

WAVE-CURRENT INTERACTION

OVER UNEVEN BOTTOM

by

Chakib Benmoussa

Dipl. Ing. Ecole Polytechnique, Palaiseau, France
(1979)

Dipl. Ing. Ecole Nationale des Ponts et Chaussees, Paris
(1981)

Submitted to the Department of
Civil Engineering
in Partial Fulfillment of the
Requirements of the
Degree of

MASTER OF SCIENCE

at the

MASSACHUSETTS INSTITUTE OF TECHNOLOGY

January 1983

© Massachusetts Institute of Technology 1983

Signature of Author _____

Department of Civil Engineering
January 10, 1983

Certified by _____

Chiang C. Mei
Thesis Supervisor

Accepted by _____

Chairman, Department Committee

Archives

MASSACHUSETTS INSTITUTE
OF TECHNOLOGY

APR 26 1983

LIBRARIES

WAVE-CURRENT INTERACTION

OVER UNEVEN BOTTOM

by

Chakib Benmoussa

Submitted to the Department of Civil Engineering
on January 10, 1983 in partial fulfillment of the
requirements for the Degree of Master of Science in
Civil Engineering

ABSTRACT

Wave-current interaction over slowly varying depth is studied by considering two extreme cases. In the first case the current is assumed to affect the waves without being affected by them. Using the method of Multiple Scales, the wave envelope is found to satisfy a cubic Schrodinger equation with variable coefficients. Benjamin-Feir's side band instability criterion is extended. By numerical integration, the evolution of a sech profile over variable depth and current is found and, Djordjevic and Redekopp's assumption of conservation of the shape of a soliton descending a shelf is assessed. In the second case, a second order mean current is assumed to be generated by a slowly varying wave group. The method of Multiple Scales and the method of Averaging are used to find the governing equations for the mean current and mean free surface displacement. They are shown to yield equivalent results. The free surface displacement is decomposed into an averaged mean set down, plus two different waves: one locked to the wave envelope and the second forced by the depth variation. Depending on the

angle of incidence and the water depth, the later can either be trapped in the region of varying depth or radiate progressive long free waves outside that region. A numerical computation using a 'Hybrid Element Method' is performed to find the forced waves.

Thesis Supervisor : Dr. Chiang C. Mei

Title : Professor of Civil Engineering

ACKNOWLEDGMENTS

I would like to express my gratitude to my thesis advisor and supervisor, Professor Chiang C. Mei whose encouragements and enthusiasm were very helpful for the completion of this study. This work was developed in a close cooperative effort with much discussions and interactions. These have always been a constant source of insight and guidance.

I also want to thank Ms. Lauren Lucszcz who typed this thesis with much patience and efficiency.

This research was sponsored by the Office of Naval Research, Contract # N00014-80-C-0531 , and the National Science Foundation, Grant # MEA 707-17817 A04 .

TABLE OF CONTENTS

	PAGES
Title Page	1
Abstract	2
Acknowledgments	4
Table of Contents	5
Part I: Evolution of Surface Wave Packets Over Slowly Varying Depth and Current	8
1. Introduction	9
2. Governing Equations	11
2.a. Governing Equations for the Current	12
2.b. Governing Equations for the Waves	14
3. Derivation of the Evolution Equation	19
3.a. Multiple Scale Procedure	19
3.b. First Order Waves	22
3.c. Second Order Waves	23
3.d. Third Order Waves	26
3.e. Evolution Equation	30
4. Wave Packet over an Uneven Bottom Profile and a Stationary Current	35
4.a. Properties of the Stationary Current	35
4.b. Wave Kinematics	42

4.c.	Evolution Equation	45
4.d.	Generalization of Stokes Waves	48
4.e.	Side Band Instability	49
5.	Numerical Approach	58
5.a.	Numerical Method	58
5.b.	Check of the Numerical Results	62
5.c.	Geometry of the Problem	65
6.	Propagation of a Wave Packet Over Varying Depth	69
6.a.	Djordjevic-Redekopp's Solution	69
6.b.	Numerical Results	71
7.	Propagation of a Wave Packet Over Varying Depth and Current	89
7.a.	Subcritical Current	89
7.b.	Supercritical Current	92
7.c.	Subcritical Opposing Current	95
8.	Conclusion	101
	Figure Captions	104
II.	Generation of Second Order Long Waves in Water of Varying Depth	109
1.	Introduction	110
2.	Governing Equations for the Mean Current and Set-Down	112
2.a.	The Multiple Scale Method	112
2.b.	The Averaging Method	117
3.	Generation of Forced Waves	124
3.a.	Locked Waves on Constant Depth	134
3.b.	Forced Waves on Variable Depth	136

4. Numerical Procedure	142
4.a. Numerical Method	142
4.b. Check of the Numerical Results	146
5. Numerical Results	149
5.a. Linear Depth Variation	149
5.b. Canyons and Ridges	162
6. Conclusion	170
Figure Captions	172
Appendix A1	175
Appendix A2	179
Appendix B1	187
Appendix B2	188
References	199

PART I :

EVOLUTION OF SURFACE WAVE PACKETS OVER

SLOWLY VARYING DEPTH AND CURRENT

1. Introduction

Wave propagation in near shore waters is often affected by depth variation and current. This interaction is of practical interest in some coastal engineering problems. At a harbor entrance, strong currents can be induced by tides, by a river flow or during storms by local wind. Waves propagating in the same direction as a current are lengthened and flattened while waves propagating in the opposite direction are shortened and steepened. These effects can be enhanced by the existence of submarine ridges and therefore can present serious hazards to navigation.

The evolution of progressive gravity waves on large scale currents was studied first by Longuet-Higgins and Stewart (1960-1961) who introduced the concept of radiation stress. The use of Whitham's approach based on averaging a Lagrangian and the introduction of the concept of wave action (Bretherton and Garrett (1968)) have further improved the understanding of wave-current interaction. A general survey by Peregrine (1976) gives more details of previous work. So far the study of waves moving over a current has been made within the limits of the linear theory, our purpose is to derive a nonlinear extension of the equation of conservation of wave action for the case of waves propagating on a strong current over variable depth. We will focus on strong currents which affect waves but are not affected by waves, and assume, as is frequently the case in nature, that the characteristic time and distance of the current are much greater than those of the waves. The method used to solve the problem is an extension of the method used by Djordjevic and Redekopp

(1978) who studied nonlinear evolution of a wave packet moving over variable depth, and the method used by Mei (1982) who showed that the results of linear theory for waves-current interaction, obtained by using Whitham's method can be derived by making use of the method of multiple scales. This method has the advantage of showing explicitly the small parameter ϵ and the assumptions made.

Turpin began this work in his M.S.thesis(1981).Because of some missing terms in the third order wave, the governing equation he found was not consistent with the linearized limit. Therefore, he assumed the value of some of the coefficients of the governing equation, in order to avoid the inconsistency. Using this equation, he then computed numerically, the evolution of a soliton over variable depth and current, for some cases. The purpose of this work is to derive the correct governing equation and to perform a comprehensive numerical study.

A nonlinear cubic Schrodinger equation with variable coefficients is shown to govern the evolution of waves amplitude. In the case of a stationary current a slight generation of Stokes wave train propagating on variable depth is found. These waves are shown to be unstable in the region where $k(\xi+h)$ is larger than 1.363 (k is the wave number, h the depth, ξ the free surface displacement due to the current). This result corresponds to the well known Benjamin-Feir (1967) instability. The evolution of a soliton propagating in the same direction or in the opposite direction of a stationary current, over variable depth is then computed numerically, using the finite difference method with an implicit scheme of the Crank-Nicholson type as applied by Yue (1980).

2. Governing Equations

We consider a unidirectional progressive wave packet moving on the free surface of a colinear current along the x-direction. The depth $h = h(x)$, is measured from the still water level and is allowed to vary along the direction of propagation. The vertical z-axis is oriented upward. We restrict the study to weakly nonlinear waves propagating over an intermediate depth i.e. the amplitude of the waves is assumed to be much smaller than their wavelength, while the depth is assumed to be of the same order:

$$\epsilon = ka \ll 1 \quad \mu = kh = O(1) \quad (2.1)$$

where k and a are the characteristic wavenumber and wave amplitude of the waves. It is further assumed that the current could be much stronger than the waves and hence the current is not affected by the waves while the waves are affected by the current at the leading order i.e.:

$$U_c = O(\sqrt{gh}) \quad \text{and} \quad (u, w) = O(\epsilon\sqrt{gh}) \quad (2.2)$$

where U_c is the horizontal current velocity, u and w the horizontal and vertical components of the wave velocity.

As is frequently the case in nature, the current U_c , the depth h , the wavenumber k and the wave period $2\pi/\omega$ are assumed to vary much more slowly than the wave induced velocity, pressure or displacement. Let introduce the slow coordinates

$$x_1 = \epsilon x \quad x_2 = \epsilon^2 x \quad t_1 = \epsilon t \quad t_2 = \epsilon^2 t \quad (2.3)$$

we have

$$\vec{U}_c = \vec{U}_c(x_2, z, t_2) \quad h = h(x_2) \quad k = k(x_2, t_2) \quad \omega = \omega(x_2, t_2) \quad (2.4)$$

while the wave related quantities depend on both fast and slow coordinates:

$$\vec{u} = \vec{u}(x, x_1, x_2, z, t, t_1, t_2) \quad (2.5)$$

2.a. Governing Equations for the Current

We first consider the current $\vec{U}_c = (U_c, W_c)$ without waves.

Following Mei (1982) we show that if the current is weakly rotational then the horizontal component U_c , and the free surface displacement ξ_c are governed, at the order $O(\epsilon^4)$, by Airy's equations.

Considering the fluid to be inviscid and incompressible, the current then satisfies Euler's equations:

$$\frac{\partial U_c}{\partial x} + \frac{\partial W_c}{\partial z} = 0 \quad (2.6)$$

$$\frac{\partial U_c}{\partial t} + U_c \frac{\partial U_c}{\partial x} + W_c \frac{\partial U_c}{\partial z} = -\frac{1}{\rho} \frac{\partial P_c}{\partial x} \quad (2.7)$$

$$\frac{\partial W_c}{\partial t} + U_c \frac{\partial W_c}{\partial x} + W_c \frac{\partial W_c}{\partial z} = -\frac{1}{\rho} \frac{\partial P_c}{\partial z} - g \quad (2.8)$$

Since the current depends on the coordinates x_2, z, t_2 the operators $\frac{\partial}{\partial t}$ and $\frac{\partial}{\partial x}$ are $O(\epsilon^2)$ while the operator $\frac{\partial}{\partial z}$ is $O(1)$ when acting on a current related quantity i.e.

$$\frac{1}{kU_c} \frac{\partial U_c}{\partial x} = \frac{1}{\omega U_c} \frac{\partial U_c}{\partial t} = \frac{1}{kh} \frac{dh}{dx} = O(\epsilon^2), \quad \frac{1}{kU_c} \frac{\partial U_c}{\partial z} = O(1) \quad (2.9)$$

Using (2.9), the continuity equation (2.6) gives:

$$W_c(x_2, z, t_2) = O(\epsilon^2) \quad (2.10)$$

Integrating with respect to z the vertical momentum equation (2.8) we find that, at the order $O(\epsilon^4)$, the pressure is hydrostatic:

$$P_c = \rho g(\xi - z) + O(\epsilon^4) \quad (2.11)$$

where $\xi = \xi(x_2, t_2)$ is the elevation of the free surface above the water level due to the current. If we further assume that the current is weakly rotational in the horizontal direction

$$\Omega = \frac{\partial U_c}{\partial z} - \frac{\partial W_c}{\partial x} = O(\epsilon^4) \quad (2.12)$$

we then deduce after using (2.10) that the horizontal component of the current could be considered to the fourth order to be independent on depth:

$$U_c = U(x_2, t_2) + O(\epsilon^4) \quad (2.13)$$

Plugging (2.13) and (2.11) into the horizontal momentum equation yields:

$$\frac{\partial U}{\partial t} + U \frac{\partial U}{\partial x} + g \frac{\partial \xi}{\partial x} = O(\epsilon^4) \quad (2.14)$$

The kinematic boundary conditions on the free surface and at the sea bottom are:

$$W_c = \frac{\partial \xi}{\partial t} + U_c \frac{\partial \xi}{\partial x} \quad z = \xi(x, t) \quad (2.15)$$

$$W_c = -U_c \frac{\partial h}{\partial x} \quad z = -h(x) \quad (2.16)$$

Integrating then the continuity equation (2.6) and using the boundary conditions (2.15) and (2.16) we obtain:

$$\frac{\partial \xi}{\partial t} + \frac{\partial}{\partial x} [U(\xi+h)] = O(\epsilon^4) \quad (2.17)$$

Equations (2.11), (2.14) and (2.17) are the so called Airy's equations.

They can be written in terms of the slow coordinates

$$\frac{\partial \xi}{\partial t_2} + \frac{\partial}{\partial x_2} (U(\xi+h)) = O(\epsilon^2) \quad (2.18)$$

$$\frac{\partial U}{\partial t_2} + U \frac{\partial U}{\partial x_2} + g \frac{\partial \xi}{\partial x_2} = O(\epsilon^2) \quad (2.19)$$

$$P_c = \rho g(\xi-z) + O(\epsilon^4) \quad (2.20)$$

The vertical current component can be found by integrating the continuity equation from $z = -h$ to z

$$W_c(x_2, z, t_2) = \epsilon^2 \left((z+h) \frac{\partial U}{\partial x_2} - \frac{\partial h}{\partial x_2} U \right) + O(\epsilon^4) \quad (2.21)$$

2.b. Governing Equations for the Waves

When we superpose waves on the current, the total velocity $\vec{U}_T = (U_c + u, W_c + w)$, the total pressure $P_T = P_c + p$ and the total free surface elevation $\xi_T = \xi + \eta$ are governed by Euler's equations with appropriate boundary conditions. [The lower case variables are related to waves, the upper case variables are related to the current]. The wave related quantities (u, w, p, η) are $O(\epsilon)$ and depends on the fast coordinates (x, z, t) so that the operators $\frac{\partial}{\partial x}$, $\frac{\partial}{\partial z}$, $\frac{\partial}{\partial t}$ are $O(1)$ when applied to these quantities.

i. Continuity and Momentum Equations

Continuity equation:

$$\frac{\partial(U_c + u)}{\partial x} + \frac{\partial(W_c + w)}{\partial z} = 0 \quad (2.22)$$

Since the current satisfies a similar equation (2.6), we have

$$\frac{\partial u}{\partial x} + \frac{\partial w}{\partial z} = 0 \quad (2.23)$$

x-momentum equation:

$$\frac{\partial(U_c + u)}{\partial t} + (U_c + u) \frac{\partial(U_c + u)}{\partial x} + (W_c + w) \frac{\partial(U_c + u)}{\partial z} = -\frac{1}{\rho} \frac{\partial(P_c + p)}{\partial x} \quad (2.24)$$

using the x-momentum equation satisfied by the current and the approximations (2.10) and (2.13) we obtain:

$$\frac{\partial u}{\partial t} + u \frac{\partial U}{\partial x} + U \frac{\partial u}{\partial x} + W \frac{\partial u}{\partial z} + u \frac{\partial u}{\partial x} + w \frac{\partial u}{\partial z} = -\frac{1}{\rho} \frac{\partial p}{\partial x} + O(\epsilon^5) \quad (2.25)$$

z-momentum equation:

$$\frac{\partial(W_c + w)}{\partial t} + (U_c + u) \frac{\partial(W_c + w)}{\partial x} + (W_c + w) \frac{\partial(W_c + w)}{\partial z} = -\frac{1}{\rho} \frac{\partial(P_c + p)}{\partial z} - g \quad (2.26)$$

using the z-momentum equation satisfied by the current we have:

$$\frac{\partial w}{\partial t} + w \frac{\partial W}{\partial z} + U \frac{\partial w}{\partial z} + W \frac{\partial w}{\partial x} + u \frac{\partial w}{\partial x} + w \frac{\partial w}{\partial z} = -\frac{1}{\rho} \frac{\partial p}{\partial z} + O(\epsilon^5) \quad (2.27)$$

If we take the second derivative with respect to z of the vertical component of the current given by (2.21), we find that

$$\frac{\partial^2 W}{\partial z^2} = O(\epsilon^4) \quad (2.28)$$

Finally taking $\frac{\partial}{\partial x}$ (2.25) + $\frac{\partial}{\partial z}$ (2.27) and using the approximations for the current (2.10), (2.13) and (2.28) and the continuity equation for the waves we get the governing equation for the wave pressure

$$\nabla^2 p = -2\rho\left\{\left(\frac{\partial u}{\partial x}\right)^2 + \frac{\partial u}{\partial z} \frac{\partial w}{\partial x} + 2 \frac{\partial u}{\partial x} \frac{\partial U}{\partial x}\right\} \quad -h < z < \xi + \eta \quad (2.29)$$

ii. Boundary Conditions

The kinematic condition at the sea bottom is:

$$(\vec{U}_c + \vec{u}) \cdot \vec{n} = 0 \quad (2.30)$$

where \vec{n} is the normal at the depth profile at the point x . Using the fact that the current satisfies a similar condition (2.16), the waves should satisfy the following equation:

$$w = -u \frac{dh}{dx} \quad \text{on } z = -h(x) \quad (2.31)$$

It should be noted that since u is $O(\epsilon)$ and $\frac{dh}{dx}$ is $O(\epsilon^2)$, the vertical velocity at the sea bottom is $O(\epsilon^3)$

$$w = O(\epsilon^3) \quad \text{on } z = -h(x) \quad (2.32)$$

From the kinematic condition (2.31) we want to infer a boundary condition for the pressure. For this purpose we differentiate (2.32) with respect to x :

$$\frac{\partial w}{\partial x} - \frac{dh}{dx} \frac{\partial w}{\partial z} = -\frac{\partial u}{\partial x} \frac{dh}{dx} + O(\epsilon^5) \quad \text{on } z = -h(x) \quad (2.33)$$

The x -momentum equation at the order $O(\epsilon^2)$ reduces to:

$$-\frac{1}{\rho} \frac{\partial p}{\partial x} = \frac{\partial u}{\partial t} + U \frac{\partial u}{\partial x} + O(\epsilon^2) \quad (2.34)$$

The z -momentum equation (2.27) applied at the sea bottom with the conditions (2.10) and (2.32) gives

$$-\frac{1}{\rho} \frac{\partial p}{\partial z} = \frac{\partial w}{\partial t} + U \frac{\partial w}{\partial x} + W \frac{\partial w}{\partial z} + O(\epsilon^4) \quad \text{on } z = -h(x) \quad (2.35)$$

Using the kinematic condition at the bottom of the sea, (2.31), (2.33) and (2.16) and the continuity equation (2.6) and (2.23) into (2.35) gives

$$-\frac{1}{\rho} \frac{\partial p}{\partial z} = -\frac{dh}{dx} \left(\frac{\partial u}{\partial t} + U \frac{\partial u}{\partial x} \right) + O(\epsilon^4) \quad \text{on } z = -h(x) \quad (2.36)$$

we finally combine (2.34) and (2.36) to obtain the boundary condition for the pressure

$$\frac{\partial p}{\partial z} = -\frac{dh}{dx} \frac{\partial p}{\partial x} + O(\epsilon^4) \quad \text{on } z = -h(x) \quad (2.37)$$

The kinematic condition at the free surface ($\xi+\eta$) is

$$\frac{\partial(\xi+\eta)}{\partial t} + (U_c + u) \frac{\partial(\xi+\eta)}{\partial x} = W_c + w \quad \text{on } z = \xi + \eta \quad (2.38)$$

Since the waves induced displacement η is $O(\epsilon)$ we expand \vec{U}_c , \vec{u} and p in Taylor series about $z = \xi$

$$\begin{aligned} U_c(x, \xi+\eta, t) &= U(x, t) + O(\epsilon^4) \\ W_c(x, \xi+\eta, t) &= W(x, \xi, t) + \eta \left. \frac{\partial W}{\partial z} \right|_{z=\xi} + O(\epsilon^4) \end{aligned} \quad (2.39)$$

$$u(x, \xi+\eta, t) = u(x, \xi, t) + \eta \left. \frac{\partial u}{\partial z} \right|_{z=\xi} + \frac{\eta^2}{2} \left. \frac{\partial^2 u}{\partial z^2} \right|_{z=\xi} + O(\epsilon^4)$$

similar equations to (2.39.c) are obtained for w and p . Substituting these expansions into equation (2.38) and using the kinematic condition (2.15) and the continuity equation (2.6) gives

$$\frac{\partial \eta}{\partial t} + u \frac{\partial \xi}{\partial x} + U \frac{\partial \eta}{\partial x} = -\eta \frac{\partial U}{\partial x} + w + \eta \frac{\partial w}{\partial z} - u \frac{\partial \eta}{\partial x} - \eta \frac{\partial \eta}{\partial x} \frac{\partial u}{\partial z} + \frac{\eta^2}{2} \frac{\partial^2 w}{\partial z^2} + O(\epsilon^4)$$

on $z = \xi$ (2.40)

The dynamic boundary conditions at the free surface ($\xi + \eta$) is that the total pressure does not vary following the fluid motion along the free surface i.e.

$$\frac{\partial (P_c + p)}{\partial t} + (U_c + u) \frac{\partial (P_c + p)}{\partial x} + (W_c + w) \frac{\partial (P_c + p)}{\partial z} = 0 \quad \text{on } z = \xi + \eta \quad (2.41)$$

plugging the previous expansions (2.39) into (2.41) and using the expression for the pressure P_c given in (2.11) and the continuity equation (2.6) we have:

$$\begin{aligned} \frac{\partial p}{\partial t} + \eta \frac{\partial^2 p}{\partial t \partial z} + \frac{\eta^2}{2} \frac{\partial^3 p}{\partial t \partial z^2} + U \frac{\partial p}{\partial x} + U\eta \frac{\partial^2 p}{\partial z \partial x} + \frac{U\eta^2}{2} \frac{\partial^3 p}{\partial z^2 \partial x} + u \frac{\partial p}{\partial x} + \\ \eta \frac{\partial p}{\partial x} \frac{\partial u}{\partial z} + u\eta \frac{\partial^2 p}{\partial x \partial z} + w \frac{\partial p}{\partial z} + \eta \frac{\partial p}{\partial z} \frac{\partial w}{\partial z} + w\eta \frac{\partial^2 p}{\partial z^2} + \rho g u \frac{\partial \xi}{\partial x} + W \frac{\partial p}{\partial z} + \\ \rho g \eta \frac{\partial U}{\partial x} - \rho g (w + \eta) \frac{\partial w}{\partial z} + \frac{\eta^2}{2} \frac{\partial^2 w}{\partial z^2} = O(\epsilon^4) \end{aligned}$$

on $z = \xi$ (2.42)

In conclusion, the governing equations for the waves are given by (2.23), (2.25) and (2.29) with the boundary conditions (2.37), (2.40) and (2.42).

3. Derivation of the Evolution Equation

3.a Multiple Scale Procedure

The depth and the current vary slowly in space and time so the parameters characterizing the waves will change over the same scales, i.e.

$$k = k(X,T) \quad \omega = \omega(X,T) \quad (3.1)$$

where $X = x_2 = \epsilon^2 x$, $T = t_2 = \epsilon^2 t$. The variation of the wavenumber k and the frequency ω are related by the law of conservation of wave crests:

$$\frac{\partial k}{\partial T} + \frac{\partial \omega}{\partial X} = 0 \quad (3.2)$$

We shall restrict our attention to slowly varying wave packet of length $1/\epsilon$, propagating in a fixed frame at the group velocity $C_g(X,T)$, therefore, by following Djordjevic and Redekopp (1978) we introduce the multiple scale variables:

$$\tau = \epsilon \left(\int \frac{dx}{C_g(X;T)} - t \right), \quad X, \quad T \quad (3.3)$$

since we are dealing with progressive waves, for small enough ϵ we can expand the wave pressure, velocity and free surface elevation in the following form:

$$p(x,z,t) = \sum_{n=1}^{\infty} \epsilon^n \sum_{m=-n}^n P_{nm}(X,T,\tau,z) e^{im\phi} \quad (3.4.a)$$

$$\eta(x,t) = \sum_{n=1}^{\infty} \epsilon^n \sum_{m=-n}^n \eta_{nm}(X,T,\tau) e^{im\phi} \quad (3.4.b)$$

where ϕ is defined by:

$$\frac{\partial \phi}{\partial x} = k \quad \frac{\partial \phi}{\partial t} = -\omega \quad (3.5)$$

and since all the left hand side quantities are real we have:

$$P_{n,-m} = P_{n,m}^* \quad \eta_{n,-m} = \eta_{n,m}^* \quad (3.6)$$

where $(\cdot)^*$ denotes the complex conjugate. The expansions for u and w are similar to Eq. (3.4.a).

We substitute the expansions (3.4) into the governing equations (2.23), (2.25) and (2.29) and the boundary conditions (2.37), (2.40) and (2.42) and then separate terms of different orders and different harmonics. It should be noted that the multiple scale method implies that the derivatives with respect to space and time are

$$\frac{\partial \cdot}{\partial x} \rightarrow \epsilon^2 \frac{\partial \cdot}{\partial X} \quad \frac{\partial \cdot}{\partial z} \rightarrow \frac{\partial \cdot}{\partial z} \quad \frac{\partial \cdot}{\partial t} \rightarrow \epsilon^2 \frac{\partial \cdot}{\partial T} \quad (3.7)$$

when applied to quantities related to the current, but they become:

$$\frac{\partial \cdot}{\partial x} \rightarrow (imk) \cdot + \frac{\epsilon}{C_g} \frac{\partial \cdot}{\partial \tau} \cdot + \epsilon^2 \frac{\partial \cdot}{\partial X} \cdot \quad (3.8)$$

$$\frac{\partial^2 \cdot}{\partial x^2} \rightarrow (-m^2 k^2) \cdot + \epsilon \frac{2imk}{C_g} \frac{\partial \cdot}{\partial \tau} \cdot + \epsilon^2 \left(2imk \frac{\partial \cdot}{\partial X} \cdot + \frac{1}{C_g^2} \frac{\partial^2 \cdot}{\partial \tau^2} \cdot + im \frac{\partial k \cdot}{\partial X} \cdot \right) \quad (3.9.a)$$

$$\frac{\partial \cdot}{\partial z} \rightarrow \frac{\partial \cdot}{\partial z} \quad (3.9.b)$$

$$\frac{\partial \cdot}{\partial t} \rightarrow (-im\omega) \cdot - \frac{\epsilon}{C_g} \frac{\partial \cdot}{\partial \tau} \cdot + \epsilon^2 \frac{\partial \cdot}{\partial T} \cdot \quad (3.9.c)$$

when applied to quantities related to the waves .

For the n^{th} order and m^{th} harmonic we then obtain the following set of equations:

$$(2.29) \rightarrow \left(\frac{\partial^2}{\partial z^2} - m^2 k^2 \right) P_{nm} = I_{nm} \quad - h < z < \xi \quad (3.10.a)$$

$$(2.37) \rightarrow \frac{\partial P_{nm}}{\partial z} = J_{nm} \quad z = -h(x) \quad (3.10.b)$$

$$(2.25) \rightarrow -im\sigma U_{nm} + \frac{imk}{\rho} P_{nm} = K_{nm} \quad - h < z < \xi \quad (3.10.c)$$

$$(2.23) \rightarrow \frac{\partial W_{nm}}{\partial z} + imk U_{nm} = L_{nm} \quad - h < z < \xi \quad (3.10.d)$$

$$(2.40) \rightarrow -im\sigma \eta_{nm} - W_{nm} = M_{nm} \quad z = \xi \quad (3.10.e)$$

$$(2.42) \rightarrow -im\sigma P_{nm} - \rho g W_{nm} = N_{nm} \quad z = \xi \quad (3.10.f)$$

where the right hand side terms are lower order terms and are listed in Appendix A1 and σ is the intrinsic frequency of the waves: $\sigma = \omega - kU$.

The procedure of solution is as follows. Once the problem at orders $1, 2, \dots, n-1$ are solved, we use (3.10.a) and (3.10.b) to find the pressure P_{nm} for $m = 0, 1, \dots, n$, then (3.10.c) and (3.10.d) to find the horizontal and vertical velocity U_{nm} , W_{nm} and (3.10.e) to find the surface displacement η_{nm} . Finally by substituting the previous results into (3.10.f) we find a solvability condition which determines the arbitrary functions introduced at lower orders.

3.b First Order Solution

Solving the set of equations (3.10) for the first order and zeroth harmonic wave, it is found that the pressure P_{10} is not dependent on z i.e. $P_{10}(X, T, \tau)$ and that there is no vertical velocity i.e.

$$W_{10} = 0 \quad (3.11)$$

At the first harmonic the usual linear wave solution is found. In particular the pressure, wave velocity and surface elevation are given respectively by:

$$P_{11} = A \frac{\cosh k(z+h)}{\cosh kd} \quad (3.12)$$

$$U_{11} = \frac{k}{\rho\sigma} A \frac{\cosh k(z+h)}{\cosh kd} \quad (3.13)$$

$$W_{11} = -\frac{ikA}{\rho\sigma} \frac{\sinh k(z+h)}{\cosh kd} \quad (3.14)$$

$$\eta_{11} = \frac{A}{\rho g} \quad (3.15)$$

where

$$d = \xi + h \quad (3.16)$$

denotes the mean water depth including the current set-up. The wavelength is also found to satisfy the following dispersion relation

$$\sigma^2 \equiv (\omega - Uk)^2 = gk \tanh kd \quad (3.17)$$

At this point the amplitude of the waves $\frac{A}{\rho g}(X, T, \tau)$ the zeroth harmonic component of the pressure $P_{10}(X, T, \tau)$ and of the horizontal velocity $U_{10}(X, T, \tau)$ are still unknown. We need to go to higher order to find their governing equations.

3.c Second Order Solution

At the second order zeroth-harmonic, Eqs. (3.10.a) and (3.10.b) can be solved to yield the pressure

$$P_{20} = -\frac{k^2 |A|^2}{\rho \sigma^2} \frac{\cosh 2k(z+h)}{\cosh^2 kd} + P_{20}(X, T, \tau) \quad (3.18)$$

where P_{20} is an arbitrary function of X, T, τ which will contribute to the mean pressure. At the zeroth harmonic the left hand side of Eq. (3.10.c) is zero, and implies that

$$\frac{\partial U_{10}}{\partial \tau} = \frac{1}{\rho(C_g - U)} \frac{\partial P_{10}}{\partial \tau} \quad (3.19)$$

This equation also shows that the horizontal, first order velocity has no z dependence. Integrating Eq. (3.10.d) with respect to z we then obtain:

$$W_{20} = -\frac{(z+h)}{C_g} \frac{\partial U_{10}}{\partial \tau} \quad (3.20)$$

The remaining two equations (3.10.e) and (3.10.f) give :

$$W_{20} = -\frac{(C_g - U)}{C_g} \frac{\partial \eta_{10}}{\partial \tau} \quad \text{on } z = \xi \quad (3.21)$$

$$-\rho g W_{20} = \frac{(C_g - U)}{C_g} \frac{\partial P_{10}}{\partial \tau} \quad \text{on } z = \xi \quad (3.22)$$

Eqs. (3.19) - (3.22) imply that

$$\frac{\partial U_{10}}{\partial \tau} = 0 \quad \frac{\partial \eta_{10}}{\partial \tau} = 0 \quad \frac{\partial P_{10}}{\partial \tau} = 0 \quad W_{20} = 0 \quad (3.23)$$

U_{10} , η_{10} , P_{10} are therefore three arbitrary functions of X, T which represent a current of order ϵ . By assuming that far downstream ($\tau \rightarrow +\infty$) their values are zero, we can take these arbitrary functions to be zero, i.e.

$$U_{10} = \eta_{10} = P_{10} = 0 \quad (3.24)$$

Similarly the first harmonic of the second order wave is obtained by setting $n = 2$, $m = 1$. The solution of (3.10.a) and (3.10.b) gives

$$P_{21} = D(X, T, \tau) \frac{\cosh k(z+h)}{\cosh kd} - \frac{iA}{C} \tau (z+h) \frac{\sinh k(z+h)}{\cosh kd} \quad (3.25)$$

where D is an arbitrary function associated with an homogeneous solution.

From Eq. (3.10.c) after using (3.25) we have:

$$U_{21} = \frac{k}{\rho\sigma} D \frac{\cosh k(z+h)}{\cosh kd} - \frac{ik A}{\rho\sigma C} \frac{\tau}{g} [(z+h) \sinh k(z+h) + \left(\frac{1}{k} - \frac{C-U}{\sigma}\right) \cosh k(z+h)] \quad (3.26)$$

which gives after plugging it into (3.10.d) and integrating with respect to z

$$W_{21} = -\frac{ik}{\rho\sigma} D \frac{\sinh k(z+h)}{\cosh kd} - \frac{k A}{\rho\sigma C} \frac{\tau}{g} [(z+h) \cosh k(z+h) + \left(\frac{1}{k} - \frac{C-U}{\sigma}\right) \sinh k(z+h)] \quad (3.27)$$

The free surface elevation at the second order and first harmonic is then obtained from (3.10.e)

$$\eta_{21} = \frac{D}{\rho g} - \frac{ikA\tau}{\rho\sigma^2 C_g} \left[d + \left(\frac{1}{k} - 2 \left(\frac{C_g - U}{\sigma} \right) \right) \tanh kd \right] \quad (3.28)$$

The dynamic free surface condition (3.10.f) gives after using (3.25) and (3.27)

$$C_g = U + \frac{\sigma}{2k} \left(1 + \frac{2kd}{\sinh 2kd} \right) \quad (3.29)$$

which is just the usual formula for the group velocity in a fixed frame

$$\text{i.e. } C_g = \frac{\partial \omega}{\partial k}$$

The second harmonic of the second order wave is obtained in a similar way.

$$P_{22} = F(X, T, \tau) \frac{\cosh 2k(z+h)}{\cosh 2kd} - \frac{k^2 A^2}{2\rho\sigma^2 \cosh^2 kd} \quad (3.30)$$

where F is a function which would be determined by the dynamic condition (3.10.f). We notice that, as usual, the second harmonic does not introduce any homogeneous solution. The horizontal and vertical velocities and the free surface elevation are:

$$U_{22} = \frac{k}{\rho\sigma} F \frac{\cosh 2k(z+h)}{\cosh 2kd} \quad (3.31)$$

$$W_{22} = - \frac{ik}{\rho\sigma} F \frac{\sinh 2k(z+h)}{\cosh 2kd} \quad (3.32)$$

$$\eta_{22} = \frac{kF}{2\rho\sigma^2} \tanh 2kd + \frac{A^2 k^2}{\rho^2 g \sigma^2} \quad (3.33)$$

The condition (3.10.f) with the results (3.30) and (3.32) give as expected the value of the function F

$$F = \frac{3k^2 \cosh 2kd}{2\rho\sigma^2 \cosh^2 kd \sinh^2 kd} A^2 \quad (3.34)$$

At this point we have only three arbitrary functions left: A , \underline{P}_{20} , D . The dynamic boundary condition (2.12) will give for the zeroth and first harmonic of the third order two equations which relate these functions. (It should be noted that as in the case of constant depth and no current, D is expected not to appear in these equations).

3.d Third Order Solution

The dynamic boundary condition at the zeroth harmonic can be determined without calculating P_{30} . From Eq. (3.10.c) we find that K_{30} is zero which yields

$$\frac{\partial U_{20}}{\partial \tau} = \frac{1}{\rho(C_g - U)} \frac{\partial \underline{P}_{20}}{\partial \tau} \quad (3.35)$$

or by integration with respect to τ

$$U_{20} = \frac{1}{\rho(C_g - U)} \underline{P}_{20} + F_1(X, T) \quad (3.36)$$

where F_1 is an arbitrary real function. It should be noted that since \underline{P}_{20} has no z -dependence, U_{20} will not be dependent on z . Using (3.36) to calculate L_{30} and integrating (3.10.d) with respect to z we obtain:

$$W_{30} = - \frac{(z+h)}{\rho g(C_g - U)} \frac{\partial \underline{P}_{20}}{\partial \tau} \quad (3.37)$$

Equation (3.10.e) gives a relation between W_{30} and M_{30} which is

$$(C_g - U) \frac{\partial \eta_{20}}{\partial \tau} - \frac{d}{\rho(C_g - U)} \frac{\partial \tilde{P}_{20}}{\partial \tau} - \frac{2k|A|_{\tau}^2}{\rho^2 g \sigma} = 0 \quad (3.38)$$

after using (3.37). By integrating with respect to τ , we get

$$\eta_{20} = \frac{d \tilde{P}_{20}}{\rho(C_g - U)^2} + \frac{2k|A|_{\tau}^2}{\rho^2 \sigma C_g (C_g - U)} + F_2(X, T) \quad (3.39)$$

where F_2 is another arbitrary function. Equation (3.10.f) is then used with (3.37) to obtain a relation between A and \tilde{P}_{20}

$$\left(1 - \frac{(C_g - U)^2}{gd}\right) \frac{\partial \tilde{P}_{20}}{\partial \tau} = -\frac{C_g (C_g - U) k^2}{gd \rho \sigma^2} \left(\frac{2\sigma}{k C_g} + \frac{(C_g - U)}{C_g} \frac{1}{\cosh^2 kd}\right) |A|_{\tau}^2 \quad (3.40)$$

or integrating it with respect to τ

$$\left(1 - \frac{(C_g - U)^2}{gd}\right) \tilde{P}_{20} = \frac{-k^2 C_g (C_g - U)}{\rho \sigma^2 gd} \left(\frac{2\sigma}{k C_g} + \frac{C_g - U}{C_g} \frac{1}{\cosh^2 kd}\right) |A|_{\tau}^2 + F_3(X, T) \quad (3.41)$$

where F_3 is an arbitrary real function. We note that $(C_g - U)^2 < gd$ always. In very shallow water $(C_g - U)^2 \rightarrow gd$, the assumption of intermediate depth i.e. $kh = O(1)$ breaks down and our weakly nonlinear theory is no longer valid. \tilde{P}_{20} is the pressure due to the mean flow which is produced by the wave modulation. In the limiting case of no current, its expression has been given by Longuet-Higgins and Stewart (1962).

To get the governing equation for A we need to apply the dynamic boundary condition at the first harmonic. For this purpose P_{31} and W_{31} must be calculated. From (3.10.a) and (3.10.b)

$$\begin{aligned}
P_{31} = & G(X, T, \tau) \frac{\cosh k(z+h)}{\cosh kd} - \frac{i}{C_g} D_\tau \frac{\sinh k(z+h)}{\cosh kd} - \frac{i(z+h)\sinh k(z+h)}{\cosh kd} A_X \\
& - \frac{3}{2} \frac{k^4}{\rho^2 \sigma^4} \frac{\cosh 3k(z+h)}{\cosh^3 kd \sinh^2 kd} |A|^2 A - (z+h)^2 \frac{\cosh k(z+h)}{2C_g^2 \cosh kd} A_\tau \frac{-iA}{\cosh kd} \\
& \left\{ \left[\frac{k(z+h)^2}{2} \right]_X \cosh k(z+h) + \left(\frac{2k}{\sigma} U_X - (kd)_X \tanh kd \right) (z+h) \sinh k(z+h) \right\}
\end{aligned} \tag{3.42}$$

where G is a new arbitrary function which corresponds to an homogeneous solution. To obtain W_{31} it is easier to use directly the z -momentum equation (2.27) at the order $O(\epsilon^3)$ for $m = 1$. This equation can be put in the form

$$-i\sigma W_{31} + \frac{1}{\rho} \frac{\partial P_{31}}{\partial z} = Q_{31} \tag{3.43}$$

where Q_{31} is a sum of lower order terms and is listed in Appendix A1. Using (3.42) in (3.43) and replacing the lower order term by their respective values we get:

$$\begin{aligned}
W_{31} = & - \frac{ik^2 \sinh k(z+h)}{\rho^2 \sigma^2 (C_g - U) \cosh kd} P_{20} A - \frac{ik \sinh k(z+h)}{\rho \sigma \cosh kd} G + 0 \cdot |A|^2 A \\
& - \frac{k D_\tau}{\rho \sigma C_g \cosh kd} \left[(z+h) \cosh k(z+h) + \left(\frac{1}{k} - \frac{(C_g - U)}{\sigma} \right) \sinh k(z+h) \right] \\
& - \frac{k A_X}{\rho \sigma \cosh kd} \left[(z+h) \cosh k(z+h) + \left(\frac{1}{k} + \frac{U}{\sigma} \right) \sinh k(z+h) \right] \\
& - \frac{k \sinh k(z+h)}{\rho \sigma^2 \cosh kd} A_\tau + \frac{ikA}{\rho \sigma C_g^2 \cosh kd} \left[\frac{(z+h)^2}{2} \sinh k(z+h) + \left(\frac{1}{k} - \frac{(C_g - U)}{\sigma} \right) \right]
\end{aligned}$$

$$\begin{aligned}
& (z+h) \cosh k(z+h) - \frac{(C_g - U)}{\sigma} \left[\frac{1}{k} - \frac{C_g - U}{\sigma} \right] \sinh k(z+h) \Big] - \frac{A}{\rho \sigma \cosh kd} \\
& \left[\frac{(k^2)}{4} X (z+h)^2 \sinh k(z+h) + (z+h) \cosh k(z+h) (k_X + k k_X \frac{U}{\sigma} + k^2 \frac{U_X}{\sigma} \right. \\
& \left. - k(kd)_X \tanh kd) + k h_X \cosh k(z+h) + k^2 h_X (z+h) \sinh k(z+h) \right. \\
& \left. + \sin k(z+h) \left(\frac{kU}{\sigma} - (kd)_X \tanh kd \left(1 + \frac{kU}{\sigma} \right) \right) + \cosh k(z+h) \right. \\
& \left. \frac{\left(\frac{k}{\sigma} \frac{\sinh k(z+h)}{\cosh kd} \right)_T \right] - \frac{i k^2 \sinh k(z+h)}{\rho \sigma^2 \cosh kd} A F_1 \tag{3.44}
\end{aligned}$$

This expression is similar to Turpin's (1981) except for the terms which are underlined. This difference in the two results is due to the fact that a term is missing in his expression for Q_{31} and that an error has been made in the evaluation of two other terms (see Appendix A1).

Finally using (3.42) and (3.44) in (3.10.f) gives the governing equation for A:

$$\alpha_1 A + \frac{1}{C_g} A_T + A_X + i \alpha_2 A_{TT} + i \alpha_3 |A|^2 A + i Q A + \alpha_4 G + \alpha_5 D_T = 0 \tag{3.45}$$

After a lengthy algebra the coefficients of this equation are found to be:

$$\begin{aligned}
\alpha_1(X, T) = & \frac{1}{2C_g} \left\{ \left(\frac{\cosh k(z+h)}{\cosh kd} \right)_T \Big|_{z=\xi} + \frac{\sigma}{k\beta} \left(\frac{k}{\sigma} \frac{\sinh k(z+h)}{\cosh kd} \right)_T \Big|_{z=\xi} \right. \\
& + U_X \left(2 + \frac{kd}{\beta} (1-3\beta^2) \right) + \sigma d_X (kd(\beta^2-1) - \frac{(\beta^2-1)}{\beta} - \frac{2k\beta U}{\sigma}) \\
& \left. + \sigma k_X (d^2(\beta^2-1) + \frac{d}{k} \frac{(1-\beta^2)}{\beta} (1 + \frac{kU}{\sigma}) + \frac{U}{\sigma k}) - \frac{U\sigma_X}{\sigma} \right\} \tag{3.46}
\end{aligned}$$

$$\alpha_2(X,T) = \frac{1}{2C_g \sigma (1-\beta^2)} \left[\left(\frac{C_g - U}{C_g} \right)^2 (1+3\beta^2) + \left(\frac{C_p}{C_g} \right)^2 - \frac{2C_p (C_g - U)}{C_g^2} (1+\beta^2) \right] \quad (3.47)$$

$$\alpha_3(X,T) = \frac{k^4}{4\rho^2 \sigma^3 \beta^2 C_g} \left[9 - 12\beta^2 + 13\beta^4 - 2\beta^6 - \frac{2\beta^2 (C_g - U)^2}{gd - (C_g - U)^2} \left(\frac{2C_p}{C_g - U} + 1 - \beta^2 \right)^2 \right] \quad (3.48)$$

$$Q(X,T) = \frac{2k}{C_g} F_1 + \frac{k\sigma}{\beta C_g} (1 - \beta^2) F_2 + \left[\frac{k^2}{\rho \sigma C_g} \left(\frac{2C_p}{C_g - U} + 1 - \beta^2 \right) \frac{gd}{gd - (C_g - U)^2} \right] F_3 \quad (3.49)$$

$$\alpha_4 = \alpha_5 = 0 \quad (3.50)$$

where $\beta = \tanh kd$ and $C_p = \frac{\sigma}{k}$ (relative phase velocity). It should be noted that the arbitrary functions G and D representing the second and third order homogeneous solutions disappear from (3.45) because of (3.50) and that Q is a real function of (X,T) depending on the unknown functions F_1, F_2, F_3 .

3.e. Evolution Equation

So far the evolution equation depends on the unknown function Q(X,T). Lets consider a wave group started from rest, at a finite distance, the wave group will be still localized i.e. the motion becomes zero as $T \rightarrow +\infty$. Therefore, from Eqs. (3.36), (3.39) and (3.41) we deduce that

$$F_1 = F_2 = F_3 = 0 \quad (3.51)$$

so Q will be identically equal to zero. In the particular case of a stationary current i.e. with no dependence on T, we can get rid of Q without saying that there is no motion at $\tau = \infty$. Since Q is then a function of X only we introduce

$$B = A \exp i \int^X Q(u) du \quad (3.52)$$

Because Q is real B and A have the same amplitude, however B satisfies an equation similar to (3.45) without the Q term. In this case Q affects the phase of A only. For these reasons Q will not be considered in what follows. The governing equation of the first order wave amplitude becomes

$$\alpha_1 A + \frac{1}{C_g} A_T + A_X + i\alpha_2 A_{TT} + i\alpha_3 |A|^2 A = 0 \quad (3.53)$$

It is a nonlinear cubic Schrodinger equation with variable coefficients. These coefficients can be further simplified by using the governing equation for the current (2.18, 2.15), the conservation of wave crest (3.2), the dispersion relation (3.17) and the expression of the group velocity (3.29).

$$\alpha_1(X, T) = -\frac{1}{2\sigma C_g} \frac{\partial \sigma}{\partial T} + \frac{\sigma}{2C_g} \frac{\partial (C_g/\sigma)}{\partial X} \quad (3.54.a)$$

$$\alpha_2(X, T) = \frac{1}{2\sigma} \frac{(C_g - U)^2}{C_g^3} \left[1 - \frac{gd}{(C_g - U)^2} (1 - \beta^2)(1 - \beta kd) \right] = -\frac{1}{2C_g^3} \frac{\partial^2 \omega}{\partial k^2} \quad (3.54.b)$$

$$\alpha_3(X, T) = \frac{k^4}{4C_g \rho^2 \sigma^3 \beta^2} \left\{ 9 - 10\beta^2 + 9\beta^4 - \frac{2\beta^2 (C_g - U)^2}{gd - (C_g - U)^2} \left[4 \left(\frac{C_p}{C_g - U} \right)^2 + 4 \left(\frac{C_p}{C_g - U} \right) (1 - \beta^2) + \frac{gd}{(C_g - U)^2} (1 - \beta^2)^2 \right] \right\} \quad (3.54.c)$$

From the linear theory Turpin (1981) guessed that α_1 should have the form (3.54.a), however he was unable to deduce it because of the errors made in the third order velocity. Our derivation shows the validity of this assumption.

In the particular case where there is no current ($U = 0$) and no dependence on T we recover the evolution equation found by Djordjevic and Redekopp (1978):

$$\alpha_1' A + A_X + i\alpha_2' A_{TT} + i\alpha_3' |A|^2 A = 0 \quad (3.55)$$

where α_1' can be put in the same form as Djordjevic and Redekopp's parameter μ by using the dispersion relation and the expression of the group velocity.

$$\alpha_1'(X) = \frac{\omega}{2C_g} \frac{\partial(C_g/\omega)}{\partial X} = \frac{\omega}{2k\beta C_g} (1-\beta^2)(1-kh\beta) \frac{dkh}{dX} \quad (3.56.a)$$

$$\alpha_2'(X) = \frac{1}{2\omega C_g} \left[1 - \frac{gh}{C_g^2} (1-\beta^2)(1-\beta kh) \right] \quad (3.56.b)$$

$$\alpha_3'(X) = \frac{k^4}{4C_g \omega^3 \beta^2} \left\{ 9 - 10\beta^2 + 9\beta^4 - \frac{2\beta^2 C_g^2}{gh - C_g^2} \left(\frac{4C_p^2}{C_g^2} + 4 \frac{C_p}{C_g} (1-\beta^2) + \frac{gh}{C_g^2} (1-\beta^2)^2 \right) \right\} \quad (3.56.c)$$

where $\beta = \tanh kh$ and $C_p = \frac{\omega}{k}$

As a limiting case, the result of linear theory can be found by neglecting the nonlinear term $|A|^2 A$ and taking A to be a function of the very slow variables (X, T) only. (3.53) becomes then:

$$\frac{1}{C} A_T + \frac{\sigma}{2C} \frac{\partial(C/\sigma)}{\partial X} A - \frac{1}{2\sigma C} A + A_X = 0 \quad (3.57)$$

Let's take (3.57)* $\cdot \frac{C}{\sigma} A + (3.57) \cdot \frac{C}{\sigma} A^*$ we obtain:

$$\frac{\partial}{\partial T} \left(\frac{|A|^2}{\sigma} \right) + \frac{\partial}{\partial X} \left(\frac{C}{\sigma} |A|^2 \right) = 0 \quad (3.58)$$

which is just the conservation of wave action. The evolution equation (3.53) is therefore an extended law of conservation of wave action.

The coefficient α_2 of the evolution equation is a measure of the wave dispersion. From (3.54.b) it can be seen that α_2 remains positive for any value of the wave period, the current velocity and depth. The coefficient α_3 is a measure of the nonlinearity. Let us introduce.

$$Y = \frac{4C \rho^2 \sigma^3 \beta^2}{k^4} \alpha_3(X, T)$$

Y can be easily seen to be a function of kd only. Y is plotted in fig. (3.1). It shows that Y increases from -9 when $kd \rightarrow 0$ to the asymptotic value 8 when $kd \rightarrow +\infty$. Its sign changes from negative to positive across $kd \approx 1.363$. So even if the value of α_3 depends on several parameters as ω , U, h, its sign only depends on the value of kd. It should be noted that Y(kd) is the same as X(K) defined by Eq. (30) in Benjamin's paper (1967) where he studied the stability of Stokes waves.

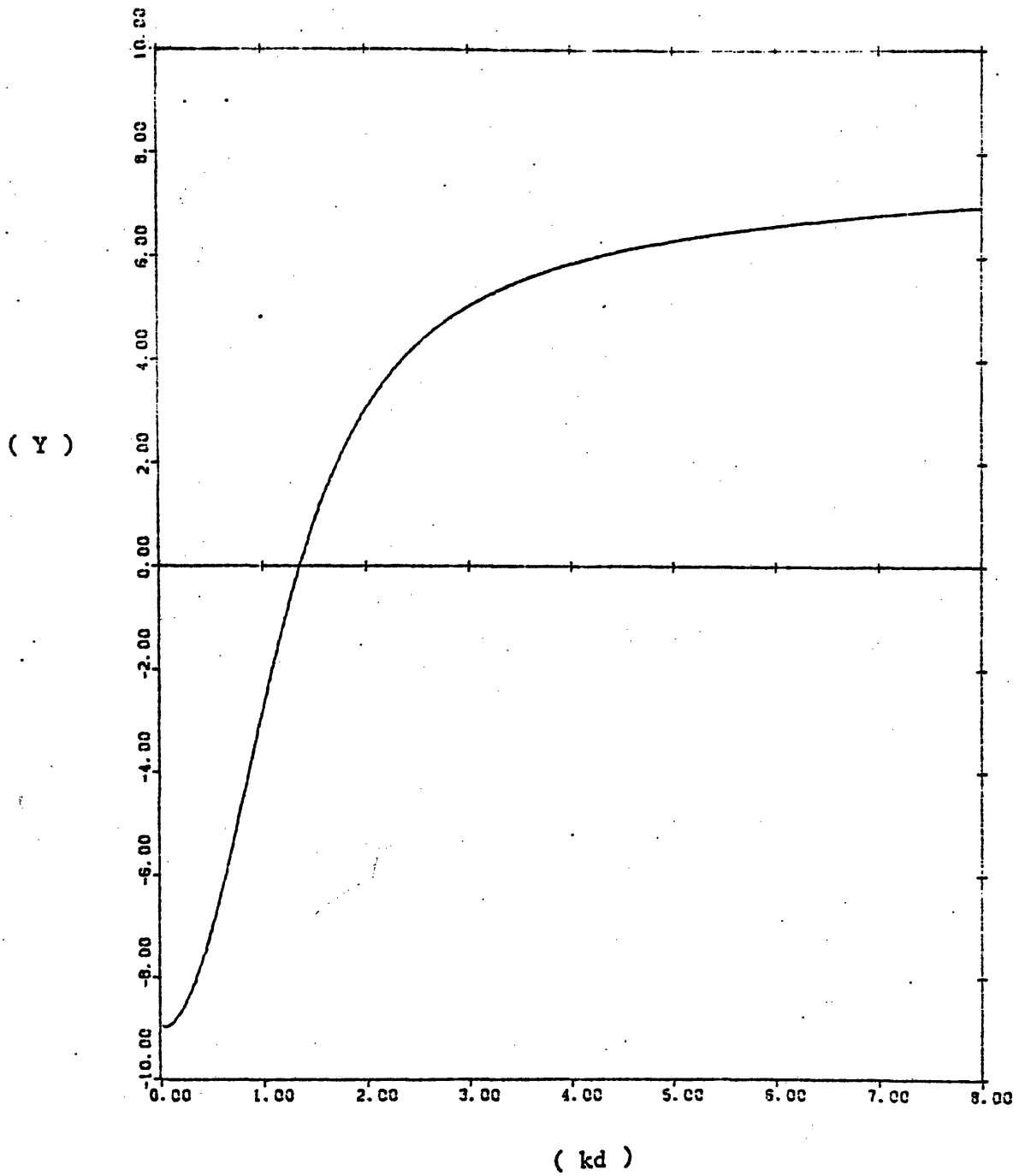


Figure 3.1 Non Linearity Coefficient

4-Wave Packets Over an Uneven Bottom Profile and a Stationary Current

To solve the evolution equation of the first order wave amplitude, we first need to solve Airy's equations for the current, which is in itself a complicated task. However the problem may be simplified in the special case of a stationary current on variable depth i.e. the current does not vary with time. By further assuming that the wave number has no time dependence the conservation of crests Eq. (3.2) implies that ω is constant. Therefore if the boundary conditions of A do not involve T, the problem is reduced to a 2-dimensional one in (X, τ) .

4.a. Properties of the Stationary Current

In the case where $\frac{\partial}{\partial T} = 0$, Airy's equations (2.18) and (2.19) can be integrated to give:

$$(\xi+h)U = \text{constant} = U_1 H_1 \quad (4.1)$$

$$\frac{1}{2} U^2 + g\xi = \text{constant} = \frac{U_1^2}{2} \quad (4.2)$$

where U_1 and H_1 are the velocity of the current and the depth as $X \rightarrow -\infty$.

Following the open channel theory we introduce the total head H and the specific head H_s defined by

$$H = \frac{1}{2} \frac{U^2}{g} + \xi \quad (4.3)$$

$$H_s = \frac{1}{2} \frac{U^2}{g} + d \quad (4.4)$$

H_s represents the height of the total head line above the sea floor.

Eq. (4.2) states that the total head is constant i.e. there is a

balance between the kinematic and potential energy. Substituting the expression of U obtained from (4.1) into H_s we get:

$$H_s = \frac{1}{2} \frac{(U_1 H_1)^2}{g d^2} + d \quad (4.5)$$

The specific head diagram in Fig. (4.1), shows that for a given specific head H_{s0} larger than a minimum value H_{sc} , two different flows are possible: The flow will be either at high velocity and small depth (i.e. $U > U_c$, $d < d_c$) or at low velocity and large depth (i.e. $U < U_c$, $d > d_c$). If the specific head is below the critical value H_{sc} , steady flow cannot occur. The magnitude of the total critical depth d_c , at which the minimum value of H_s occurs can be determined by setting to zero the derivative of H_s with respect to d .

$$\frac{dH_s}{d(d)} = -\frac{(U_1 H_1)^2}{g d_c^3} + 1 = 0 \quad \text{or} \quad d_c = \sqrt[3]{\frac{(U_1 H_1)^2}{g}} \quad (4.6)$$

The critical specific head can then be deduced from (4.6) to be

$$H_{sc} = \frac{3}{2} \sqrt[3]{\frac{(U_1 H_1)^2}{g}} \quad (4.7)$$

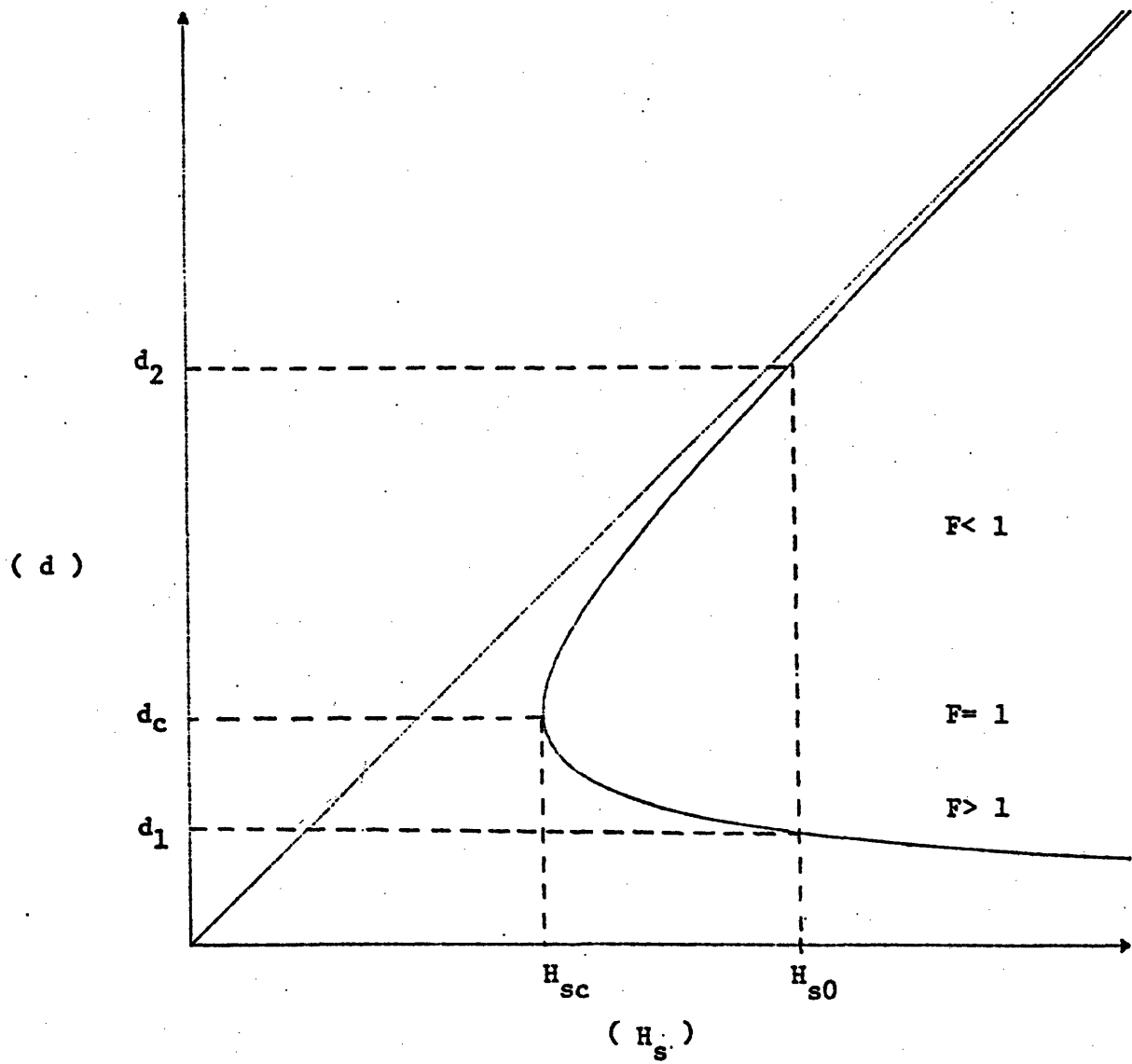


Figure 4.1 Specific Head Diagram

while the total head is found from (4.2) and (4.3):

$$H = H_s - h = \frac{U_1^2}{2g} \quad (4.8)$$

(4.7) can be used in (4.8) to obtain the critical depth h_c

$$h_c = \frac{3}{2} \sqrt{\frac{(U_1 H_1)^2}{g}} - \frac{U_1^2}{2g} \quad (4.9)$$

$\frac{h_c}{H_1}$ is plotted in fig. (4.2) as a function of $\frac{|U_1|}{\sqrt{gH_1}}$. We notice that

$h_c \leq H_1$. Therefore if $h > H_1$, $H_s > H_{sc}$ always and steady current is

possible. When $U_1^2 > 3\sqrt{3} gH_1$, h_c becomes negative i.e. for such a

current the flow is possible for any depth variation. When

$U_1^2 \leq 3\sqrt{3} gH_1$ the flow is possible only if h is larger than the critical

value h_c . At the critical depth, (4.1) and (4.6) determine the critical

velocity U_c :

$$U_c = \sqrt{gd_c} \quad (4.10)$$

The Froude number of the flow may be defined as $F = \frac{U}{\sqrt{gH_1}}$.

$F < 1$ corresponds to a subcritical flow, while $F > 1$ corresponds to

a supercritical flow. Depending on whether the flow is originally

subcritical or supercritical, Fig. (4.1) shows that two totally

different surface profiles can be produced: If originally the flow

is subcritical (i.e. $U_1 < \sqrt{gH_1}$) an increase in depth h implies an increase

of the total depth $\xi+h$. However if the original flow is supercritical

(i.e. $U_1 > \sqrt{gH_1}$) an increase in depth implies an increase of the specific

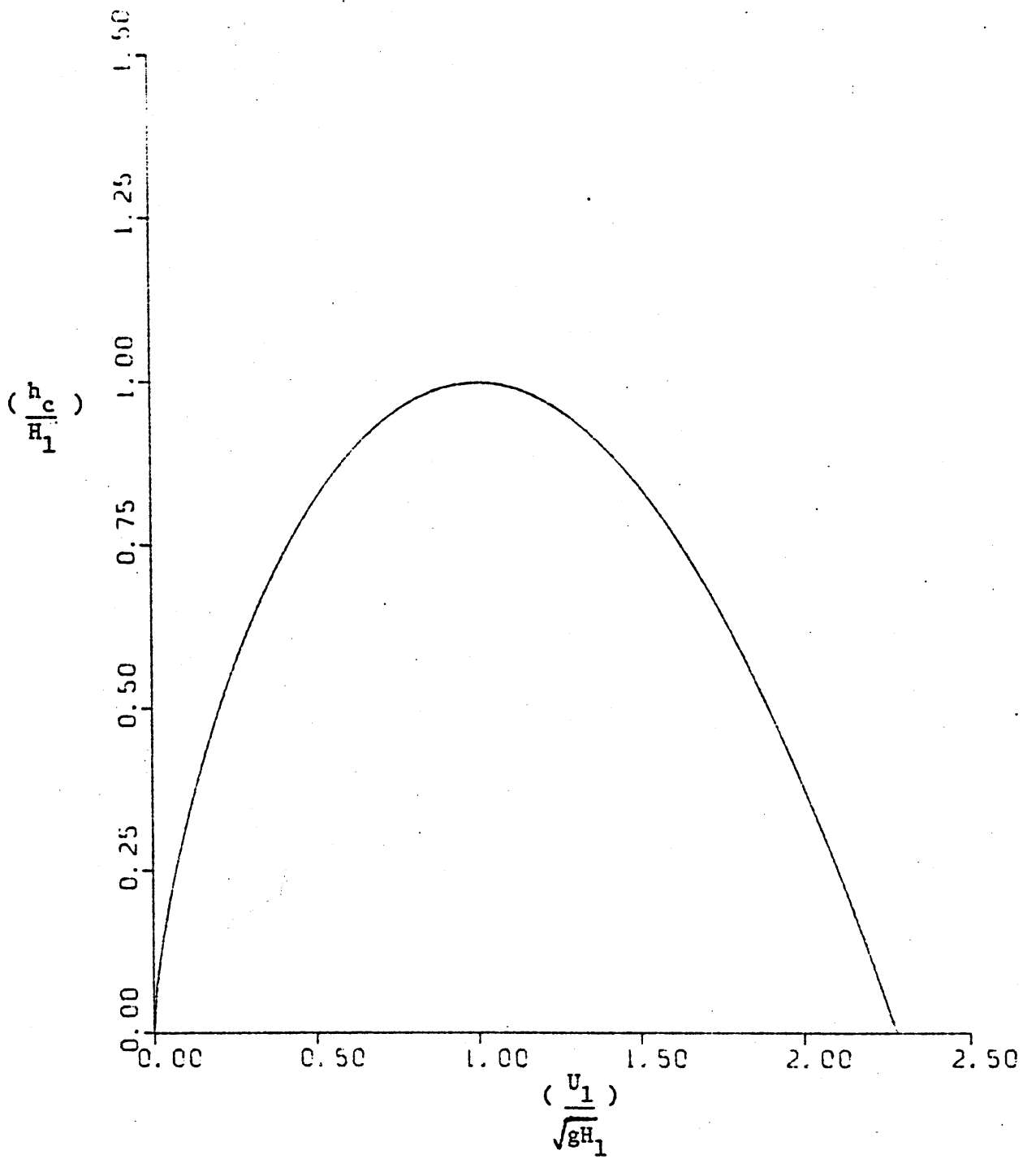


Figure 4.2 Critical Depth

head which will result in a decrease of the total depth d . If the total flow is critical i.e. $U_1 = \sqrt{gH_1}$ when the depth increases the flow will be subcritical or supercritical depending on the conditions downstream. The flow is then unstable i.e. a small perturbation will produce a large variation of the surface profile.

These qualitative results can be illustrated by solving the problem numerically in the different cases. By eliminating U from (4.1) and (4.2) we obtain the governing equation for the total depth d

$$\left(\frac{d}{H_1}\right)^3 - \left(\frac{h}{H_1} + \frac{U_1^2}{2gH_1}\right)\left(\frac{d}{H_1}\right)^2 + \frac{U_1^2}{2gH_1} = 0 \quad (4.11)$$

$\frac{d}{H_1} = \frac{\zeta+h}{H_1}$ is the root of this equation which satisfies $\left(\frac{d}{H_1}\right) \rightarrow 1$ when

$h \rightarrow H_1$. Fig. (4.3) represents the variation of the dimensionless

total depth $\frac{d}{H_1}$ as the depth varies from the critical value h_c to a given

value $h = 2H_1$ for different values of the current at $X = -\infty$. As

expected the plot shows that for a subcritical current $U_1' = \frac{U_1}{\sqrt{gH_1}} = 0.5$

the total depth increases with depth, for a supercritical current

$U_1' = \frac{U_1}{\sqrt{gH_1}} = 2$, the total depth decreases as the depth increases and for

a critical current $U_1 = \sqrt{gH_1}$, there are two possible solutions which behave very differently.

It should be noted that when the flow is supercritical, the assumptions made in the derivation of the governing equations of the current could break down in particular viscosity and turbulence could become important.

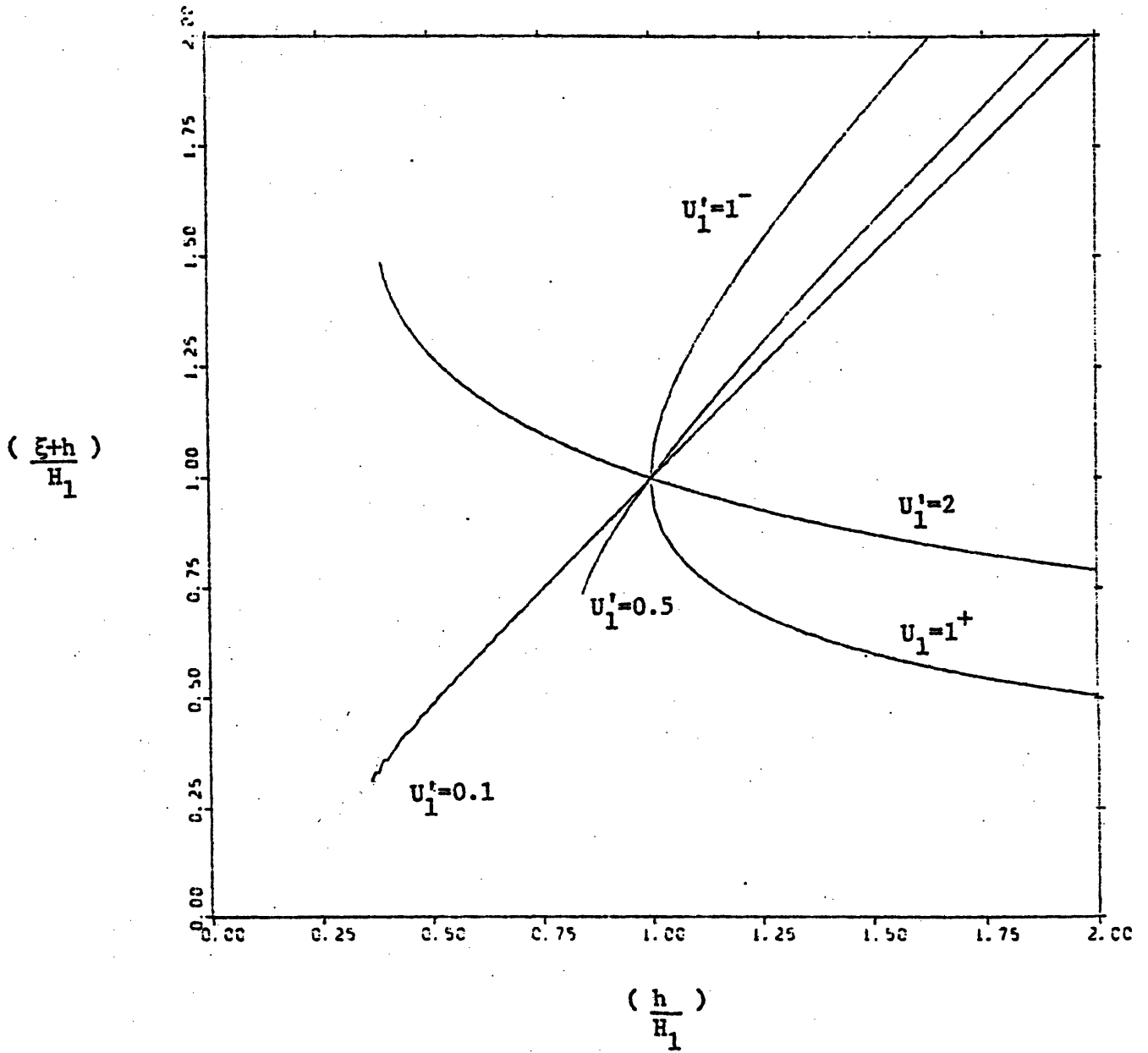


Figure 4.3 Set-up Due to the Current

4.b Wave kinematics

A second step in solving the problem is to solve the dispersion relation.

$$\sigma^2 \equiv (\omega - kU)^2 = gk \tanh kd \quad (4.12)$$

Following Peregrine (1976), we consider the intersection of the two curves:

$$\sigma(k) = \omega - kU \quad \text{and} \quad W(k) = \pm \sqrt{gk \tanh kd} \quad (4.13)$$

These curves are plotted in Fig. (4.4).

If the waves propagate in the same direction as the current i.e. $U > 0$, there are always two solution points A and B. A corresponds to waves whose phase velocity relative to the current is in the same direction as the current (i.e. $C_p = \frac{\sigma}{k} > 0$). Since the frequency of these waves in a fixed frame ω is larger than their frequency relative to the water σ , the effect of the current is to increase the wavelength. B corresponds to waves whose phase velocity and group velocity in a moving frame propagate

in the opposite direction of the current (i.e. $C_p = \frac{\sigma}{k} < 0$, $(C_g)_{rel} = \frac{\partial \sigma}{\partial k} < 0$) but a fixed observer sees the waves propagating downstream (i.e. $C_p + U > 0$).

If the waves propagate against the current, i.e. $U < 0$, the solution points, when they exist, are C and D. C represents waves whose crests and energy in a fixed frame propagate upstream (i.e. $\frac{\omega}{k} = C_p + U > 0$, $C_g = \frac{\partial \omega}{\partial k} = (C_g)_{rel} + U > 0$). Since the frequency ω is less than the relative frequency σ , the effect of the current is to shorten the wavelength. D represents waves whose crests in a fixed frame propagate upstream (i.e.

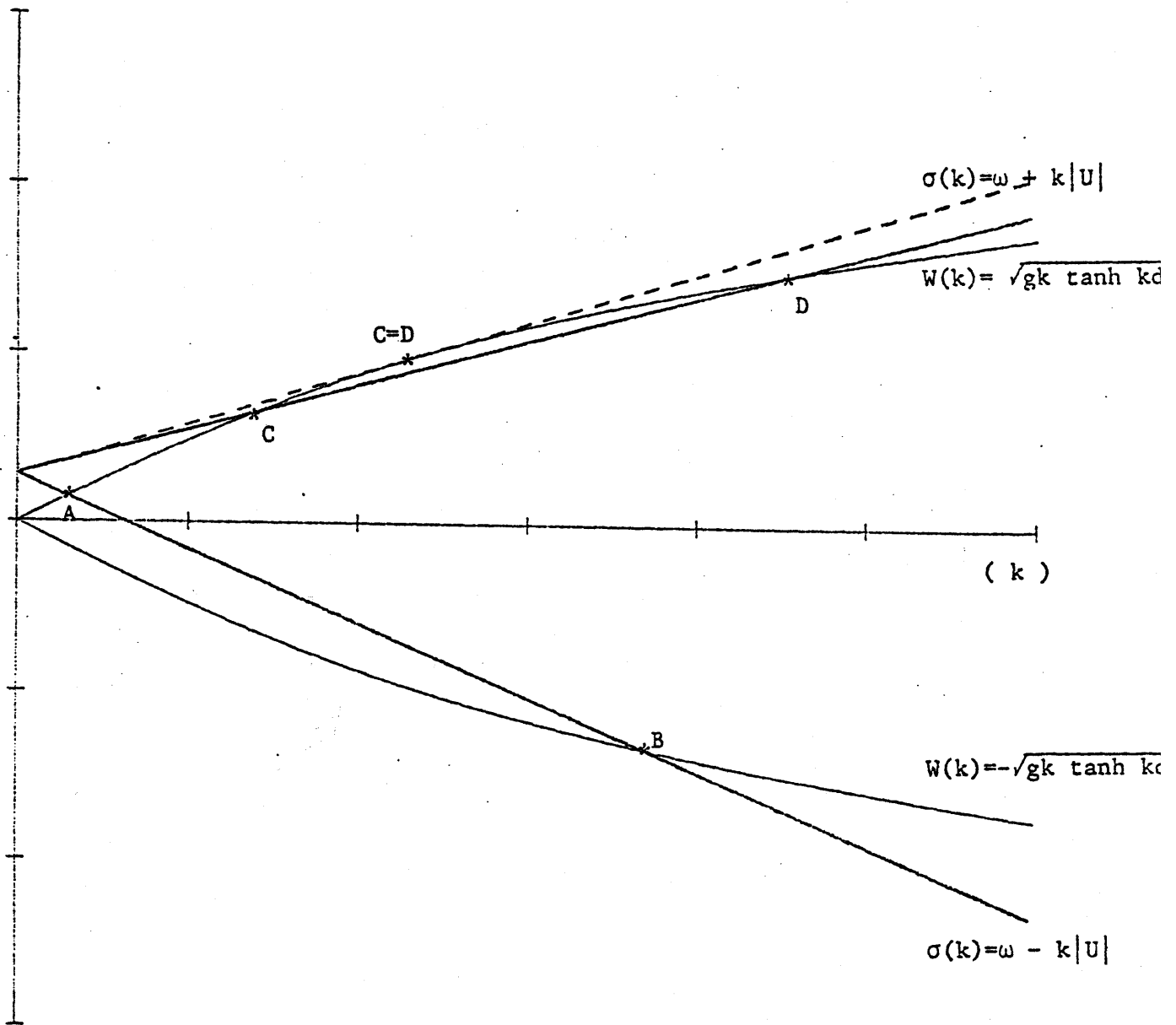


Figure 4.4 Dispersion Relation Diagram

$C_p + U > 0$) but their energy for a fixed observer propagates downstream (i.e. $C_g < 0$). When the opposite current becomes very large the solution C and D may not exist. The limiting case is when the two points C and D coalesce. This case occurs when

$$C_g = \frac{\partial \omega}{\partial k} = (C_g)_{\text{rel}} + U = 0 \quad (4.14)$$

The wave energy in a fixed frame is, then at rest. Such a current velocity is called *stopping velocity*. For this velocity the wave number and frequency are both finite but the wave energy density increases and the amplitude becomes very large. Therefore our small amplitude theory is not valid near a stopping velocity. A more refined theory has been given by Stiassnie and Dagan (1979). The stopping velocity is defined by (4.12) and (4.14) which can be combined and put in a dimensionless form. If we introduce

$$U'' = \frac{U}{\sqrt{gd}} \quad \omega'' = \omega \sqrt{\frac{d}{g}} \quad k'' = kd \quad (4.15)$$

we have:

$$U'' + \frac{1}{2} \sqrt{\frac{\tanh k''}{k''}} \left(1 + \frac{2k''}{\sinh 2k''}\right) = 0 \quad (4.16)$$

$$\omega'' = k'' U'' + \sqrt{k'' \tanh k''} \quad (4.17)$$

(4.16) and (4.17) define implicitly ω'' as a function of U'' or if we use the dimensionless period $T'' = \frac{2\pi}{\omega''}$, T'' as a function of U'' . This function is plotted in figure (4.5.a). It can be easily seen from (4.16) that when $U'' \rightarrow -1$, $k'' \rightarrow 0$ so $T'' \rightarrow \infty$. This means that for an opposite current $U'' < -1$, waves cannot propagate no matter how large

their period is. On the other hand when the current tends to zero, waves of any period can always propagate.

In the case of a stationary currents propagating over variable depth the velocity U is dependent on its value U_1 at $-\infty$ and on the depth variation (cf. Eq. 4.1). For given values of $\frac{U_1}{\sqrt{gH_1}} = U'_1$ and $\frac{h}{H_1} = h'$ waves of period $T_s \sqrt{\frac{g}{H_1}} = T'_s$ will be stopped. From U'_1 and h' , $\frac{d}{H_1}$ and $\frac{U}{U_1}$ can be found by using (4.11) and (4.1) therefore from $T''(U'')$ we can deduce $T'_s(U'_1, h')$. Fig. (4.5.b) shows in dimensionless form how the stopping period T'_s varies with h' for different currents $U'_1 = -0.1, -0.3, -0.6, -0.9$. Alternatively this plot also shows the depth at which stopping occurs for given T'_s and U'_1 .

In subsequent numerical computation we shall only consider the solution A and C of the dispersive relation which corresponds to the cases where the phase and group velocity are positive whether in a moving or in a fixed frame.

4.c. Evolution Equation

In the case of a steady current the evolution equation (3.53) can be further simplified. Let us introduce the following normalized variables:

$$(U', C'_g, C'_p) = (U, C_g, C_p)(gH_1)^{-1/2}$$

$$X' = \frac{X}{H_1} \left(\frac{a}{H_1}\right)^2 \quad \tau' = \tau \sqrt{\frac{g}{H_1}} \left(\frac{a}{H_1}\right)$$

(4.18)

$$A' = A/\rho g a \quad k' = kH_1$$

$$d' = \frac{d}{H_1} = \frac{(\xi+h)}{H_1} \quad \sigma' = \sqrt{\frac{g}{H_1}} \sigma \quad T' = \frac{2\pi}{\omega} \sqrt{\frac{H_1}{g}}$$

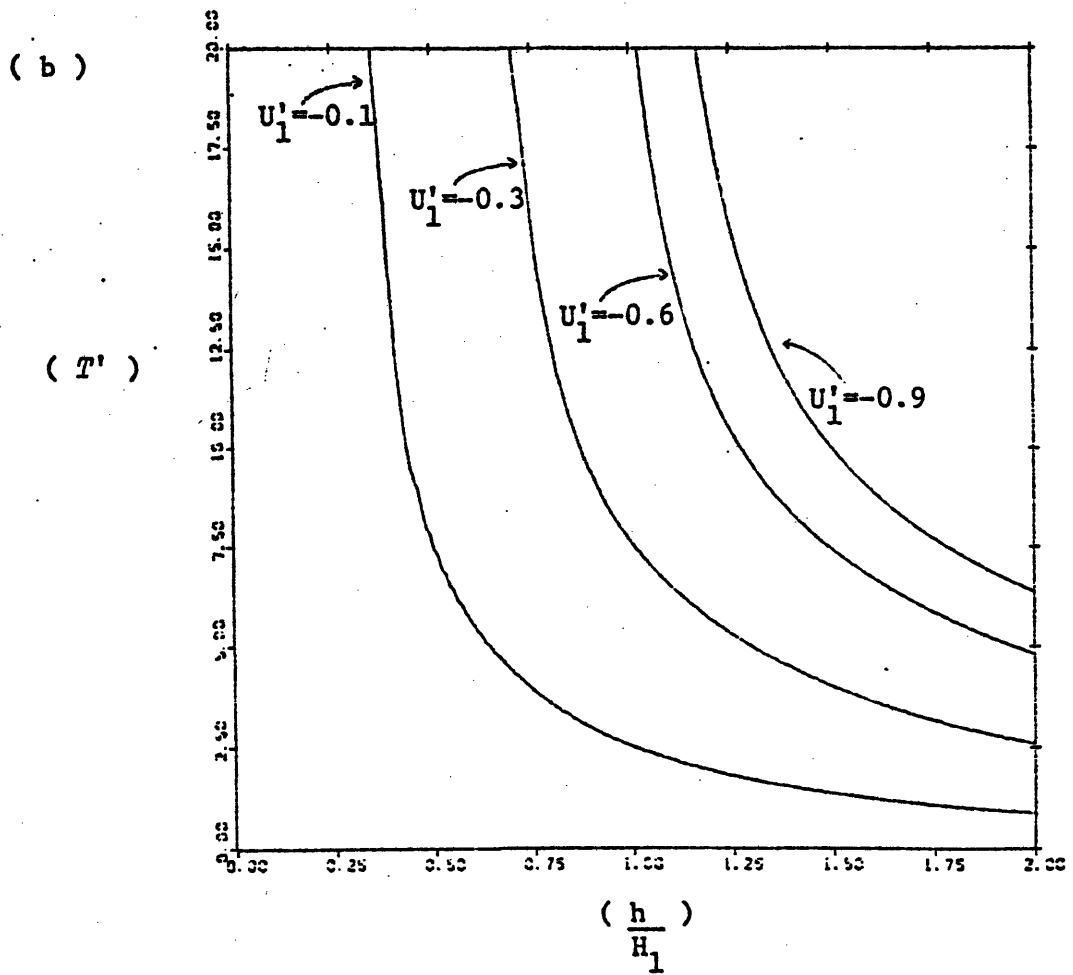
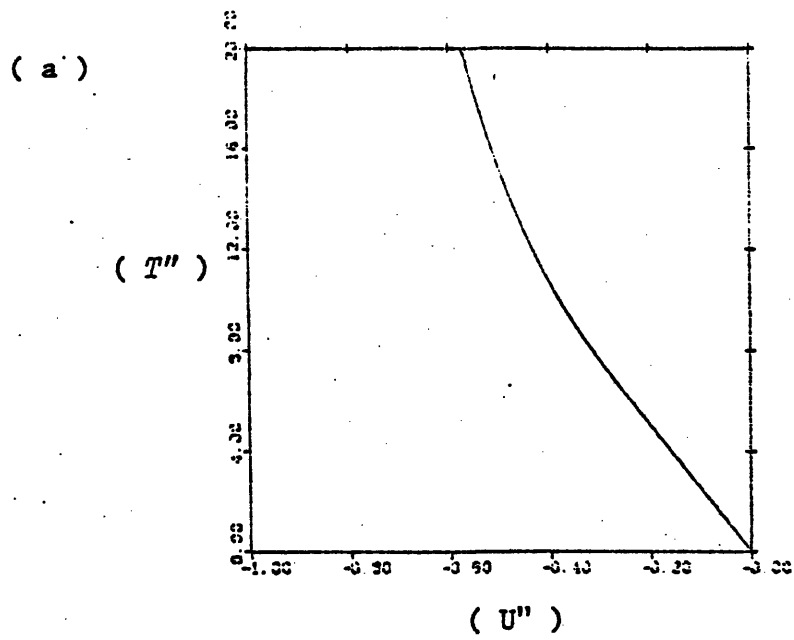


Figure 4.5 Stopping Periods

where a represents the wave amplitude and H_1 represents a reference depth.

The evolution equation then becomes after omitting the primes

$$\alpha_1 A + A_X + i\alpha_2 A_{\tau\tau} + i\alpha_3 |A|^2 A = 0 \quad (4.19)$$

$$\alpha_1(X) = \frac{\sigma}{2C_g} \frac{\partial(C_g/\sigma)}{\partial X} \quad (4.20)$$

$$\alpha_2(X) = \frac{1}{2\sigma C_g} \left(\frac{C_g - U}{C_g}\right)^2 \left[1 - \frac{d}{(C_g - U)^2} (1 - \beta^2)(1 - \beta kd)\right] \quad (4.21)$$

$$\alpha_3(X) = \frac{k^4}{4\sigma^3 \beta^2 C_g} \left\{9 - 10\beta^2 + 9\beta^4 - 2\beta^2 \frac{(C_g - U)}{d - (C_g - U)^2} \left(\frac{C_p}{C_g - U}\right)^2 + \frac{4C_p}{C_g - U} (1 - \beta^2) + \frac{d(1 - \beta^2)^2}{(C_g - U)^2}\right\} \quad (4.22)$$

For later purposes we introduce the following transformation (Djordjevic and Redekopp (1978))

$$\bar{X} = \int_0^X \alpha_2(u) du \quad (4.23)$$

$$A = B \exp\left(-\int_0^X \alpha_1(u) du\right) = sB \quad (4.24)$$

Equation (4.19) can be put in its canonical form:

$$-iB \frac{\partial}{\partial \bar{X}} + B_{\tau\tau} + K|B|^2 B = 0 \quad (4.25)$$

where $K = \frac{\alpha_3}{\alpha_2} s^2$

and $s = \exp\left(-\int_0^X \alpha_1(u) du\right) = \left(\frac{C_g/\sigma}{(C_g/\sigma)}\right)^{1/2} \quad (4.26)$

The subscript 1 denotes the value at $X = 0$. The quantity s depends only on X or \bar{X} and is known to be the shoaling factor of infinitesimal waves.

4.d Generalization of Stokes Waves

In the case of constant depth, the coefficients α_2, α_3 are constants and $\alpha_1 = 0$. The evolution equation (4.19) is just a nonlinear-cubic Schrodinger equation with constant coefficients. Such an equation was first obtained by Zakharov and Shabat (1968) in the case of deep water and then generalized to the case of intermediate depth by Hasimoto and Ono (1972). Its general solution has been obtained by Zakharov and Shabat (1972 - 1973) for both cases $\alpha_2\alpha_3 > 0$ and $\alpha_2\alpha_3 < 0$, by using the Inverse Scattering method. General or particular solutions could also be found in Tappert and Zakusky (1971), Hasimoto and Ono (1972), Satsuma and Yajima (1975).

In the case of variable coefficients, no general solution has been reported and one has to solve the evolution equation numerically. However if the initial and boundary conditions are such that a Stokes wave train is unmodulated on the length scale and time scale $O(\epsilon^{-1})$, then A depends only on X but not on τ and so does B (Eq. 4.24). The governing equation for B becomes

$$\frac{B}{\bar{X}} + iK|B|^2B = 0 \quad (4.27)$$

Let us take (4.27)* $B - (4.11)B^*$ we deduce that

$$|B| = \text{constant} = B(0) \quad (4.28)$$

Substituting into (4.24) we have:

$$B(\bar{X}) = B(0) \exp(-i B^2(0) \int_0^{\bar{X}} K \, dv + \phi) \quad (4.29)$$

where ϕ is an arbitrary constant. In terms of the amplitude A, (4.29) can be written as

$$A(X) = B(0)s \exp(-i B^2(0) \int_0^X K(v) \, dv + \phi) \quad (4.30)$$

Since $A(0) = B(0)$ we have:

$$\left| \frac{A(X)}{A(0)} \right| = s = ((C_g/\sigma)_1 / (C_g/\sigma))^{1/2} \quad (4.31)$$

which is nothing but the shoaling law of infinitesimal waves. Thus at the leading order the amplitude of Stokes waves on a variable medium varies with X according to the shoaling law.

4.e Side Band Instability

In the case of constant depth, (4.30) just gives the classical Stokes wave with spatial modulation. It is known that a Stokes wave train is stable to side band disturbance if $K < 0$ or $kh < 1.36$ and is unstable if $K > 0$ or $kh > 1.36$. This result can be extended to the solution (4.30), (4.31). We let B have a dependence on τ :

$$B(X, \tau) = b(X, \tau) \exp if (X, \tau) \quad (4.32)$$

where b and f are real functions of X and τ . Substituting into the evolution equation (4.27) and taking the real and imaginary part we obtain:

$$\begin{aligned} \frac{\partial b^2}{\partial X} - \frac{\partial}{\partial \tau} (b^2 W) &= 0 \\ \frac{\partial W}{\partial X} + \frac{\partial}{\partial \tau} \left(\frac{b_{\tau\tau}}{b} - W^2 + Kb^2 \right) &= 0 \end{aligned} \quad (4.33)$$

where $W = f_\tau$. With reference to (4.30) Stokes wave solution is obtained for b constant and f independent of τ , i.e. $b = B(0) = b_0$, $W = 0$. To consider the linear stability of the Stokes waves we superpose on them a small disturbance $b' \ll b_0$ and $W' \ll 1$. Since b' and W' are very small the equation for $b = b_0$ and $W = W'$ is obtained from (4.33) after linearization.

$$\begin{aligned}
 b'_X - b_0 W'_\tau &= 0 \\
 W'_X + \frac{b'_\tau \tau}{b_0} + b_0 b'_\tau &= 0
 \end{aligned}
 \tag{4.34}$$

We assume a wavelike disturbance

$$\begin{pmatrix} b' \\ W' \end{pmatrix} = \begin{pmatrix} \hat{b} \\ \hat{W} \end{pmatrix} \exp i(\rho(x) - \Omega\tau)
 \tag{4.35}$$

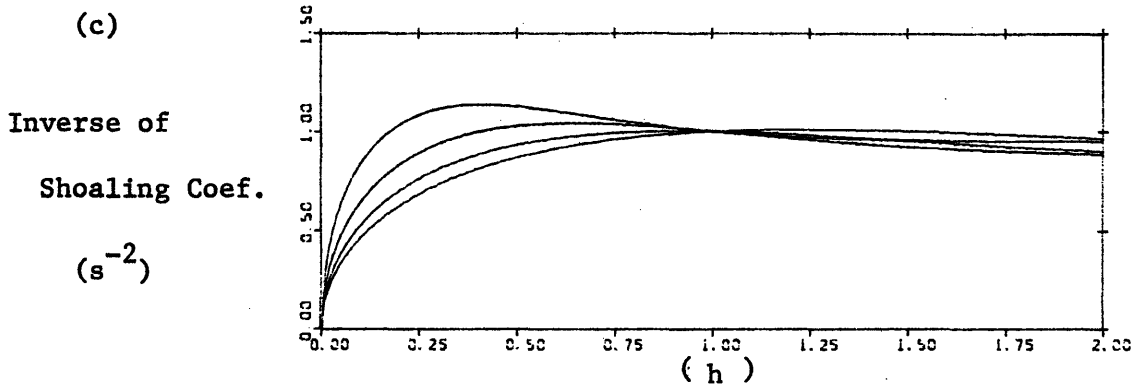
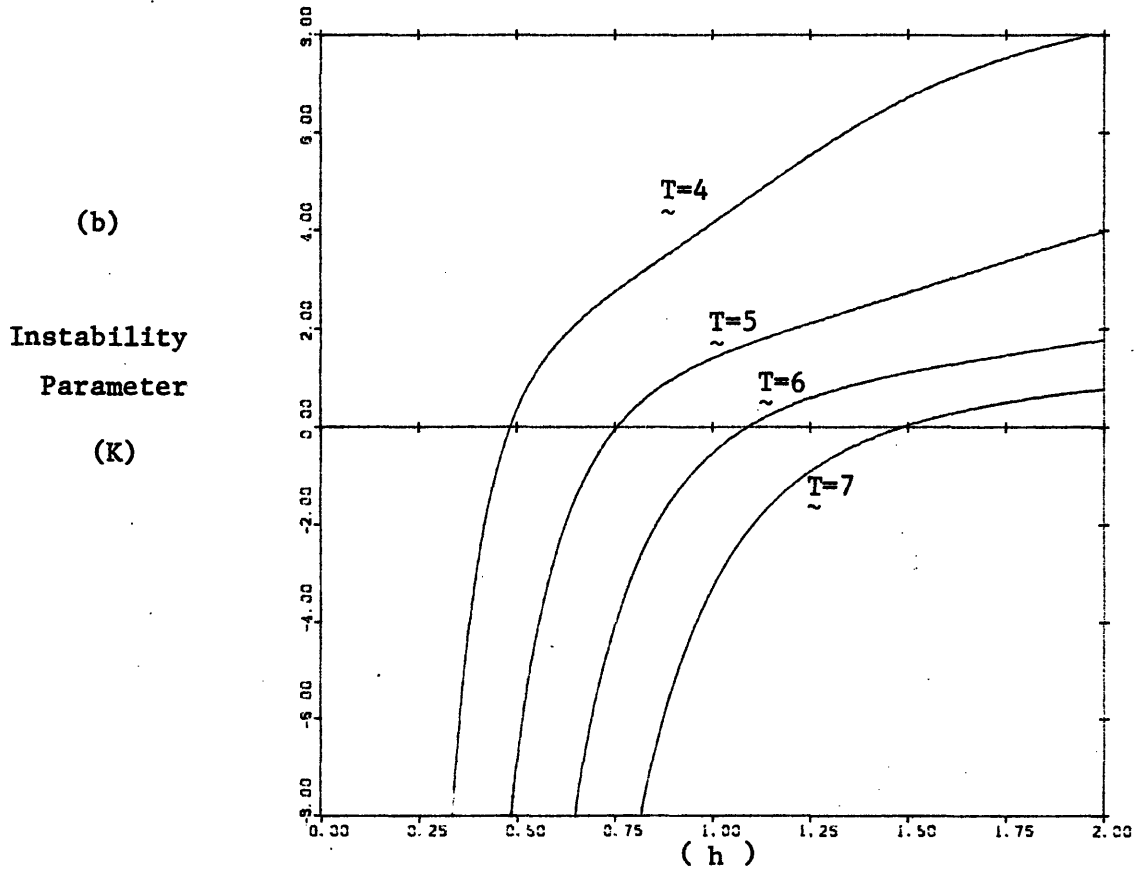
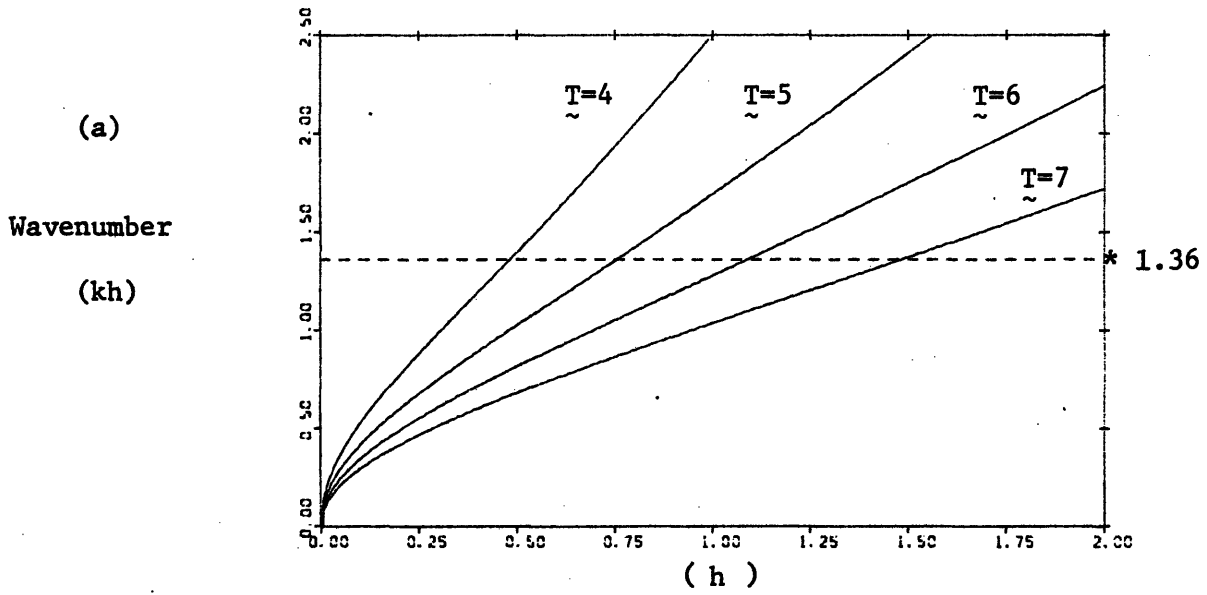
Plugging these expressions into (4.34) we find the eigenvalue condition

$$\frac{d\rho}{dx} = \Omega b_0 \sqrt{\frac{\Omega^2}{2b_0^2} - K}
 \tag{4.36}$$

From the definition of K (4.26), it can be noticed that K has the same sign as $\frac{\alpha_3}{\alpha_2}(X)$. But as shown in section 3, α_2 is always positive and the sign of α_3 is just dependent on the value of $kd = k(\xi+h)$ with respect to 1.363. When $kd < 1.363$, K is negative. Therefore (4.36) shows that $\frac{d\rho}{dx}$ is real and the disturbance will not be amplified. When $kd > 1.363$ K is positive. For small Ω , $\frac{d\rho}{dx}$ is imaginary so 'ip' will be real and monotonic and the disturbance will be unstable i.e. it will decrease or grow exponentially with X while the wave propagates. The quantity kd varies with the current velocity at $X = -\infty$, the wave period and the depth variation.

When the waves propagate over variable depth, as long as $k(\xi+h)$ is larger than 1.363 the disturbance will grow but if $k(\xi+h)$ becomes smaller than 1.363 the disturbance will stop growing. So we can have a situation where a periodic wavetrain is unstable at a given depth but becomes stable while it propagates into a region of different depth. Similarly a wavetrain which is stable in one region could become unstable in a region of different depth. To illustrate the effect of variable depth and current on the solution found previously, we have plotted in figures 4.6, 4.7, 4.8 and 4.9 for different values of the current velocity U_1 , the variation with depth of the dimensionless wave number kh , of the instability parameter $K = \frac{\alpha_3}{\alpha_2} s^2$ and of the inverse of the shoaling coefficient $s^{-2} = \frac{(C_g/\sigma)}{(C_g/\sigma)_1}$. All the quantities are normalized according to (4.18). Figure (4.6) corresponds to the case without current (i.e. $U_1 = 0$). It shows the variation of kh , K , and s^{-2} as the depth increases from zero to a given value $h = 2$, for different wave periods $T = 4, 5, 6, 7$. From the dispersion relationship, we have $kh = 0(\omega\sqrt{h})$ in very shallow water (i.e. $h \rightarrow 0$) and $kh = 0(\omega^2 h)$ in deep water (i.e. $h \rightarrow \infty$). Therefore as shown in figure (4.6.a) kh increases with depth and passes through the value 1.363. Figure (4.6.b) shows that K will then increase from negative to positive values and cross zero at the point where $kh \approx 1.363$. This is the well known result of Benjamin-Feir (1967): Stokes wave train are stable in a region where the depth is such that $kh < 1.363$. The effect of increasing the wave period is to move the instability zone toward deeper water. Figure (4.6.c) shows that except for very shallow water, the shoaling coefficient does not

Figure 4.6 No Current $U_1=0$



vary rapidly. So outside the very shallow region where our solution breaks down, Stokes waves amplitude will vary very slowly with depth.

In the case where waves propagate in the same direction as a sub-critical current, the variation with depth of kd , K is similar to that of figure (4.6). Figure (4.7) illustrates this case for a current $U_1 = 0.5$ and wave periods $T = 3, 4, 5, 6$. The depth varies from the critical depth $h_c = 0.82$ (see fig. 4.2) to a given depth $h = 2$. By comparison with figure (4.6), the effect of the current is to increase the wave length. Therefore, for a given wave period $k(\xi+h)$ crosses 1.363 in deeper water i.e. the instability region moves toward deeper water when the current velocity increases. Figure (4.7.b) shows that K crosses zero at the point where $k(\xi+h) = 1.363$ as predicted in section(4.7). The variations of K are more rapid than in the case without current. Figure (4.7.c) shows that the shoaling coefficient has larger amplitude variation with depth than in the case without current. Stokes waves amplitude will increase substantially with increasing depth.

When the current velocity U_1 , becomes supercritical, the total depth $(\xi+h)$ decreases drastically with increasing depth (see Fig. 4.3). Such a behavior implies that $k(\xi+h)$ will decrease as the depth increases. In this case, Stokes waves will be unstable in shallow water and stable in deep water, since K decreases from positive to negative values. Figure (4.8) illustrates these features for a current $U_1 = 2$ and wave periods $T = 1, 1.5, 2, 2.5$. The depth varies from a critical depth h_c to $h = 2$. Comparing figure (4.8) with figure (4.7) we notice that the variation of $k(\xi+h)$, K and s^{-2} are opposite in each figure. For $U_1 = 2$,

Figure 4.7 Subcritical Current $U_1=0.5$

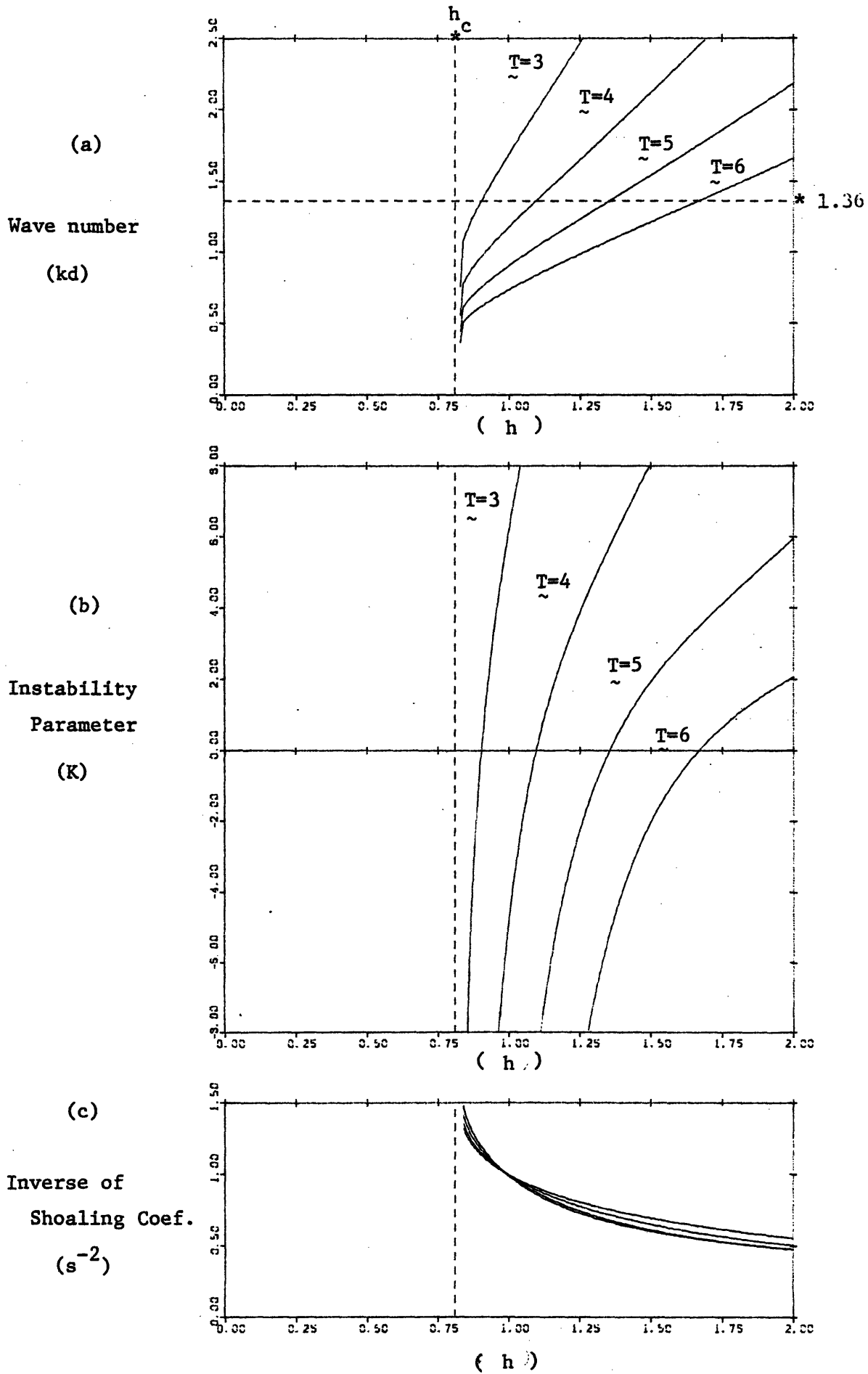
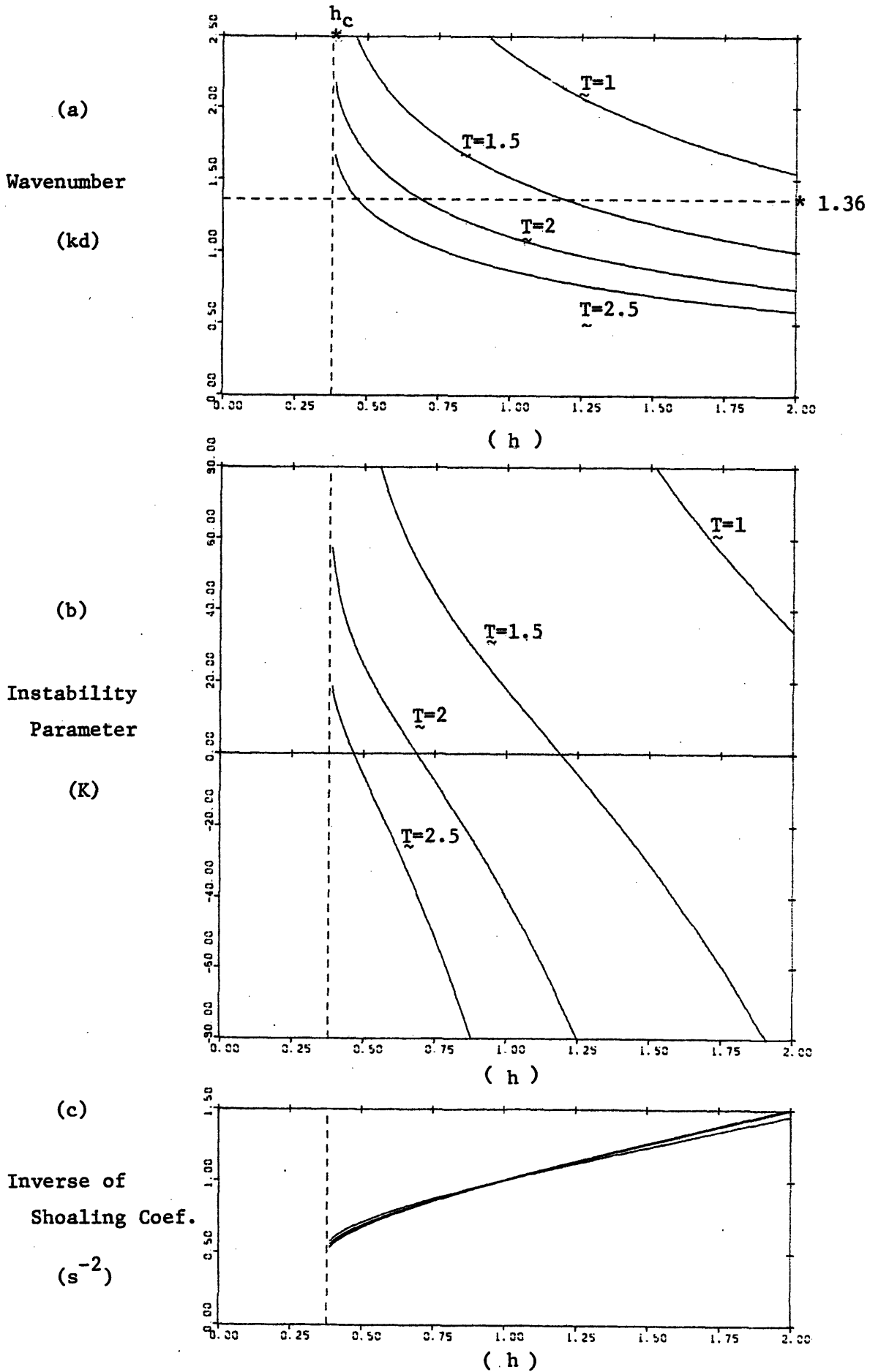


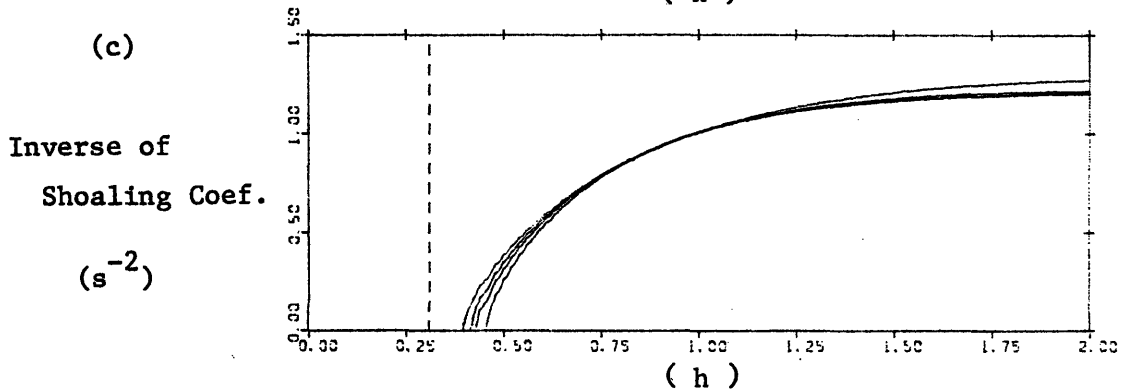
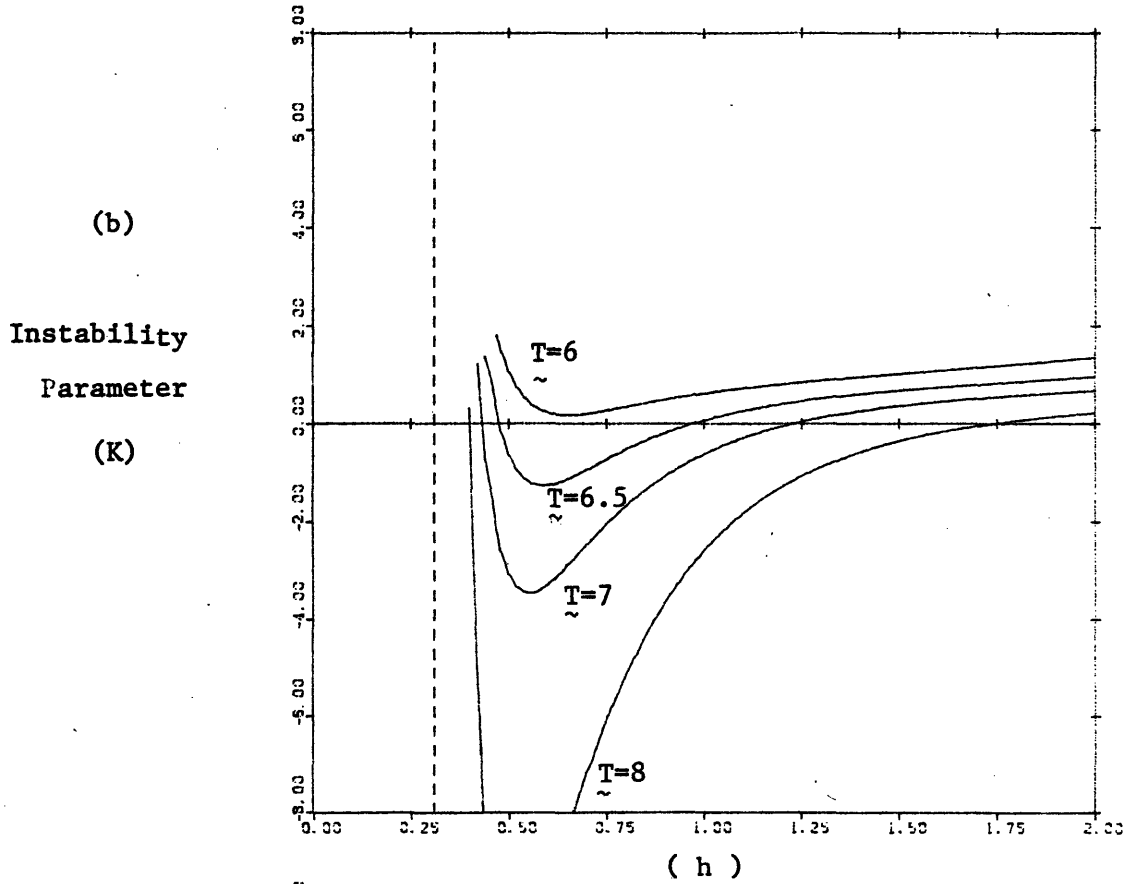
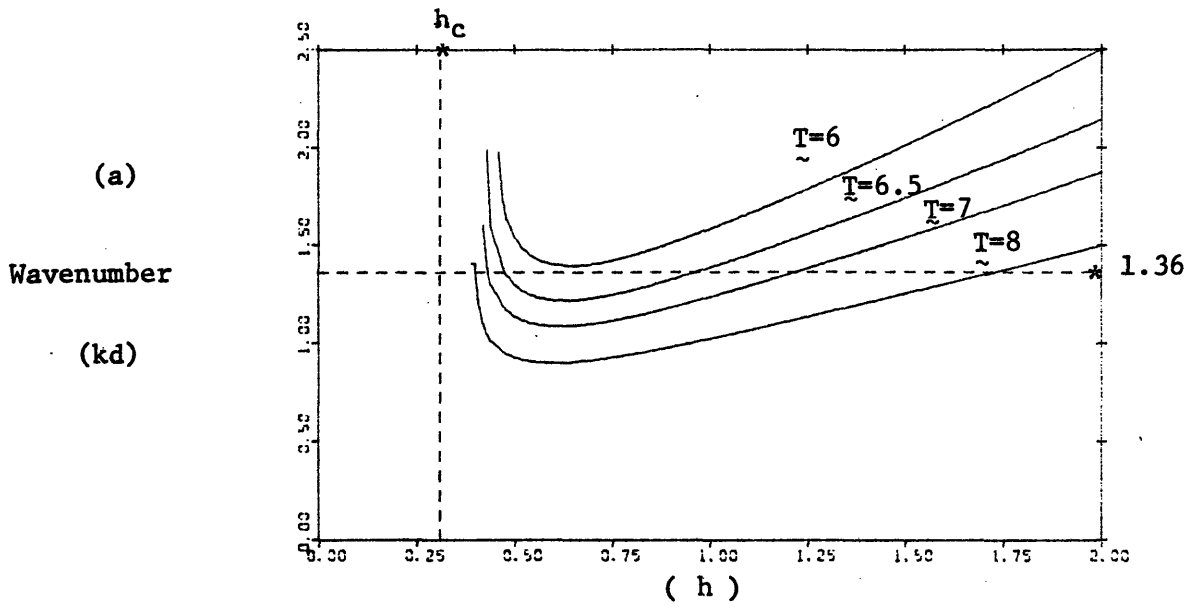
Figure 4.8 Supercritical Current $U_1 = 2.0$



K varies more rapidly (For this range of period $T = 1, 2.5$, α_2 is very small i.e. $\alpha_2 = O(10^{-2})$ and hence $K = \frac{\alpha_3}{\alpha_2} s^2$ varies very rapidly).

In the case where waves propagate against a current, for a given velocity and wave period there is a depth h_0 for which waves are stopped i.e. $C_g \rightarrow 0$ (cf. figure 4.5.b). This depth which could be called the stopping depth corresponds to a caustic. In the neighborhood of this point our nonlinear theory breaks down. Figure (4.9) illustrates this case for a current $U_1 = -0.1$. The wave periods considered in the plot are $T = 6, 6.5, 7, 8$ and the depth varies from the stopping point h_0 to $h = 2$. For large depth the variation of $k(\xi+h)$, K, s^{-2} is similar to the variation of these quantities in the case without current, but in the neighborhood of the stopping point $k(\xi+h)$ and K admit a minimum value. This minimum value proceeds from the fact that near the stopping depth the wavelength becomes shorter (i.e. k is larger). When we move away from h_0 towards deep water, k decreases rapidly and so does $k(\xi+h)$; but far enough from h_0 , the increase in depth becomes larger than the decrease in the wave number, so the trend is reversed and $k(\xi+h)$ increases. For short wave period K can be positive everywhere implying that Stokes waves with a small period will be unstable at any depth, but as the wave period increases K decreases and becomes negative in shallow water. For a given wave period and depth, when the opposite current increases in magnitude the wavelength decreases and so does $k(\xi+h)$. The point where $k(\xi+h)$ crosses the value 1.363 moves toward deeper water so Stokes wave train becomes stable in shallow and intermediate depth.

Figure 4.9 Opposing Current $U_1 = -0.1$



5. Numerical Approach

While the non-linear cubic Schrodinger equation with constant coefficients, has been solved analytically using inverse scattering transform method (Zakharov and Shabat), very few results have been obtained in the case of variable coefficients. Djordjevic and Redekopp (1978) studied analytically the problem of the evolution of a soliton moving over a slowly varying depth, without current. To solve the problem, they made very strong assumptions about the shape of the soliton on the shelf. In order to check these assumptions, it is necessary to solve numerically Eq. (4.19). Furthermore in the case of waves propagating over stationary current and varying depth from a region where $K = \alpha_3/\alpha_2 s^2 < 0$ into a region where $K > 0$ or inversely, no analytical results are available. One must then resort to numerical solutions. In the following numerical study we restrict ourselves to the case of a compact wave packet propagating over variable depth in the same direction as a stationary current or in the opposite direction.

5.a Numerical Method

The problem we have to solve is:

$$A_X + \alpha_1(X)A + i \alpha_2(X) A_{\tau\tau} + i \alpha_3(X) |A|^2 A = 0 \quad (5.1.a)$$

$$\text{on } D = \{0 < X < \infty, +\infty < \tau < -\infty\} \quad (5.1.b)$$

$$A(X=0, \tau) = f(\tau) \quad (5.1.c)$$

$$A(X, \tau) \rightarrow 0 \quad \text{as } |\tau| \rightarrow \infty \quad (5.1.d)$$

where f is a prescribed initial wave envelope. The assumption that f is compact (i.e. $f \rightarrow 0$ as $|\tau| \rightarrow +\infty$) implies that at any finite X the wave envelope is still compact. For our numerical computation, we restrict the region D to a finite region.

$$D_F = \{0 < X < X_2 ; -\tau_0 < \tau < \tau_0\} \quad (5.2)$$

where τ_0 is chosen sufficiently large to avoid any boundary effect when the condition (5.1.d) is applied at $\tau = \pm \tau_0$.

To solve numerically Eq. (5.1.a) an implicit scheme of Crank-Nicholson type for integration in X , and centered second order for differentiation in τ , is used. This scheme is known to be unconditionally stable for the linear case with constant coefficients. It has been used by Yue (1980) for the nonlinear case with constant coefficients and extended by Turpin (1981) for the case with variable coefficients and is found to be stable for reasonable choice of δX and $\delta \tau$. The error due to discretisation is $O((\delta X)^2, (\delta \tau)^2)$. Eq. (5.1.a) then becomes

$$\begin{aligned} \frac{A_j^{n+1} - A_j^n}{\delta X} + \frac{\alpha_1(n+1) + \alpha_1(n)}{2} A_j^n + i \frac{\alpha_2(n+1) + \alpha_2(n)}{2} \frac{A_{j+1}^{n+1} - 2A_j^{n+1} + A_{j-1}^{n+1}}{2(\delta \tau)^2} \\ + \frac{A_{j+1}^n - 2A_j^n + A_{j-1}^n}{2(\delta \tau)^2} + i \frac{\alpha_3(n+1) + \alpha_3(n)}{2} \frac{|A_j^{n+1}|^2 A_j^{n+1} + |A_j^n|^2 A_j^n}{2} = 0 \end{aligned} \quad (5.3)$$

where

$$\tilde{A}_j^{n+1} = A_j^n - \delta X \{ \alpha_1(n) A_j^n + i \alpha_2(n) \frac{(A_{j+1}^n - 2A_j^n + A_{j-1}^n)}{(\delta \tau)^2} + i \alpha_3(n) |A_j^n|^2 A_j^n \} \quad (5.4)$$

$$A_j^n = A((n-1)\delta X, (j - J + 1)\delta\tau) \quad n = 1, 2, \dots, N; \quad j = 1, \dots, 2J+1 \quad (5.5)$$

N and J are defined by

$$(N-1) \delta X = X_2 \quad \text{and} \quad J\delta\tau = \tau_0 \quad (5.6)$$

If the initial data $f(\tau)$ is even in τ , then, since τ appears in (5.1.a) through $A_{\tau\tau}$, the solution $A(X, \tau)$ will be even in τ . By imposing at $\tau=0$ the condition $\frac{\partial A}{\partial X} = 0$ the problem can be solved for $\tau \geq 0$ only. In this case A_n^j will be defined by the following:

$$A_j^n = A((n-1)\delta X, (j-2)\delta\tau) \quad n = 1, \dots, N; \quad j = 1, \dots, 2J+1 \quad (5.7)$$

$$\text{where } (N-1)\delta X = X_2 \quad \text{and} \quad (2J-1)\delta\tau = \tau_0 \quad (5.8)$$

Applying (5.3) for a fixed n and $j = 2, \dots, 2J$ we obtain a linear system in A_j^{n+1} :

$$\begin{aligned} \gamma_1^n A_3^{n+1} + \beta_1^n A_2^{n+1} + \alpha_1^n A_1^{n+1} &= W_1^n \\ \gamma_j^n A_{j+2}^{n+1} + \beta_j^n A_{j+1}^{n+1} + \alpha_j^n A_j^{n+1} &= W_j^n \\ \gamma_{2J-1}^n A_{2J+1}^{n+1} + \beta_{2J-1}^n A_{2J}^{n+1} + \alpha_{2J-1}^n A_{2J-1}^{n+1} &= W_{2J-1}^n \end{aligned} \quad (5.9)$$

where

$$\begin{aligned} \gamma_j^n &= \alpha_j^n = i \frac{\delta X}{2(\delta\tau)^2} \frac{(\alpha_2(n+1) + \alpha_2(n))}{2} \\ \beta_j^n &= 1 + \frac{\delta X}{2} \left[\frac{\alpha_1(n+1) + \alpha_1(n)}{2} - i \frac{\alpha_2(n+1) + \alpha_2(n)}{(\delta\tau)^2} + i \frac{\alpha_3(n+1) + \alpha_3(n)}{2} |A_j^{n+1}|^2 \right] \\ W_j^n &= A_j^n \left[1 - \frac{\delta X}{2} \left(\frac{\alpha_1(n+1) + \alpha_1(n)}{2} - i \frac{\alpha_2(n+1) + \alpha_2(n)}{(\delta\tau)^2} + i \frac{\alpha_3(n+1) + \alpha_3(n)}{2} |A_j^n|^2 \right) \right. \\ &\quad \left. - i \frac{\delta X}{2(\delta\tau)^2} \frac{\alpha_2(n+1) + \alpha_2(n)}{2} (A_{j+1}^n + A_{j-1}^n) \right] \end{aligned} \quad (5.10)$$

Following D. Potter, the solution of the linear system (5.9) can be found by introducing:

$$A_{j+1}^{n+1} = X_j^{n+1} A_j^{n+1} + y_j^{n+1} \quad j = 1, \dots, 2J \quad (5.11)$$

By plugging (5.11) in the set of equations (5.9) we find the general recurrence relations:

$$X_j^{n+1} = \frac{-\alpha_1^n}{\gamma_j^n X_{j+1}^{n+1} + \beta_j^n} \quad y_j^{n+1} = \frac{W_j^n - y_{j+1}^{n+1}}{\gamma_j^n X_{j+1}^{n+1} + \beta_j^n} \quad j = 2J-2, \dots, 1 \quad (5.12)$$

Since $A \rightarrow 0$ as $\tau \rightarrow +\infty$ we have $A_{2J+1}^{n+1} = 0$ which implies from (5.9.c)

$$X_{2J-1}^{n+1} = \frac{-\alpha_{2J-1}^n}{\beta_{2J-1}^n} \quad y_{2J-1}^{n+1} = \frac{W_{2J-1}^n}{\beta_{2J-1}^n} \quad (5.13)$$

If the initial perturbation $A(0, \tau)$ is not even in τ , the condition $A \rightarrow 0$ as $\tau \rightarrow -\infty$ gives $A_1^n = 0$ which implies from (5.9.a)

$$A_2^{n+1} = \frac{W_1^n - \gamma_1^n y_2^{n+1}}{\gamma_1^n x_2^{n+1} + \beta_i^n} \quad (5.14)$$

If the initial perturbation $A(0, \tau)$ is even in τ , we solve the problem for $\tau \geq 0$ only by imposing the condition $\frac{\partial A}{\partial \tau}(X, \tau) = 0$. Using the notations (5.7) and (5.8), this condition becomes:

$$\frac{A_3^{n+1} - A_1^{n+1}}{2(\delta\tau)} = 0 \quad \text{or} \quad A_3^{n+1} = A_1^{n+1} \quad (5.15)$$

which gives after using (5.11):

$$A_1^{n+1} = \frac{x_2^{n+1} y_1^{n+1} + y_2^{n+1}}{1 - x_2^{n+1} x_1^{n+1}} \quad (5.16)$$

The numerical procedure can be summarized as follows:

A_j^1 $j = 1 \dots 2J+1$ is the initial data $A(0, \tau) = f(\tau)$ which is given. The coefficients (5.10) can then be calculated for $j = 1, \dots, 2J-1$. Using (5.12) and (5.13) x_j^2 and y_j^2 $j = 1, \dots, 2J=1$ are found by recurrence. If the initial data is not even in τ , A_2^2 is given by (5.14) and A_j^2 $j = 3 \dots 2J$ can be determined using (5.11). If the initial data is even in τ , A_1^2 is given by (5.16) and A_j^2 $j = 2 \dots 2J$ can be determined using (5.11). Once A_j^2 is known, $A_j^3 \dots A_j^N$ $j = 1 \dots 2J+1$ can be solved using the same procedure.

5.b Check of the Numerical Results

i. Case of Constant Depth

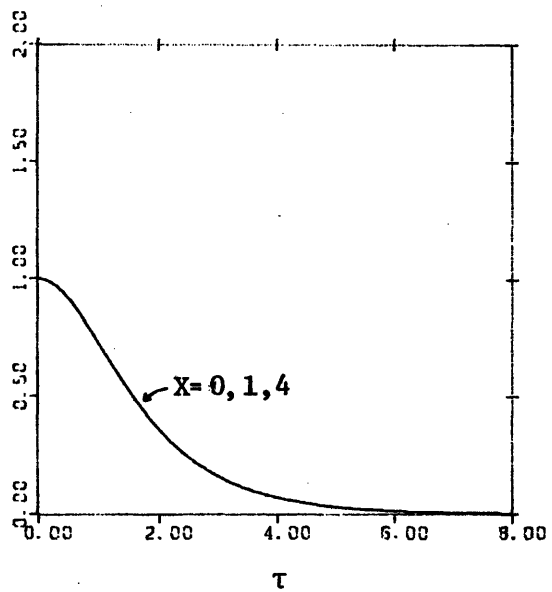
The program has been checked in the case of constant depth, where some exact solutions are known. In particular for $K > 0$ it is known that an initial solution

$$A(X = 0, \tau) = \operatorname{sech} \left(\sqrt{\frac{\alpha_3}{2\alpha_2}} \tau \right) \quad (5.17)$$

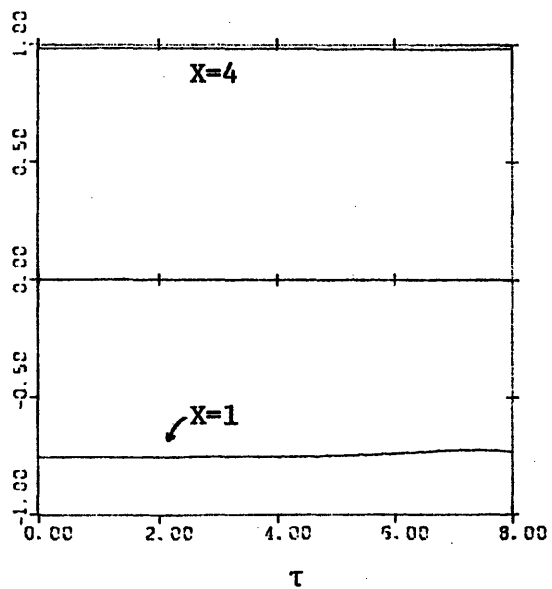
preserve the same shape while it propagates on constant depth (See Hasimoto and Ono (1972)). Fig. (5.1) shows the wave envelope as a function of X and τ . The current velocity at $X = -\infty$, the wave period and the depth have been chosen to be $U_1 = 0$, $T = 5$, $h = 1$ such that $K = (1.4)$. Since $A(X, \tau)$ is even in τ , the wave envelope has been plotted for $\tau \geq 0$ only. Fig. (5.1.a) is a general view of the wave envelope during its propagation from $X = 0$ to $X = 4$ and for $\tau = 0$ to $\tau_0 = 15$. In Fig. (5.1.b) the wave envelope profiles at $X = 0$, $X = 1$ and $X = 4$ have been superposed. It shows that the initial soliton profile is conserved for a distance of propagation larger than $X_2 = 4$. Fig. (5.1.c) gives the phase of the wave at $X = 1$ and $X = 4$. We can notice that, as expected the phase is independent of τ but varies with X .

ii. Evolution Law

The cubic Schrodinger equation with constant coefficients admits an infinite number of conservation laws, some of them express the conservation of physical quantities as the mass and the energy conservation. When the coefficients are not constants, laws allowing to follow the evolution of certain quantities can be found but they are not of the type of conservation laws (see Turpin, 1981). Here we derive the first evolution law and use it to check our numerical result. For this purpose we use the canonical evolution equation (4.25). Let us take (4.25)* B- (4.25) B*:



(b) Wave Amplitude $|A(X, \tau)|$



(c) Wave Phase $\text{Arg}(a(X, \tau))$

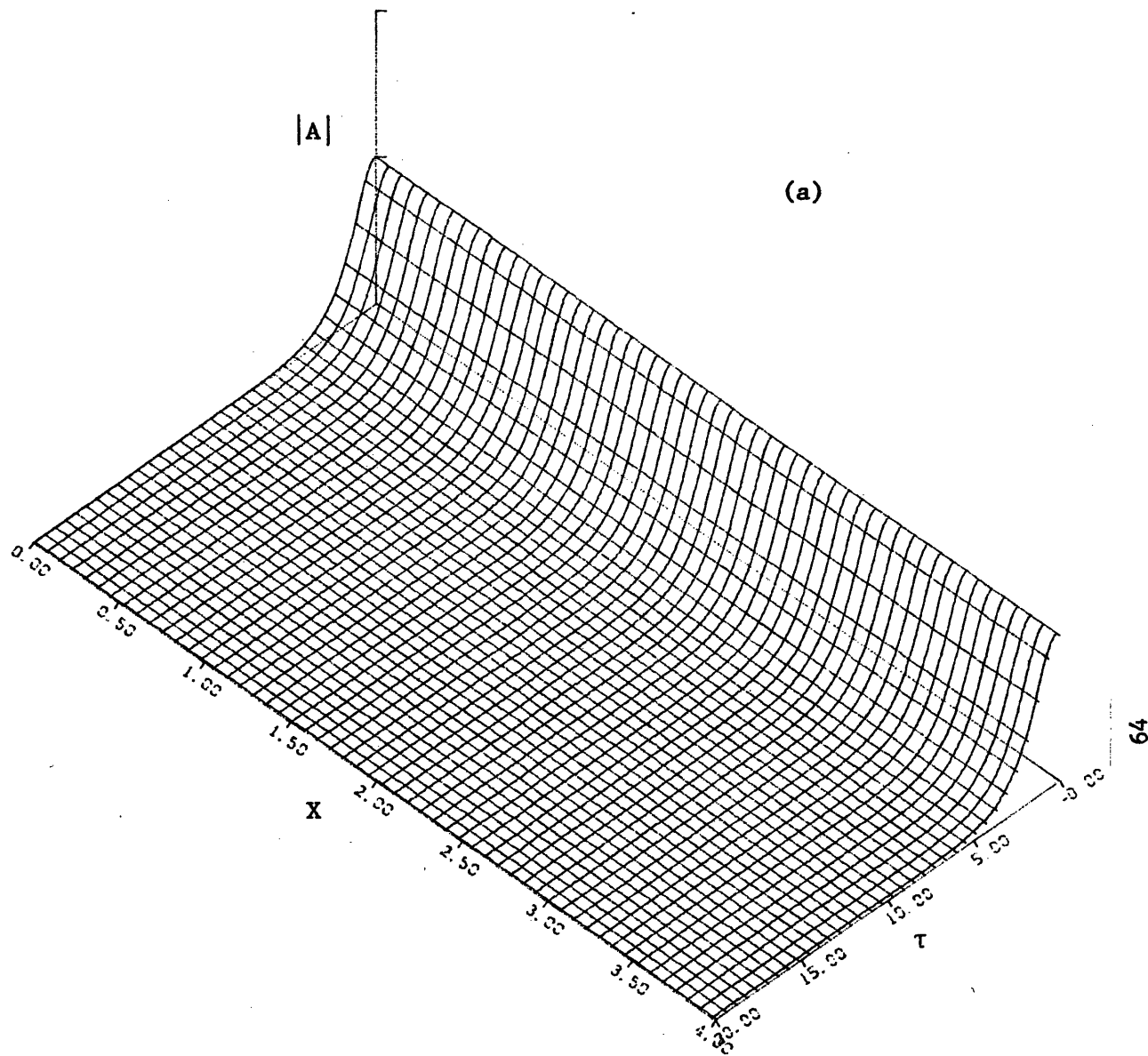


Figure 5.1 Evolution of a Sech Profile over Constant Depth,
No Current, K Positive

$$i \frac{\partial |B|^2}{\partial X} + \frac{\partial}{\partial \tau} (B_{\tau}^* B - B_{\tau} B^*) = 0 \quad (5.18)$$

If we assume B and $B_{\tau} \rightarrow 0$ as $\tau \rightarrow \pm \infty$, (5.18) gives by integration with respect to τ :

$$\frac{\partial}{\partial X} \int_{-\infty}^{+\infty} |B|^2 d\tau = 0 \quad (5.19)$$

which implies by using (4.24)

$$(C_g / \sigma)(X) \int_{-\infty}^{+\infty} |A(X, \tau)|^2 d\tau = \text{constant} \quad (5.20)$$

This result shows that for waves propagating against a current, when

$$C_g \rightarrow 0 \quad \int_{-\infty}^{+\infty} |A(X, \tau)|^2 d\tau \rightarrow +\infty. \quad \text{This is just an extension of the linear}$$

result $|A(X, \tau)| \rightarrow \infty$ in the neighborhood of a caustic. The evolution law (5.20) is used as a measure of the total error due to discretization, round-off and truncation of τ and is satisfied within few percents (less than 5%) for all computed cases in the following sections.

5.c. Geometry of the Problem

In our numerical computation we consider a more specific problem which is summarized in Fig. (5.2). The depth is considered to be constant and equal to 1 for $X < 0$, it varies as a cosine curve in the transition zone $0 \leq X \leq L$ i.e. $h = 1 + \frac{dh}{2} (\cos(\frac{\pi X}{L}) - 1)$ and becomes constant and equal to $1 - dh$ in the region $X \geq L$. dh is the height of the step. It is positive when the depth decreases and negative when

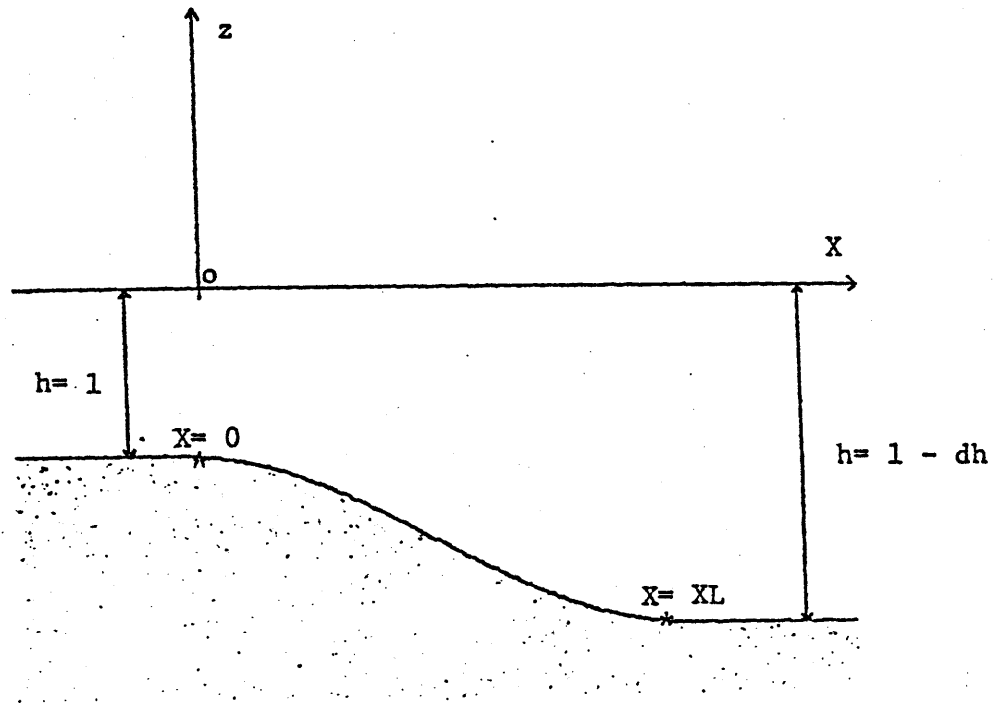


Figure 5.2 Geometry of the Problem

the depth increases. The transition zone L , has been taken equal to 1 in all the computed cases. It should be noted that the depth is normalized with respect to H_1 while the distance L is normalized as X , so the assumption of slowly varying depth is satisfied. U_1 is the current in the region $X \leq 0$. If U_1 is positive waves propagate in the same direction as the current, if U_1 is negative waves propagate in the opposite direction. The current induces a free water displacement $\xi(X)$ which can be found as shown in section (4.a). The origin of the vertical axis has been chosen such that $\xi = 0$ in the region $X \leq 0$. T is the wave period. T is constant during the propagation of the waves. $A(0, \tau)$ is the initial wave envelope profile. It has been chosen in all the cases to be of the form

$$A(0, \tau) = \text{sech} \left(\sqrt{\frac{\alpha_3}{2\alpha_2}} (X=0) \tau \right) \quad (5.21)$$

where α_3 and α_2 are the coefficients of the nonlinear cubic Schrodinger equation as defined in (4.21) and (4.22). This initial profile represents a soliton solution which is appropriate for the depth $h = 1$ i.e. if the depth remains constant the wave envelope profile would not change. Since the initial profile is even in τ , we only consider the wave envelope profile for $\tau \geq 0$. τ_0 must be chosen sufficiently large so that the condition $A(X, \tau_0) = 0$ does not induce any noise effect in the solution. From (5.21) we can see that τ_0 depends on $\frac{\alpha_3}{\alpha_2}$. It also depends on X_2 , the distance of propagation considered: the larger X_2 is the larger

τ_0 should be. X_2 is the distance of propagation over which the wave envelope is studied. To limit the computation time, in most of the cases this distance has not been chosen to be very large. The program used for the numerical computation has been developed by Turpin (1981) and has been slightly modified to include the case of waves propagating against current. This program is given in appendix A2 .

6. Propagation of a Wave Packet Over Varying Depth

6.a Djordevic - Redekopp's Solution

One purpose of the numerical study is to check the validity of the assumptions made by Djordevic and Redekopp (1978) in solving the problem of a soliton moving over a slowly varying depth in a region where K is positive everywhere. In this section, we present the method they used. It should be noted that their method can be generalized without modifications to the case of a stationary current. In what follows, we refer to Djordevic and Redekopp's paper as D-R. We use the same transformation as in section (4.c):

$$s = \exp - \int_0^{\bar{X}} \alpha_1 du \quad \text{where} \quad \bar{X} = \int_0^X \alpha_2(u) du \quad (6.1)$$

$$A(X, \tau) = s(X) P(X, \tau)$$

By substituting into (4.19) P is shown to be solution of the equation

$$-i P_{\bar{X}} + P_{\tau\tau} + K|P|^2 P = 0 \quad (6.2)$$

We consider an initial perturbation in region (1) ($X < 0$) which is a soliton, whose amplitude length ratio is adapted to this region of constant depth i.e.

$$P = P_0 \operatorname{sech} \tilde{K}\tau \quad \text{and} \quad \tilde{K} = P_0 \sqrt{\frac{\alpha_3}{2\alpha_2}} \quad (1) \quad (6.3)$$

Djordjevic and Redekopp made the assumption that at the end of the depth variation $X = L$, P conserves its original shape and can be considered as

the initial condition for propagation in region (2). This assumption means that if in region (1):

$$A(0, \tau) = P_0 \operatorname{sech} \left(P_0 \sqrt{\frac{\alpha_3}{2\alpha_2}}(1) \tau \right) \quad (6.4)$$

At the end of the depth variation it is assumed to be:

$$A(L, \tau) = s(L) P_0 \operatorname{sech} \left(P_0 \sqrt{\frac{\alpha_3}{2\alpha_2}}(1) (\tau - \tau_0) \right) \quad (6.5)$$

where $s(L) = \sqrt{\frac{(C_g/\sigma)(1)}{(C_g/\sigma)(2)}}$

In region (2) $X \gg L$, this initial condition will in general evolve into N solitons where N is determined from the Zakharov - Shabat eigen-value problem (cf Zakharov and Shabat (1972)). If the potential q of the eigen value problem is of the form $q(\tau) = a \operatorname{sech} K(\tau - \tau_0)$ then, the number of discrete eigen values with positive real parts i.e. the number of solitons which will emerge as $X \rightarrow \infty$ is the largest integer smaller than $\frac{a}{K} + \frac{1}{2}$. Using the wave envelope (6.5), the associated Zakharov and Shabat eigen value problem has the potential

$$q(z) = \sqrt{\frac{1}{2} \frac{\alpha_3}{\alpha_2}}(2) s P_0 \operatorname{sech} K(\tau - \tau_0) \quad (6.6)$$

So the asymptotic number of solitons as $X \rightarrow +\infty$ is:

$$N = \text{largest integer smaller than} \left[\left(\frac{\alpha_3}{\alpha_2}(2) \frac{\alpha_2}{\alpha_3}(1) \frac{C_g}{\sigma}(1) \frac{\sigma}{C_g}(2) \right)^{1/2} + \frac{1}{2} \right] \quad (6.7)$$

This result is given by Eqs. (5.5), (5.7) and (5.8) in Djordjevic and Redekopp's paper (1978). Let us introduce S the area under the wave profile at the end of the transition zone.

$$A = \int_{-\infty}^{+\infty} A(L, \tau) d\tau \quad (6.8)$$

From Djordjevic - Redekopp's theory, this area can be calculated by using (6.5). It gives

$$A_s = \pi \left(\frac{C_g}{\sigma}(1) \frac{\sigma}{C_g}(2) \frac{2\alpha_2}{\alpha_3}(1) \right)^{1/2} \quad (6.9)$$

To check the validity of the assumptions which have been made to find (6.7) the asymptotic number of solitons N , the value of A_s expected by D-R theory is compared to the value A obtained from the numerical computation. We define

$$\Delta = 1 - \frac{A_s}{A} \quad (6.10)$$

Δ measures the relative error between the numerical computation and D-R theory.

6.b Numerical Results

i . Constant Depth

We first consider the evolution of an initial sech profile on constant depth. The results of this case are known both analytically (Zakharov and Shabat, Satsuma and Yajima) and numerically (Yue, 1980). However it is important to present here some of these results in order to compare them with those of the case of variable depth. Let us consider the initial profile to be :

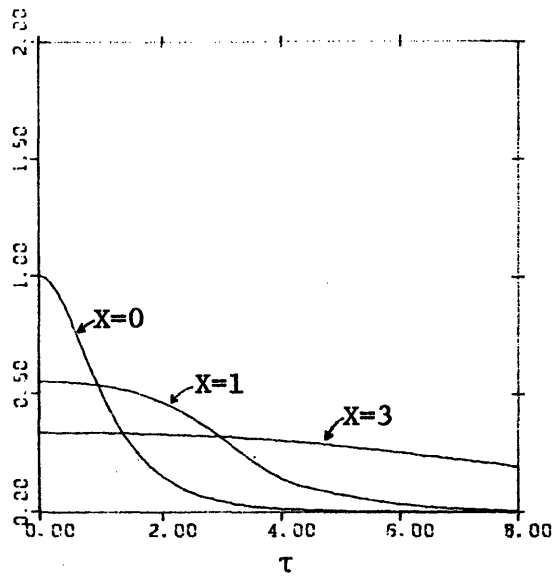
$$A = a \operatorname{sech}(\tau/\lambda) \quad (6.11)$$

Then, we know that in a region where $K < 0$, the initial wave packet flattens and spreads toward large τ . The decay of the envelope is as $\frac{1}{\sqrt{X}}$ and no soliton emerges. Fig. (6.1) illustrates this case, the parameter λ is 1 and the wave period is $\underline{T} = 7$ so that $K = \frac{\alpha_3}{\alpha_2} = -3.33 < 0$. It shows the steadily decrease of the maximum height of the envelope which is associated with the radiation of energy towards large τ .

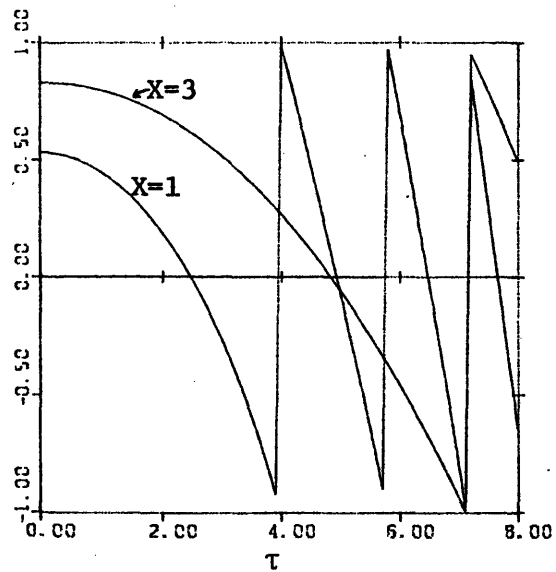
In region where $K > 0$, the asymptotic state consists of N solitons plus decaying oscillations where N is the largest integer less than

$$m = \sqrt{\frac{\alpha_3}{2\alpha_2}} \frac{A}{\pi} + \frac{1}{2} \quad (6.12)$$

where $A = \pi a \lambda$ is the area of the initial profile (6.11). If $1 < m < 1.5$, the asymptotic state consists of one soliton. The evolution picture is shown in Fig. (6.2) in the case of $\underline{T} = 5, K = 1.4, m = 1.25$. It shows a dispersive decay of the wave envelope and does not reveal any recurrence period. If $1.5 < m \leq 2$ only one soliton emerges for large X while if $2 < m < 2.5$ two soliton emerge. However the evolution pictures of these two cases are similar. There is a single 'recurrence period' after which the profile repeats itself with a slow decay of the maximum amplitude and a slight spreading towards large τ , signalling radiation. This result is shown in Fig. (6.3) in the case of $\underline{T} = 5, K = 1.4$ and $m = 2$. It should



(b) Wave Amplitude $|A(X, \tau)|$



(c) Wave Phase $\text{Arg}(A(X, \tau))$

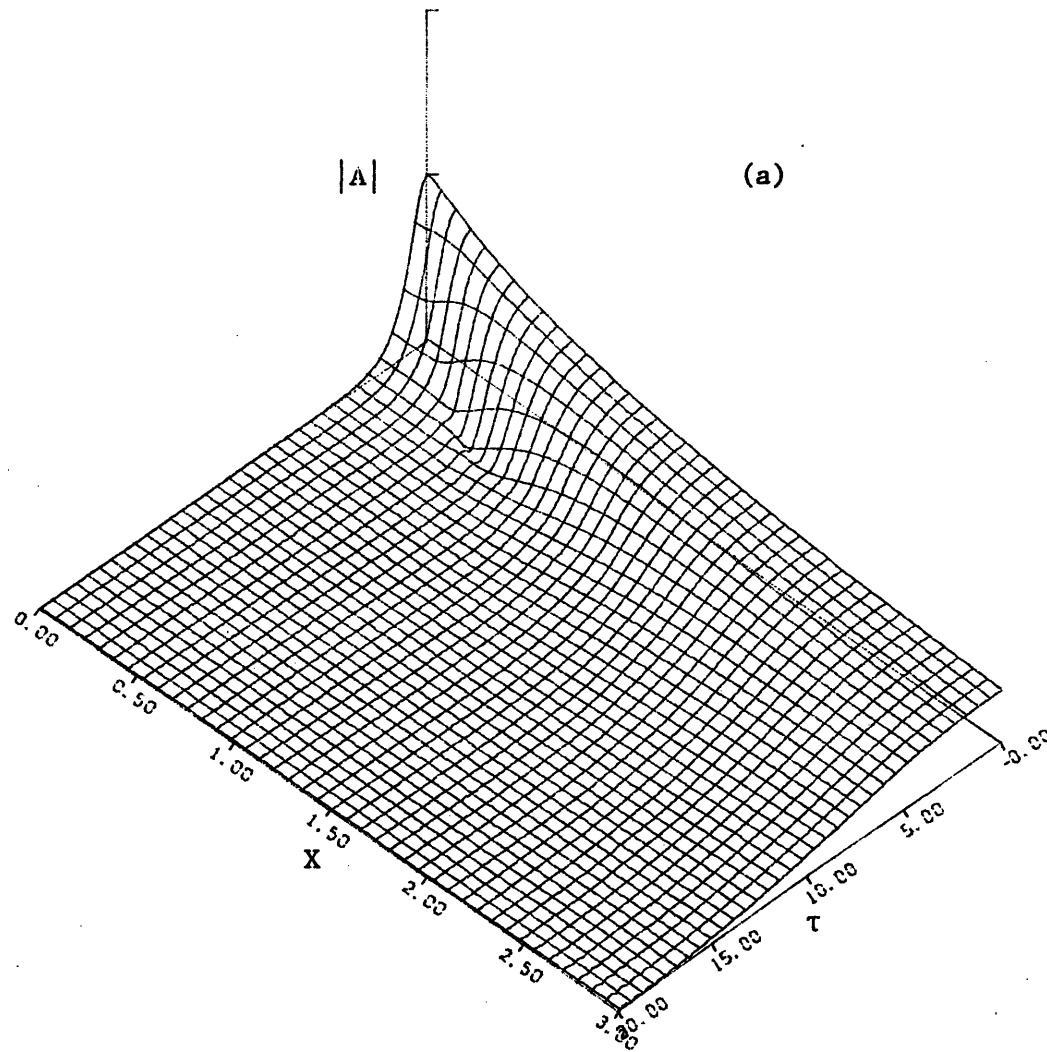
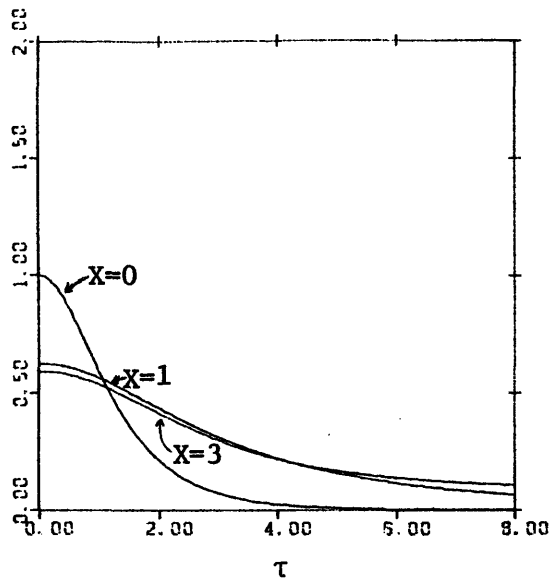
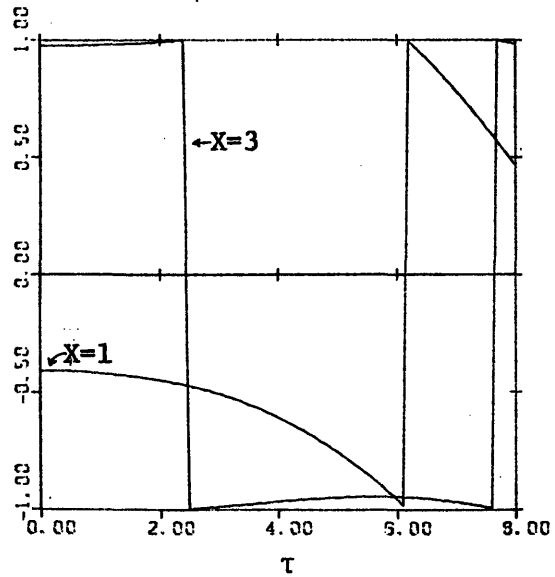


Figure 6.1 Evolution of a Sech Profile over Constant Depth,
No Current, K Negative



(b) Wave Amplitude $|A(X, \tau)|$



(c) Wave Phase $\text{Arg}(A(X, \tau))$

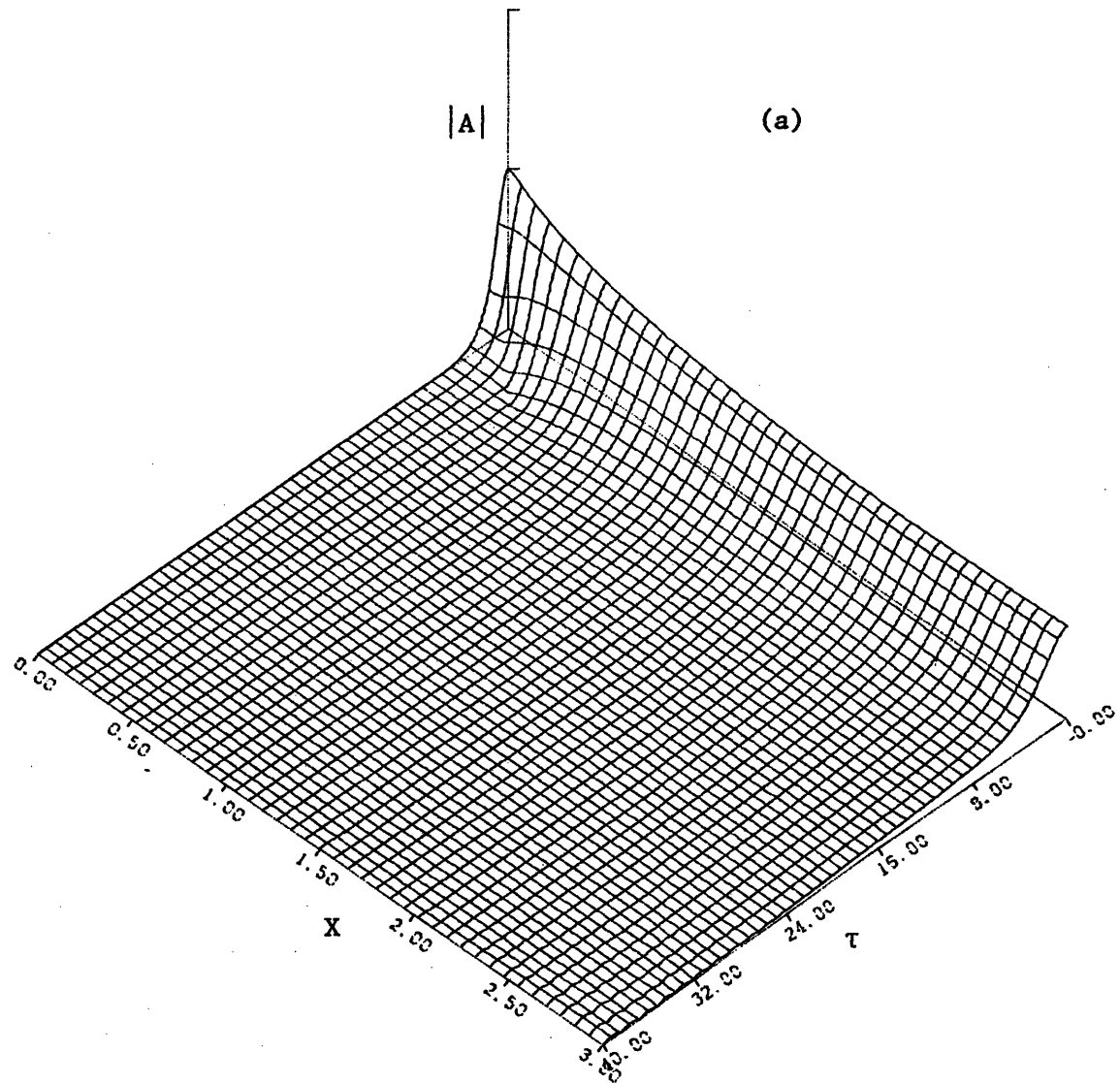
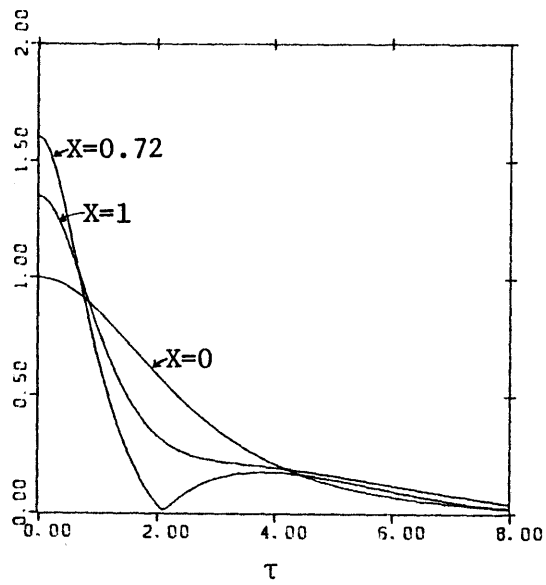
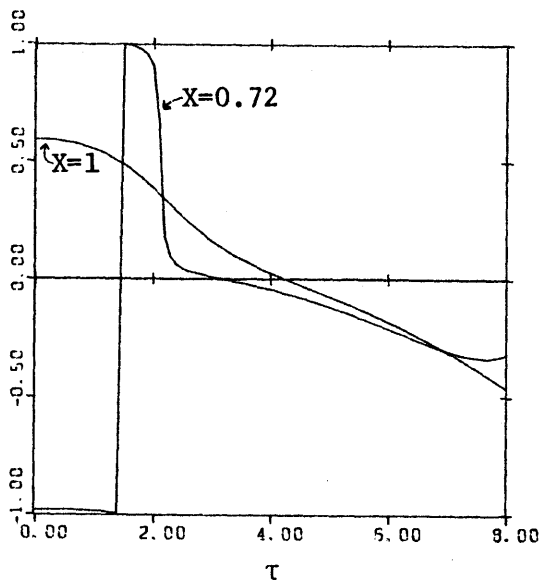


Figure 6.2 Evolution of a Sech profile over Constant Depth,
No Current, K Positive, $m=1.25$



(b) Wave Amplitude $|A(X, \tau)|$



(c) Wave Phase $\frac{\text{Arg}(A(X, \tau))}{\pi}$

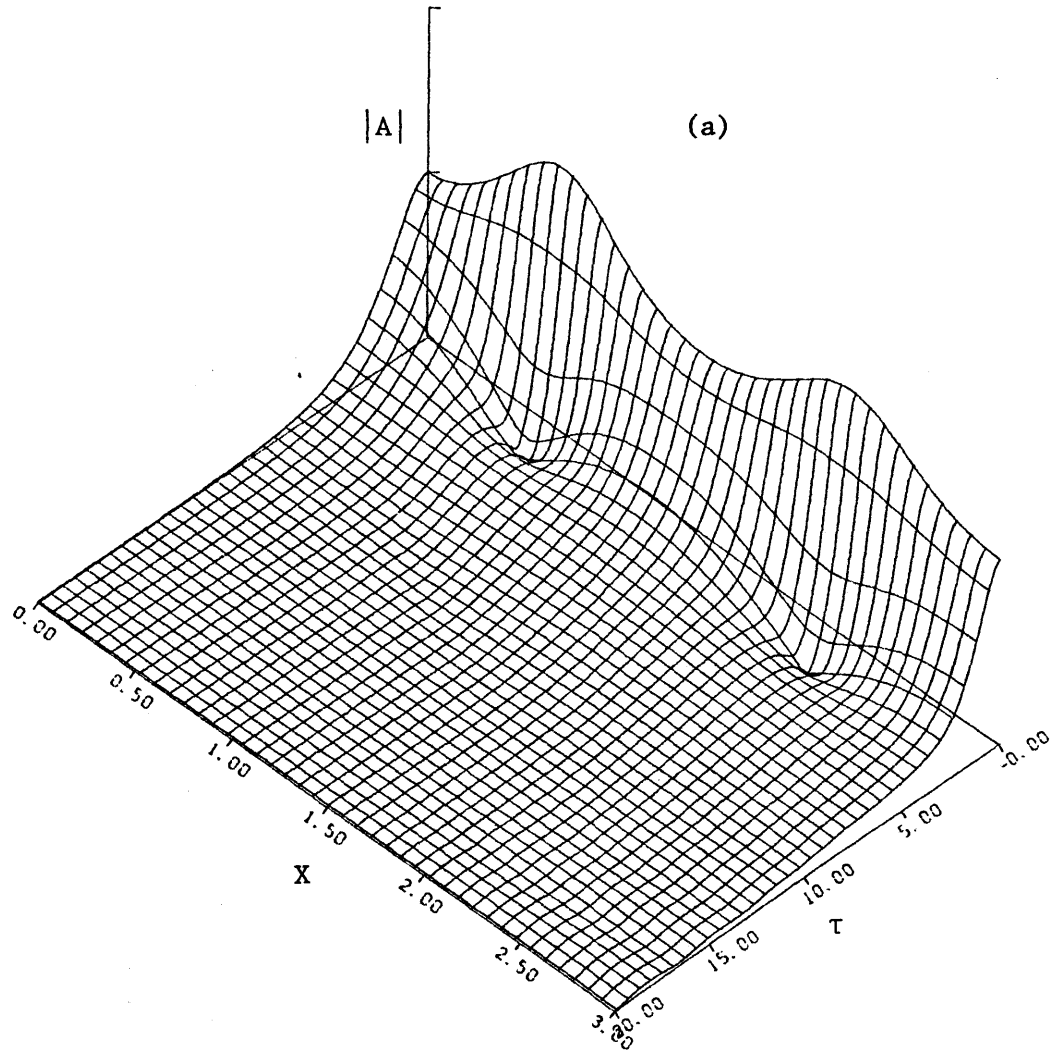


Figure 6.3 Evolution of a Sech Profile over Constant Depth,
No current, K Positive, $m=2.0$

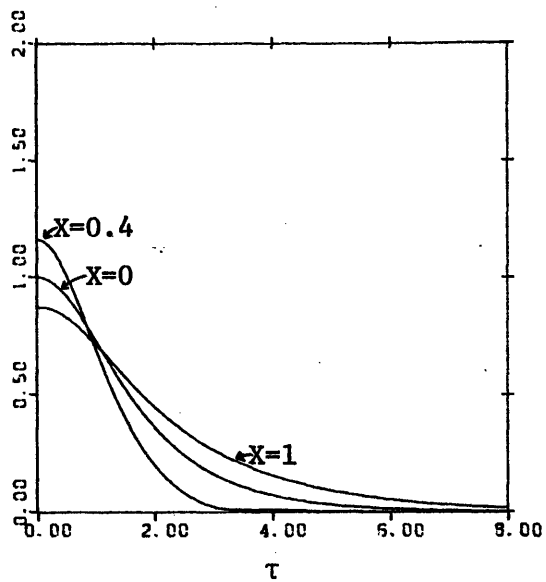
be noted that for two initial envelopes of the same area and height, the evolution towards the final state can be quite different if their shapes or phase distributions are different. This statement is illustrated in Fig. (6.4) where the propagation of the initial profile:

$$A(0, \tau) = \operatorname{sech} \left(\sqrt{\frac{\alpha_3}{2\alpha_2}}(1) \tau \right) e^{i0.1\tau^2} \quad (6.13)$$

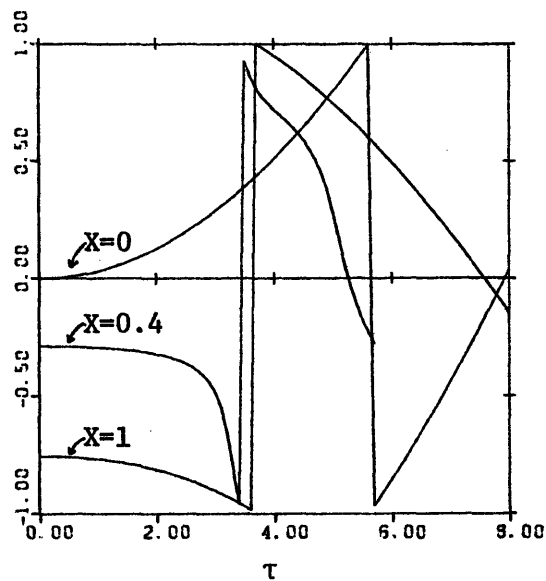
is shown. Comparing Fig. (6.4) and Fig. (5.1) we note that a difference in the phase distribution of the initial profiles induces a qualitative difference in the subsequent evolution of the wave envelope.

ii. Variable Depth

In what follows we consider the initial profile (5.21) such that if the nonlinearity parameter K is positive everywhere and the depth constant the wave envelope will evolve without change in amplitude. However when the depth varies, K changes according to Fig. (4.6.b) and the initial profile must adapt to its new environment: its shape is not conserved. In Fig. (6.5) we present the evolution of an initial sech profile, corresponding to the envelope of waves with a period $T = 5$, during its propagation into deeper water ($dh = -0.5$). We know from Fig. (4.6.b) that K is positive and increases from $K_1 = 1.4$ to $K_2 = 2.8$. The 3-dimensional plot gives the amplitude of the waves as a function of τ and X . As the depth increases the initial data becomes steeper and steeper. At $X = 1$ the envelope is no longer a soliton, it has two side groups separated by nodes as could be seen from Fig. (6.5.b). The



(b) Wave Amplitude $|A(X, \tau)|$



(c) Wave Phase $\text{Arg}(A(X, \tau))$

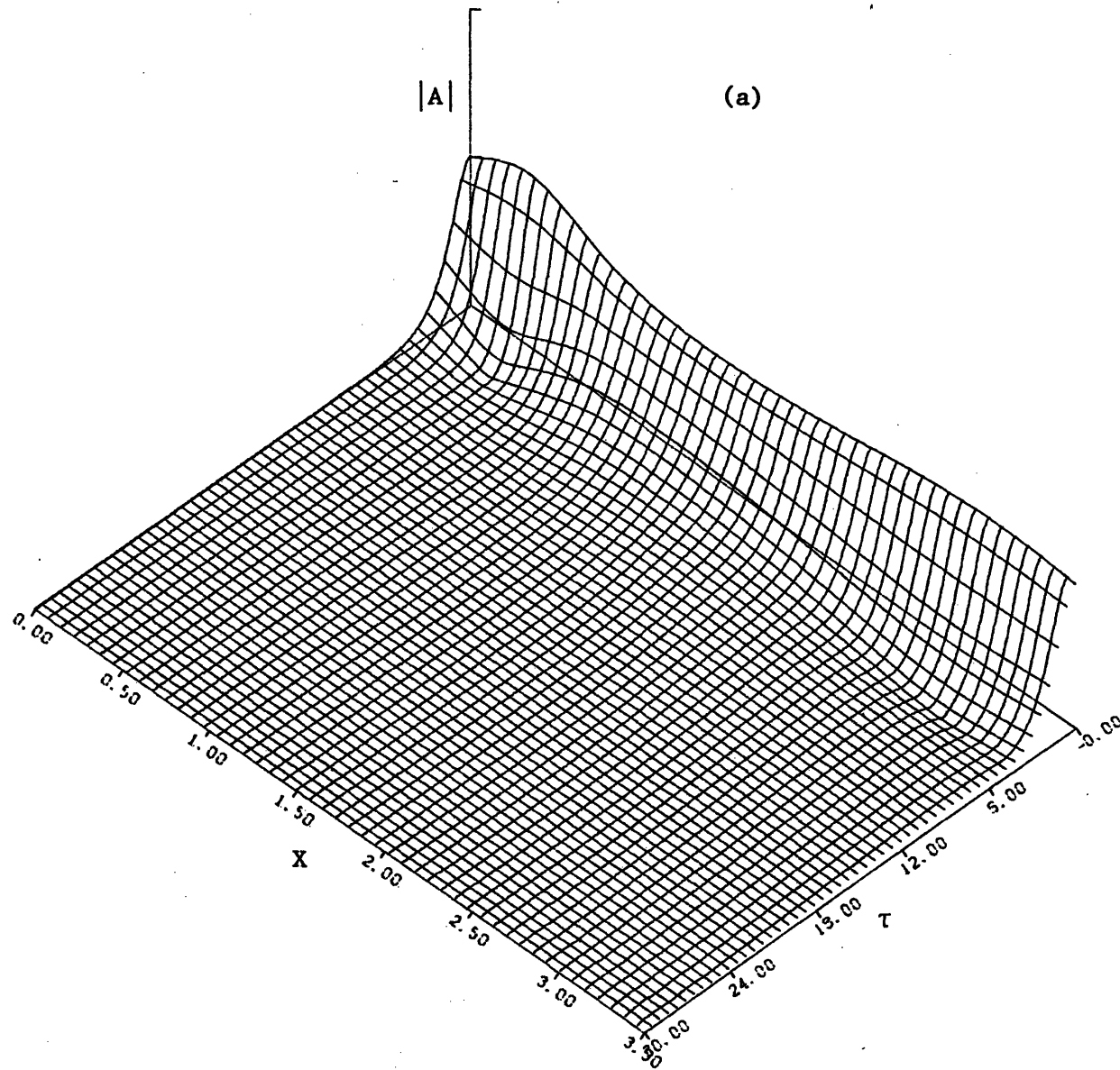
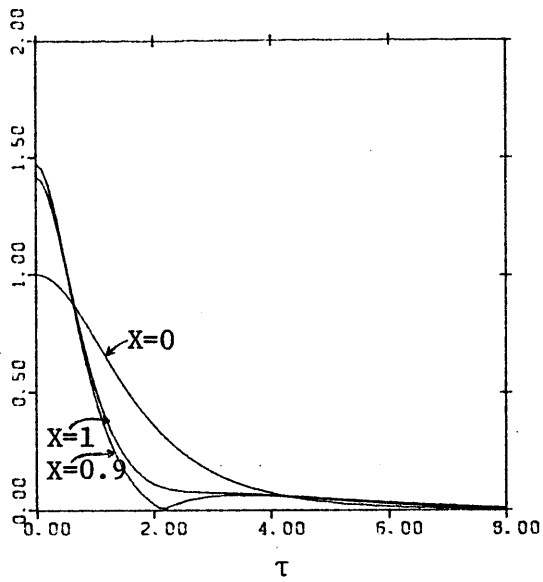
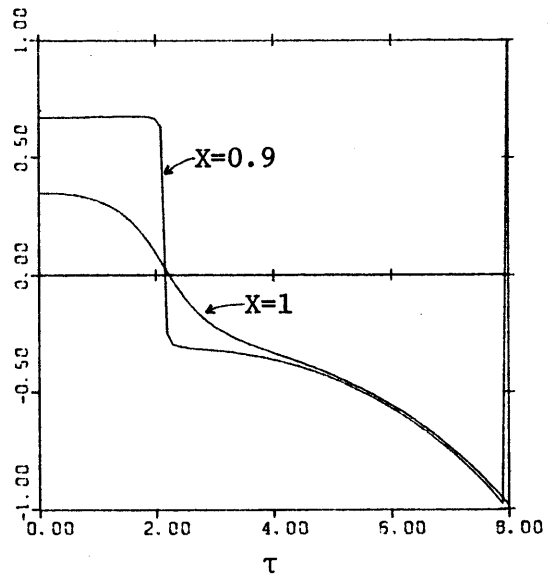


Figure 6.4 Evolution of a Sech Profile with Parabolic Phase Distribution over Constant Depth, No Current, K Positive



(b) Wave Amplitude $|A(X, \tau)|$



(c) Wave Phase $\frac{\text{Arg}(A(X, \tau))}{\pi}$

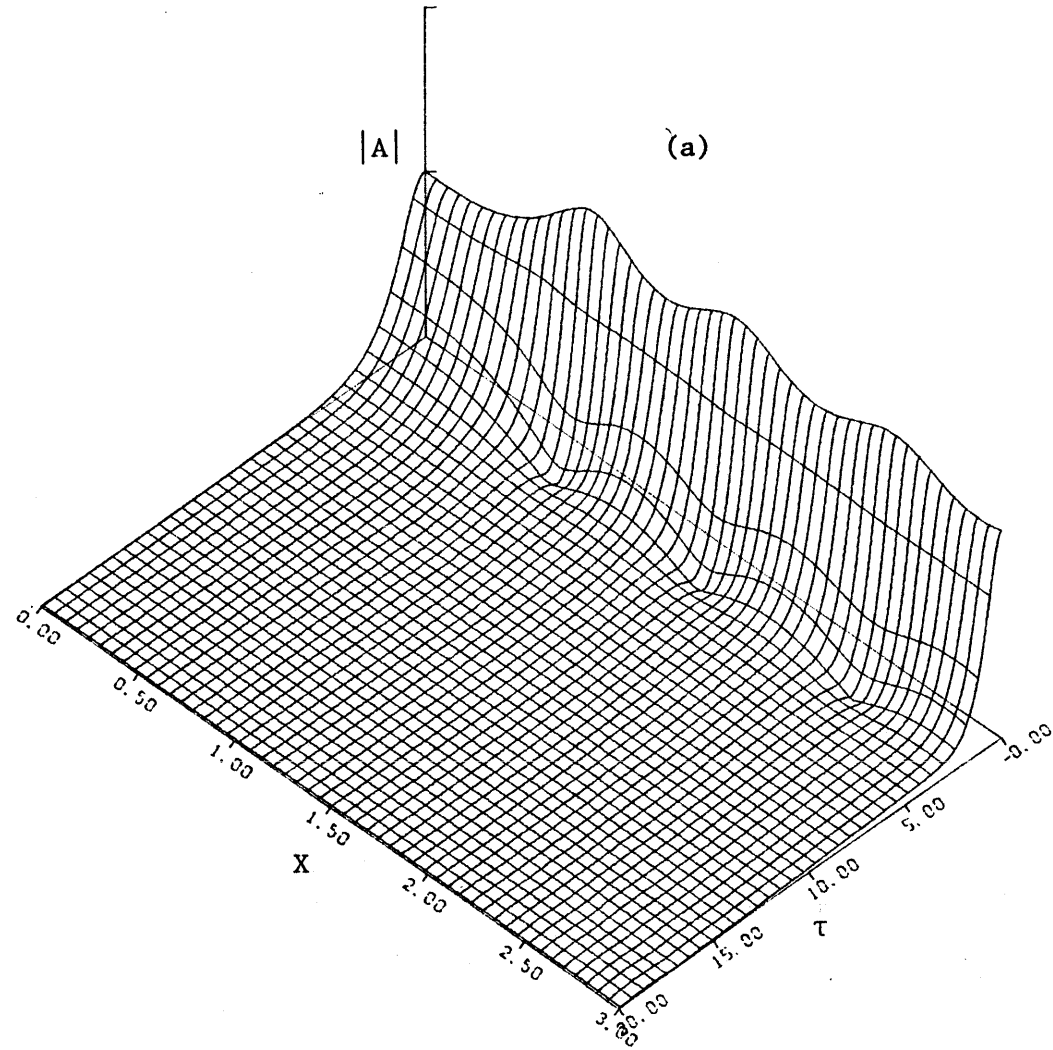


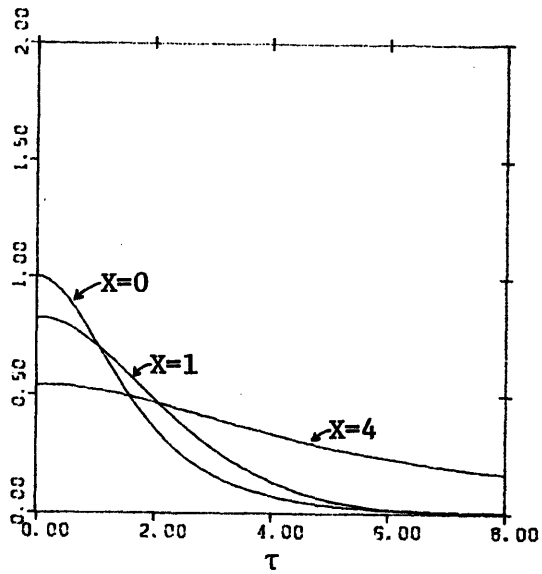
Figure 6.5 Evolution of a Sech Profile over Increasing Depth

No Current, K Positive

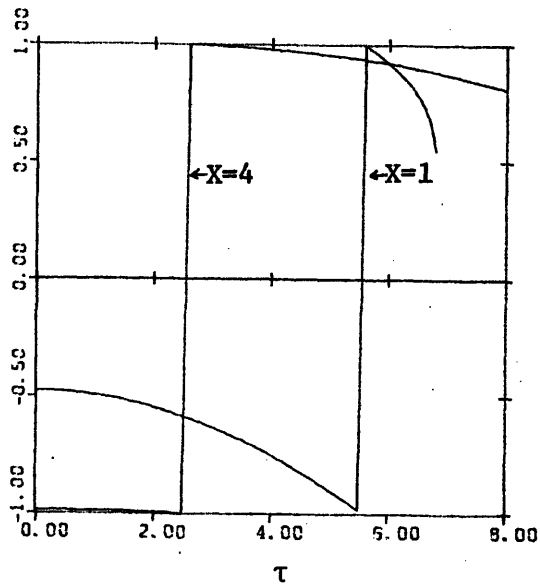
evolution picture is qualitatively similar to Fig. (6.3). It shows that the profile repeats itself with some decay after a recurrence period which is approximately $X \approx 0.9$. As pointed by Yue (1980) it can be noted that the node of the wave amplitude is accompanied by a sudden jump by π of the phase (see Fig. (6.5.c)). In the complex plane it means that A crosses zero without discontinuity of its derivatives. It also implies that the wave frequency has a peak at the node.

Fig. (6.6) presents the evolution of the same initial profile during its propagation into shallower water ($dh = 0.15$). The depth variation has been chosen such that K is positive everywhere. As shown in Fig. (4.6.b) K decreases with decreasing depth: $K_1 = 1.4$, $K_2 = 0.72$. The 3-D plot shows that as the depth decreases the initial profile becomes flatter and flatter. A more quantitative picture is obtained by superposing the wave envelope profile at different locations $X = 0, 1, 2, 4$ as a function of τ (Fig. 6.6.b). It shows the continuous decrease in the profile steepness during the evolution. Fig. (6.6.c) shows that, at each location X , the phase decreases slightly as a function of τ .

Since K is positive everywhere in the two previous cases, their results can be used to check Djorjevic and Redekopp's assumptions (see section 6.a). The relative difference between the numerical results and the D-R results as defined by (6.10) is for the case presented in Fig. (6.5) $\Delta = -22\%$ and for the case presented in Fig. (6.6) $\Delta = 11\%$. It should be recalled that in all the cases the evolution law (5.20) is satisfied within 5%. Therefore these differences are larger than the numerical errors and hence could affect the prediction of the number of solitons emitted. We note that $\Delta \lesssim 0$ when $dh \gtrsim 0$, this result has been found to be valid in all



(b) Wave Amplitude $|A(X, \tau)|$



(c) Wave Phase $\text{Arg}(A(X, \tau))$

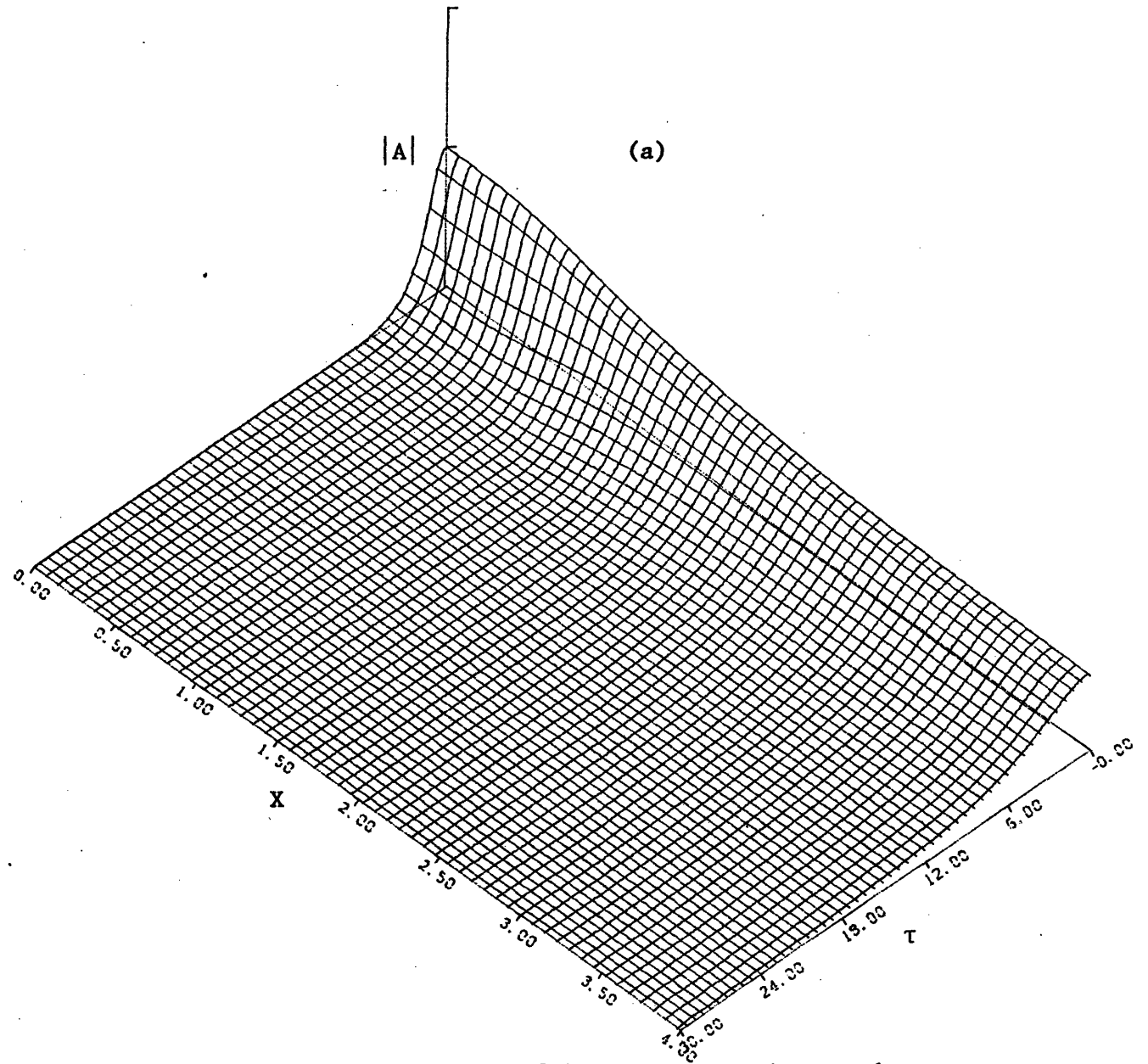


Figure 6.6 Evolution of a Sech Profile over Decreasing Depth,
No Current, K Positive

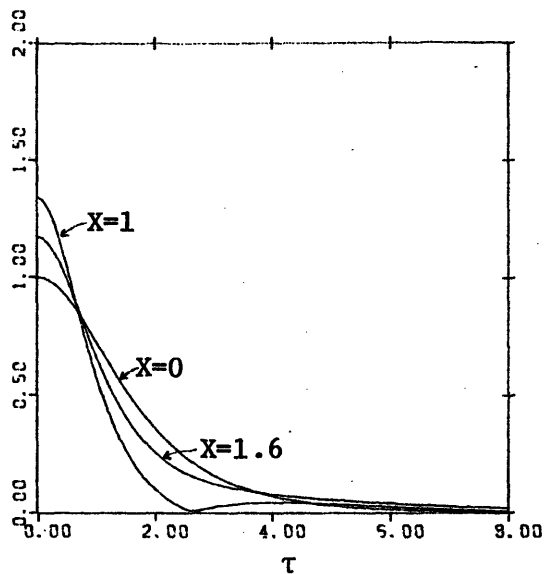
the cases treated. It implies that for waves propagating into deeper water, the area under the wave envelope becomes smaller than expected by D-R while for waves propagating into shallower water the area under the wave envelope becomes larger than expected by D-R. Furthermore D-R assumes that the profile at the end of the depth variation is still a sech profile (Eq. 6.5) but a comparison between the initial profile and the profile at $X = 1$ in Figs. (6.5) and (6.6) shows that this assumption is not satisfied. Based on D-R theory the number of solitons which will appear as $X \rightarrow \infty$ is N the largest integer smaller than $m_s = 1.87$ in the first case and $m_s = 1.22$ in the second. So in both cases the initial profile would evolve into one soliton plus residual oscillations which decay as $(X)^{-1/2}$. Since our computation has been limited to a small distance of propagation ($X_2 = 3, X_2 = 4$ respectively) these predictions could not be checked numerically. However based on the numerical value of the area of the wave envelope at $X = 1$ one can find a more accurate value for m (Eq. 6.12): $m = 1.5$ for the case of Fig. (6.5). This result implies that if the profile at $X = 1$ was a sech profile then it would evolve without shape variation. The fact that we see in Fig. (6.5) both recurrence and radiation is due to the initial departure from (6.11). In the case of Fig. (6.6) $m = 1.3$ and the evolution of the wave envelope is qualitatively similar to the one presented in Fig. (6.2).

It should be noted that in the case where K is positive everywhere and where the depth increases the effect of increasing the magnitude of

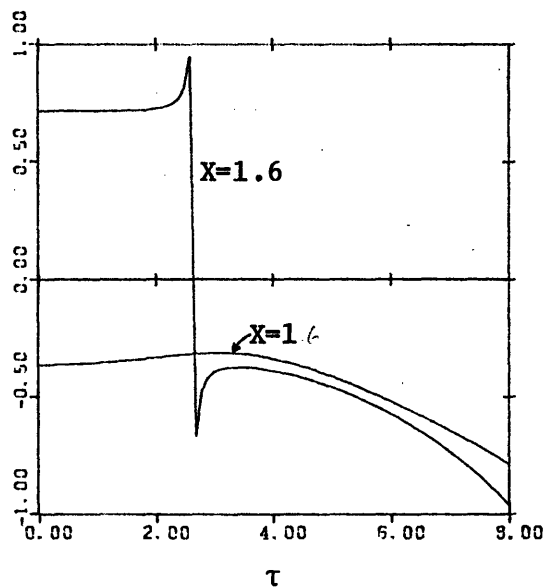
the depth variation dh , letting all the other parameters fixed is to increase the maximum amplitude and to shorten the inter-nodal distance. This result can be seen by comparing Fig. (6.7) where $dh = -0.3$ and Fig. (6.5) where $dh = -0.5$.

In the case where $K < 0$ everywhere, we know that the initial sech profile does not conserve its shape even on constant depth (see Fig. 6.1). We present the evolution of a sech profile corresponding to waves of period $T = 7$ which are propagating into deeper water (Fig. (6.8), $dh = -0.3$) and shallower water (Fig. (6.9), $dh = 0.3$). These figures are qualitatively very similar to Fig. (6.1). The three of them can be superposed with a good agreement at least during the initial stage of propagation. It shows that in the case where $K < 0$ depth variation has very little effect on the qualitative features of the evolution which is dominated by radiation.

Fig. (6.10) illustrates the case where K crosses zero during the propagation of the wave. It shows the evolution of an initial sech profile corresponding to waves with period $T = 6$, which propagates into deeper water, $dh = -0.5$. Fig. (4.6.b) shows that K is negative initially but becomes positive as the depth increases: $K_1 = -0.56$, $K_2 = 0.73$. The initial profile first decays and radiates as in the case $K < 0$, then begins to steepen as it propagates into deeper water. Soliton emission is clear in the deeper water, numerical computation of m at $X = 1$ gives $m = 1.7$. In the case where K decreases from positive to negative values an initial soliton flattens. The evolution of a wave



(b) Wave Amplitude $|A(X, \tau)|$



(c) Wave Phase $\text{Arg}(A(X, \tau))$

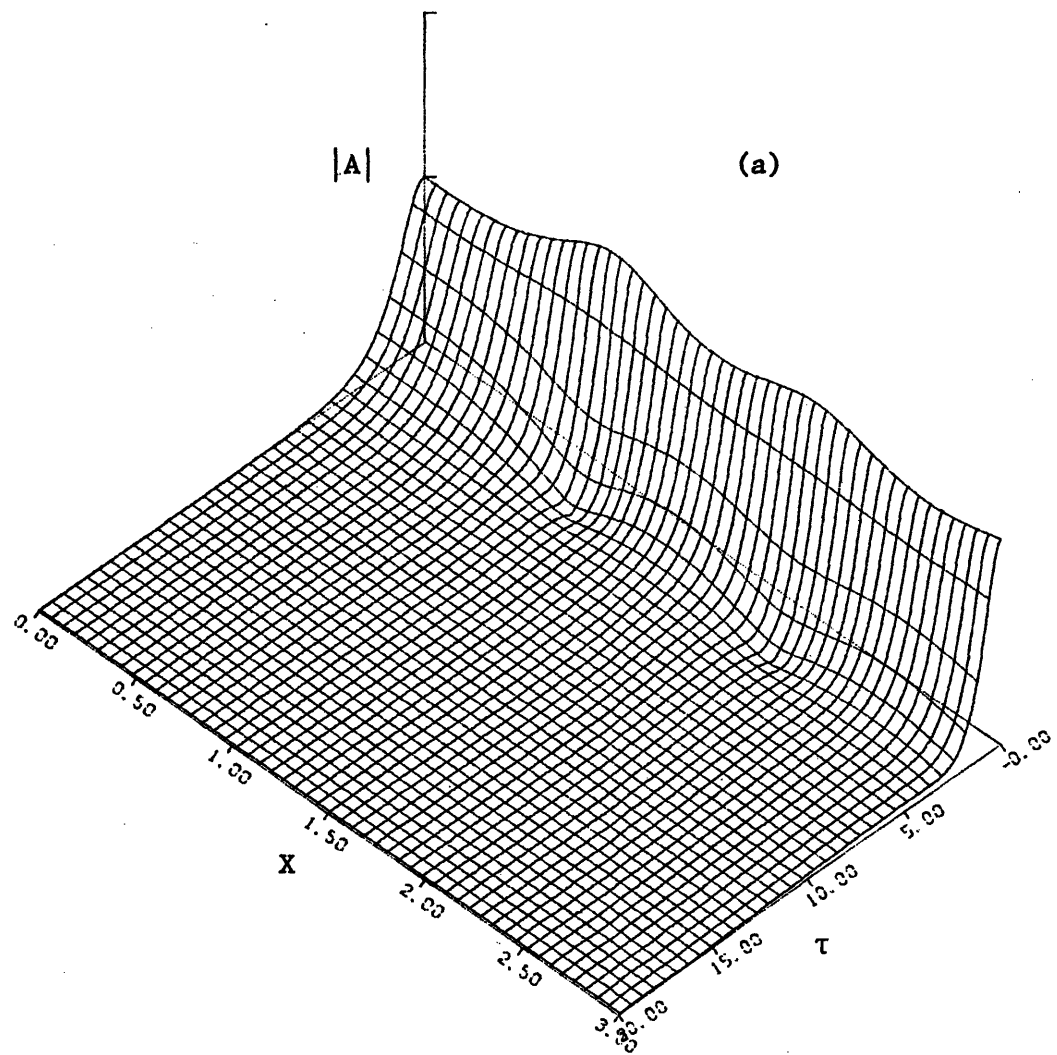
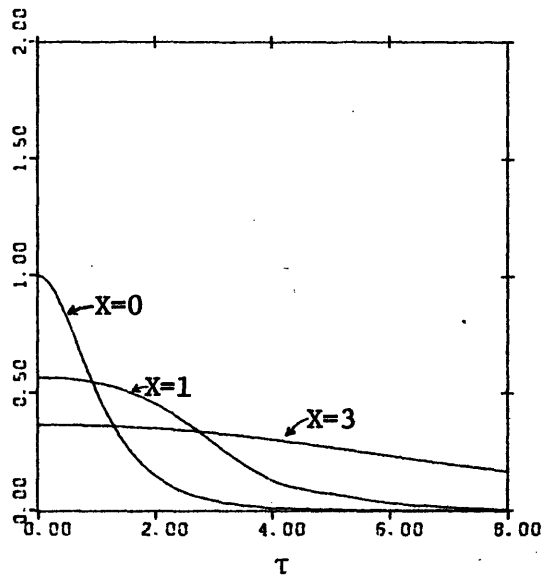
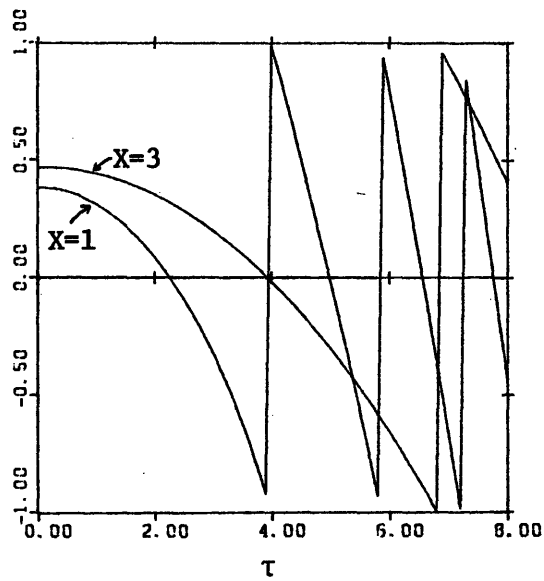


Figure 6.7 Evolution of a Sech Profile over Increasing Depth,
No Current, K Positive



(b) Wave Amplitude $|A(X, \tau)|$



(c) Wave Phase $\frac{\text{Arg}(A(X, \tau))}{\pi}$

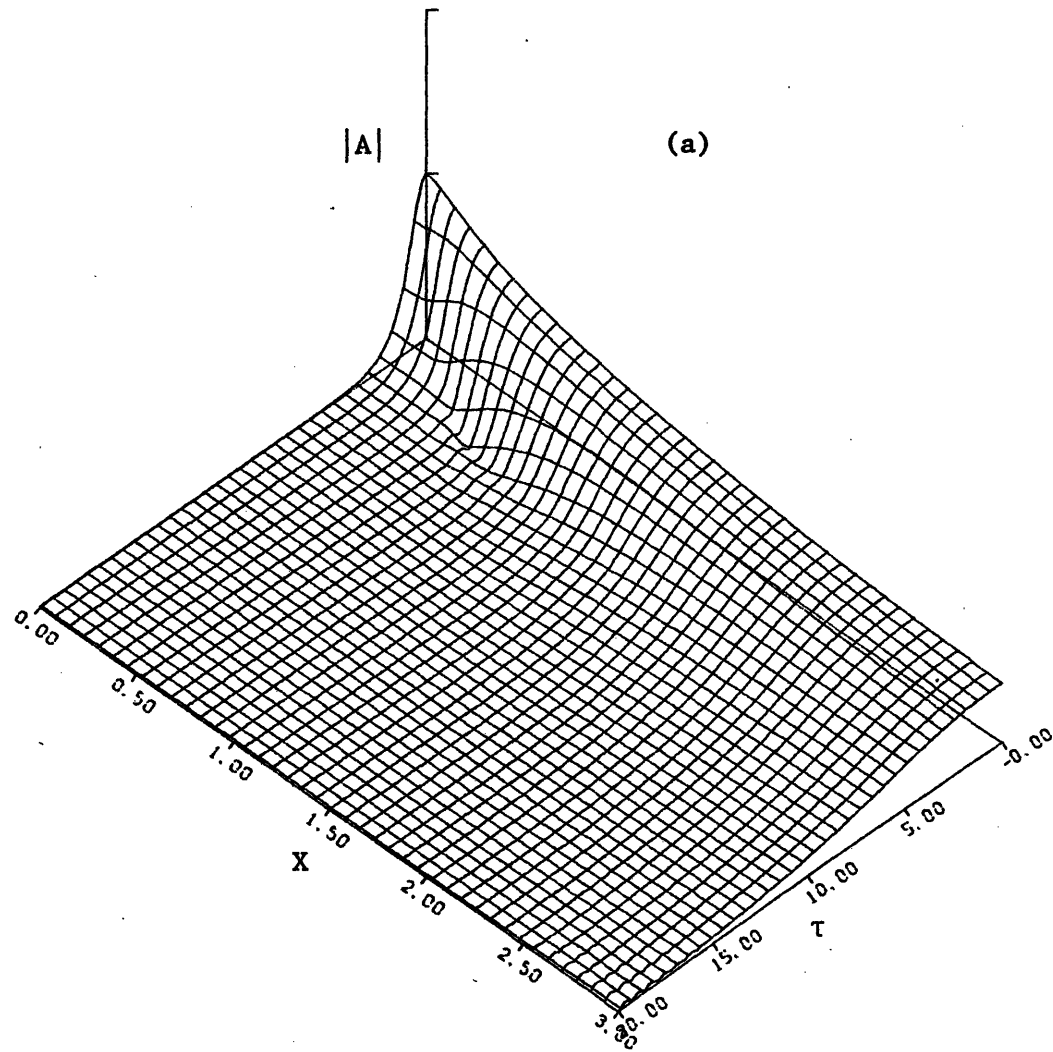
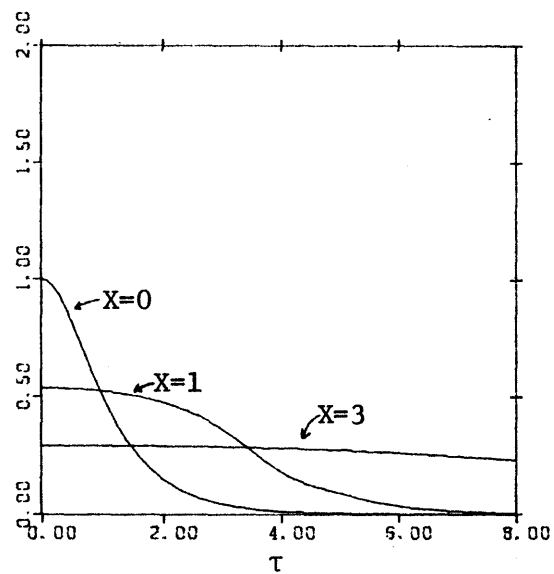
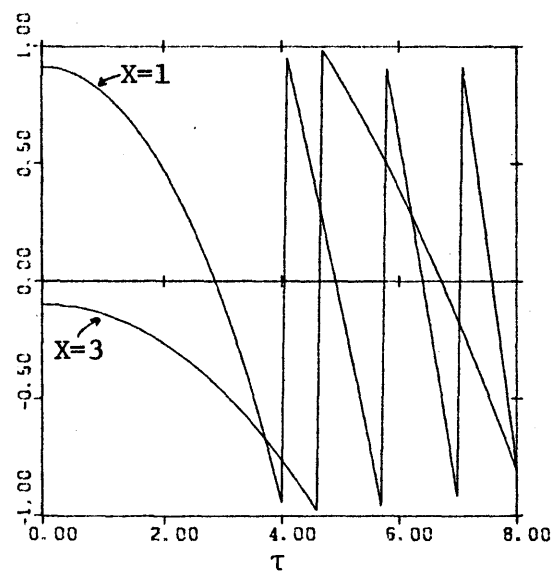


Figure 6.8 Evolution of a Sech Profile over Increasing Depth,
No Current, K Negative



(b) Wave Amplitude $|A(X, \tau)|$



(c) Wave Phase $\frac{\text{Arg}(A(X, \tau))}{\pi}$

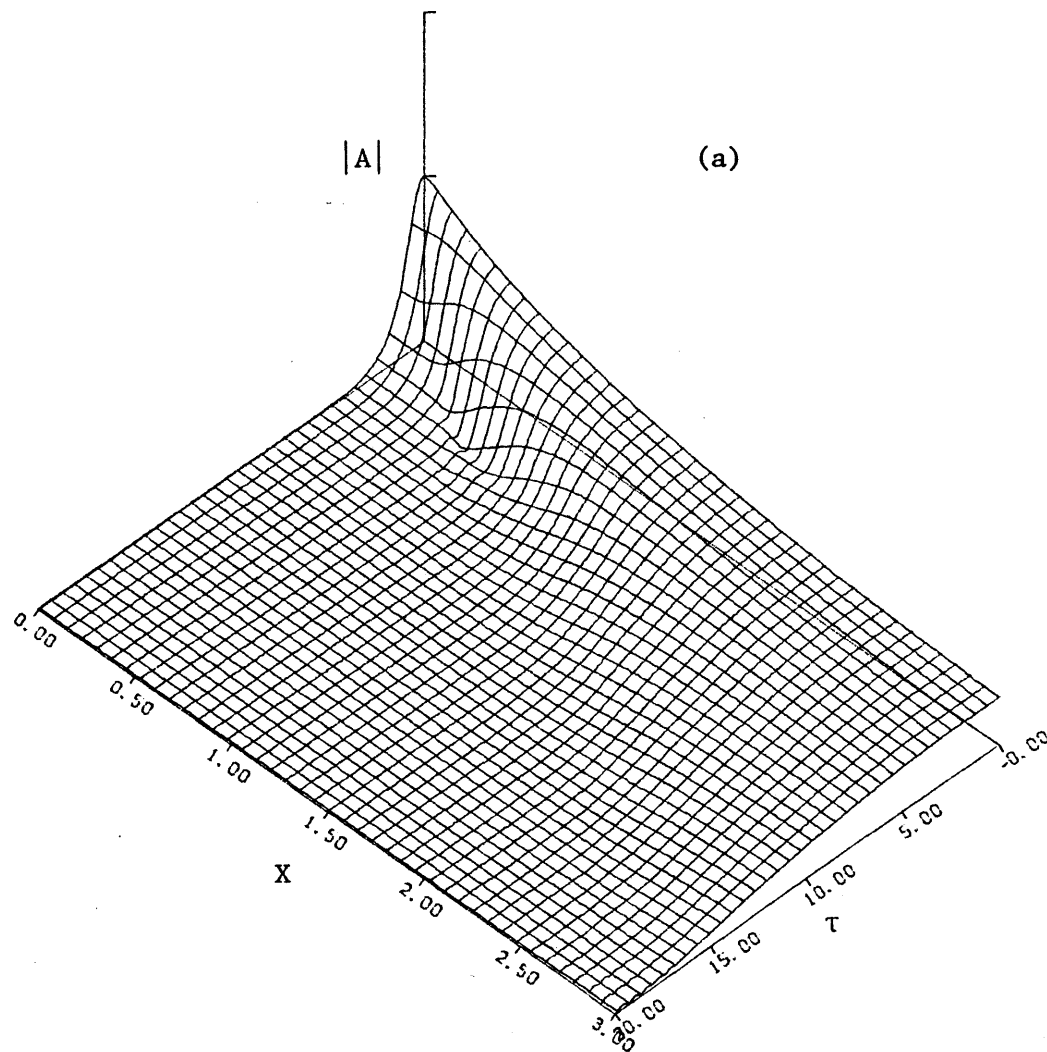
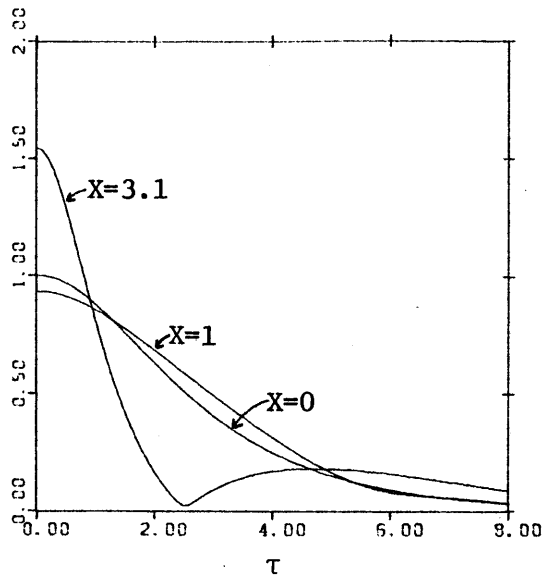
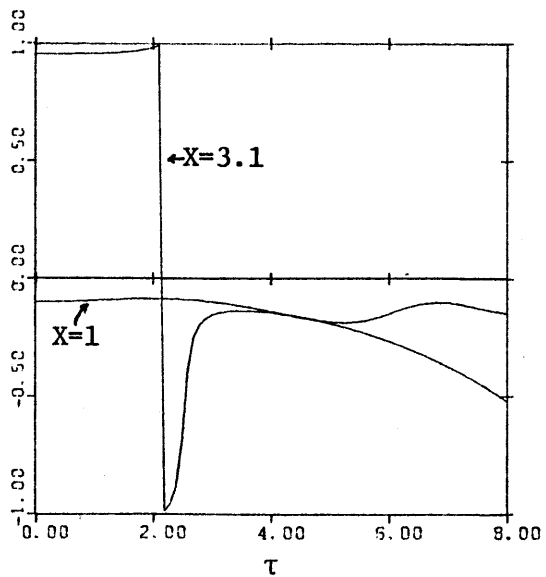


Figure 6.9 Evolution of a Sech Profile over Decreasing Depth,
No Current, K Negative



(b) Wave Amplitude $|A(X, \tau)|$



(c) Wave Phase $\text{Arg}(A(X, \tau))$

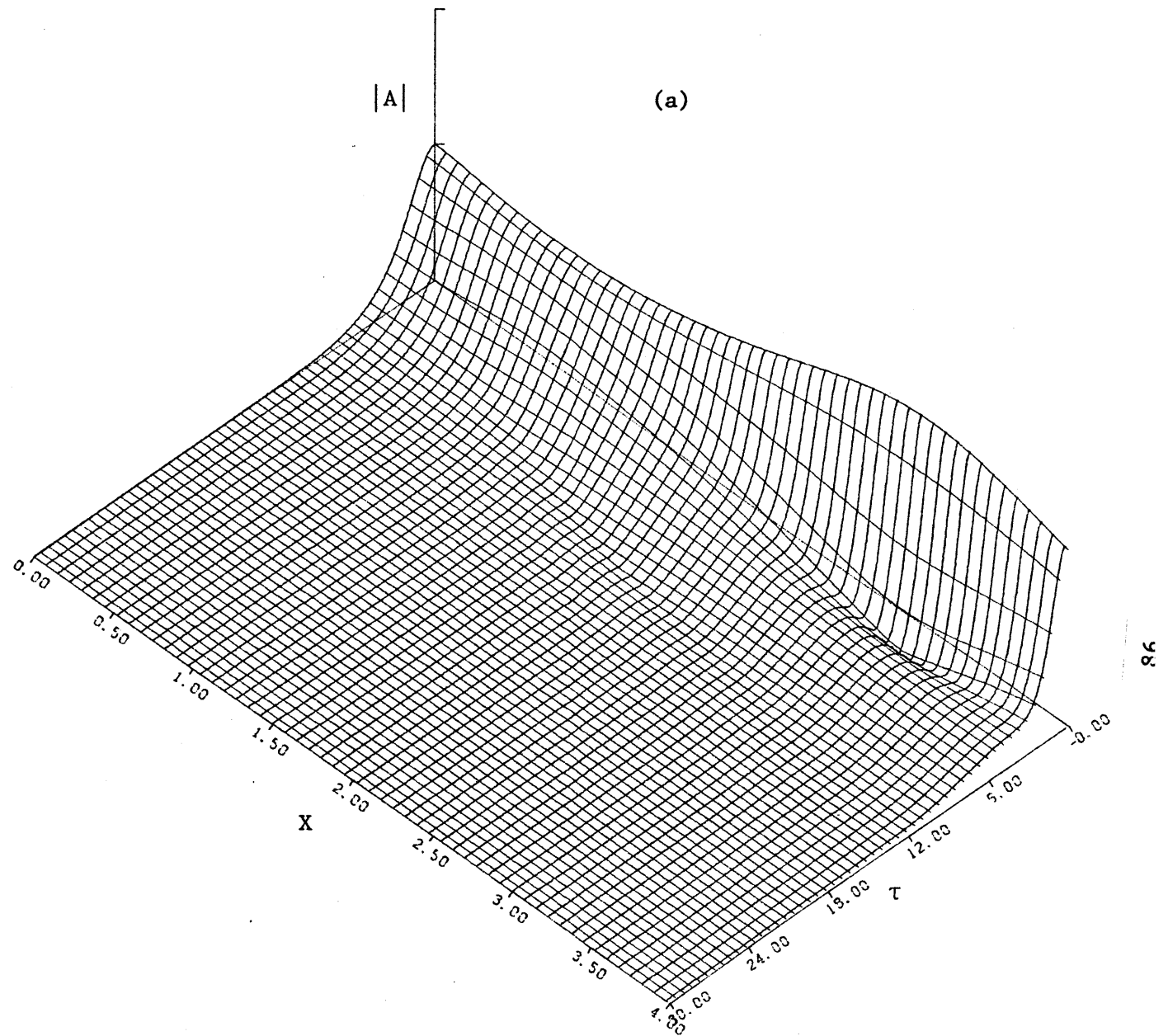
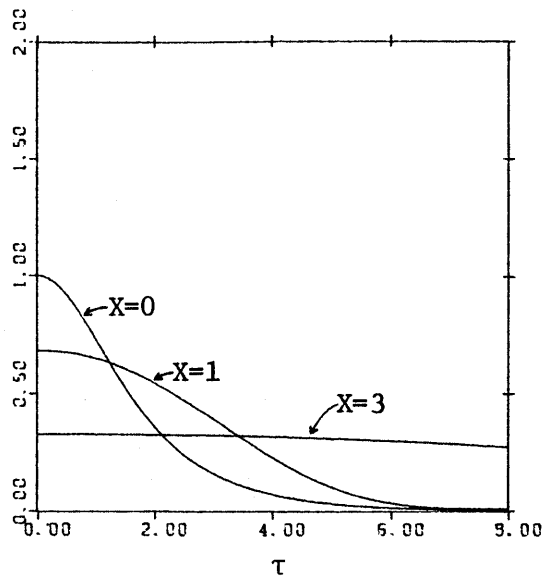
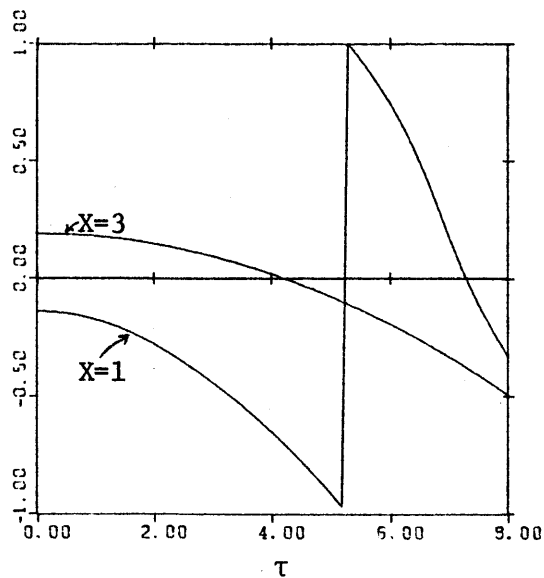


Figure 6.10 Evolution of a Sech Profile over Increasing Depth,
No Current, K Increases from Negative to Positive
Values

envelope (see Fig. 6.11) is a combination of an initial slow decay similar to Fig. (6.6), followed by a very strong radiation similar to Fig. (6.8) or (6.9).



(b) Wave Amplitude $|A(X, \tau)|$



(c) Wave Phase $\frac{\text{Arg}(A(X, \tau))}{\pi}$

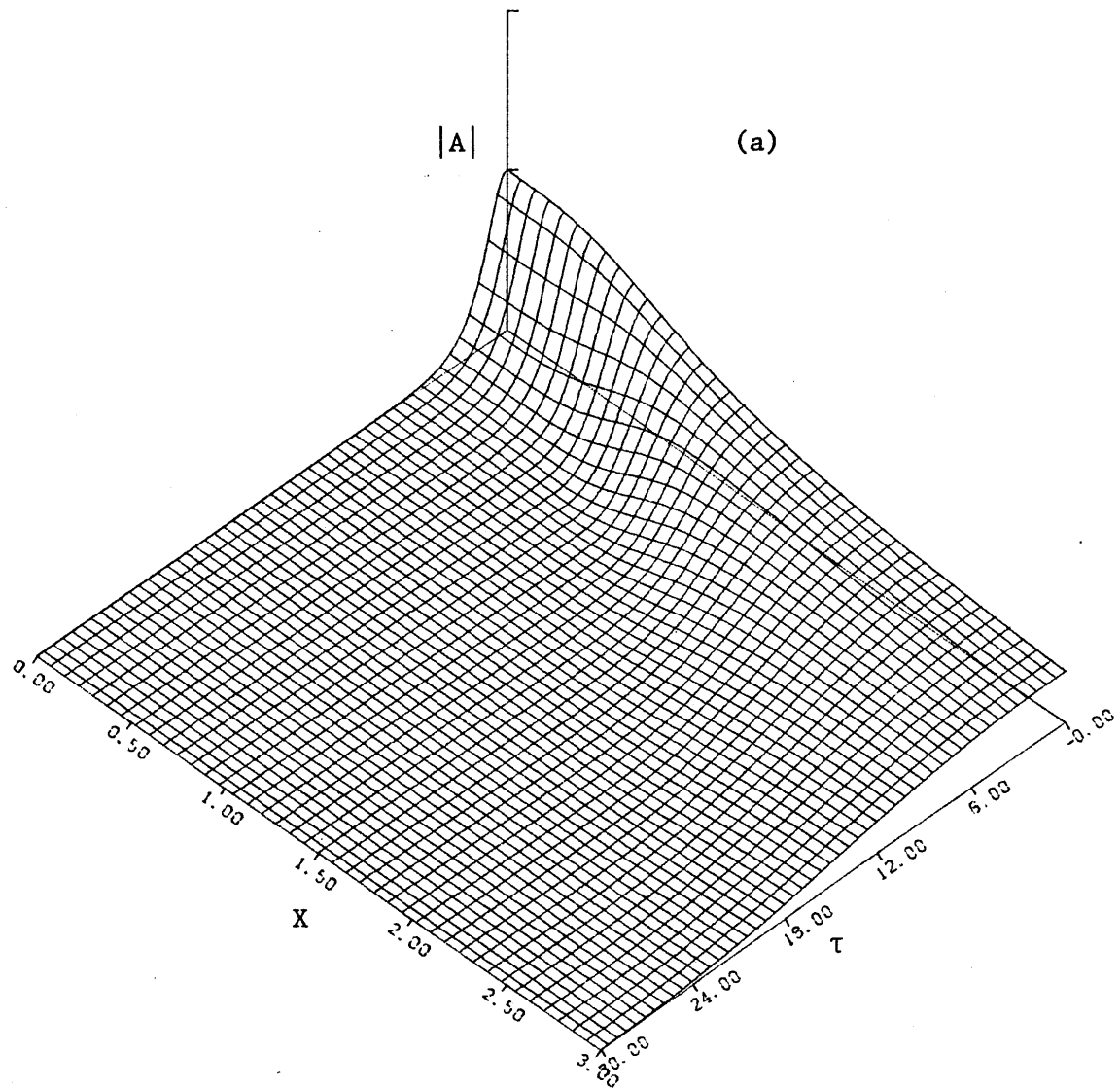
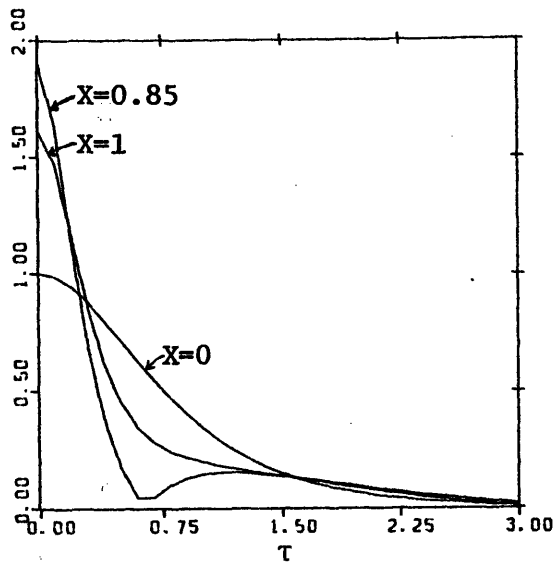


Figure 6.11 Evolution of a Sech Profile over Decreasing Depth,
No Current, K Decreases from Positive to Negative
Values

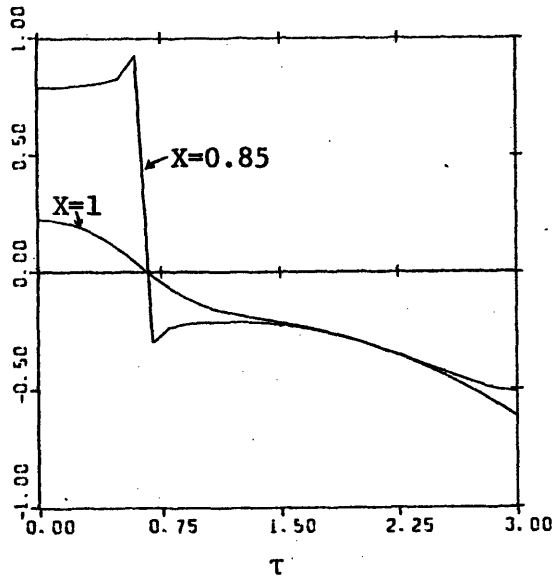
7. Propagation of a Wave Packet Over Varying Depth and Current

7.a Subcritical Current

As discussed at the end of section (4.e), one effect of the current is to increase the wavelength and hence to move the point where K crosses zero towards deeper water. Assuming the geometry of the problem to be fixed as defined in section (5.c) then at $h = 1$ (i.e. $X = 0$) K is positive for small periods only (see Fig. 4.7). For such periods the initial sech profile evolves into N solitons during its propagation over increasing depth, while for larger periods K is negative at $h = 1$ and the initial profile tends to radiate during its evolution. Figs. (7.1) and (7.2) illustrate the effect of a subcritical current $U_1 = 0.5$ propagating in the same direction as the waves. Fig. (7.1) corresponds to waves of period $T = 3$ propagating into deeper water $dh = -0.3$. As it can be seen in Fig. (4.7.b) K is positive everywhere and increases with depth. The initial profile becomes steeper during its propagation into deeper water. It desintegrates and then rebuilds with smaller amplitude with a recurrence distance of the order of 0.6. The qualitative features of the evolution of the initial profile in Fig.(7.1) are similar to those presented in Fig. (6.5) in the case of no currents. The numerical computation gives $m = 1.9$ so that asymptotically only one soliton evolves. However applying D-R's assumption to this case gives $m_s = 2.1$ i.e. two solitons instead of one. It should be noted that this difference becomes important only when X is large. Fig. (7.2) presents the case where $K < 0$



(b) Wave Amplitude $|A(X, \tau)|$



(c) Wave Phase $\text{Arg}(A(X, \tau))$

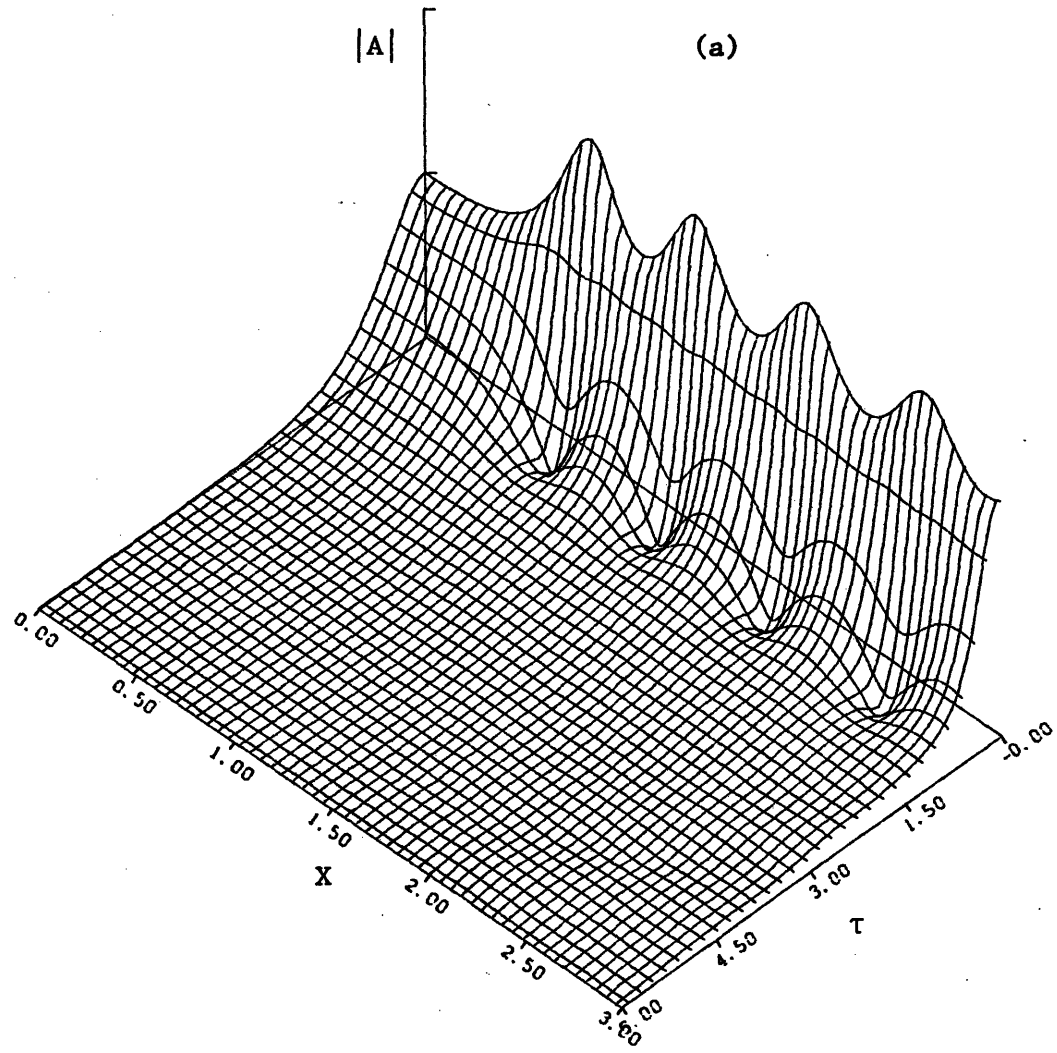
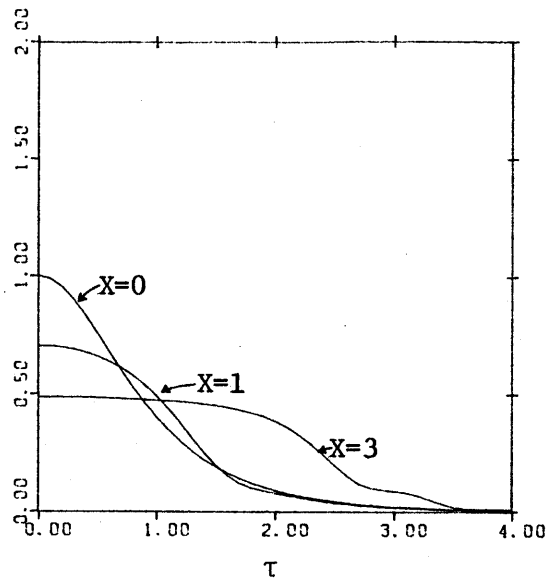
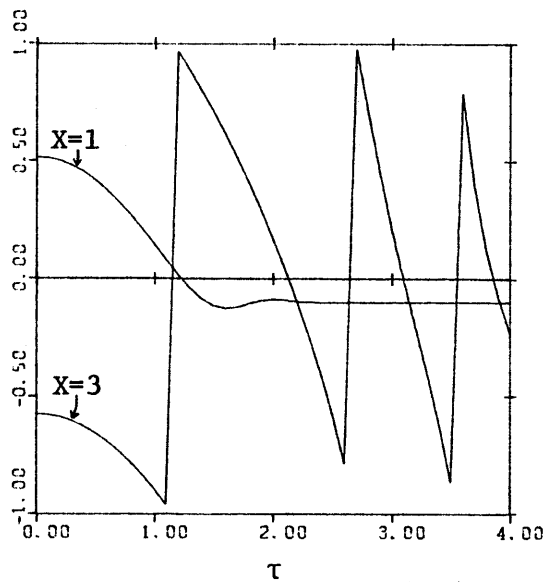


Figure 7.1 Evolution of a Sech Profile over Increasing Depth,
Subcritical Current, K Positive



(b) Wave Amplitude $|A(X, \tau)|$



(c) Wave Phase $\text{Arg}(A(X, \tau))$

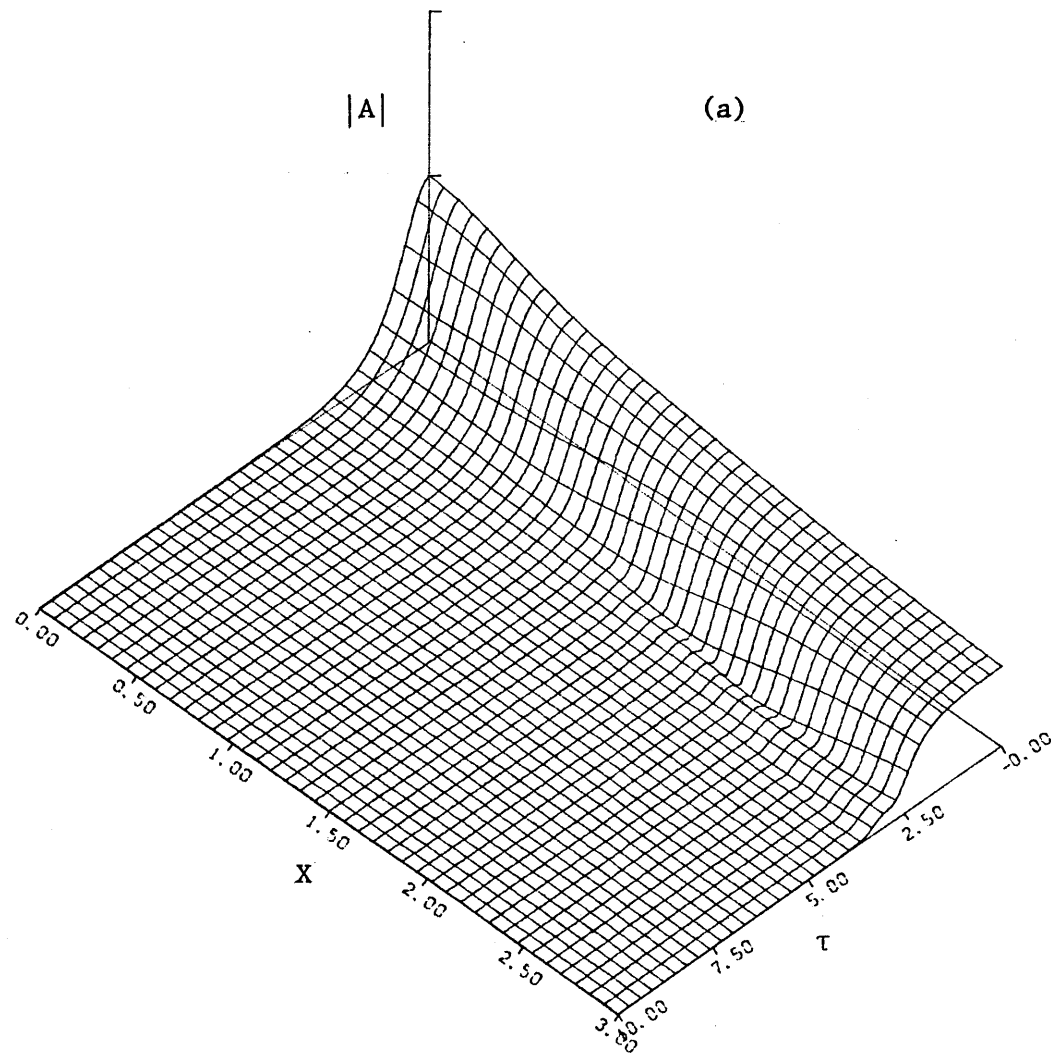
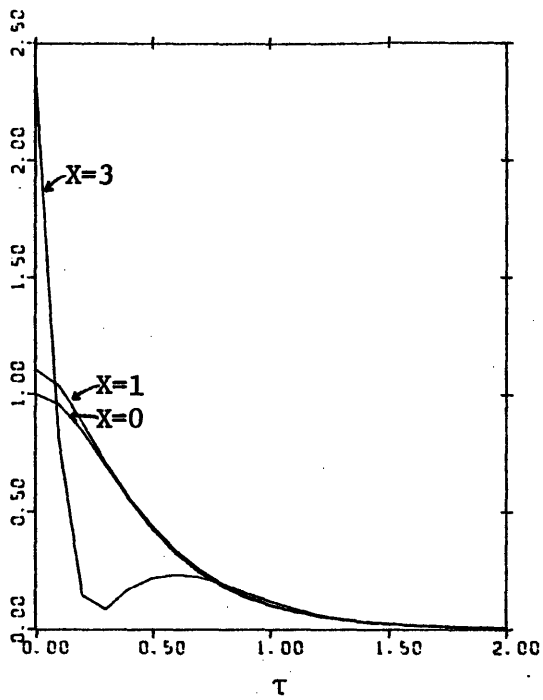


Figure 7.2 Evolution of a Sech Profile over Decreasing Depth,
Subcritical Current, K Negative

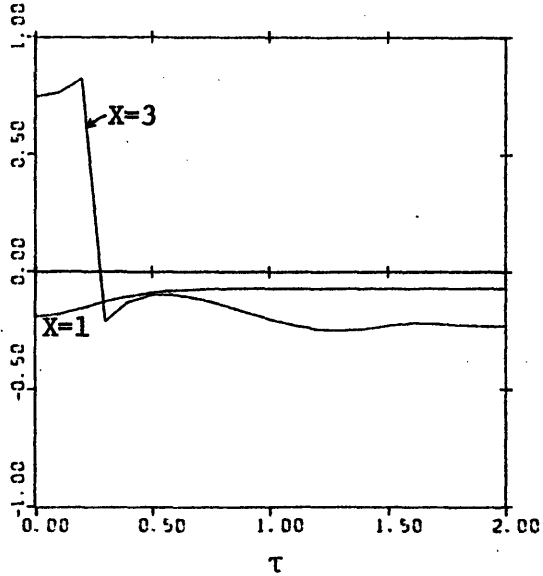
everywhere. Waves of period $\underline{T} = 4$ are propagating towards shallower water $dh = 0.15$. The depth variation has been limited to 0.15 to avoid the critical depth $h_c = 0.82$ (see Fig. 4.7). For such period and depth variation K is negative and decreases with decreasing depth. Fig. (7.2) shows that there is a radiation of the initial profile which becomes flatter and spread towards large τ . Nevertheless the rate of decay is much smaller than in the case of no current see Fig. (6.9).

7.b Supercritical Current

As noted in section (4.e), when the current becomes supercritical turbulence cannot be neglected and our theory is incomplete. Nevertheless in order to show that the evolution of an initial profile depends mainly on the sign of K , we have plotted in Fig. (7.3) and Fig. (7.4) this evolution in the case of a current $U_1 = 2$. It should be recalled that for a supercritical current the variations of $k(\xi+h)$, K and s^{-2} with depth are the opposite of those presented in the case of subcritical current (see Fig. 4.8). Therefore we expect the features of the evolution of an initial profile to be reversed: for example if $K > 0$ the initial profile should steepen with decreasing depth and flatten with increasing depth. We also note that for $U_1 = 2$, $\alpha_2 = 0$ (10^{-2}) so the dispersion has no effect but after a very long distance of propagation. Finally Fig. (4.8) suggests that at the depth $h = 1$, K is negative except for very small periods (say $\underline{T} < 1.75$). Fig. (7.3) illustrates the case of waves of period $\underline{T} = 1.5$ propagating into shallower water $dh = 0.3$. It shows the appearance of the first node after a long distance of propagation $X = 3$. The result is opposite to that obtained in the case of subcritical current where the initial sech profile flattened when propagating into shallower water. The numerical computation of m gives $m = 2.1$ which



(b) Wave Amplitude $|A(X, \tau)|$



(c) Wave Phase $\frac{\text{Arg}(A(X, \tau))}{\pi}$

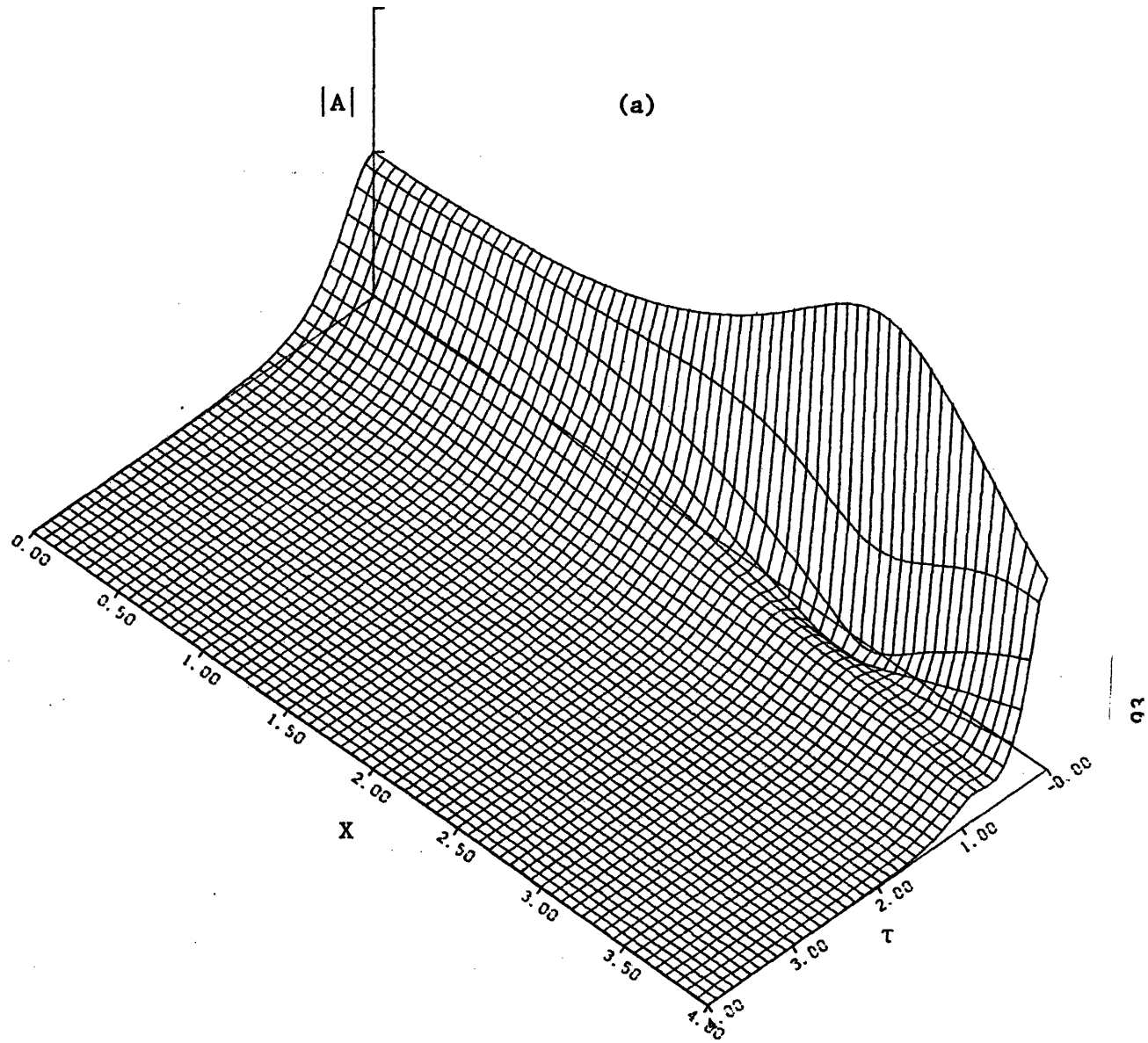
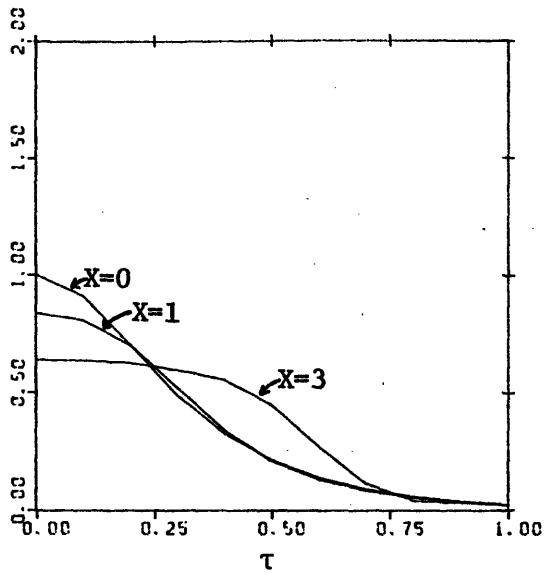
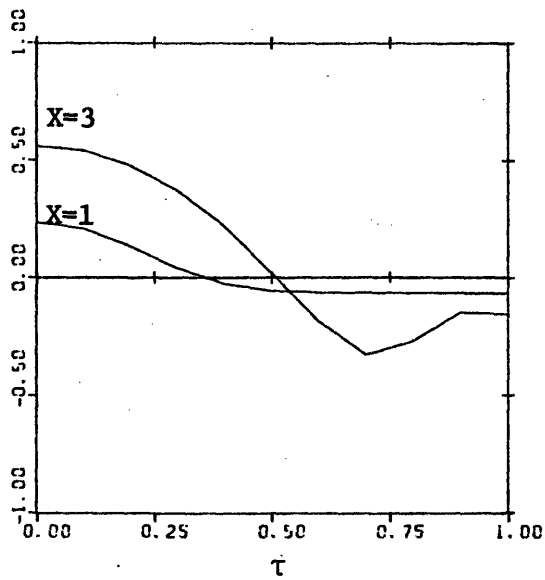


Figure 7.3 Evolution of a Sech Profile over Decreasing Depth,
Supercritical Current, K Positive



(b) Wave Amplitude $|A(X, \tau)|$



(c) Wave Phase $\text{Arg}(A(X, \tau))$

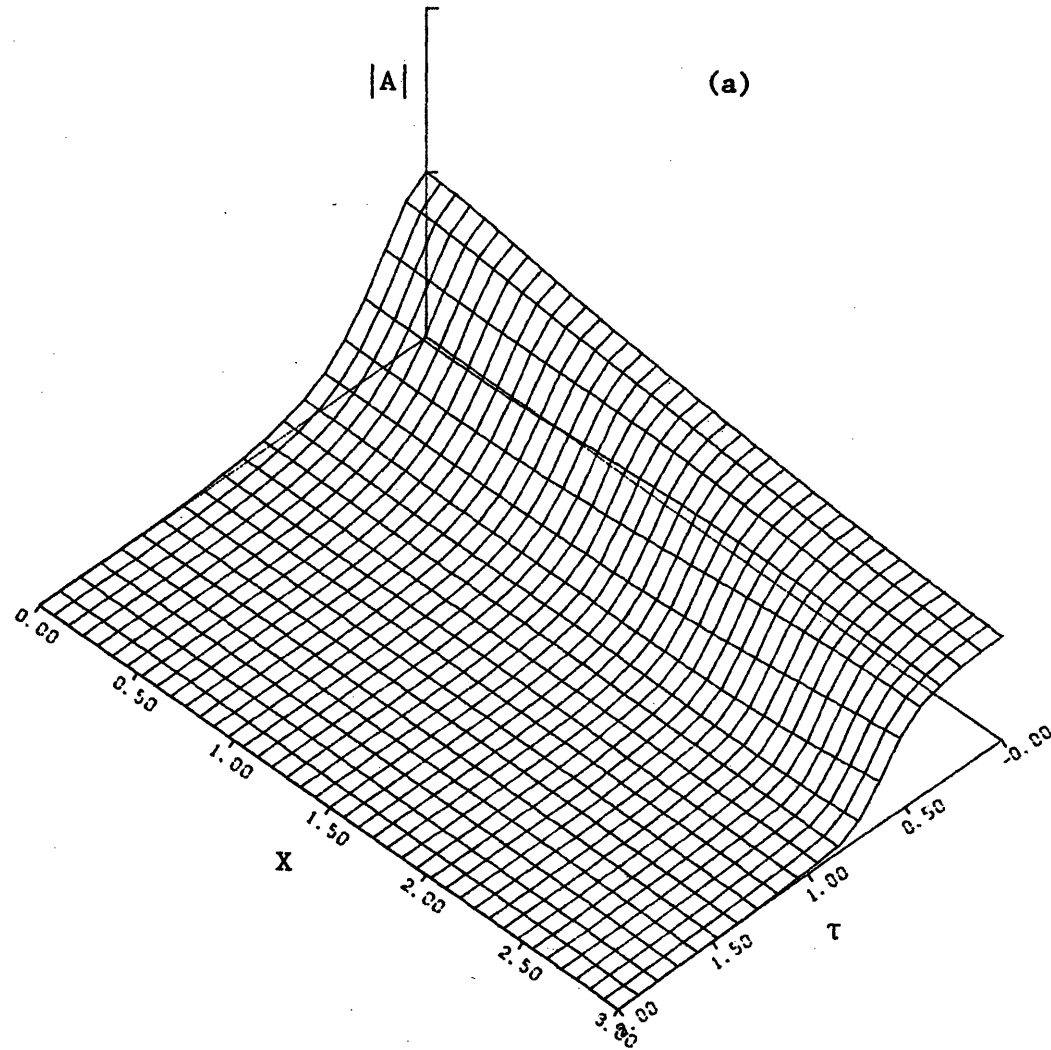
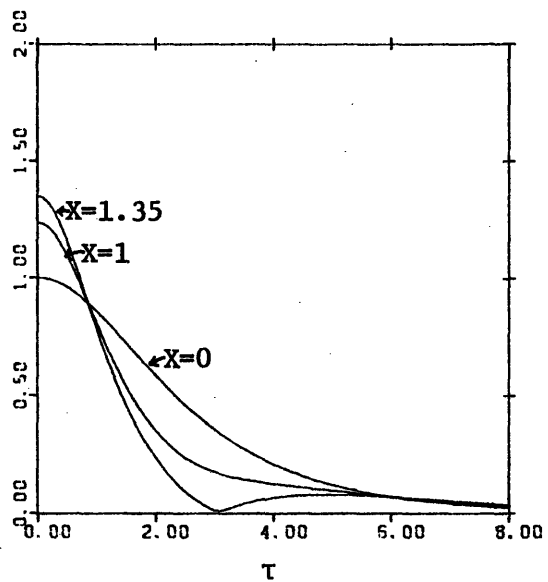


Figure 7.4 Evolution of a Sech Profile over Increasing Depth,
Supercritical Current, K Negative

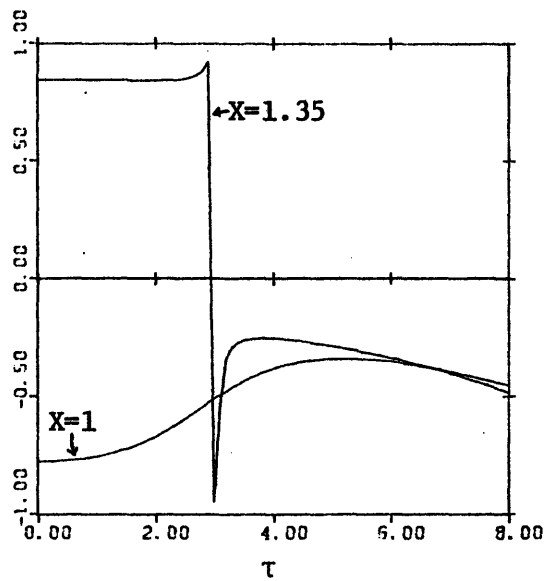
suggests that the wave envelope evolves into two solitons plus some oscillations which dies for large X . Fig. (7.4) corresponds to waves of period $T = 2$ propagating into deeper water $dh = - 0.3$. In this case K is negative everywhere and the initial profile decays. The radiation is very small. At this point the sign of K and its variations with depth appear to be essential in determining the qualitative features of the evolution of an initial sech profile.

7.c Subcritical Opposing Current

A current propagating against waves tends to decrease their wavelength and hence moves the point where K crosses zero towards shallower water (see Fig. (4.9)). But as shown in Fig. (4.5) for any given current velocity and depth there exist a critical period such that waves with smaller period can not propagate against that current. For example waves of period less than ~ 2.5 cannot propagate at $h = 1$ against a current $U_1 = - 0.1$. Near the stopping point, our assumption of weakly nonlinear wave breakdown; the dispersion effect represented by α_2 becomes very large and hence the initial profile will change over a very short distance of propagation. Several cases have been studied to illustrate the effect of an opposite current on the evolution of waves. Fig. (7.5) - (7.6) present the case where K is positive everywhere. Fig. (7.5) represents waves of period $T = 6$ propagating into deeper water $dh = 0.5$, against a current $U_1 = - 0.1$. The initial soliton profile increases in steepness during its propagation, disintegrates and then rebuilds itself after a near recurrence period of order 2. The evolution picture is very



(b) Wave Amplitude $|A(X, \tau)|$



(c) Wave Phase $\text{Arg}(A(X, \tau))$

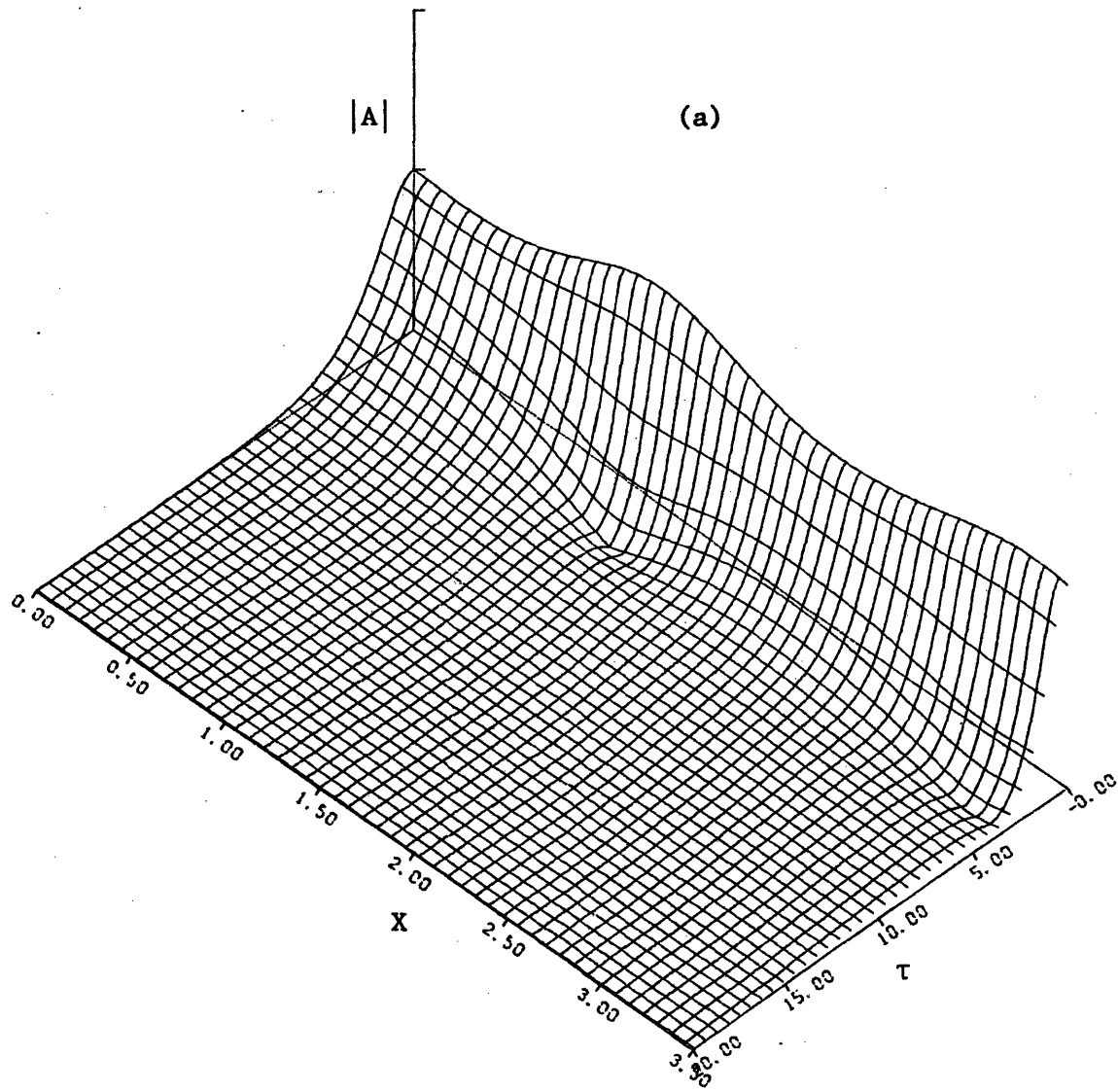
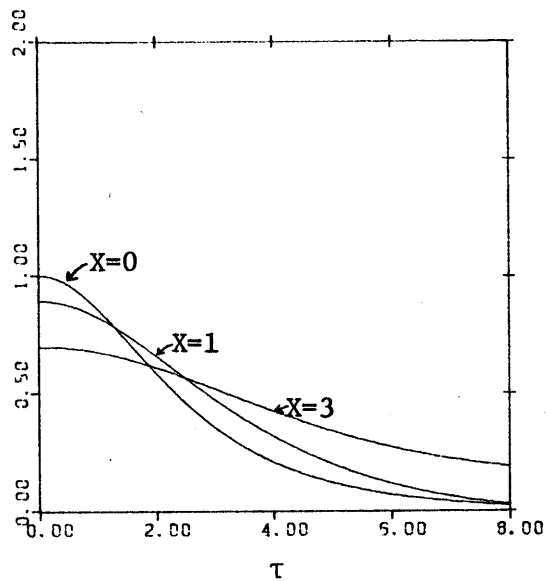
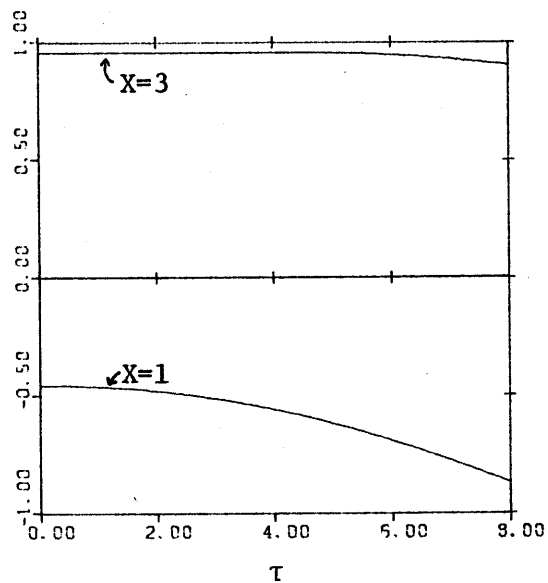


Figure 7.5 Evolution of a Sech Profile over Increasing Depth,
Opposing Current, K Positive

similar to the one obtained in Fig. (6.5). In Fig. (7.6) the wave period \underline{T} is still $\underline{T} = 6$, however the waves propagate towards decreasing depth $dh = 0.15$ and against a current $U_1 = -0.1$. In this case $K > 0$ but decreases. The plot shows a small decay in the wave envelope maximum amplitude very similar to the one obtained in Fig. (6.6). Since K is positive everywhere in the two previous cases we have calculated Δ , the relative difference between the area under the wave envelope at $X = L$ as expected by D-R theory and as computed numerically. In the case of Fig. (7.5) $\Delta = 8.4\%$. The large values obtained for Δ shows once again that the D-R assumption is not reliable. According to the numerical results $m = 1.61$ for Fig.(7.5). A soliton would evolve for large X . To point out the effect of the magnitude of the depth variation we have plotted in Fig. (7.7) the propagation of a soliton corresponding to waves of period $\underline{T} = 6$ over an increasing depth $dh = -0.3$. By comparing this figure to the previous one, we can see that the effect of decreasing the magnitude of dh is to lengthen the near recurrence period and to decrease the maximum amplitude. As the opposite current increases, the only waves which can propagate at $h = 1$ without being stopped are those having a large period. For such waves the parameter K tends to become negative in the neighborhood of $h = 1$ (see Fig. 4.9) and therefore an initial sech profile will decay during its propagation over variable depth. This effect is illustrated in Fig. (7.8) for waves with period $\underline{T} = 7$ propagating into deeper water $dh = -0.15$, against a current $U_1 = -0.1$. The initial profile radiates during its propagation qualitatively as in the case of no current, $K < 0$ (see Fig. 6.8).



(b) Wave Amplitude $|A(X, \tau)|$



(c) Wave Phase $\frac{\text{Arg}(A(X, \tau))}{\pi}$

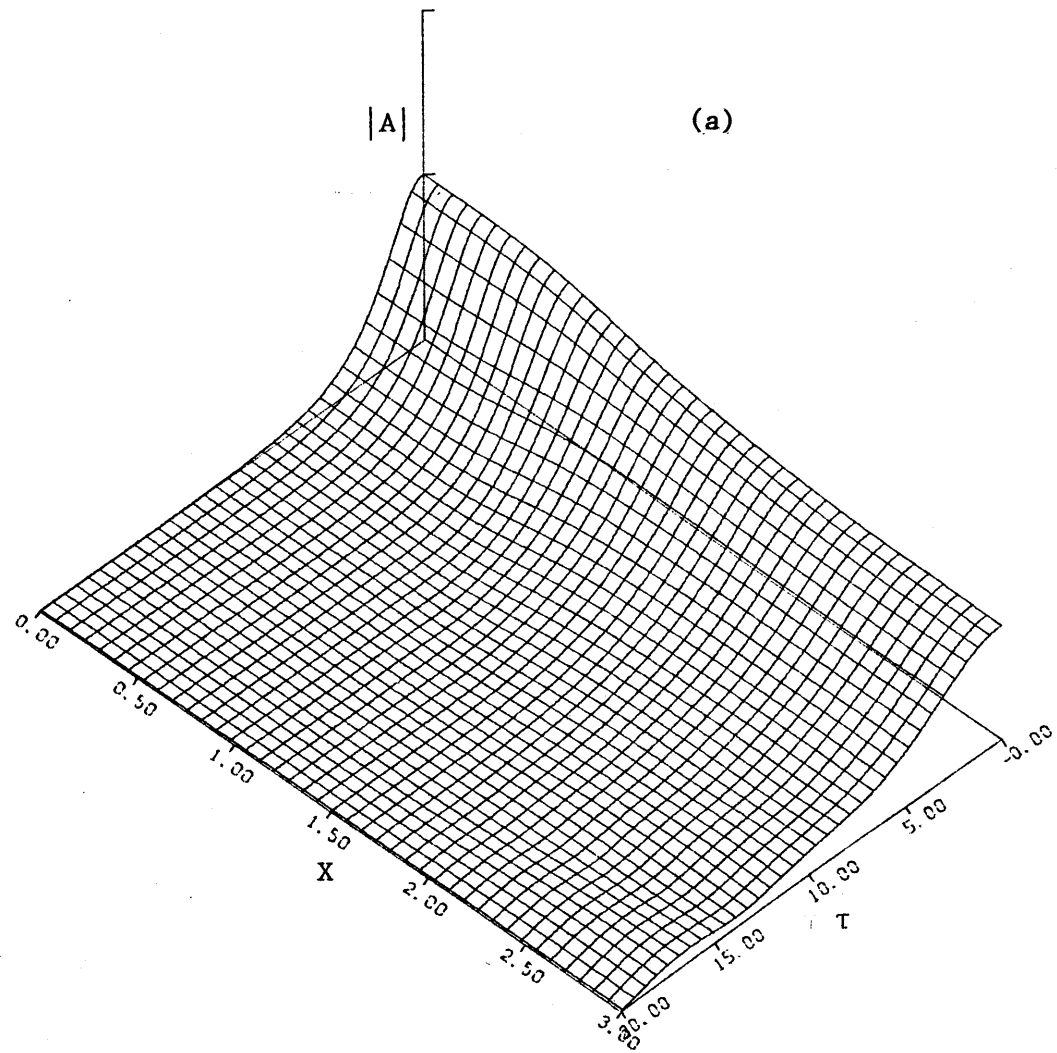
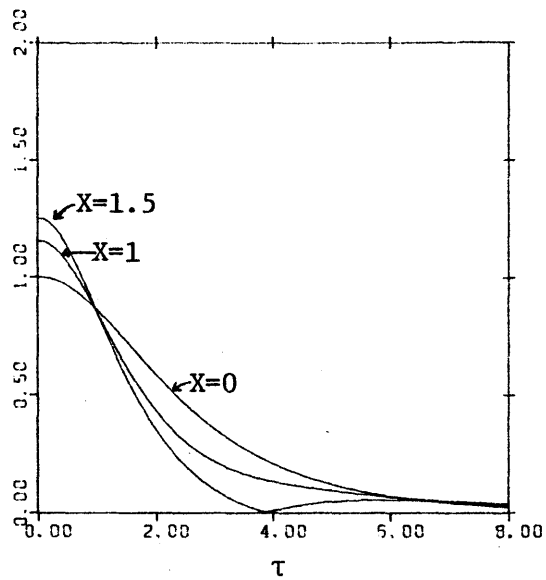
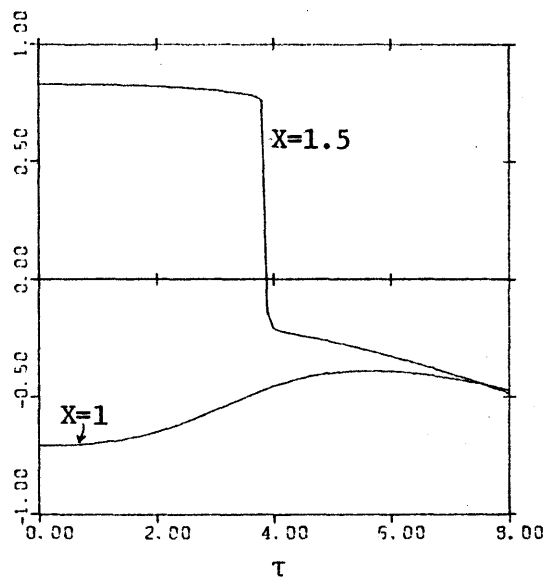


Figure 7.6 Evolution of a Sech Profile over Decreasing Depth,
Opposing Current, K Positive



(b) Wave Amplitude $|A(X, \tau)|$



(c) Wave Phase $\frac{\text{Arg}(A(X, \tau))}{\pi}$

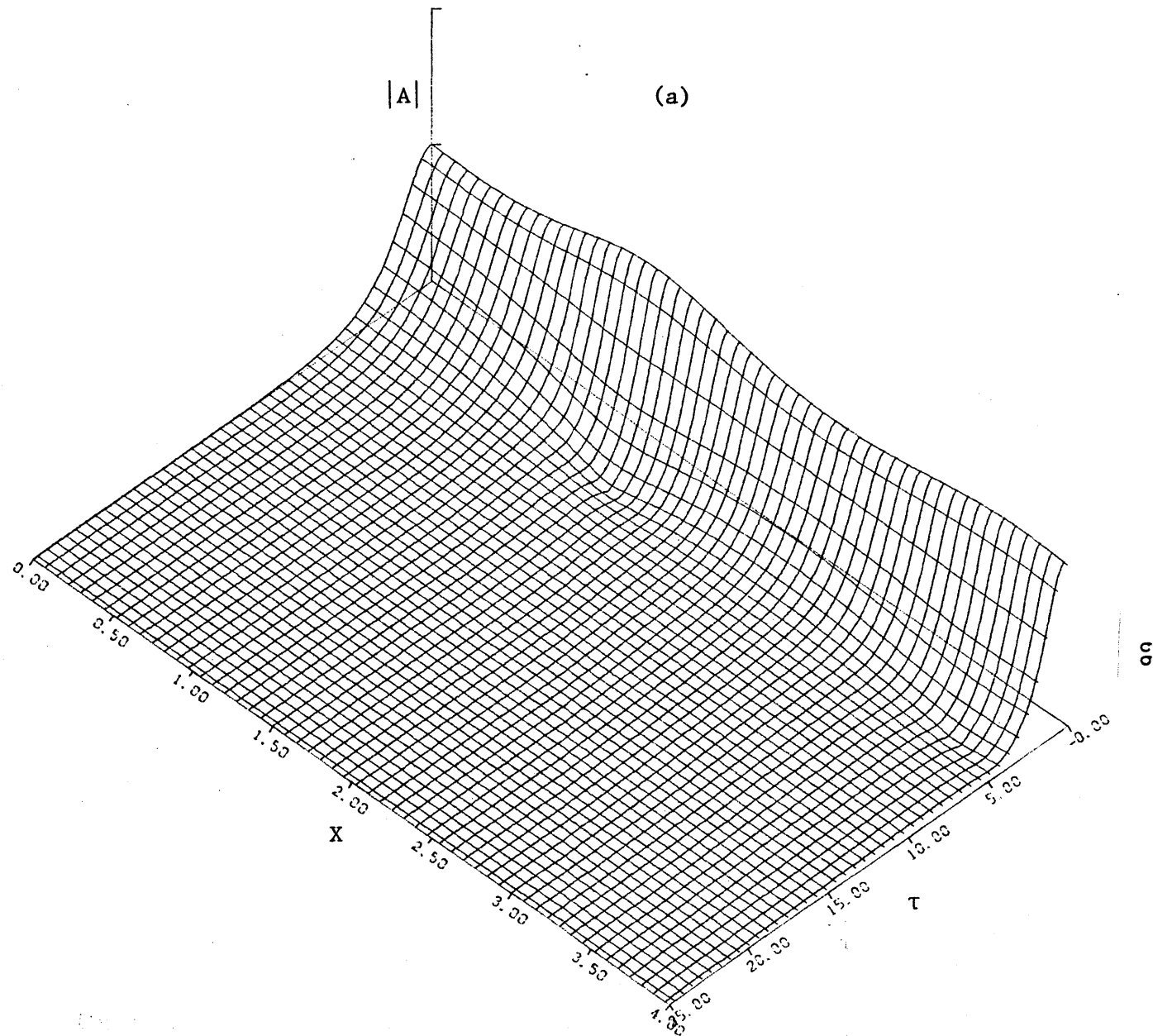
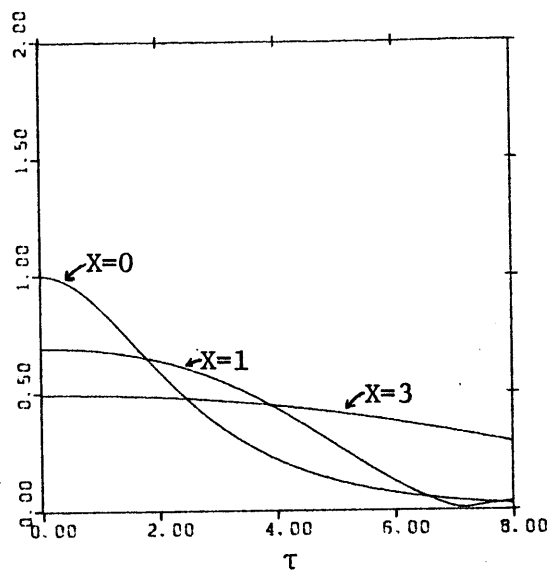
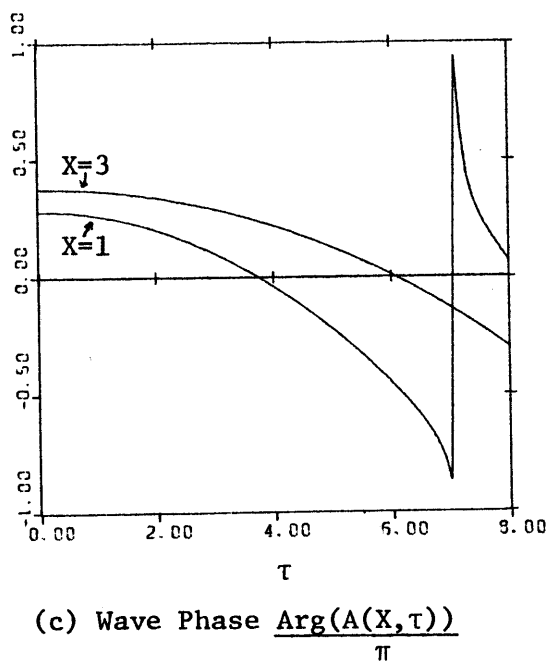


Figure 7.7 Evolution of a Sech Profile over Increasing Depth,
Opposing Current, K Positive



(b) Wave Amplitude $|A(X, \tau)|$



(c) Wave Phase $\frac{\text{Arg}(A(X, \tau))}{\pi}$

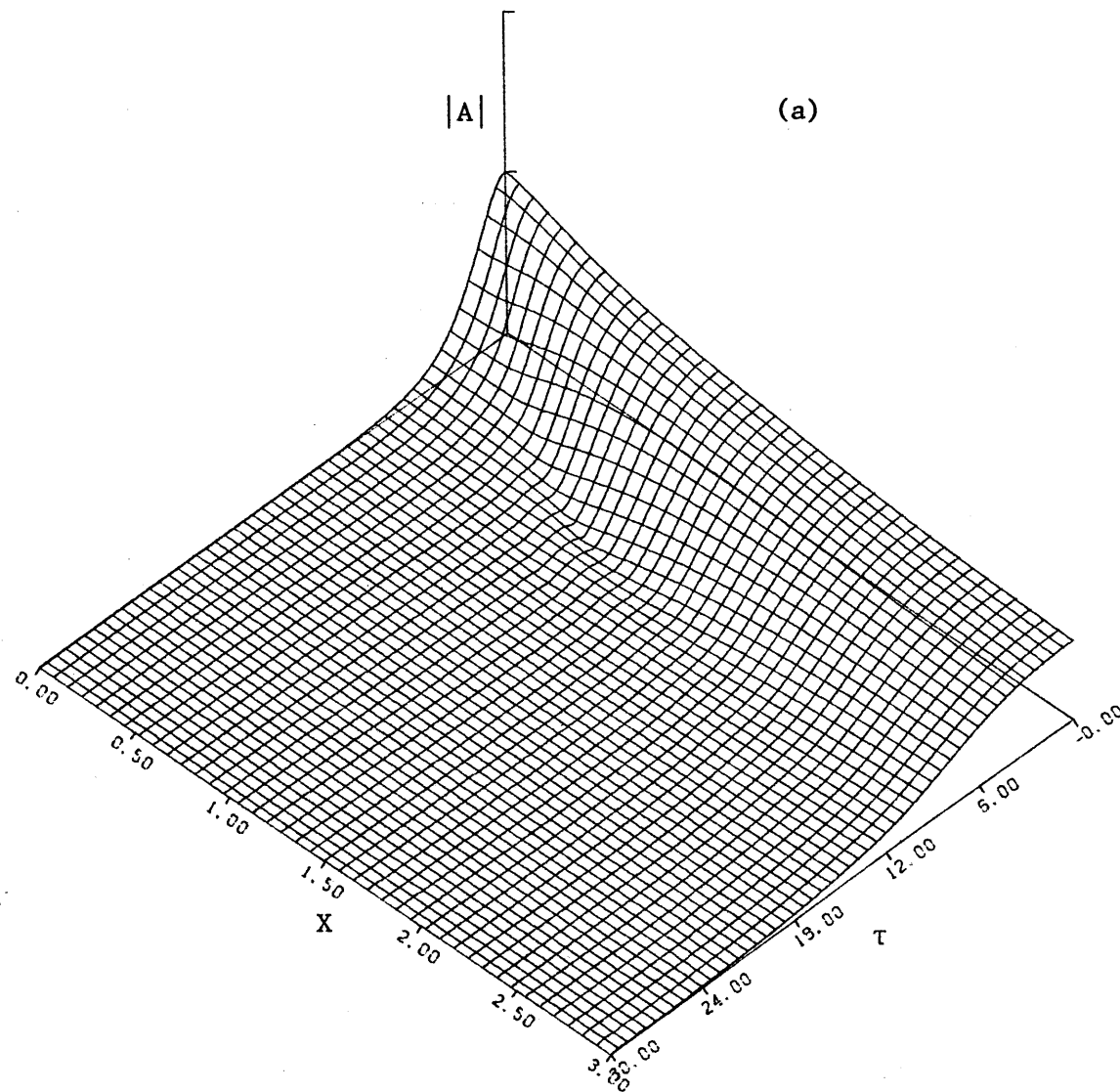


Figure 7.8 Evolution of a Sech Profile over Increasing Depth,
Opposing Current, K Negative

8. Conclusion

The previous results are a general survey of the evolution of a slowly modulated wave packet propagating over varying depth, in the same direction as a strong current or in the opposite direction. They show that for any subcritical current the qualitative features of the evolution depend only on the sign of K and its variations: K increases with increasing depth and decreases with decreasing depth.

In the case where K is positive everywhere, an initial soliton profile propagating into deeper water becomes steeper and steeper. At the end of the depth change, the wave envelope is more peaked and evolves into a soliton or a multisoliton appropriate for the new depth. Depending on the characteristics of the initial soliton, of the depth variation and of the current, the profile can fission into 2-bounded solitons with near recurrence periods. On the other hand when the initial soliton profile propagates into shallower water, it becomes flatter and flatter. At the end of the depth change, the wave envelope can either evolve into a soliton adapted to the new depth or desintegrates as $X \rightarrow \infty$.

In the case where K is negative everywhere, whatever the depth variation is, the initial profile desintegrates during its propagation. The width in τ of the wave packet increases with X while its maximum amplitude decays. The rate of decay of the maximum amplitude with X is dependent on the characteristics of the waves, the current and the depth variation.

When K changes sign as the depth varies, two cases can occur. The first one corresponds to waves propagating into shallower water, in this case K is initially positive and becomes negative as the depth decreases. The initial profile, first begins to flatten but as the sign of K changes its rate of decay increases and finally it desintegrates. The second case corresponds to waves propagating into deeper water and hence K increases from an initial negative value to a positive one. In the region where K is negative the waves envelope begins to desintegrate. If the profile of the waves envelope is very flat at the point where K becomes negative, it would just pursue its desintegration while propagating into the region where K is positive, otherwise it would evolve into a soliton or a multi-soliton.

The previous discussion pointed out the importance of the sign of K for the evolution of an initial wave packet. As shown in Figure (4.6), (4.9) this sign depends on the wave period, the depth and the current. For a given period a strong current in the same direction as the waves tends to decrease the value of K at a given depth and hence moves the point where K changes its sign towards deeper water. Therefore in the presence of the current, except for short wave packets, any initial wave period whose envelope is a sech profile desintegrates during its propagation over variable depth. Depending on the depth variation a short wave packet can desintegrate if the depth decreases or evolves into a soliton or a multisoliton if the depth increases. For a current propagating against waves the effect is to move the point where K crosses zero towards shallower water and therefore long wave packets only, desintegrates during their propagation over variable depth. (The opposite current also affects the

propagation of waves since it can stop the shortest of them; our weakly nonlinear theory is not valid in the neighborhood of this stopping depth. Therefore as the current increases only long waves can propagate at the initial depth $h = 1$ and the envelope of such a long wave desintegrates during its propagation over varying depth.

Through the numerical study we have shown that the assumption of 'shape conservation' made by Djordjevic and Redekopp to derive their analytical solution for the propagation of an initial soliton over slowly varying depth, is not valid. The difference between the areas under the wave envelope profile at the end of the depth change as predicted using D-R's assumption and as calculated numerically is in some cases about 22%. It has been checked that this large difference is not due to the numerical method.

Finally this study shows the very drastic effect of depth variation and strong current on the propagation of a wave packet. It is based on the assumption that the current is strong enough to influence the waves without being influenced by them. This assumption holds in some cases, for example a harbor entrance with a river flow; our results can then be applied directly. In nature most currents are weak i.e. of the same order of magnitude as waves. A new study is then needed to include the effect of waves on the current itself and our results should be considered as a first step to improve our understanding of this problem.

Figure Captions: Part I

Figure 3.1: Nonlinearity coefficient γ

Figure 4.1: Specific Head Diagram

Figure 4.2: Critical depth

Figure 4.3: Set-up due to the current

Figure 4.4: Dispersion Relation Diagram

Figure 4.5: (a) Stopping periods $T'' = \frac{2\pi}{\omega} \sqrt{\frac{g}{d}}$ for negative currents

$$U'' = \frac{U}{\sqrt{gd}}$$

(b) Stopping periods $T' = \frac{2\pi}{\omega} \sqrt{\frac{g}{H_1}}$ as a function of depth $\frac{h}{H_1}$.
for different current $\frac{U_1}{\sqrt{gH_1}} = -0.1, -0.3, -0.6, -0.9$

Figure 4.6: (a) Wave number kh , (b) Instability parameter K , (c) Inverse of the shoaling coefficient s^{-2} . (No current). $\underline{T} = 4, 5, 6, 7$

Figure 4.7: (a) Wave number kd , (b) Instability parameter K , (c) Inverse of the shoaling coefficient s^{-2} for a subcritical current $U_1 = 0.5$. $\underline{T} = 3, 4, 5, 6$

Figure 4.8: (a) Wave number kd , (b) Instability parameter K , (c) Inverse of the shoaling coefficient s^{-2} for a supercritical current $U_1 = 2$. $\underline{T} = 1, 1.5, 2, 2.5$

Figure 4.9: (a) Wave number kd , (b) Instability parameter K , (c) Inverse of the shoaling coefficient s^{-2} for an opposing current $U_1 = -0.1$. $\underline{T} = 6, 6.5, 7, 8$

Figure 5.1: (a) 3-dimensional plot of the wave amplitude $|A(X, \tau)|$;
(b) Wave amplitude $|A(X, \tau)|$, and (c) phase $\text{Arg}(A(X, \tau))$ for $X = 0, 1, 4$. No current, constant depth $h = 1$, wave period $\underline{T} = 5$, $K = 1.4$, $(kh) = 1.69$, $m = 1.5$

Figure 5.2: Geometry of the problem

Figure 6.1: (a) 3-dimensional plot of the wave amplitude $|A(X,\tau)|$,
(b) Wave amplitude $|A(X,\tau)|$, and (c) Phase $\text{Arg}(A(X,\tau))$
for $X = 0, 1, 3$, $U_1 = 0$, $\underline{T} = 7$, $dh = 0$, $K = -3.33$,
 $(kh) = 1.04$

Figure 6.2: (a) 3-dimensional plot of the wave amplitude $|A(X,\tau)|$,
(b) Wave amplitude $|A(X,\tau)|$, and (c) Phase $\text{Arg}(A(X,\tau))$
for $X = 0, 1, 3$, $U_1 = 0$, $\underline{T} = 5$, $dh = 0$, $K = 1.4$,
 $(kh) = 1.69$, $m = 1.25$

Figure 6.3: (a) 3-dimensional plot of the wave amplitude $|A(X,\tau)|$,
(b) Wave amplitude $|A(X,\tau)|$, and (c) Phase $\text{Arg}(A(X,\tau))$
for $X = 0, 0.72, 1$, $U_1 = 0$, $\underline{T} = 5$, $dh = 0$, $K = 1.4$,
 $(kh) = 1.69$, $m = 2.0$

Figure 6.4: (a) 3-dimensional plot of the wave amplitude $|A(X,\tau)|$,
(b) wave amplitude $|A(X,\tau)|$, and (c) Phase $\text{Arg}(A(X,\tau))$.
for $X = 0, 0.4, 1$, $U_1 = 0$, $T = 5$, $dh = 0$, $T = 5$,
 $dh = 0$, $K = 1.4$, $(kh) = 1.69$, $m = 1.5$

Figure 6.5: (a) 3-dimensional plot of the wave amplitude $|A(X,\tau)|$,
(b) Wave amplitude $|A(X,\tau)|$, and (c) Phase $\text{Arg}(A(X,\tau))$
for $X = 0, 0.9, 1$, $U_1 = 0$, $\underline{T} = 5$, $dh = -0.5$, $K_1 = 1.4$,
 $(kh)_1 = 1.69$, $K_2 = 2.6$, $(kh)_2 = 2.4$, $m = 1.62$, $\Delta = -22\%$,
global energy error = 4.2%

Figure 6.6: (a) 3-dimensional plot of the wave amplitude $|A(X,\tau)|$,
(b) Wave amplitude $|A(X,\tau)|$, and (c) Phase $\text{Arg}(A(X,\tau))$
for $X = 0, 1, 4$, $U_1 = 0$, $\underline{T} = 5$, $dh = 0.15$, $K_1 = 1.4$,
 $(kh)_1 = 1.69$, $K_2 = 0.72$, $(kh)_2 = 1.49$, $m = 1.3$,
 $\Delta = 11\%$, global energy error = 0.1%

Figure 6.7: (a) 3-dimensional plot of the wave amplitude $|A(X,\tau)|$,
 (b) Wave amplitude $|A(X,\tau)|$, and (c) Phase $\text{Arg}(A(X,\tau))$
 for $X = 0.1, 1.6, U_1 = 0, \tau = 5, dh = -0.3, K_1 = 1.4,$
 $(kh)_1 = 1.69, K_2 = 2.19, (kh)_2 = 2.11, m = 1.5,$
 $\Delta = -26.6\%, \text{ global energy error} = 2.5\%$

Figure 6.8: (a) 3-dimensional plot of the wave amplitude $|A(X,\tau)|$,
 (b) Wave amplitude $|A(X,\tau)|$, and (c) Phase $\text{Arg}(A(X,\tau))$
 for $X = 0, 1, 3, U_1 = 0, \tau = 7, dh = -0.3, K_1 = -3.3,$
 $(kh)_1 = 1.04, K_2 = -0.65, (kh)_2 = 1.24, \text{ global energy}$
 $\text{error} < 0.1\%$

Figure 6.9: (a) 3-dimensional plot of the wave amplitude $|A(X,\tau)|$,
 (b) Wave amplitude $|A(X,\tau)|$, and (c) Phase $\text{Arg}(A(X,\tau))$
 for $X = 0, 1, 3, U_1 = 0, \tau = 7, dh = 0.3, K_1 = -3.30,$
 $(kh)_1 = 1.04, K_2 = -14.6, (kh)_2 = 0.83, \text{ global energy}$
 $\text{error} = 0.1\%$

Figure 6.10: (a) 3-dimensional plot of the wave amplitude $|A(X,\tau)|$,
 (b) Wave amplitude $|A(X,\tau)|$, and (c) Phase $\text{Arg}(A(X,\tau))$
 for $X = 0, 1, 3, U_1 = 0, \tau = 6, dh = -0.5, K_1 = -0.54,$
 $(kh)_1 = 1.28, K_2 = 1.10, (kh)_2 = 1.75, m = 1.98, \text{ global}$
 $\text{energy error} = 0.05\%$

Figure 6.11: (a) 3-dimensional plot of the wave amplitude $|A(X,\tau)|$,
 (b) Wave amplitude $|A(X,\tau)|$, and (c) Phase $\text{Arg}(A(X,\tau))$
 for $X = 0, 1, 3, U_1 = 0, \tau = 5, dh = 0.3, K_1 = 1.4$
 $(kh)_1 = 1.69, K_2 = -0.68, (kh)_2 = 1.29, \text{ global energy}$
 $\text{error: } 0.1\%$

Figure 7.1: (a) 3-dimensional plot of the wave amplitude $|A(X,\tau)|$,
 (b) Wave amplitude $|A(X,\tau)|$, and (c) Phase $\text{Arg}(A(X,\tau))$
 for $X = 0, 0.85, 1$, $U_1 = 0.5$, $\underline{T} = 3$, $dh = -0.3$, $K_1 =$
 6.0 , $(kd)_1 = 1.68$, $K_2 = 15.7$, $(kd)_2 = 2.62$, $m = 1.9$,
 $\Delta = -15.2\%$ global energy error = 5%

Figure 7.2: (a) 3-dimensional plot of the wave amplitude $|A(X,\tau)|$,
 (b) Wave amplitude $|A(X,\tau)|$, and (c) Phase $\text{Arg}(A(X,\tau))$
 for $X = 0, 1, 3$, $U_1 = 0.5$, $\underline{T} = 4$, $dh = 0.15$, $K_1 =$
 -4.8 , $(dk)_1 = 1.17$, $K_2 = -42$, $(kd)_2 = 0.82$, global
 energy error.

Figure 7.3: (a) 3-dimensional plot of the wave amplitude $|A(X,\tau)|$,
 (b) Wave amplitude $|A(X,\tau)|$, and (c) Phase $\text{Arg}(A(X,\tau))$
 for $X = 0, 1, 3$, $U_1 = 2$, $\underline{T} = 1.5$, $dh = 0.3$, $K_1 = 17.9$,
 $(kd)_1 = 1.51$, $K_2 = 48.0$, $(kd)_2 = 1.86$, $m = 2.1$, $\Delta =$
 -0.9% global energy error: 0.2%

Figure 7.4: (a) 3-dimensional plot of the wave amplitude $|A(X,\tau)|$,
 (b) Wave amplitude $|A(X,\tau)|$, and (c) Phase $\text{Arg}(A(X,\tau))$
 for $X = 0, 1, 3$, $U_1 = 2$, $\underline{T} = 2$, $dh = -0.3$, $K_1 = -39.9$
 $(kd)_1 = 1.1$, $K_2 = -91.0$, $(kd)_2 = 0.95$, global energy
 error: 0.05%

Figure 7.5: (a) 3-dimensional plot of the wave amplitude $|A(X,\tau)|$,
 (b) Wave amplitude $|A(X,\tau)|$, and (c) Phase $\text{Arg}(A(X,\tau))$
 for $X = 0, 1, 1.35$, $U_1 = -0.1$, $\underline{T} = 6$, $dh = -0.5$,
 $K_1 = 0.63$, $(kd)_1 = 1.58$, $K_2 = 1.1$, $(kd)_2 = 2.01$,
 $m = 1.61$, $\Delta = -13.4\%$ global energy error = 0.5%

Figure 7.6: (a) 3-dimensional plot of the wave amplitude $|A(X,\tau)|$,
 (b) Wave amplitude $|A(X,\tau)|$, and (c) Phase $\text{Arg}(A(X,\tau))$
 for $X = 0, 1, 3$, $U_1 = -0.1$, $\tau = 6$, $dh = 0.15$, $K_1 =$
 0.63 , $(kd)_1 = 1.58$, $K_2 = 0.41$, $(kd)_2 = 1.48$, $m = 1.3$,
 $\Delta = 8.4\%$ global energy error $< 0.1\%$

Figure 7.7: (a) 3-dimensional plot of the wave amplitude $|A(X,\tau)|$,
 (b) Wave amplitude $|A(X,\tau)|$, and (c) Phase $\text{Arg}(A(X,\tau))$
 for $X = 0, 1, 1.5$, $U_1 = -0.1$, $\tau = 6$, $dh = -0.3$,
 $K_1 = 0.63$, $(kd)_1 = 1.58$, $K_2 = 0.94$, $(kd)_2 = 1.83$,
 $m = 1.6$, $\Delta = 9.4\%$ global energy error = 0.3%

Figure 7.8: (a) 3-dimensional plot of the wave amplitude $|A(X,\tau)|$,
 (b) Wave amplitude $|A(X,\tau)|$, and (c) Phase $\text{Arg}(A(X,\tau))$
 for $X = 0, 1, 3$, $U_1 = -0.1$, $\tau = 7$, $dh = -0.15$,
 $K_1 = -0.61$, $(kd)_1 = 1.23$, $K_2 = -0.15$, $(kd)_2 = 1.32$,
 global energy error = 0.05%

PART II :

GENERATION OF SECOND ORDER LONG WAVES

IN WATER OF VARYING DEPTH

1. Introduction

The interaction between waves and strong current was studied in the first part. The current is found to affect strongly the waves by changing their wavelength, their evolution properties and their stability regions while the waves do not affect the current. A second extreme case is studied in this part: the current is assumed to be weaker than the waves. The waves then do affect the current but are not affected by it, at the leading order. As an example, a slowly modulated wave evolving on constant depth can generate a mean current and a mean set-down (see Longuet-Higgins and Stewart (1962)). The mean free surface displacement, induced by the wave group envelope, is a second order long wave propagating with the group velocity and hence is bound to the wave group. As noted by Longuet-Higgins and Stewart, this locked wave is the result of the variations of the radiation stress which are induced by the slowly varying envelope. If in addition the depth varies slowly (on the same scale as the envelope), the locked wave alone will not compensate the effect of the radiation stress change due to the depth variation and a forced wave is generated in this region. After being created in the region where the depth varies, the forced wave could radiate energy towards the farfield in the form of progressive long waves traveling at the phase velocity \sqrt{gh} . In contrast to the locked waves, these long waves are not bound to the short waves. Since their period is of the order of few minutes, they can be of practical interest in some engineering problems: Harbor resonance, deep water structure dynamics... In coastal regions they have also been related to surf-beats.

Such mechanism for the generation of second order free long waves was studied by Molin (1982) in the case where the first order short waves are considered to be deep water waves while the generated second order waves are considered to be shallow water waves. He found that the waves radiated away from the region of depth variation have very small amplitude (i.e. third order) and that their amplitude increases as the water depth becomes intermediate, i.e. $kh = O(1)$. In this part we extend Molin's study to the case of plane wave in water of intermediate depth. We first derive the governing equation for the mean free surface displacement induced by a plane wave group with slow modulations in both directions x and y . For this derivation we use two different methods and show that they are equivalent; the first one is the multiple scale method which is more formal but straightforward, the second one is an averaging method which is much less straightforward but whose results can be easily interpreted physically using the radiation stress concept. Then limiting ourselves to the case where the depth variation is in the x direction only and where the wave envelope is periodic in time with constant frequency, we derive a governing equation for the forced waves which is solved numerically by using a hybrid element method.

2. Governing Equations for the Mean Current and Set-Down

We consider a weakly nonlinear wave group propagating into water of variable but intermediate depth h i.e.

$$\epsilon = ka \ll 1 \quad \mu = kh = O(1) \quad (2.1)$$

where k is the wave number and a is the wave amplitude. The wave envelope and the depth are assumed to vary slowly. Introducing the slowly varying time and horizontal space coordinates

$$T = \epsilon t \quad X = \epsilon x \quad Y = \epsilon y \quad (2.2)$$

we have

$$h = h(X,Y) \quad \text{and} \quad A = A(X,Y,T) \quad (2.3)$$

where h is the depth of the water measured from the still water level and A is the wave amplitude. Therefore the length of the wave envelope is $O(1/\epsilon)$ and is of the same order as the distance over which the depth varies. The wave envelope modulation is known to induce a second order free surface displacement and current, which vary on the same scales as the first order envelope (i.e. X, Y, T scales). The governing equations of the induced current and free surface displacement can be found either by using the multiple scale method or by averaging the equation of the flow over the short scales.

2.a. The Multiple Scale Method

This method has been applied to a slowly modulated Stokes wave train by Chu and Mei (1970). Through their derivation of the nonlinear governing equation of the wave amplitude, they obtained the governing equation

of the second-order mean free surface displacement and current (Eqs. (4.5) and (4.6)). Let us summarize the main steps of this derivation. In terms of the potential velocity ϕ , the basic governing equations are

$$\nabla_2^2 \phi + \phi_{zz} = 0 \quad -h(\vec{x}) \leq z \leq \eta(\vec{x}, t) \quad (2.4)$$

$$\phi_{tt} + g \phi_z + \left(\frac{\partial}{\partial t} + \frac{1}{2} \vec{u} \cdot \nabla_3 \right) |\vec{u}|^2 = 0 \quad z = \eta(\vec{x}, t) \quad (2.5)$$

$$\phi_z + \nabla_2 \phi \cdot \nabla h = 0 \quad z = -h(\vec{x}) \quad (2.6)$$

$$\eta = -\frac{1}{g} \left(\phi_t + \frac{1}{2} |\vec{u}|^2 \right) \quad z = \eta(\vec{x}, t) \quad (2.7)$$

where $\vec{x} = (x, y)$ denotes the horizontal spatial coordinates, $\vec{u} = (\phi_x, \phi_y, \phi_z)$ is the velocity of a fluid particle, $\nabla_2 = \left(\frac{\partial}{\partial x}, \frac{\partial}{\partial y} \right)$ and $\nabla_3 = \left(\frac{\partial}{\partial x}, \frac{\partial}{\partial y}, \frac{\partial}{\partial z} \right)$ represent respectively the horizontal and total gradient operators, and η is the free surface elevation. Since $\eta = O(\epsilon)$, the free surface conditions (2.5) and (2.7) can be expanded about $z = 0$. Now we assume the following expansions

$$\phi(\vec{x}, z, t) = \sum_{n=1}^{\infty} \epsilon^n \sum_{m=-n}^{+n} \phi_{nm}(\vec{X}, T) e^{imS} \quad (2.8)$$

$$\eta(\vec{x}, t) = \sum_{n=1}^{\infty} \epsilon^n \sum_{m=-n}^{+n} \eta_{nm}(\vec{X}, T) e^{imS} \quad (2.9)$$

where $\vec{X} = (X, Y) = (\epsilon x, \epsilon y)$ and $T = \epsilon t$. The phase function $S(\vec{x}, t)$ then defines the wavenumber \vec{k} and frequency ω .

$$\vec{k} = \nabla_2 S \quad (2.10.a)$$

$$\omega = - S_t \quad (2.10.b)$$

If ω is assumed to be constant, then the previous equations imply that \vec{k} is independent of t and satisfies

$$\nabla_2 \times \vec{k} = 0 \quad (2.11)$$

Substituting the expansions (2.8) and (2.9) into the governing equations (2.4), (2.6) and the expanded form of (2.5) and (2.7) about $z = 0$, and separating different orders and harmonics give a set of equations:

$$\phi_{nmzz} - m^2 k^2 \phi_{nm} = R_{nm}(\vec{X}, z, T) \quad -h \leq z \leq 0 \quad (2.12.a)$$

$$g \phi_{nmz} - m^2 \omega^2 \phi_{nm} = G_{nm}(\vec{X}, T) \quad z = 0 \quad (2.12.b)$$

$$\phi_{nmz} = F_{nm}(\vec{X}, T) \quad z = -h \quad (2.12.c)$$

$$\eta_{nm} = \frac{1}{g} (im\omega \phi_{nm} - H_{nm}(\vec{X}, T)) \quad z = 0 \quad (2.12.d)$$

where R_{nm} , G_{nm} , F_{nm} and H_{nm} depend on lower order terms and are given in Appendix (B1). At the first order $n = 1$ the system of equations (2.12) yields that ϕ_{10} is independent of depth and ϕ_{11} is the classical linear wave solution

$$\phi_{10} = \phi_{10}(\vec{X}, T) \quad (2.13.a)$$

$$\phi_{11} = -iA(\vec{X}, T) \frac{g}{2\omega} \frac{\cosh k(z+h)}{\cosh kh} \quad (2.13.b)$$

$$\eta_{11} = \frac{A}{2} (\vec{X}, T) \quad (2.13.c)$$

where $\omega^2 = kg \tanh kh$ (2.14)

At the second order zeroth harmonic Eq. (2.12.d) gives an equation relating the mean quantities ϕ_{10} and η_{20} :

$$\eta_{20} = -\frac{1}{4} A^2 \frac{\omega^2}{g} \frac{1}{\sinh^2(kh)} - \frac{1}{g} \phi_{10t} \quad (2.15)$$

From the set of equation (2.12) it can be seen by using Green's formula that a necessary condition for the second order first harmonic solution to exist is that the following solvability condition is satisfied.

$$\frac{1}{g} G_{21} = \int_{-h}^0 dz R_{21} \frac{\cosh k(z+h)}{\cosh kh} + \frac{F_{21}}{\cosh kh} \quad (2.16)$$

which gives

$$\frac{\partial A^2}{\partial T} + \nabla \cdot (\vec{C}_g A^2) = 0 \quad (2.17)$$

after using the expressions for G_{21} and R_{21} . Where $\nabla = (\frac{\partial}{\partial x}, \frac{\partial}{\partial y})$ and \vec{C}_g is the group velocity defined as:

$$\vec{C}_g = \frac{k\omega}{2k^2} \left(1 + \frac{2kh}{\sinh 2kh}\right) \quad (2.18)$$

Equation (2.17) represents the conservation of energy.

Similarly at the third order zeroth harmonic, using the Green's formula we find the solvability condition:

$$\frac{1}{g} G_{30} = \int_{-h}^0 dz R_{30} + F_{30} \quad (2.19)$$

which gives a second equation relating η_{20} and ϕ_{10}

$$\frac{\partial \eta_{20}}{\partial T} + \nabla \cdot (h \nabla \phi_{10} + \frac{\vec{k}}{\omega} \frac{1}{2} g A^2) = 0 \quad (2.20)$$

Taking the derivative with respect to time of (2.20) and using (2.15), we obtain the governing equation for the mean free surface displacement

$$\nabla \cdot (gh \nabla \eta_{20}) - \frac{\partial^2 \eta_{20}}{\partial T^2} = \nabla \cdot \left(\frac{\vec{k}g}{2\omega} (A^2)_T \right) - \nabla \cdot \left(h \nabla \left(\frac{\omega^2 A^2}{4 \sinh^2 kh} \right) \right) \quad (2.21)$$

Eq. (2.21) can be written in a slightly different form. Let us differentiate the dispersion relation (2.14)

$$\nabla k = - \frac{k\omega}{C_g \sinh 2kh} \nabla h \quad (2.22)$$

Using (2.17) and (2.22) in the right hand side of Eq. (2.21), this equation becomes:

$$\nabla \cdot (gh \nabla \eta_{20}) - \frac{\partial^2 \eta_{20}}{\partial T^2} = - \nabla \cdot \left[\nabla \left(\frac{gA^2 kh}{2 \sinh 2kh} \right) + \frac{g}{2\omega} (\vec{k} \nabla \cdot (\vec{C}_g A^2) + A^2 C_g \nabla k) \right] \quad (2.23.a)$$

Using the irrotationality of \vec{k} Eq. (2.23.a) reduces to

$$\nabla \cdot (gh \nabla \eta_{20}) - \frac{\partial^2 \eta_{20}}{\partial T^2} = - \frac{\partial^2}{\partial X_1^2} \left(\frac{gA^2 C_g}{2} \left(\frac{C_g}{C} - \frac{1}{2} \right) \right) - \frac{\partial}{\partial X_1} \frac{\partial}{\partial X_j} \left(\frac{gA^2 C_g}{2C} \frac{k_i k_j}{k^2} \right) \quad (2.23.b)$$

2.b. The Averaging Method

Since we are interested in the governing equations of mean quantities, arguments similar to those leading to the Reynolds equations for the mean turbulent flow, can be applied. Therefore by averaging the Euler's equations over the rapidly varying scales, we would expect to obtain the conservation laws of mass and horizontal momentum for the mean current. This method have been applied by Longuet-Higgins and Stewart (1962). They introduced the radiation stress concept which is the equivalent of the Reynold stress in the case of turbulent flow. In what follows we rederive their results in the context of our problem.

The basic equations are Euler's equations with appropriate boundary conditions

$$\nabla \cdot \vec{u} = 0 \quad (2.24)$$

$$\frac{\partial \vec{u}}{\partial t} + (\vec{u} \cdot \nabla) \vec{u} = -\frac{1}{\rho} \nabla (P + \rho g z) \quad (2.25)$$

$$w + \vec{u} \cdot \nabla h = 0 \quad z = -h(x, y) \quad (2.26)$$

$$\frac{\partial \xi}{\partial t} + \vec{u} \cdot \nabla \xi = w \quad z = \xi(x, y, t) \quad (2.27)$$

$$P = 0 \quad z = \xi(x, y, t) \quad (2.28)$$

where $\vec{u} = (u_1, u_2, w)$ is the flow velocity, P the pressure and ξ the free surface displacement. We now define the mean velocity U_i ($i = 1, 2$) by integrating u_i over the water depth and then over the short time scale T ($T = \frac{2\pi}{\omega}$ represents the period of the short waves)

$$U_i = \frac{1}{\bar{\xi}+h} \int_{-h}^{\bar{\xi}} u_i dz \quad i = 1,2 \quad (2.29)$$

where the time averaging of a quantity (Q) is defined as:

$$\bar{Q} = \frac{1}{T} \int_t^{t+T} Q dt \quad (2.30)$$

Physically $\rho(\bar{\xi}+h)U_i$ represents the mean rate of mass flux across a vertical plane of unit width along $x_i = \text{constant}$ and is called the mass flux velocity (see Mei (1982)). Let \tilde{u}_i be the deviation of the velocity from its mean i.e.

$$u_i = U_i + \tilde{u}_i \quad (2.31)$$

then it follows from the definition (2.29) that

$$\int_{-h}^{\bar{\xi}} \tilde{u}_i dz = 0 \quad (2.32)$$

The continuity equation (2.24) integrated with respect to depth gives

$$\frac{\partial \bar{\xi}}{\partial t} + \frac{\partial}{\partial x_i} \left(\int_{-h}^{\bar{\xi}} u_i dx \right) = 0 \quad (2.33)$$

after using the boundary conditions (2.25) and (2.26). Substituting (2.31) into (2.33) and averaging over the short time scale we get

$$\frac{\partial \bar{\xi}}{\partial t} + \frac{\partial}{\partial x_i} ((\bar{\xi} + h)U_i) = 0 \quad (2.34)$$

where Eq. (2.32) has been used.

Since the flow is inviscid, the equations of momentum conservation can be written as follows:

$$\frac{\partial u_j}{\partial t} + \frac{\partial u_i u_j}{\partial x_i} + \frac{\partial u_j w}{\partial z} = \frac{1}{\rho} \frac{\partial}{\partial x_i} (-P \delta_{ij}) \quad i = 1, 2 \quad (2.35)$$

$$\frac{\partial w}{\partial t} + \frac{\partial u_i w}{\partial x_i} + \frac{\partial w^2}{\partial z} = -\frac{1}{\rho} \frac{\partial}{\partial z} (P + \rho g z) \quad (2.36)$$

Let us now integrate (2.35) with respect to depth, use Leibnitz rule to inverse the respective position of the derivative with respect to t or x_i and the integration with respect to z and use the boundary conditions (2.26) - (2.28):

$$\frac{\partial}{\partial t} \left(\int_{-h}^{\xi} u_j dz \right) + \frac{\partial}{\partial x_i} \int_{-h}^{\xi} (u_i u_j + \frac{P}{\rho} \delta_{ij}) dz - \frac{P|_h}{\rho} \frac{\partial h}{\partial x_j} = 0 \quad (2.37)$$

Using (2.31) and averaging with respect to time gives:

$$\frac{\partial}{\partial t} ((\bar{\xi} + h) U_j) + \frac{\partial}{\partial x_i} ((h + \bar{\xi}) U_i U_j) = \frac{\bar{P}|_h}{\rho} \frac{\partial h}{\partial x_j} - \frac{\partial}{\partial x_i} \left(\int_{-h}^{\bar{\xi}} (\bar{u}_i \bar{u}_j + \frac{P}{\rho} \delta_{ij}) dz \right) \quad (2.38)$$

Introducing \bar{p} , the mean dynamic pressure at the bottom

$$\bar{p} = \bar{P}|_h - \rho g(\bar{\xi} + h) \quad (2.39)$$

Eq. (2.38) can be written in a slightly different way:

$$\frac{\partial}{\partial t} ((\bar{\xi} + h) U_j) + \frac{\partial}{\partial x_i} ((h + \bar{\xi}) U_i U_j) = \frac{\bar{p}}{\rho} \frac{\partial h}{\partial x_j} - g(\bar{\xi} + h) \frac{\partial \bar{\xi}}{\partial x_j} - \frac{1}{\rho} \frac{\partial (S_{ij})}{\partial x_i} \quad (2.40)$$

$$\text{where } S_{ij} = \int_{-h}^{\xi} dz [\rho \tilde{u}_i \tilde{u}_j + (P - \rho g(\xi - z)) \delta_{ij}] \quad (2.41)$$

S_{ij} represents the sum of the i^{th} component of the net momentum flux across and the excess hydrodynamic pressure on, a surface normal to the j -th direction. This tensor representing the excess momentum fluxes is called the radiation stress (see Longuet-Higgins and Stewart, 1960). In order to obtain the average pressure we integrate Eq. (2.36) from z to ξ

$$P(z) = \rho g(\xi - z) + \frac{\partial}{\partial x_i} \left(\int_z^{\xi} \rho u_i w dz \right) - \rho w^2 + \rho \frac{\partial}{\partial t} \left(\int_z^{\xi} w dz \right) \quad (2.42)$$

where the Leibnitz rule has been used to inverse derivation and integration and the boundary conditions (2.27) and (2.28) have been applied. So far the equations found are very general but to go further we need to make some assumptions. First we assume that the depth is slowly varying, i.e.

$$\nabla h = O(\epsilon) \quad (2.43)$$

we also assume that at the leading order the flow corresponds to the propagation of an infinitesimal wave with slowly varying amplitude over the variable depth. Therefore the wave velocity and the free surface displacement are:

$$u_j = \frac{k_j g A}{2\omega} \frac{\cosh k(z+h)}{\cosh kh} e^{iS} + * + O(\epsilon^2) \quad j = 1, 2 \quad (2.44)$$

$$w = - \frac{ikgA}{2\omega} \frac{\sinh k(z+h)e^{iS}}{\cosh kh} + * + 0(\epsilon^2) \quad (2.45)$$

$$\xi = \frac{A}{2} e^{iS} + * + 0(\epsilon^2) \quad (2.46)$$

$$\text{where } S = \int k_1 dx + \int k_2 dy - \omega t \quad (2.47)$$

and * denotes the complex conjugate. Eqs. (2.44) - (2.47) imply that the derivative with respect to time or horizontal space coordinate of an averaged quantity is of higher order i.e.

$$\frac{\partial}{\partial t} (\bar{\cdot}), \quad \frac{\partial}{\partial x_j} (\bar{\cdot}) = 0(\epsilon) \quad (2.48)$$

we also deduce that

$$\bar{u}_j, \bar{\xi}, \bar{w} \leq 0(\epsilon^2) \quad (2.49)$$

As a comment, we note from Eq. (2.26) that $w|_{-h} = 0(\epsilon^3)$. From Eqs. (2.44) it can be seen that u_j and $\frac{\partial \xi}{\partial x_j}$ are out of phase therefore $\overline{u_j \frac{\partial \xi}{\partial x_j}} = 0(\epsilon^3)$ and Eq. (2.27) implies that $\bar{w}|_{\xi} = 0(\epsilon^3)$. Averaging Eq. (2.49) with respect to time and using the previous assumptions give

$$\bar{P}(z) = \rho g (\bar{\xi} - z) - \overline{\rho w^2} + 0(\epsilon^3) \quad (2.50)$$

The dynamical pressure at the bottom is

$$\bar{p} \leq 0(\epsilon^3) \quad (2.51)$$

Similarly, the radiation stress tensor can be estimated to the second order, by plugging the expression for the pressure (2.42) into (2.40)

$$S_{ij} = \int_{-h}^{\xi} \overline{u_i u_j} dz + \left(\int_{-h}^{\xi} dz \left(\frac{\partial}{\partial t} \int_z^{\xi} w dz' \right) \right) + \int_{-h}^{\xi} dz \left(\frac{\partial}{\partial x_i} \int_z^{\xi} u_i w dz' \right) - \int_{-h}^{\xi} \overline{w^2} dz + \frac{1}{2} \overline{g \xi^2} \delta_{ij} \quad (2.52)$$

where $\tilde{\xi} = \xi - \bar{\xi}$. Applying the rules (2.48) and (2.49) we obtain:

$$S_{ij} = \int_{-h}^0 \overline{\tilde{u}_i \tilde{u}_j} dz + \int_{-h}^0 \overline{w^2} dz + \frac{1}{2} \overline{g \tilde{\xi}^2} + O(\epsilon^3) \quad (2.53)$$

To have S_{ij} to the second order we only need the first order approximation of the velocities and free surface displacement as given by Eqs. (2.44) - (2.47)

$$S_{ij} = \frac{gA^2}{2} \left(\frac{C_g}{C} - 1/2 \right) \delta_{ij} + \frac{gA^2}{2} \frac{C_g}{C} \frac{k_i k_j}{k^2} + O(\epsilon^3) \quad (2.54)$$

where $C_g = \frac{C}{2} \left(1 + \frac{2kh}{\sinh 2kh} \right)$ is the group velocity and $C = \frac{\omega}{k}$ is the phase velocity. Since U_i and $\bar{\xi}$ are $O(\epsilon^2)$ Eqs. (2.34) and (2.38) become

$$\frac{\partial \bar{\xi}}{\partial t} + \frac{\partial}{\partial x_i} (h U_i) = O(\epsilon^5) \quad (2.55)$$

$$h \frac{\partial U_j}{\partial t} + gh \frac{\partial \bar{\xi}}{\partial x_j} = - \frac{1}{\rho} \frac{\partial}{\partial x_i} S_{ij} + O(\epsilon^4) \quad (2.56)$$

Taking $-\frac{\partial}{\partial t} (2.55) + \frac{\partial}{\partial x_j} (2.56)$ we finally find the governing equation for the mean free surface displacement

$$-\frac{\partial^2 \bar{\xi}}{\partial t^2} + \frac{\partial}{\partial x_j} \left(gh \frac{\partial \bar{\xi}}{\partial x_j} \right) = - \frac{1}{\rho} \frac{\partial}{\partial x_j} \frac{\partial}{\partial x_i} (S_{ij}) \quad (2.57)$$

which is identical to Eq. (2.23.b). This equation shows that $\bar{\xi}$ is equivalent to the surface elevation of a long wave when a horizontal force $-\frac{\partial S_{11}}{\partial x_1}$ is applied to the fluid i.e. gradients of the excess momentum fluxes tend to change the mean free surface level.

3. Generation of Forced Waves

The governing equation for the mean free surface displacement is Eq. (2.57) or Eq. (2.21). However to solve it, one needs to find the variations of the wavenumber, the wave direction and the wave amplitude with respect to the slow coordinates X_i , T . These quantities are governed by the dispersion relation (2.14), the irrotationality condition (2.11) and the equation of conservation of energy (2.17).

Using the following normalization

$$\begin{aligned} X'_i &= k_\infty X_i & h' &= k_\infty h & k' &= \frac{k}{k_\infty} \\ A' &= \frac{A}{a_0} & \bar{\xi}' &= \frac{\bar{\xi}}{k_\infty a_0^2} & C'_g &= \frac{k_\infty}{\omega} C_g & T' &= \frac{T}{\omega} \end{aligned} \quad (3.1)$$

where $k_\infty = \frac{\omega^2}{g}$ is the wavenumber in deep water and a_0 is the wave amplitude at some reference depth h_0 ; these equations become

$$\frac{\partial}{\partial X_i} \left(h \frac{\partial \bar{\xi}}{\partial X_i} \right) - \frac{\partial^2 \bar{\xi}}{\partial T^2} = - \frac{\partial}{\partial X_i} \left(h \frac{\partial}{\partial X_i} \left(\frac{A^2}{4 \sinh^2 kh} \right) \right) + \frac{\partial}{\partial X_i} \left(\frac{k_i}{2} \frac{\partial A^2}{\partial T} \right) \quad (3.2)$$

$$\frac{\partial A^2}{\partial T} + \frac{\partial}{\partial X_i} (A^2 C_{gi}) = 0 \quad (3.3)$$

$$1 = k \tanh kh \quad (3.4)$$

$$\frac{\partial k_1}{\partial X_2} = \frac{\partial k_2}{\partial X_1} \quad (3.5)$$

In the most general case these two dimensional equations need to be solved numerically. To simplify the analysis we assume the depth to vary in one direction only i.e. $h = h(X_1)$. Then Eq. (3.4) and (3.5) imply:

$$k = k(X_1) \quad k_1 = k_1(X_1) \quad k_2 = \text{constant} \quad (3.6)$$

or by introducing $\alpha(X_1)$ the angle between the direction of propagation of the wave and the X_1 - axis.

$$k_1 = k \cos \alpha \quad k_2 = k \sin \alpha = k_0 \sin \alpha_0 \quad (3.7)$$

where the subscript 'o' refers to the values at the reference depth h_0 . In what follows we will use (X, Y) as representing (X_1, X_2) . We further assume the wave envelope to be periodic in T with a constant frequency ω .

$$A(X, Y, T) = \frac{1}{2} (\tilde{A}(X, Y) e^{-i\omega T} + *) \quad (3.8)$$

and to satisfy the boundary condition:

$$\tilde{A}(X, Y) = e^{i\nu k_2 Y} \quad \text{at} \quad X = X_0 \quad (3.9)$$

where $X = X_0$ is a reference line in the region of constant depth $h = h_0$.

Then Eq. (3.3) becomes

$$k_1 \frac{\partial \tilde{A}^2}{\partial X} + k_2 \frac{\partial \tilde{A}^2}{\partial Y} + \left(\frac{k}{C_g} \frac{\partial C_{g1}}{\partial X} - \frac{2i\nu\Omega k}{C_g} \right) \tilde{A}^2 = 0 \quad (3.10)$$

$$k_1 \frac{\partial |\tilde{A}|^2}{\partial X} + k_2 \frac{\partial |\tilde{A}|^2}{\partial Y} + \frac{k}{C_g} \frac{\partial C_{g1}}{\partial X} |\tilde{A}|^2 = 0$$

where C_{g1} is the group velocity in the X direction. The solution of Eqs. (3.10) which satisfies the boundary condition (3.9) is:

$$\tilde{A} = \sqrt{\frac{C_{g10}}{C_{g1}}} e^{i\nu \left(\int_{x_0}^X K dx + k_2 Y \right)} \quad (3.11)$$

where $K = \frac{\Omega}{C_{g1}} - \frac{k_2^2}{k_1}$. The wave envelope is then a progressive wave whose direction of propagation is at the angle β with respect to the X-axis

$$\tan \beta = \frac{k_2}{K} \quad (3.12)$$

and whose phase velocity is

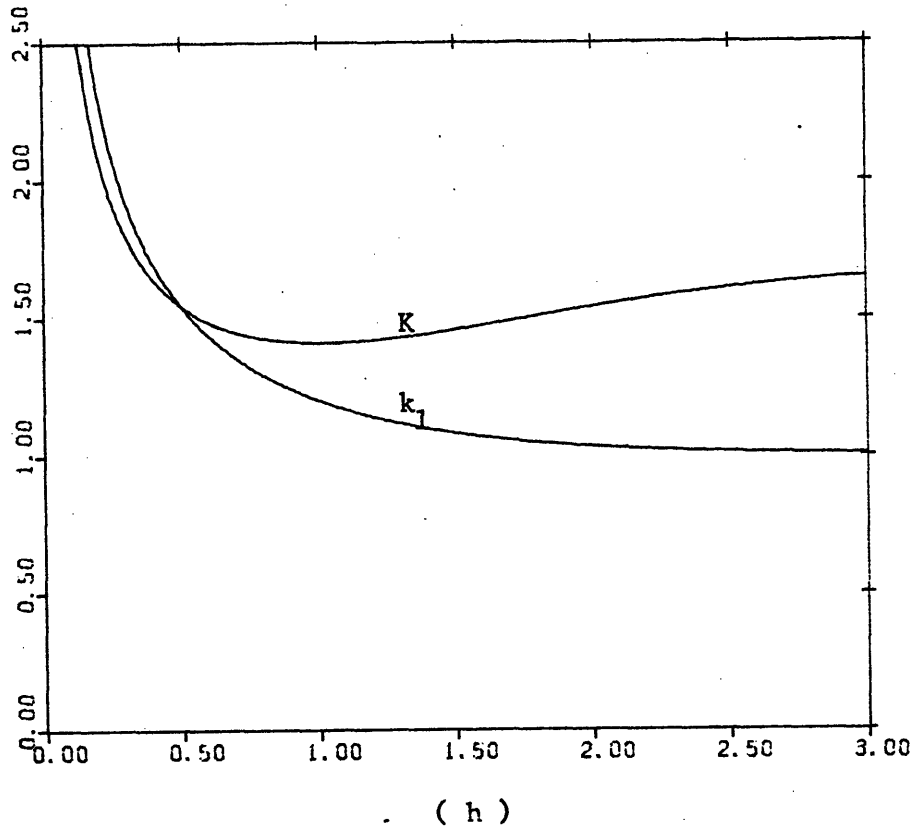
$$C = \frac{\Omega}{\sqrt{K^2 + k_2^2}} \quad (3.13)$$

We choose $\Omega = C_{g0} k_0$ such that at the reference depth h_0 , $K = k_{10}$,

$C = C_{g0}$ i.e. the wave envelope is propagating at the group velocity in the same direction as that of the short waves. We have plotted in fig. (3.1) the variation of K and k_1 with depth for different values

$\alpha_0 = 0, \frac{\pi}{6}, \frac{\pi}{4}, \frac{\pi}{3}$. The reference depth is taken to be $h_0 = 0.5$. As expected

(a)
Normal incidence
 $\alpha_0 = 0$



(b)
Oblique Incidence
 $\alpha_0 = \frac{\pi}{6}$

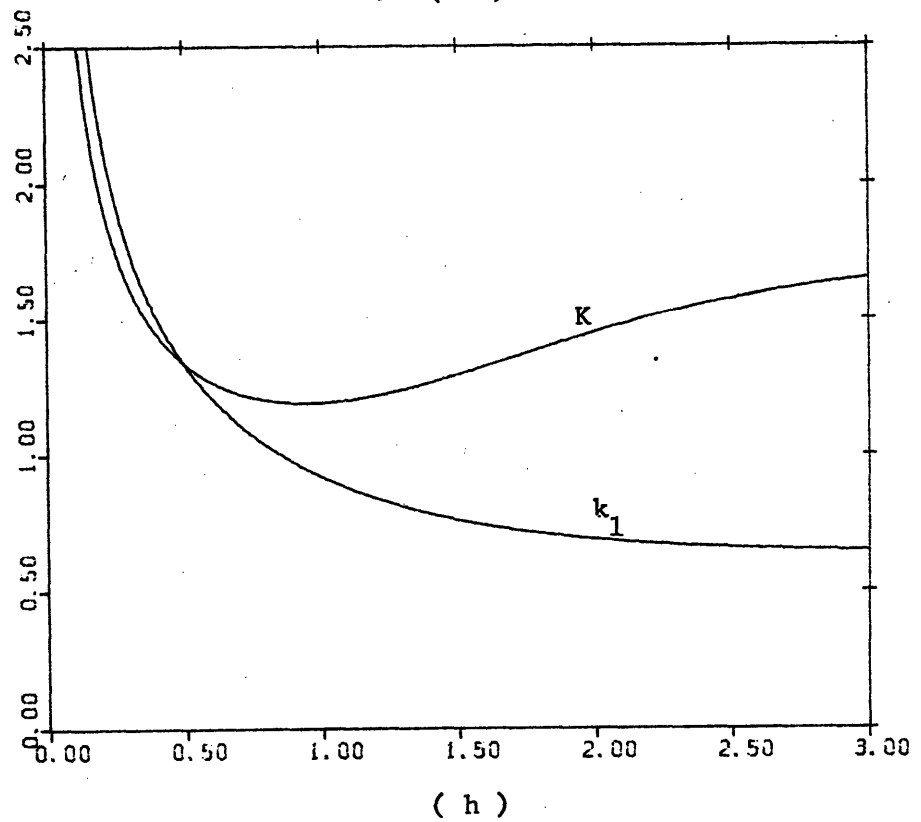
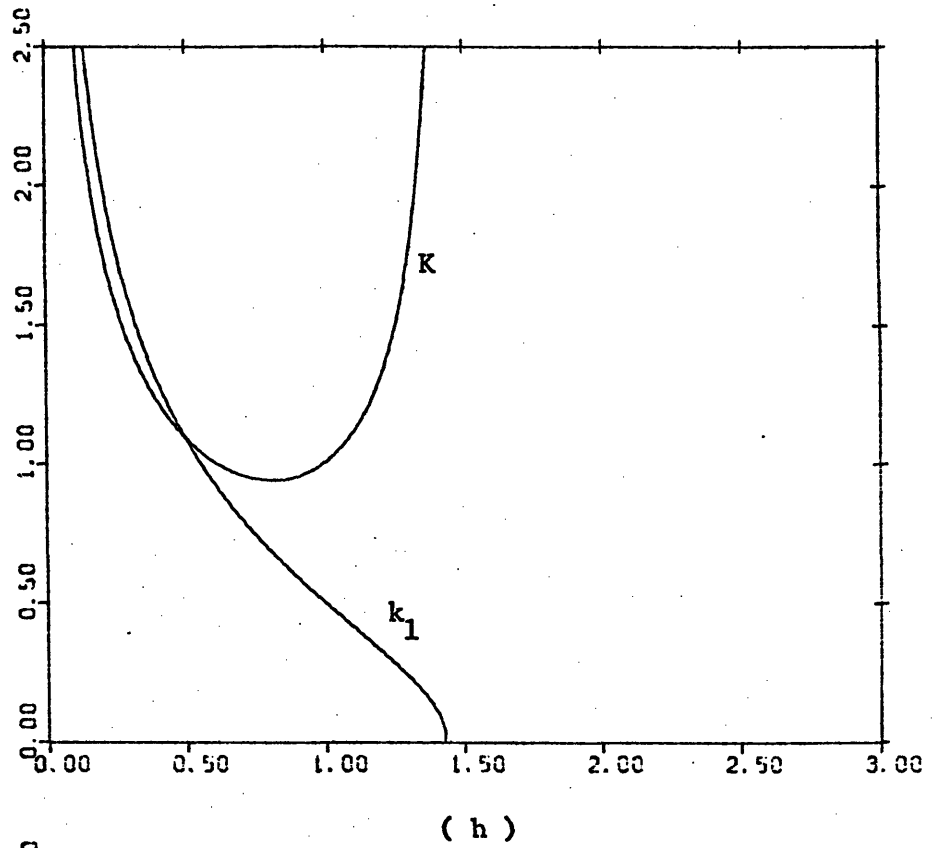


Figure 3.1 Wavenumbers in X-Direction, Reference Depth $h_0 = 0.5$.

(c)
Oblique Incidence
 $\alpha_0 = \frac{\pi}{4}$



(d)
Oblique Incidence
 $\alpha_0 = \frac{\pi}{3}$

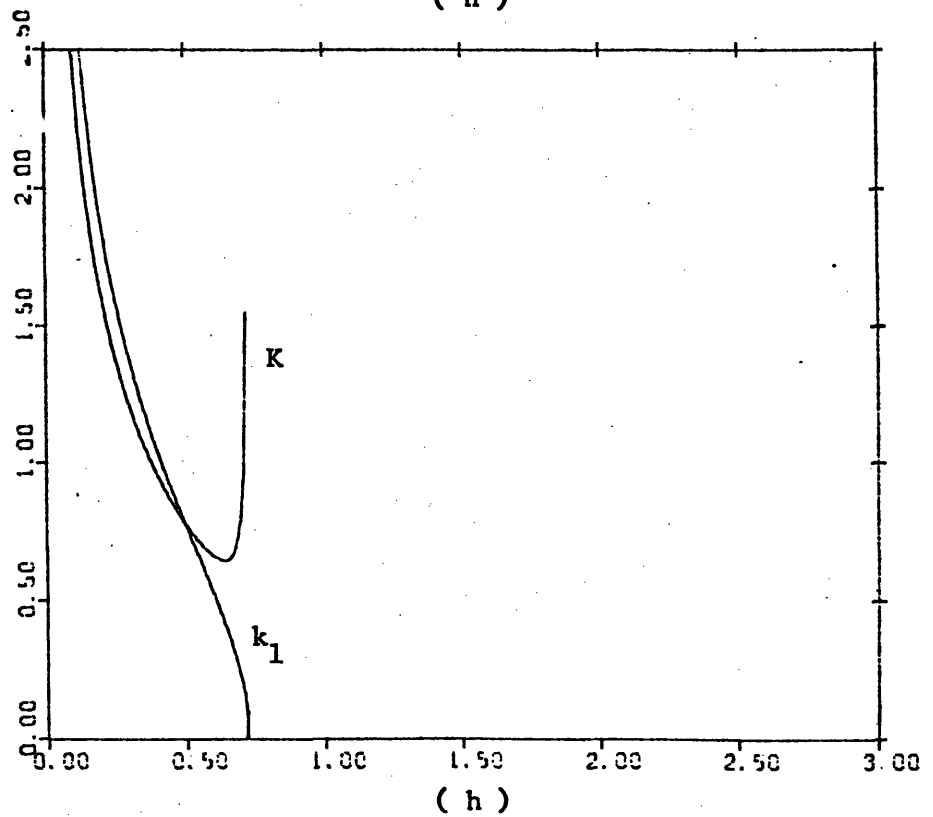


Figure 3.1 (Cont.)

at $h = h_0$ we have $K = k_1$, $\beta = \alpha$. In shallower water $K < k_1$ and therefore $\beta > \alpha$. As $h \rightarrow 0$, k_1 and $K \rightarrow \infty$ i.e. α and $\beta \rightarrow 0$. In deeper water $K > k_1$ and $\beta < \alpha$. Depending on the reference depth and the initial angle of incidence α_0 , short waves propagating into deeper water can be reflected back by a Caustic (A line corresponding to the envelope of all the rays). The Caustic line is defined by :

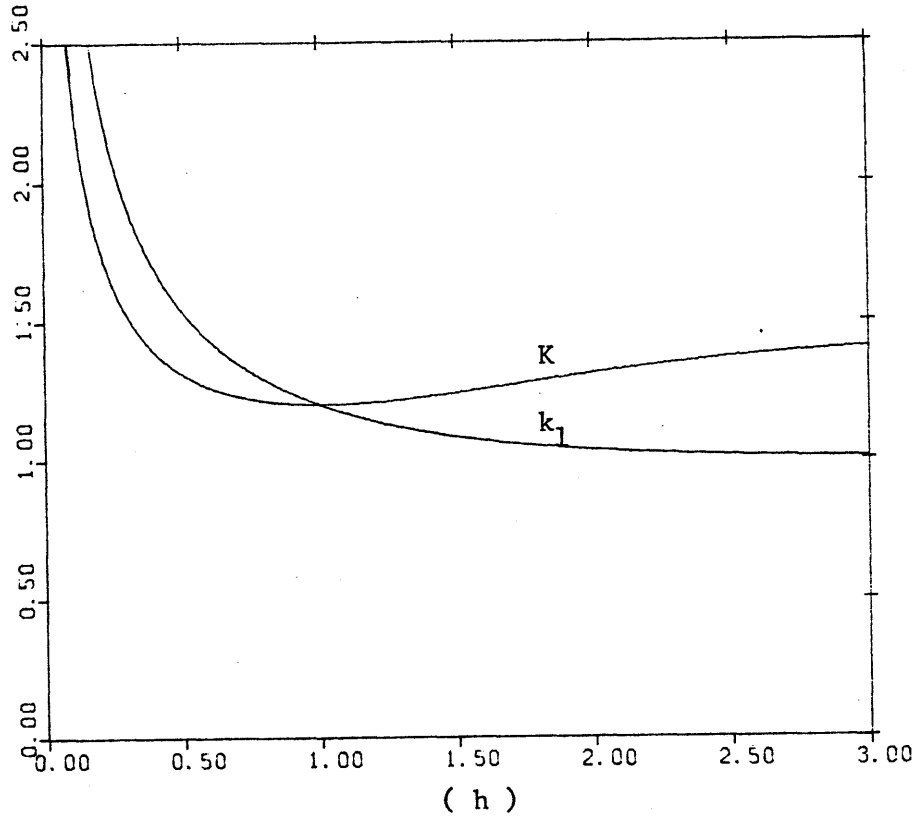
$$k_2 = k \quad \text{or} \quad \frac{k_0 \sin \alpha_0}{k} = 1 \quad (3.14)$$

In the neighborhood of the caustic $k_1 \rightarrow 0$ but $K \rightarrow \infty$: The short waves reach the caustic with an angle of incidence $\alpha \rightarrow \pi/2$ (i.e., glancing incidence) while their envelope reaches it with an angle $\beta \rightarrow 0$ (i.e. normal incidence). In the neighborhood of the caustic, Eq. (3.11) shows that $|A| \rightarrow \infty$, our small amplitude theory ceases to be valid and a more refined treatment is needed. In fig. (3.2), K and k_1 are shown for $h_0 = 1$, before the caustic is approached. The variations of K and k_1 with depth are qualitatively similar to those presented in fig. (3.1).

From Eq. (3.8) and (3.11), we note that A^2 consists of zeroth and second harmonic so the right hand side of Eq. (3.2) consists of the same harmonics, therefore we expect $\bar{\xi}$ to be of the form:

$$\bar{\xi} = \xi_0(x) + \frac{1}{2} (\tilde{\xi}(x) e^{2iv(k_2 Y - \Omega T)} + *) \quad (3.15)$$

(a)
 Normal Incidence
 $\alpha_0 = 0$



(b)
 Oblique Incidence
 $\alpha_0 = \frac{\pi}{6}$

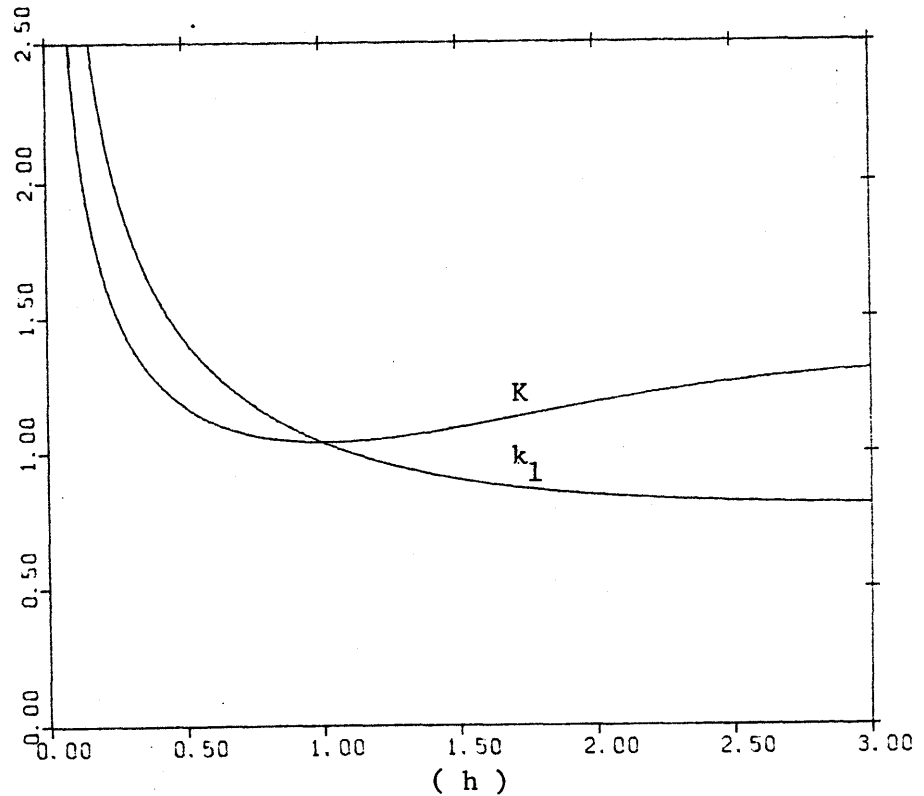
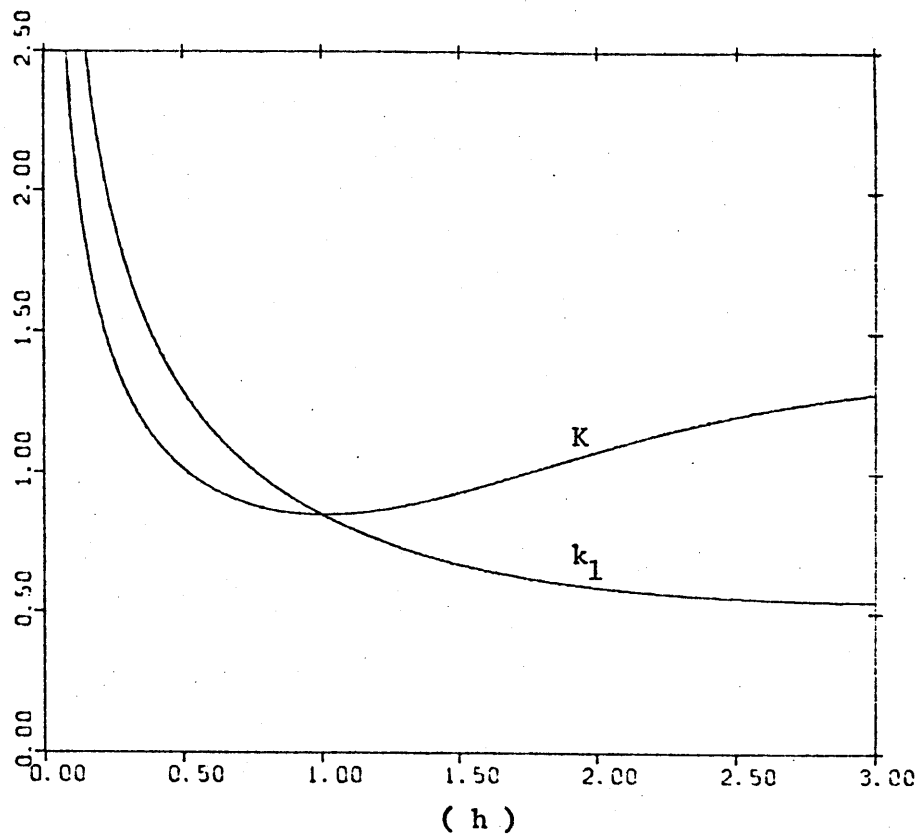


Figure 3.2 Wavenumbers in X-Direction, Reference Depth $h_0 = 1$

(c)
Oblique Incidence
 $\alpha_0 = \frac{\pi}{4}$



(d)
Oblique Incidence
 $\alpha_0 = \frac{\pi}{3}$

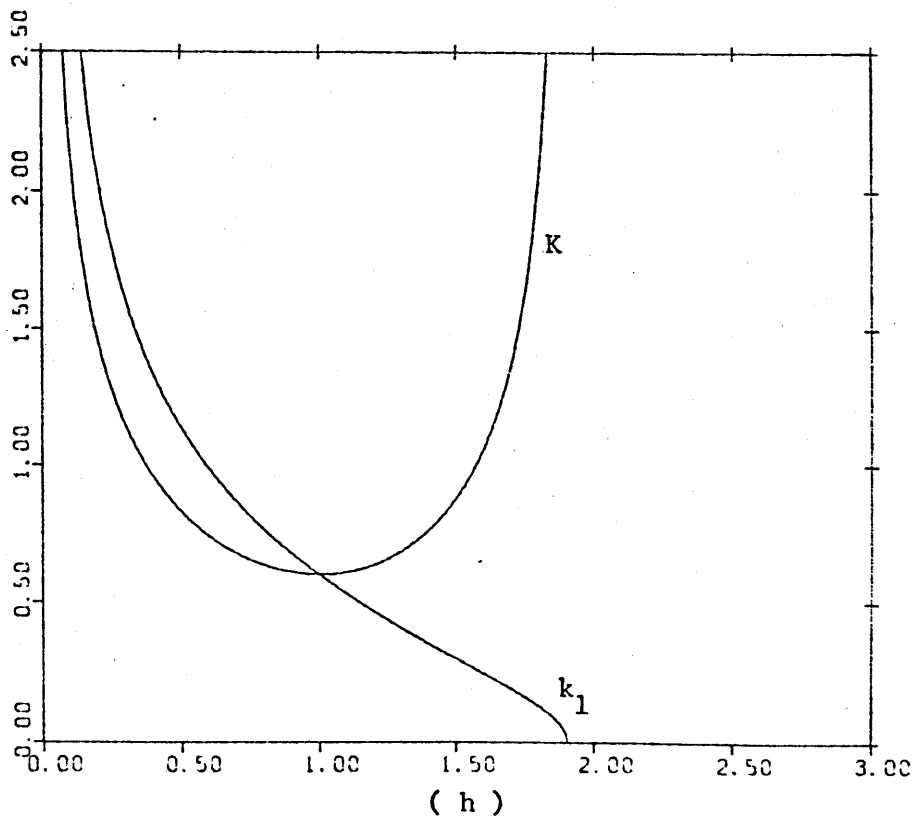


Figure 3.2 (Cont.)

Plugging (3.15) into (3.2) we obtain the expression for ξ_0 and the governing equation for $\tilde{\xi}$:

$$\xi_0(X) = - \frac{C_{g10}}{8C_{g1} \sinh^2 kh} = - \frac{|\tilde{A}|^2}{8 \sinh^2 kh} \quad (3.16)$$

$$\frac{d}{dX} \left(h \frac{d\tilde{\xi}}{dX} \right) + 4v^2 (\Omega^2 - k_2^2 h) \tilde{\xi} = \left[\frac{kh (K^2 + k_2^2)}{\sinh 2kh} + \frac{\Omega^2 k_1^2}{C_g} \right] v^2 \frac{C_{g10}}{C_{g1}} e^{2iv \int_{X_0}^X K dX} +$$

$$\left[\frac{d}{dX} \left(h \frac{d\xi_0}{dX} \right) + iv(4Kh \frac{d\xi_0}{dX} + 2\xi_0 \frac{d}{dX} (Kh) - \frac{\Omega C_{g10}}{2} \frac{d}{dX} \left(\frac{k}{C_g} \right) \right] e^{2iv \int_{X_0}^X K dX} \quad (3.17)$$

Eq. (3.17) is then an ordinary differential equation in X .

For normal incidence $\alpha_0 = 0$, a limiting case was studied by Molin (1982) by considering the first order waves to be deep water waves and the second order waves to be long waves. In this limit $kh = 0 \left(\frac{1}{\sqrt{\epsilon}} \right)$, $C_g \rightarrow \frac{1}{2}$, $k \rightarrow 1$

$$\frac{d}{dX} \left(h \frac{d\tilde{\xi}}{dX} \right) + 4v^2 \Omega^2 \tilde{\xi} = 2 \Omega^2 v^2 e^{\frac{2iv\Omega X}{C_g}} \quad (3.18)$$

Taking $\Omega v = 1$, Eq. (3.18) is equivalent to the governing equation obtained by Molin.

For $kh = 0 \left(\frac{1}{\sqrt{\epsilon}} \right)$, the steady state set-down, $\xi_0(X)$ is plotted in fig. (3.3) for different angles of incidence $\alpha_0 = 0, \frac{\pi}{6}, \frac{\pi}{4}, \frac{\pi}{3}$. The

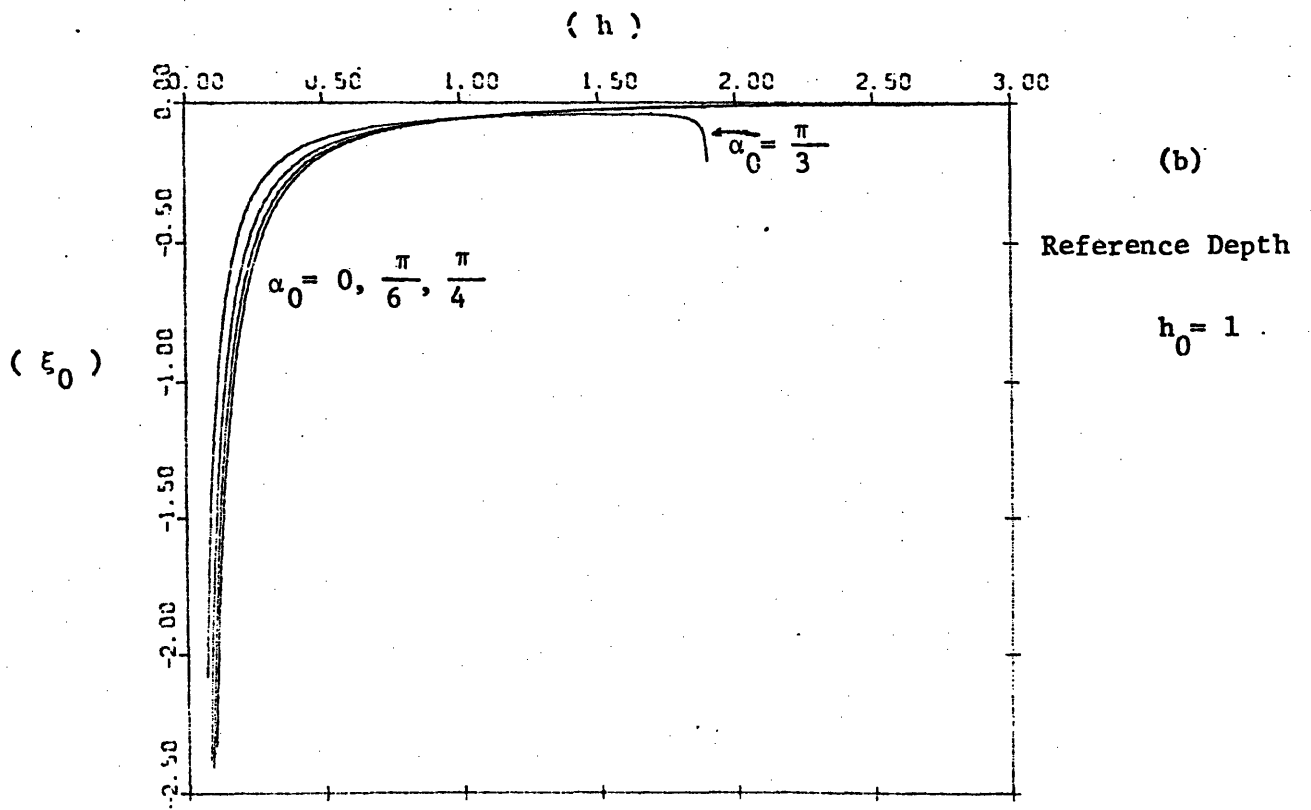
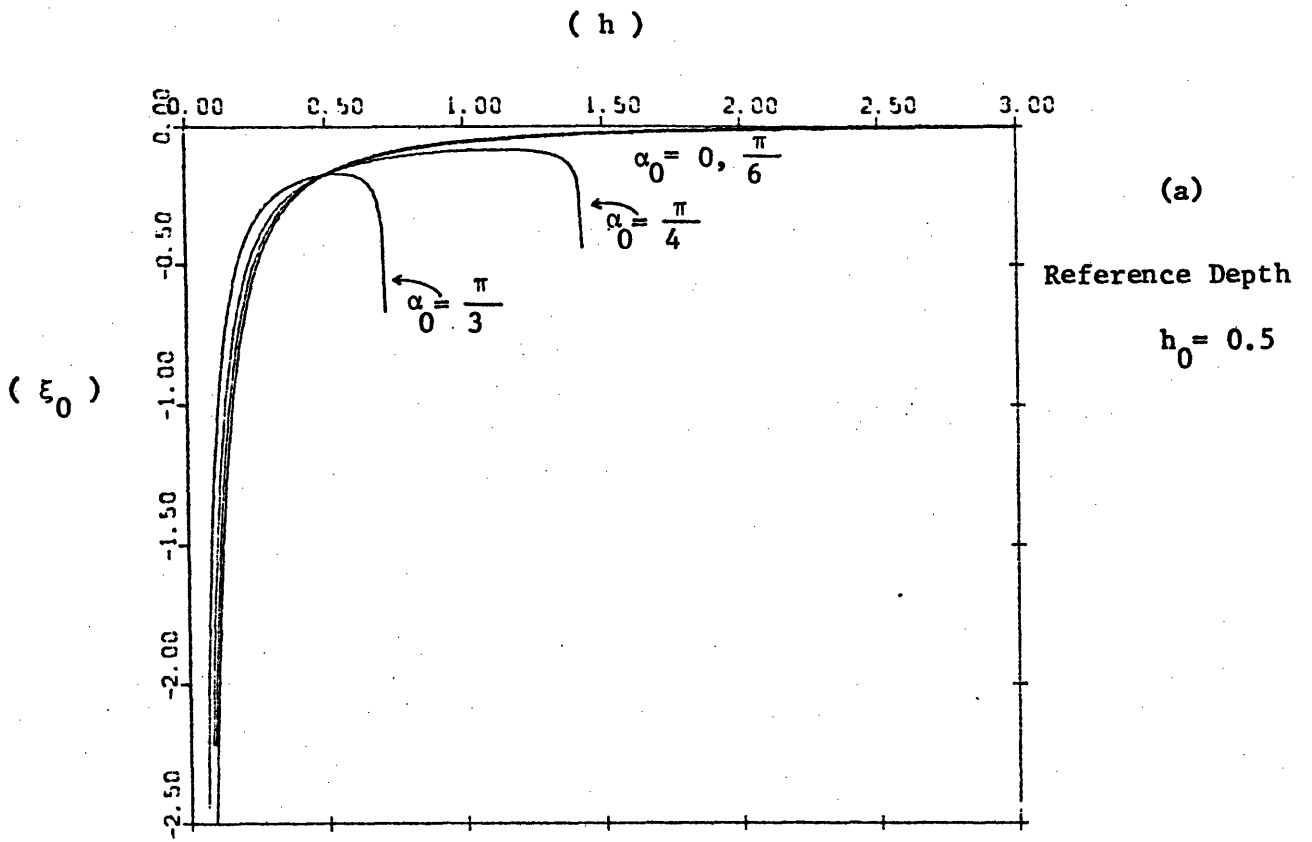


Figure 3.3 Mean Set-Down

reference depths in figs. (3.3.a) and (3.3.b) are respectively $h_0 = 0.5$ and $h_0 = 1$. As expected from Eq. (3.16), ξ_0 is always negative and increases from $-\infty$ in very shallow water to zero in deep water. Near a caustic $k_1 \rightarrow 0$ and $\xi_0 \rightarrow -\infty$. The effect of increasing angle of incidence is very small before the caustic is approached.

3.a Locked Waves on Constant Depth

In the case of constant depth, the second term on the right hand side of (3.17) is zero. The equation admits a solution of the form

$$\xi = \xi_L e^{2iv \int_X^X K dx}$$

$$\text{with } \xi_L = \frac{-C}{8C} \frac{g_{10} \left(\frac{2kh (K^2 + k^2)}{\sinh 2kh} + \frac{2\Omega^2 k}{C} \right)}{g_1 (h(K^2 + k^2) - \Omega^2)} \quad (3.19)$$

ξ_L represents the amplitude of a wave travelling in the same direction and with the same velocity as those of the envelope of the short waves. It is therefore locked to the wave group. Note that the directions of the short waves and their envelopes are different. In the case of normal incidence $\alpha_0 = \beta = 0$ and at a depth $h = h_0$, ξ_L reduces to the expression of the mean free surface displacement given by Longuet-Higgins and Stewart (1962):

$$\xi_L = - \frac{(4k_0 C g_0 - 1)}{8C g_0 (h_0 - C^2 g_0)} \quad (3.20)$$

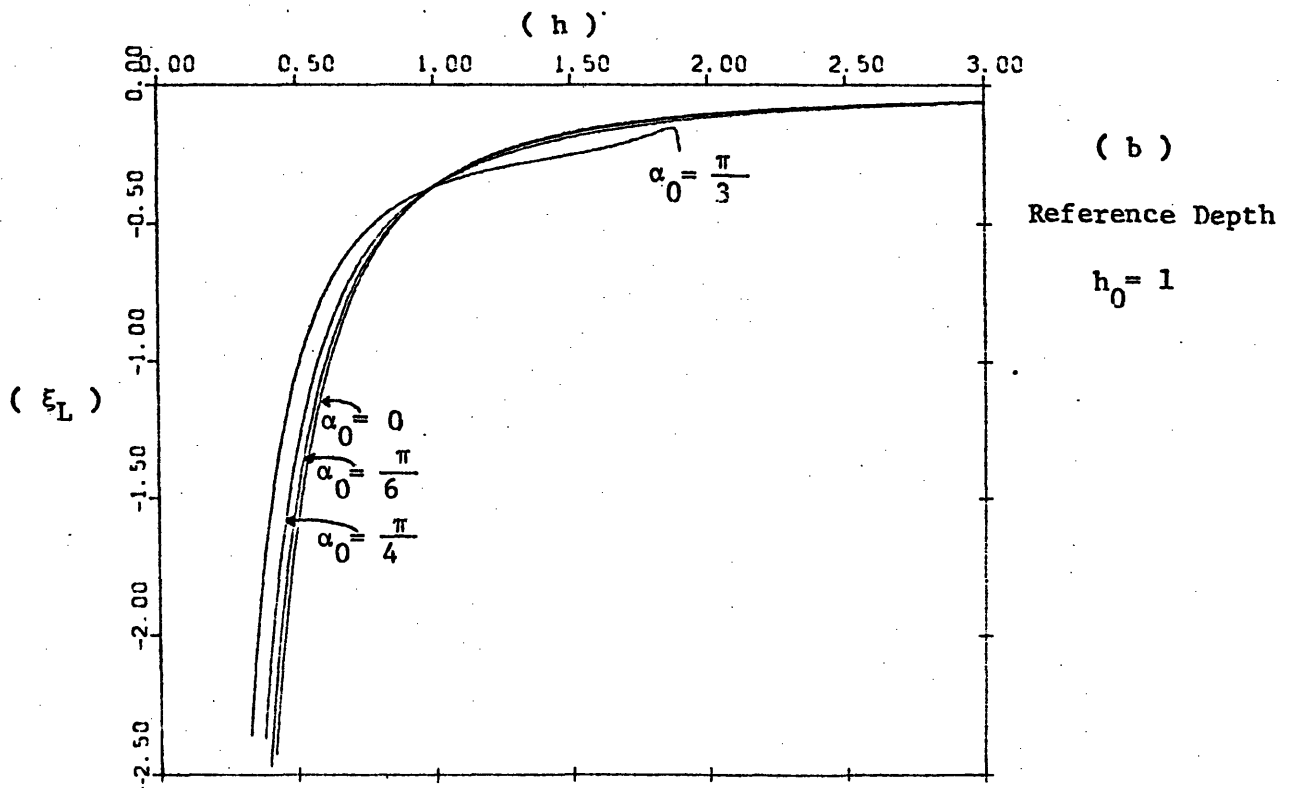
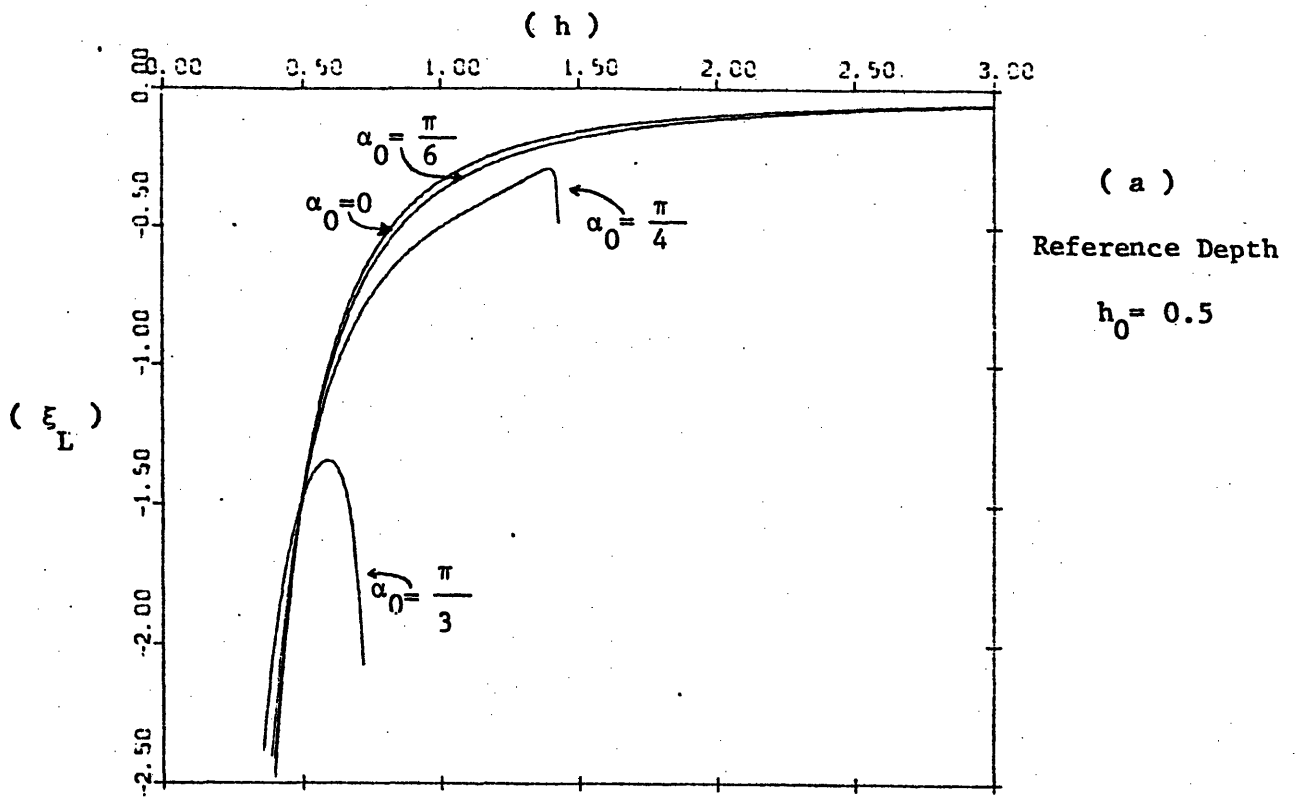


Figure 3.4 Set-Down Associated with the Locked Waves

ξ_L is plotted in Fig. (3.4) as a function of depth for different angle of incidence $\alpha_0 = 0, \frac{\pi}{6}, \frac{\pi}{4}, \frac{\pi}{3}$. The reference depths in figs. (3.4.a) and (3.4.b) are respectively $h_0 = 0.5$ and $h_0 = 1$. ξ_L is always negative. It corresponds therefore to a set down of the mean free surface elevation. $|\xi_L|$ is larger than $|\xi_0|$ but their variation with depth are similar. The effect of increasing the angle of incidence remains very small except in the neighborhood of a caustic.

3.b. Forced Waves on Variable Depth

In the case of variable depth, the second term in the right hand side of Eq. (3.17) is non zero and contribute to the forcing of $\tilde{\xi}$. This equation has then to be solved numerically in the region where the depth varies. We assume the depth to vary from h_0 in the region $X < X_0$ to h_1 in the region $X > X_1$. In the regions of constant depth, the solutions are of the form

$$\tilde{\xi} = \xi_{L0} e^{2iv \int_{X_0}^X K_0 dx} + \xi_{F0} \quad \text{for } X < X_0 \quad (3.21)$$

$$\tilde{\xi} = \xi_{L1} e^{2iv \int_{X_0}^X K_1 dx} + \xi_{F1} \quad \text{for } X > X_1 \quad (3.22)$$

where ξ_{L0} and ξ_{L1} are respectively the values of the locked wave amplitude at depths h_0 and h_1 . ξ_{F0} and ξ_{F1} are homogeneous solutions of Eq. (3.17), in regions of constant depth. These solutions depend on the sign of λ^2

$$\lambda^2 = \frac{1}{h}(\Omega^2 - k_2^2 h) = \frac{k_0^2}{h} (C_{g_0}^2 - \sin^2 \alpha_0 h) \quad (3.23)$$

In the case where $\lambda_1^2 > 0$ at $h = h_1$, the solutions of (3.17) are of the form $e^{\pm 2i\nu|\lambda_1|X}$. By imposing the radiation condition we deduce that

$$\xi_{F1} = A_1 e^{2i\nu|\lambda_1|X} \quad \text{for } X > X_1 \quad (3.24.a)$$

In the case where λ_1^2 is negative at $h = h_1$, the solution of (3.17) are of the form $e^{\pm 2\nu|\lambda_1|X}$. By imposing the condition that $\xi_{F1} \rightarrow 0$ as $X \rightarrow +\infty$ we deduce

$$\xi_{F1} = A_1 e^{-2\nu|\lambda_1|X} \quad \text{for } X > X_1 \quad (3.24.b)$$

Similarly in the region $X < X_0$, depending on the sign of λ^2 we have

$$\xi_{F0} = A_0 e^{2i\nu\lambda_0 X} \quad \text{for } X < X_0 \quad (3.25)$$

where $\lambda_0 = -|\lambda_0|$ if $\lambda_0^2 > 0$ and $\lambda_0 = -i|\lambda_0|$ if $\lambda_0^2 < 0$

A_0 and A_1 are complex constants which can be found by matching together the solutions in regions of constant and variable depth. Outside the region of varying depth the free surface displacement is the sum of three terms: a mean set down ξ_0 , a progressive locked wave

$$\xi_L e^{2i\nu\left(\int_{X_0}^X K dX + k_2 Y - \Omega T\right)} \quad \text{and a progressive 'Forced Wave'}$$

$$A_j e^{2i\nu(\lambda_j X + k_2 Y - \Omega T)} \quad j = 0 \text{ or } 1$$

If λ_j^2 is positive the forced waves are radiated towards large $|X|$ and propagate in a direction defined by

$$\tan \theta = \frac{k_2}{\lambda_j} \quad (3.26)$$

with the phase velocity

$$c_F = \frac{\Omega}{\sqrt{\lambda_j^2 + k_2^2}} = \frac{\Omega}{\sqrt{\frac{\Omega^2 + k_2^2(1-h_j)}{h_j}}} \quad (3.27)$$

The phase velocity and the direction of propagation of these radiated waves are constants which depend on the depths h_j . In general they are different from those of the locked waves. As imposed by the radiation condition θ_0 is negative and θ_1 is positive.

If λ_j^2 negative the forced waves are propagating in Y direction with a phase velocity $\frac{\Omega}{k_2}$. Their amplitude is not constant as in the case $\lambda_j^2 > 0$ but decreases exponentially as we move away from the zone of variable depth. The forced waves are then trapped in this zone.

Depending on the values of the parameters h_0, α_0, h_1 , any combination of the two previous cases can occur. We can have either radiated waves in both regions '0' and '1' or radiated waves in one region and trapped waves in the other or trapped waves in both of them. Table (3.1) illustrates these cases. For given values of h_0 and α_0 it gives the depth h^* at which λ^2 is zero. The value X at which h^* is reached, is called a turning point in the theory of differential equations. If h is smaller than h^* , λ^2 is positive but if h larger than h^* , λ^2 is negative.

$h_0 \backslash \alpha_0$	0°	30°	45°	60°
0.5	∞	1.20	0.60	0.40
1.0	∞	1.44	0.72	0.48
1.5	∞	1.34	0.77	0.45
2.0	∞	1.20	0.60	0.40
2.5	∞	1.10	0.55	0.38

Table 3.1 Critical Values of h^* at which $\lambda = 0$
(Turning Point)

	h	k_2	k_1	K	λ	α°	β°	θ°
$h_0 = 0.5$	0.50	0.77	1.33	1.33	1.05	30.0	30.0	143.8
	1.00	0.77	0.92	1.19	0.50	39.9	32.9	57.0
$h_0 = 1.0$	0.50	0.60	1.42	1.17	1.04	22.9	27.1	30.0
	1.00	0.60	1.04	1.04	0.60	30.0	30.0	135.0

Table 3.2 , Direction of Propagation of Short Waves α , Wave Envelope β , and Forced Waves θ

For oblique incidence, the direction of propagation of the short waves α , that of the locked waves β and that of the radiated waves θ can be different. At some constant depth, the values of these angles are only dependent on h_0 and α_0 and not on the profile of the depth variation. They are given in table (3.2) for $h_0 = 0.5$, $h_1 = 1.0$, and $h_0 = 1.0$, $h_1 = 0.5$. In both cases $\alpha_0 = 30^\circ$. As expected $\alpha_0 = \beta_0$ but $\beta_1 < \alpha_1$ when $h_1 > h_0$ and $\beta_1 > \alpha_1$ when $h_1 < h_0$. The magnitude of θ increases with depth. When $h = h^*$, $|\theta| \rightarrow 90^\circ$: glancing incidence ($h^* = 1.20$ for $h_0 = 0.5$ and $h^* = 1.44$ for $h_0 = 1.0$, according to table (3.1)).

As mentioned above, in the region of varying depth the free surface has to be found by solving numerically Eq. (3.17) with the appropriate matching conditions. By analogy with the form of the solutions in the regions of constant depth (see Eqs. (3.21) and (3.22)) we decompose $\tilde{\xi}$ in two parts:

$$\tilde{\xi} = \xi_L(x) e^{2iv \int_x^X K dx} + \xi_F(x) \quad (3.28)$$

where ξ_L is the locked wave amplitude as defined by Eq. (3.19) and $\xi_F(x)$ is the discrepancy of the free surface displacement from the locked wave due to the depth variation. ξ_F is a wave which is forced in varying depth and will be called the forced wave. This decomposition is mainly for numerical convenience. The governing equation for ξ_F is obtained from Eq. (3.17)

$$\frac{d}{dx} \left(h \frac{d\xi_F}{dx} \right) + 4v^2 (\Omega^2 - k_2^2 h) \xi_F = F(x) \quad (3.29)$$

where $F(x) = \left[h \frac{d^2 Z}{dx^2} + \frac{dh}{dx} \frac{dZ}{dx} + iv \left(4hK \frac{dZ}{dx} + 2Z \frac{d}{dx} (Kh) \right) \right.$

$$\left. - \frac{(C_{g_0})^2 k_0 \cos \alpha_0}{2} \frac{d}{dx} \left(\frac{k}{C_g} \right) \right] e^{2iv \int_{x_0}^x K dx}$$

$$Z(x) = \xi_0 - \xi_L$$

The boundary conditions are:

$$\xi_F = \xi_{F0} = A_0 e^{2iv\lambda_0 x} \quad \text{and} \quad \frac{\partial \xi_F}{\partial x} = 2iv\lambda_0 \xi_{F0} \quad \text{at} \quad x = x_0 \quad (3.30)$$

$$\xi_F = \xi_{F1} = A_1 e^{2iv\lambda_1 x} \quad \text{and} \quad \frac{\partial \xi_F}{\partial x} = 2iv\lambda_1 \xi_{F1} \quad \text{at} \quad x = x_1$$

where $\lambda_j = (-1)^{j+1} |\lambda_j|$ if $\lambda_j^2 > 0$, $\lambda_j = (-1)^{j+1} |\lambda_j|$ if $\lambda_j^2 < 0$

It should be noted that $|F|$ is zero in regions of constant depth and increases with increasing slope of the bottom profile. However this increase is very slow in deep water and very rapid in intermediate depth $h \approx 0.5$ (Note from figs. (3.3) and (3.4) that Z and $\frac{dZ}{dh}$ are very small in deep water but increases sharply in shallower water). Therefore $|\xi_F|$ is expected to be small (i.e. $|\xi_F| \ll 0(\epsilon^2)$) if h_0 and h_1 correspond both to deep water or if the slope of the bottom profile is small.

4. Numerical Procedure

4.a. Numerical Method

Eq. (3.29) with the boundary conditions (3.30) correspond to a boundary value problem in one dimension and can be solved easily by using a finite difference scheme. However in the most general case the governing equation is two-dimensional and the finite difference method becomes inappropriate. A different numerical method which can be easily extended to the 2-D case is the so called 'Hybrid element method' (see Mei, 1978). This method is an extension of the usual finite element method to the case where the domain is infinite but an analytical form of the solution is known in some outer region. The solution is obtained by using finite elements in the inner domain and an analytical representation in the outer domain. By choosing an adequate variational form for the finite elements problem the matching conditions can be transformed into 'stationarity conditions' for the functional at the extreme nodal points. In our case the functional can be deduced from Mei's results (Eq. 4.4 p. 407)

$$\begin{aligned}
 J(\xi) = & \int_{x_0}^{x_1} \left(-\frac{h}{2} (\xi')^2 + 2\lambda \xi^2 - F\xi \right) dx - \left[h \left(\frac{\xi_{F1}}{2} - \xi \right) \frac{\partial \xi_{F1}}{\partial x} \right]_{x_1} \\
 & + \left[h \left(\frac{\xi_{F0}}{2} - \xi \right) \frac{\partial \xi_{F0}}{\partial x} \right]_{x_0}
 \end{aligned} \tag{4.1}$$

where $\tilde{\lambda} = v^2(\Omega^2 - k_2^2 h)$, ξ_{F0} and ξ_{F1} are given in Eqs. (3.30). The Variational form of (4.1) becomes after some manipulations:

$$\begin{aligned} \delta J = & \int_{x_0}^{x_1} ((h\xi')' + 4\lambda\xi - F) \delta\xi dx + [\delta\xi h (\frac{\partial \xi_{F1}}{\partial x} - \frac{\partial \xi}{\partial x}) - \frac{\partial(\delta\xi_{F1})}{\partial x} h(\xi_{F1} - \xi) \\ & - \frac{h}{2} \delta\xi_{F1} \frac{\partial \xi_{F1}}{\partial x} - \xi_{F1} \frac{\partial(\delta\xi_{F1})}{\partial x}]_{x_1} - [\delta\xi h (\frac{\partial \xi_{F0}}{\partial x} - \frac{\partial \xi}{\partial x}) - \frac{\partial(\delta\xi_{F0})}{\partial x} \\ & h(\xi_{F0} - \xi) - \frac{h}{2} \delta\xi_{F0} \frac{\partial \xi_{F0}}{\partial x} - \xi_{F0} \frac{\partial(\delta\xi_{F0})}{\partial x}]_{x_0} \end{aligned} \quad (4.2)$$

Eq. (4.2) shows that any solution of Eqs. (3.29) - (3.30) corresponds to a stationary point for the functional J i.e. $\delta J = 0$. We subdivide the interval $[x_0, x_1]$ into (N-1) elements of equal length $\delta x = \frac{(x_1 - x_0)}{N-1}$. For each element (x_i, x_{i+1}) $i = 1 \dots N-1$, we use a linear interpolating function:

$$\begin{aligned} \xi_i(x) &= \frac{(x_{i+1} - x)}{\delta x} \bar{\xi}_i + (\frac{x - x_i}{\delta x}) \bar{\xi}_{i+1} & x_i < x < x_{i+1} \\ \xi_i &= 0 & x < x_i \text{ or } x > x_{i+1} \end{aligned} \quad (4.3)$$

where $\bar{\xi}_i, \bar{\xi}_{i+1}$ are the nodal unknowns at points x_i and x_{i+1} . The contribution of each element to the functional J is

$$E_i = \int_{X_i}^{X_{i+1}} \left(-\frac{h}{2} (\xi'_i)^2 + 2\tilde{\lambda} \xi_i^2 - F\xi_i \right) dx \quad i = 2, \dots, N-2 \quad (4.4)$$

which gives after integration:

$$E_i = \frac{a_i}{2} \bar{\xi}_i^2 + \frac{b_i}{2} \bar{\xi}_{i+1}^2 + c_i \bar{\xi}_i \bar{\xi}_{i+1} - d_i \bar{\xi}_i - e_i \bar{\xi}_{i+1} \quad (4.5)$$

The contributions of the end intervals, E_1 and E_{N-1} have an extra term coming from the boundary conditions. E_1, E_{N-1} are respectively the sum of Eq. (4.5) for $i = 1$ or $i = N-1$ and the terms $-ivh_0 \lambda_0 \bar{\xi}_1^2$ or $ivh_1 \lambda_1 \bar{\xi}_N^2$ where λ_j is defined in Eq. (3.30)

$$\begin{aligned} a_i = b_i &= \frac{1}{(\delta x)^2} \left(-\int_{X_i}^{X_{i+1}} h dx + 4 \int_{X_i}^{X_{i+1}} \tilde{\lambda}(X) (X_{i+1}-X)^2 dx \right) \\ c_i &= \frac{1}{(\delta x)^2} \left(\int_{X_i}^{X_{i+1}} h dx + 4 \int_{X_i}^{X_{i+1}} \tilde{\lambda}(X_{i+1}-X)(X-X_i) dx \right) \\ d_i &= \frac{1}{\delta x} \left(\int_{X_i}^{X_{i+1}} F(X)(X_{i+1}-X) dx \right) \\ e_i &= \frac{1}{\delta x} \left(\int_{X_i}^{X_{i+1}} F(X)(X-X_i) dx \right) \end{aligned} \quad (4.6)$$

The stationarity conditions at the nodal points (i.e. $\frac{\partial}{\partial \bar{\xi}_j} (\sum_{i=1}^{N-1} E_i) = 0$)

then leads to a set of N equations for N unknowns:

$$\begin{cases} \gamma_1 \bar{\xi}_2 + \beta_1 \bar{\xi}_1 = W_1 \\ \gamma_i \bar{\xi}_{i+1} + \beta_i \bar{\xi}_i + \alpha_i \bar{\xi}_{i-1} = W_i & i = 2, \dots, N-1 \\ \beta_N \bar{\xi}_N + \alpha_N \bar{\xi}_N = W_N \end{cases} \quad (4.7)$$

where

$$\gamma_i = c_i = \frac{2}{3} (\delta x) \left(\frac{\tilde{\lambda}_i + \tilde{\lambda}_{i+1}}{2} \right) + \left(\frac{h_i + h_{i+1}}{2\delta x} \right) \quad i = 1, \dots, N-1$$

$$\beta_i = a_i + b_{i-1} = \frac{4}{3} (\delta x) \left(\frac{\tilde{\lambda}_{i+1} + 2\tilde{\lambda}_i + \tilde{\lambda}_{i-1}}{2} \right) - \left(\frac{h_{i+1} + 2h_i + h_{i-1}}{2\delta x} \right)$$

$i = 2, \dots, N-1$

$$\alpha_i = c_{i-1} = \frac{2}{3} \delta x \left(\frac{\tilde{\lambda}_i + \tilde{\lambda}_{i-1}}{2} \right) + \frac{h_i + h_{i-1}}{2\delta x} \quad i = 2, \dots, N$$

$$W_i = d_i + e_{i-1} = F_i \delta x \quad i = 2, \dots, N-1$$

The extreme values for β and W are:

$$\beta_1 = \frac{4}{3} (\delta x) \left(\frac{\tilde{\lambda}_1 + \tilde{\lambda}_2}{2} \right) - \left(\frac{h_1 + h_2}{2\delta x} \right) - 2ivh_0 \lambda_0$$

$$\beta_N = \frac{4}{3} (\delta x) \left(\frac{\tilde{\lambda}_{N-1} + \tilde{\lambda}_N}{2} \right) - \left(\frac{h_{N-1} + h_N}{2\delta x} \right) + 2ivh_1 \lambda_1 \quad (4.9)$$

$$W_1 = \frac{F_1}{2} \delta x$$

$$W_N = \frac{F_N}{2} \delta x$$

The linear system (4.7) is solved as in section (I.5.a). Introducing the intermediate variables x_i and y_i such that:

$$\bar{\xi}_{i+1} = x_i \bar{\xi}_i + y_i \quad i = 1, \dots, N-1 \quad (4.10)$$

They are found to obey the following recurrence relations:

$$x_i = \frac{-\alpha_{i+1}}{\gamma_{i+1} x_{i+1} + \beta_{i+1}} \quad y_i = \frac{-\gamma_{i+1} y_{i+1} + W_i}{\gamma_{i+1} x_{i+1} + \beta_{i+1}} \quad i = 1, \dots, N-2$$

$$x_{N-1} = \frac{-\alpha_N}{\beta_N} \quad y_{N-1} = \frac{W_N}{\beta_N} \quad (4.11)$$

Therefore having the initial value

$$\bar{\xi}_1 = \frac{W_1 - \gamma_1 y_1}{\gamma_1 x_1 + \beta_1} \quad (4.12)$$

all the other unknowns can be calculated by using Eq. (4.10). Finally, from the values of $\bar{\xi}_1$, by using the linear relation (4.3) one can deduce the forced wave solution $\xi(X)$ for $X_0 < X < X_1$. The listing of the program is given in Appendix (B2). It should be noted that the computation is done in double precision so that the forcing term which involves second derivatives of Z can be found with sufficient accuracy. The parameter ν has been taken to be $1/\Omega$ in all the computed cases. This means that in dimensional variables, ϵ also represents the ratio between the short wave frequency and the envelope frequency i.e. $\epsilon = \frac{\Omega}{\omega}$

4.b. Check of the Numerical Results

The numerical solution was checked with a 'quasi analytical solution', in the case of normal incidence. ($\alpha_0 = 0$) and linear increasing depth. It was found to give the same results within 0.1% (see Appendix (B2)).

The 'analytical solution' is found by solving Eq. (3.29) with the boundary conditions (3.30) in the case of a linear depth variation. Let us introduce:

$$h(X) = \gamma X \quad X_0 < X < X_1 \quad (4.13)$$

Two cases have to be considered depending on whether the depth increases ($\gamma > 0$) or decreases ($\gamma < 0$). We first consider the case $\gamma > 0$. By using the transformation $v = 4 \sqrt{\frac{x}{\gamma}}$, Eq. (3.29) becomes:

$$\frac{d^2 \xi}{dv^2} + \frac{1}{v} \frac{d\xi}{dv} + \xi = \frac{F}{4} \quad (4.14)$$

whose solutions can be found in terms of Bessel's functions Y_0 and J_0 . After some manipulations, $\xi(x)$ can be written as follows:

$$\xi(x) = \frac{\pi}{\gamma} [(-E_1(x) + A)J_0(4\sqrt{\frac{x}{\gamma}}) + (E_2(x) + B)Y_0(4\sqrt{\frac{x}{\gamma}})] \quad (4.15)$$

$$\text{where } E_1(x) = \int_{x_0}^x F(x') Y_0(4\sqrt{\frac{x'}{\gamma}}) dx' \quad E_2(x) = \int_{x_0}^x F(x') J_0(4\sqrt{\frac{x'}{\gamma}}) dx'$$

A, B are two constants which are found by using the boundary conditions (4.4).

$$A = \frac{c_2(c_3 E_1(x_1) - c_4 E_2(x_1))}{c_2 c_3 - c_1 c_4} \quad B = -\frac{c_1}{c_2} A \quad (4.16)$$

$$\text{with } c_1 = -J_1(4\sqrt{\frac{x_0}{\gamma}}) + i J_0(4\sqrt{\frac{x_0}{\gamma}})$$

$$c_2 = -Y_1(4\sqrt{\frac{x_0}{\gamma}}) + i Y_0(4\sqrt{\frac{x_0}{\gamma}})$$

$$c_3 = J_1(4\sqrt{\frac{x_1}{\gamma}}) + i J_0(4\sqrt{\frac{x_1}{\gamma}})$$

$$c_4 = Y_1(4\sqrt{\frac{x_1}{\gamma}}) + i Y_0(4\sqrt{\frac{x_1}{\gamma}})$$

Actually this solution is not totally analytical in the sense that the forcing term F is rather complicated and has to be computed numerically, and similarly for $E_1(\gamma)$ and $E_2(X)$. The listing of the program is given in Appendix (B2).

In the case where $\gamma < 0$, the solution of Eq. (3.29) can be similarly expressed in terms of confluent hypergeometric functions

$$\rho_1(X) = e^{-\nu} M(1/2, 1, 2\nu) \text{ and } \rho_2(X) = e^{-\nu} U(1/2, 1, 2\nu)$$

where $\nu = 4 \frac{X}{|\gamma|}$. Since the computation of these functions is in itself a long task, no attempt was made to use this analytical solution to check the numerical results.

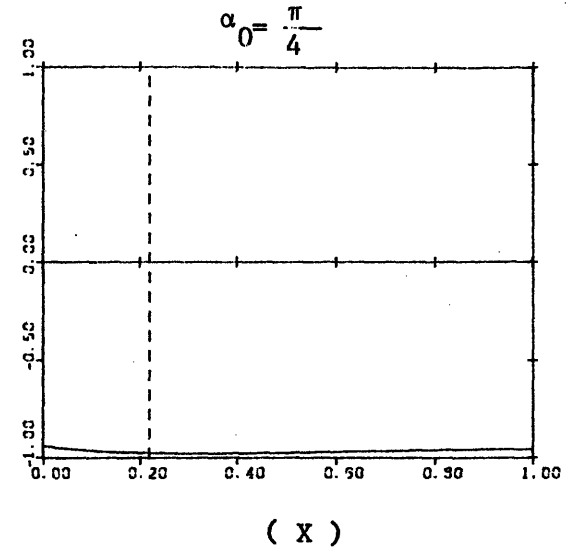
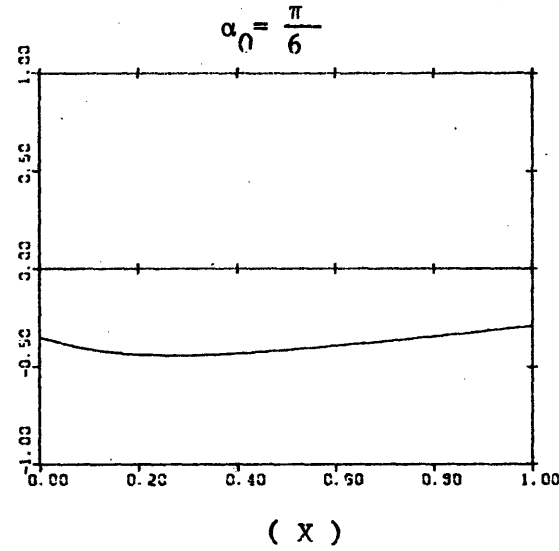
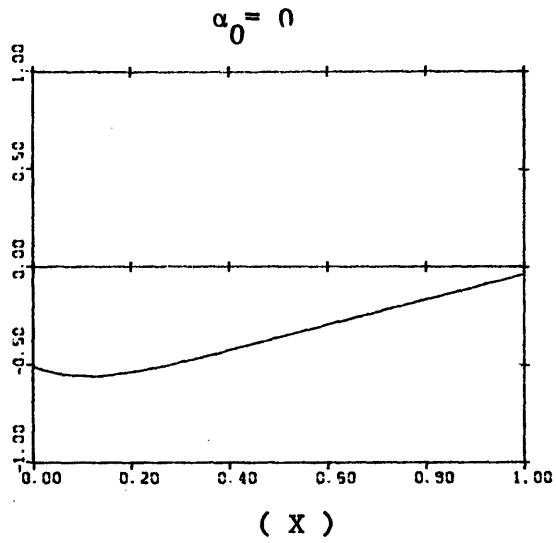
5. Numerical Results

The second order free surface displacement depends on the bottom profile. In the region of varying depth it can be decomposed into locked and forced waves. The magnitude of the forcing function depends on the water depth, the slope of the bottom profile and the initial angle of incidence. It vanishes in the region of constant depth. Depending on the wave parameters and the water depth, the forced waves can either be radiated towards large $|X|$ in the form of free waves with constant amplitude (case $\lambda^2 > 0$) or be trapped along the zone of depth variation with an amplitude decreasing exponentially with $|X|$ (case $\lambda^2 < 0$). For normally incident waves, the second order forced waves are always radiated in the X direction towards both infinities. In this section the forced wave amplitude $|\xi_F|$ and the corresponding phase are plotted for different bottom profiles. Note that $\frac{d}{dX} (\text{Arg}(\xi_F))$ gives the wave number of ξ_F in the X direction. In all the computed cases, the parameters are chosen such that there is no caustic.

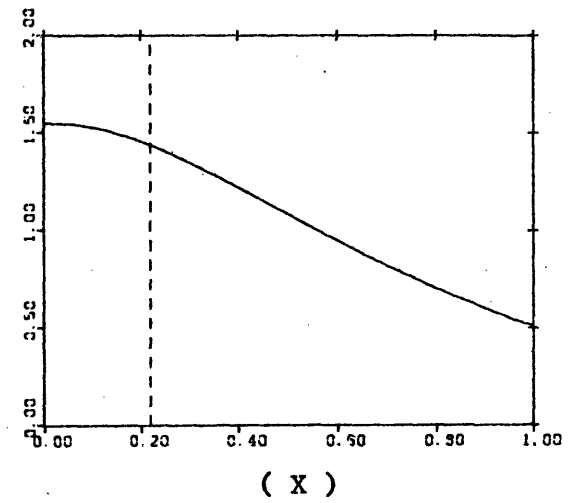
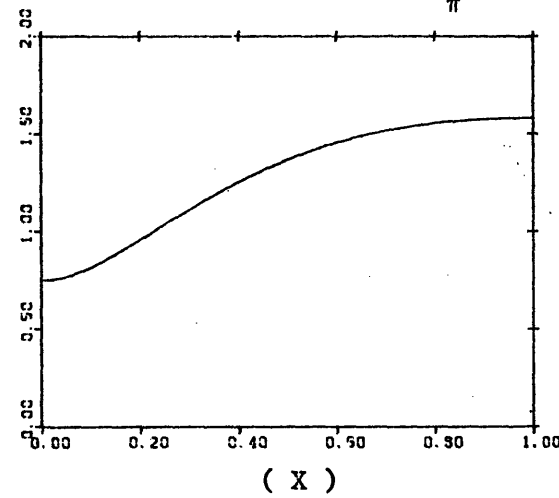
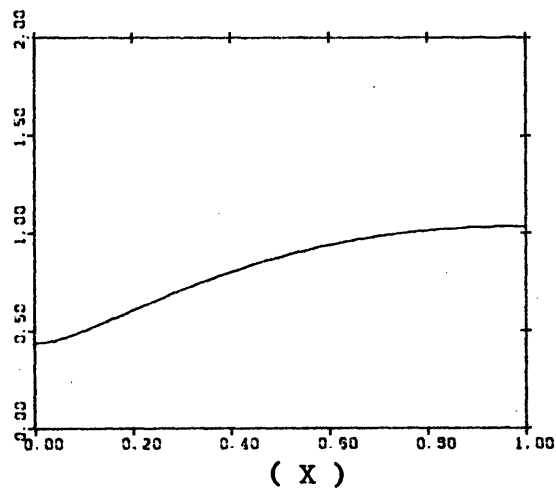
5.a. Linear Depth Variation

Fig. (5.1) presents the case where the depth increases from $h_0 = 0.5$ to $h_0 = 1$ over a distance $XL = 1$. The slope is then $\gamma = \frac{dh}{dX} = 0.5$. The forced waves are plotted for different angles of incidence $\alpha_0 = 0$ (normal incidence), $\alpha_0 = \pi/6$, $\alpha_0 = \pi/4$. For $\alpha_0 = 0$ and $\pi/6$ their amplitude is larger on the right hand side than on the left hand side. As expected their wavenumber in the X direction is positive on the right and negative

Figure 5.1 Forced Waves over Linearly Increasing Depth,
 $h_0=0.5, dh=0.5, XL=1$



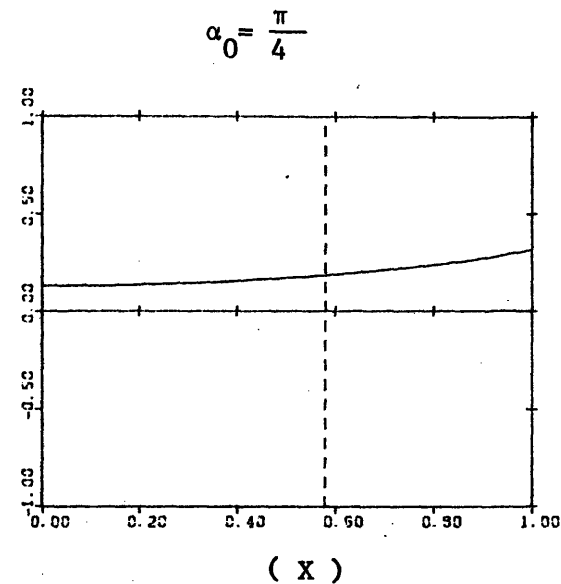
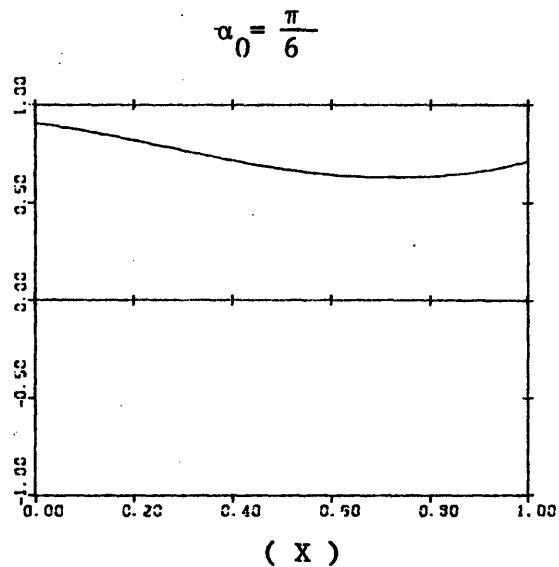
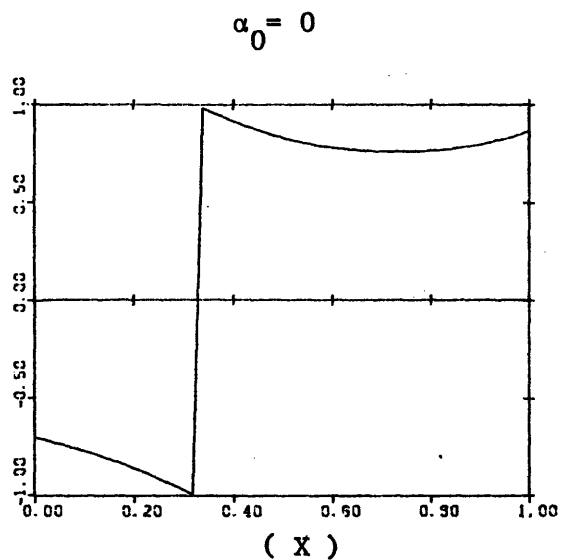
(a) Forced Wave Phase $\frac{\text{Arg}(\xi_F(X))}{\pi}$



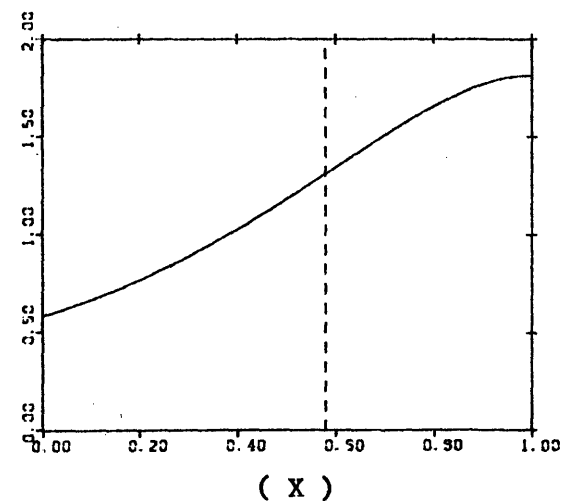
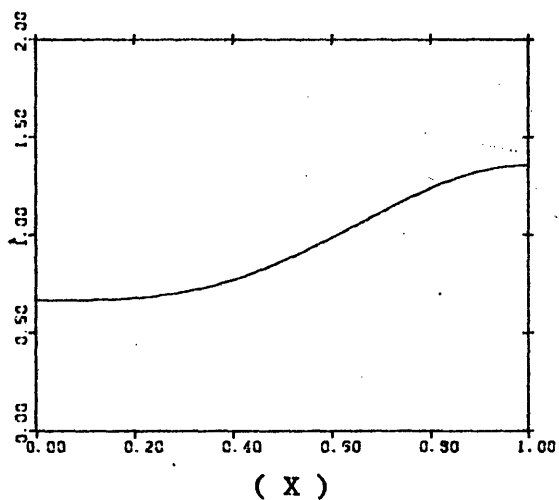
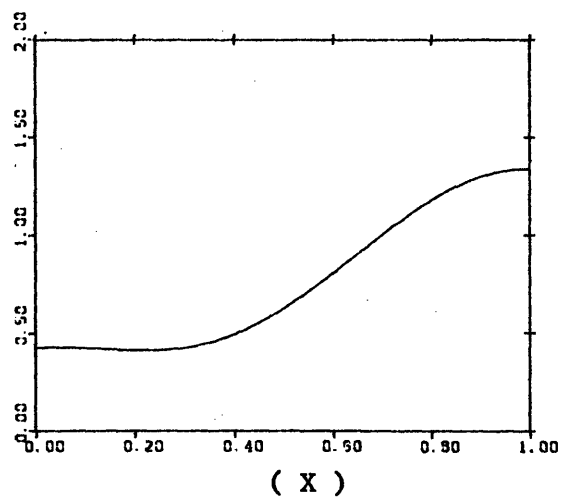
(b) Forced Wave Amplitude $|\xi_F(X)|$

Figure 5.2 Forced Waves over Linearly Decreasing Depth,

$$h_0 = 1, dh = -0.5, \gamma L = 1$$



(a) Forced Wave Phase $\frac{\text{Arg}(\xi_F(X))}{\pi}$



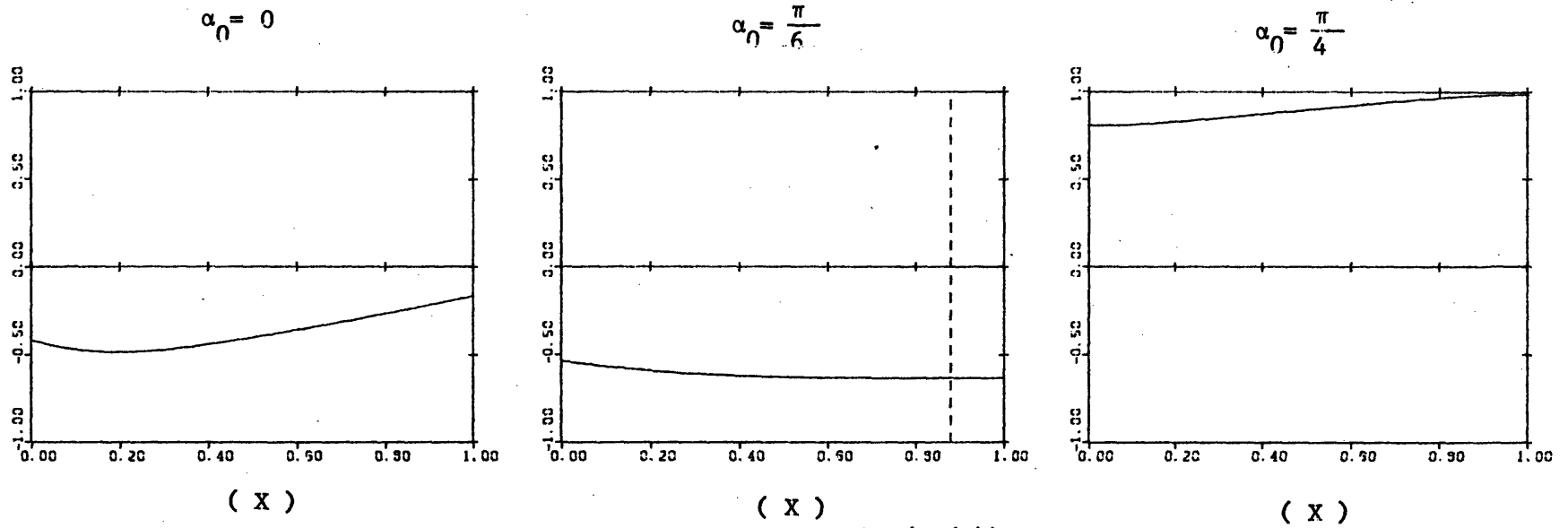
(b) Forced Wave Amplitude $|\xi_F(X)|$

on the left, i.e. the forced waves are outgoing. For $\alpha_0 = \pi/4$, the forced waves on the right hand side are trapped. The turning point is at $h^* = 0.6$, according to table (3.1), and is marked on the plot by the dash-line. The amplitude of the trapped waves is smaller than that of the outgoing waves, and decreases exponentially as X increases. Similarly fig. (5.2) illustrates the case where the depth decreases from $h_0 = 0.5$ to $h_1 = 1.0$ over a distance $XL = 1$. For $\alpha_0 = \pi/4$, the left going forced waves are trapped but the right going forced waves propagate towards increasing X with large amplitude.

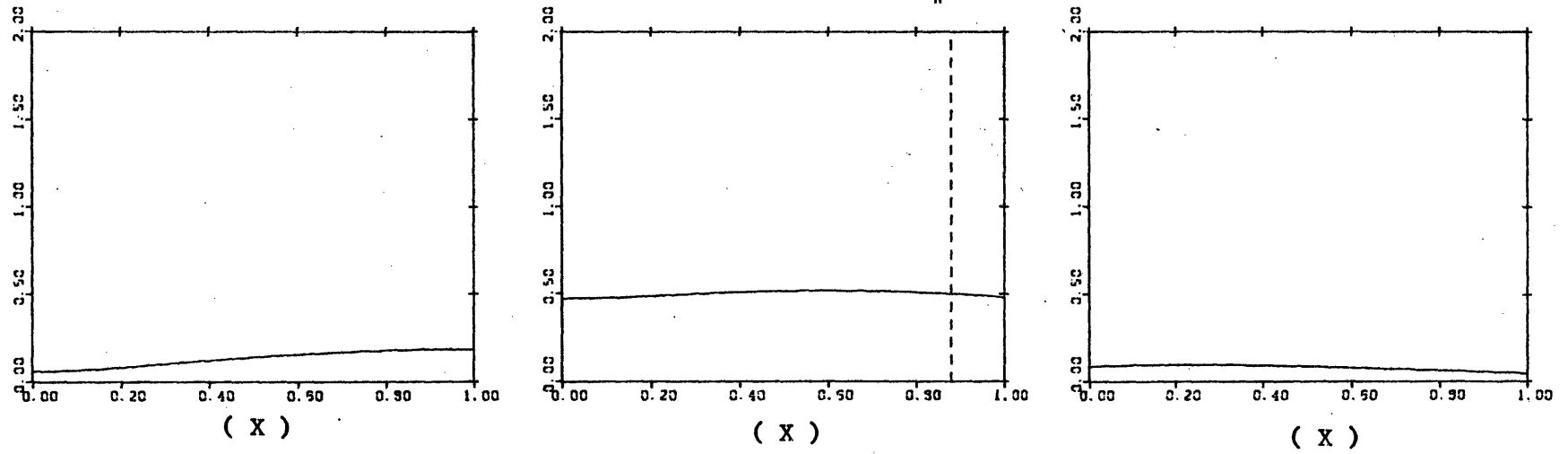
From Figs. (3.3) and (3.4) we know that $|Z|$ and $|\frac{dZ}{dy}|$ become smaller as the depth increases. The forcing is then smaller and we expect the magnitude of $|\xi_F|$ to decrease with increasing depth. Fig. (5.3) shows the forced waves in the case where the depth increases from 1 to 1.5 with a slope $\gamma = 0.5$. By comparing Fig. (5.1) and Fig. (5.3) we note that the amplitude of the forced waves is much larger in the first case than in the second. For a more complete illustration of the effect of increasing depth, we have plotted for the case of normal incidence the right going and left going radiated wave amplitudes as a function of the initial depth h_0 (see Fig. 5.4). h_0 varies from 0.5 to 3, h_1 is taken equal to $(h_0 + 0.5)$ and $XL = 1$ such that $dh = 0.5$ and $\gamma = 0.5$ always. The figure shows the rapid decrease in the amplitude of the radiated waves.

The forced waves are also determined by the slope of the bottom profile. In fig. (5.5) we consider the depth to vary from $h_0 = 0.5$ to $h_1 = 1$ but

Figure 5.3 Forced Waves over Linearly Increasing Depth,
 $h_0 = 1, dh = 0.5, XL = 1$



(a) Forced Wave Phase $\frac{\text{Arg}(\xi_p(X))}{\pi}$



(b) Forced Wave Amplitude $|\xi_p(X)|$

Figure 5.4 Forced Wave Amplitudes on the Left and Right Hand Sides
of a Linearly Increasing Depth region
Normal Incidence, $dh= 0.5$, $XL= 1$

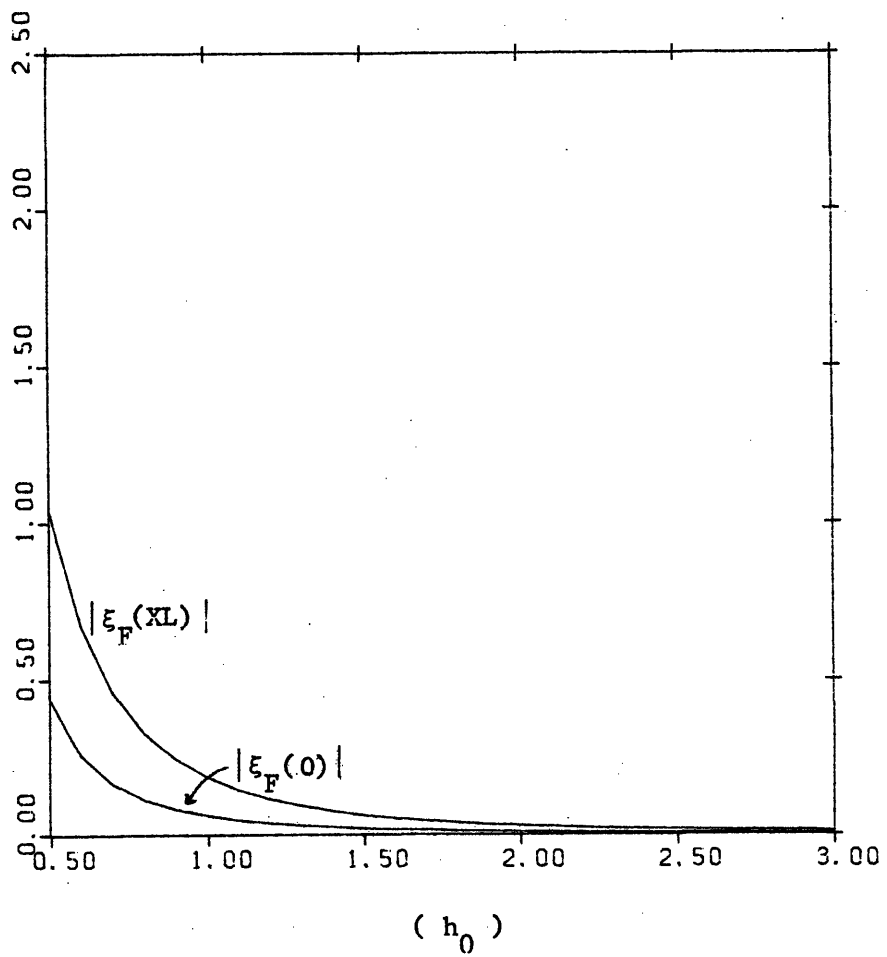
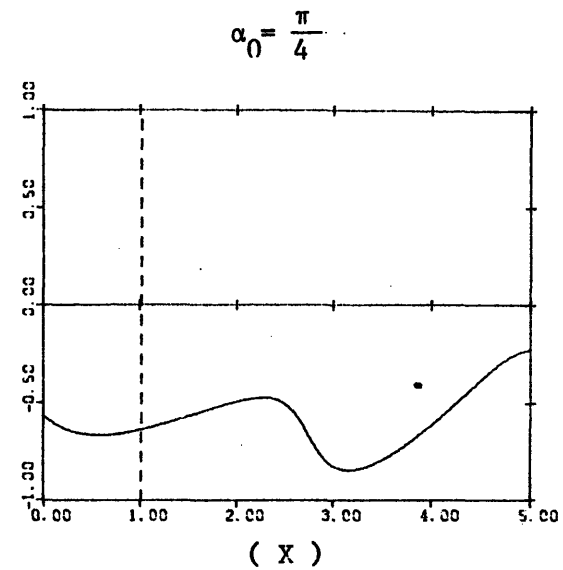
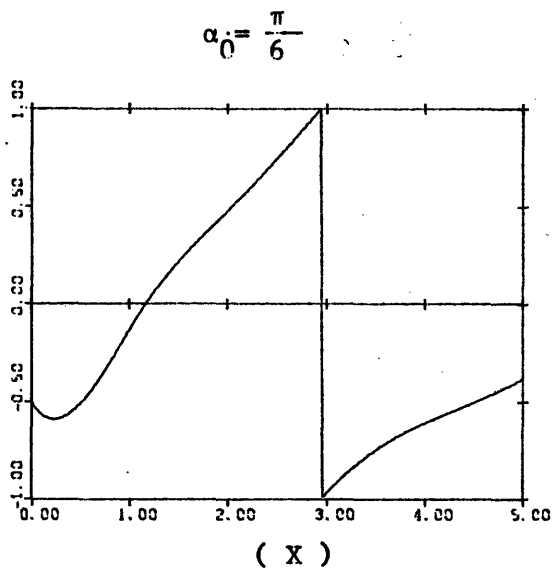
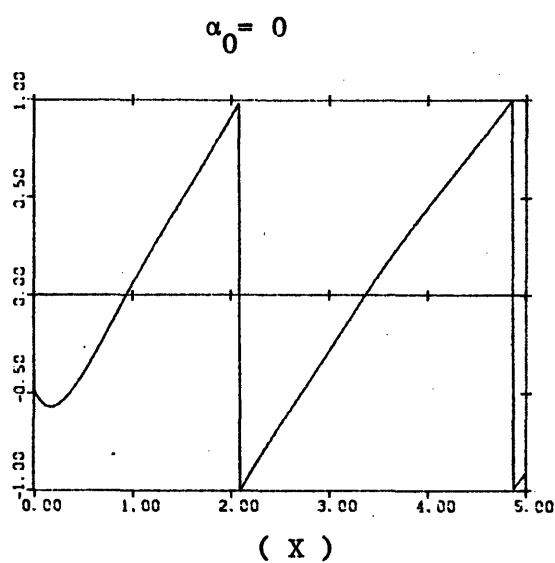
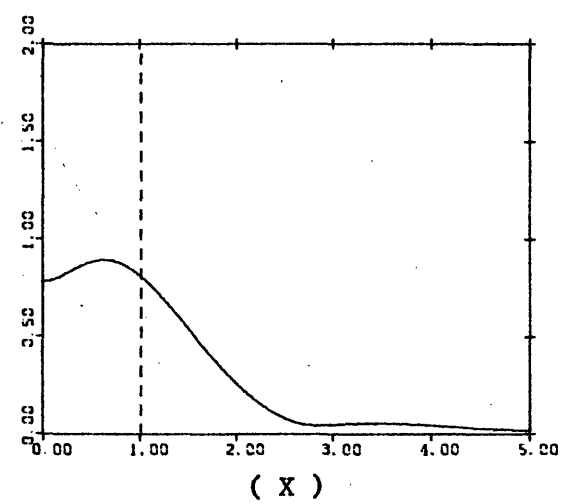
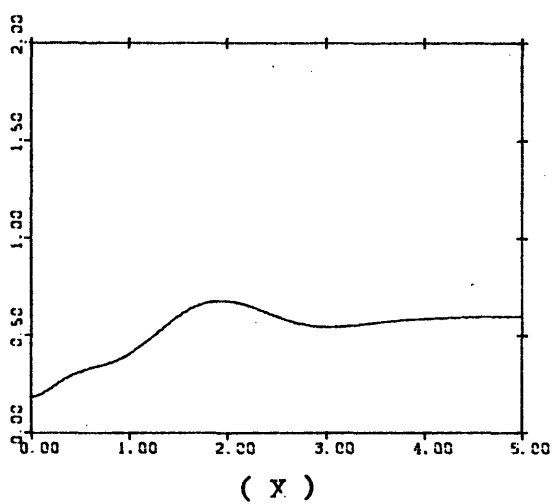
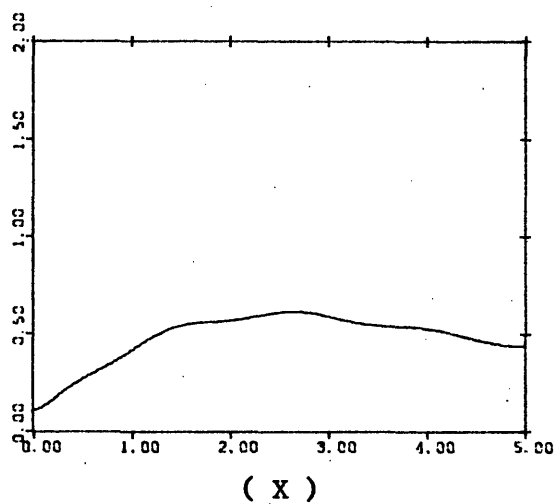


Figure 5.5 Forced Waves over Linearly Increasing Depth,
 $h_0 = 0.5, dh = 0.5, XL = 5$



(a) Forced Wave Phase $\frac{\text{Arg}(\xi_F(X))}{\pi}$



(b) Forced Wave Amplitude $|\xi_F(X)|$

the length of the transition zone is taken to be $XL = 5$, and therefore $\gamma = 0.1$. Comparing Fig. (5.1) with Fig. (5.5) we note that the forced wave amplitude is smaller in the latter. Similarly in the case where the depth varies from $h_0 = 1$ to $h_1 = 0.5$ over a distance $XL = 5$, Fig. (5.6) shows smaller wave amplitude than those in Fig. (5.2). However in this case there is in addition oscillations of the forced wave amplitude with a period increasing with the angle of incidence. The existence of these oscillations depends on the length of the transition zone. At each node of $|\xi_F|$, there is a phase jump of π . In the complex plane it means that ξ_F crosses zero and that its derivative is continuous. For a more general picture about the effect of decreasing slope we display in Figs. (5.7) and (5.8) the variations with XL of the right hand side $|\xi_F|_R$ and left hand side $|\xi_F|_L$ forced wave amplitudes. Fig. (5.7) corresponds to an increasing depth $h_0 = 0.5$, $h_1 = 1$ while Fig. (5.8) corresponds to a decreasing depth $h_0 = 1$, $h_1 = 0.5$. In both figures normal incidence $\alpha_0 = 0$, and oblique incidence $\alpha_0 = \pi/4$, are considered. We note that in the case of normal incidence the left going wave amplitude is always smaller than the right going wave amplitude. In the case of oblique incidence $\alpha_0 = \pi/4$, there is a turning point at $h^* = 0.6$, the forced wave amplitude $|\xi_F|$ is smaller in the regions where $h > h^*$ i.e. regions where forced waves are trapped. The effect of decreasing the slope is to decrease the amplitude of the forced waves on both sides. For normal incidence the decrease in the amplitude of the left going wave is accompanied with small oscillations.

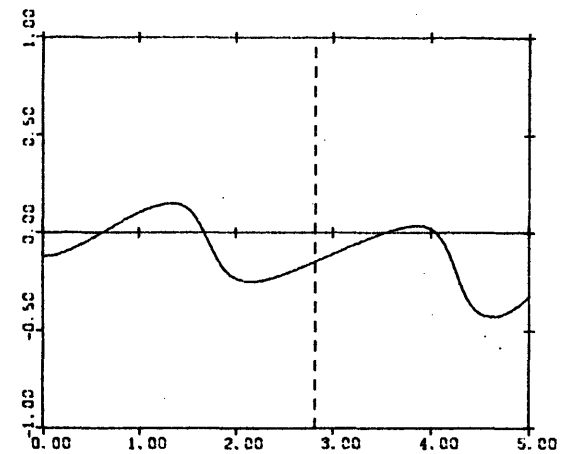
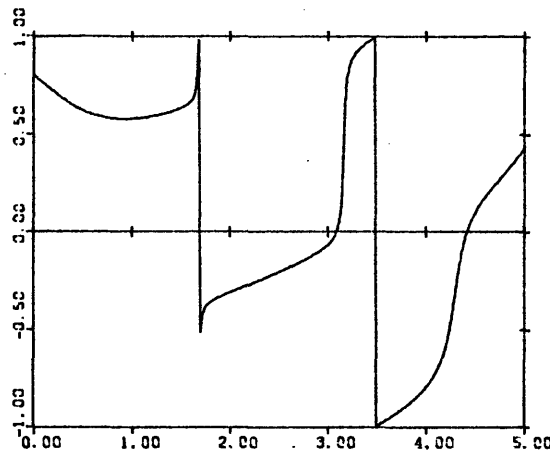
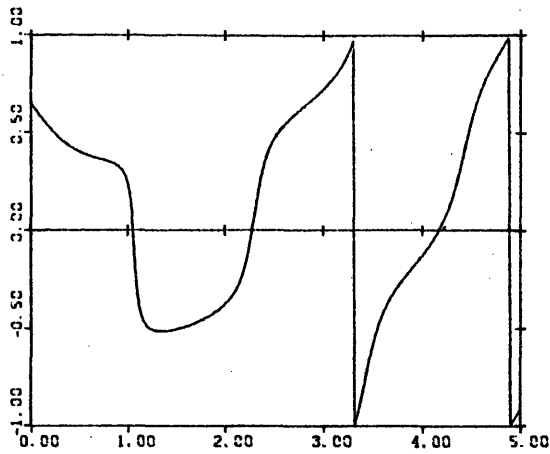
Figure 5.6 Forced Waves over Linearly Decreasing Depth,

$$h_0 = 1, dh = -0.5, XL = 5$$

$$\alpha_0 = 0$$

$$\alpha_0 = \frac{\pi}{6}$$

$$\alpha_0 = \frac{\pi}{4}$$

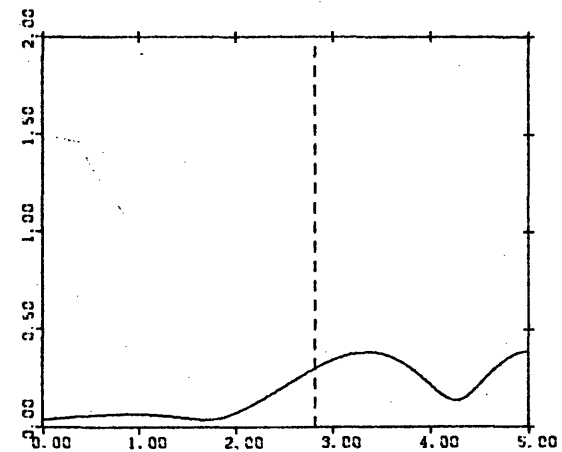
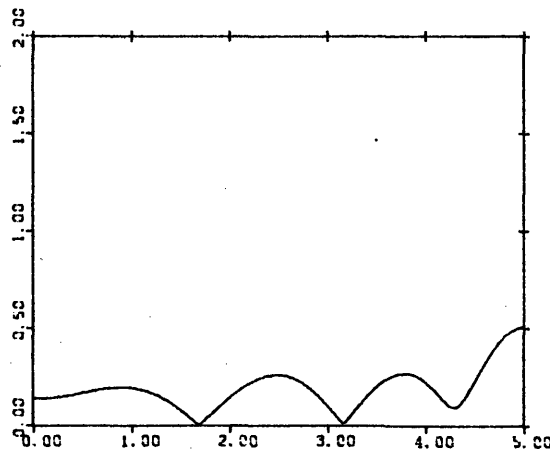
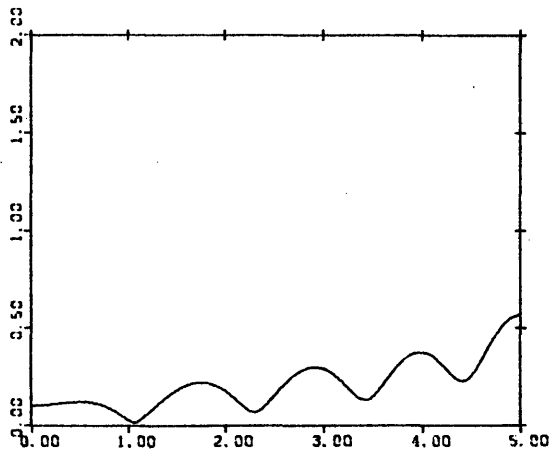


(X)

(X)

(X)

(a) Forced Wave Phase $\frac{\text{Arg}(\xi_F(X))}{\pi}$



(X)

(X)

(X)

(b) Forced Wave Amplitude $|\xi_F(X)|$

Figure 5.7 Forced Wave Amplitudes on the Left and Right Hand Sides
of the Linearly Decreasing Depth Region

$$h_0 = 1, dh = -0.5$$

(a) Normal Incidence $\alpha_0 = 0$

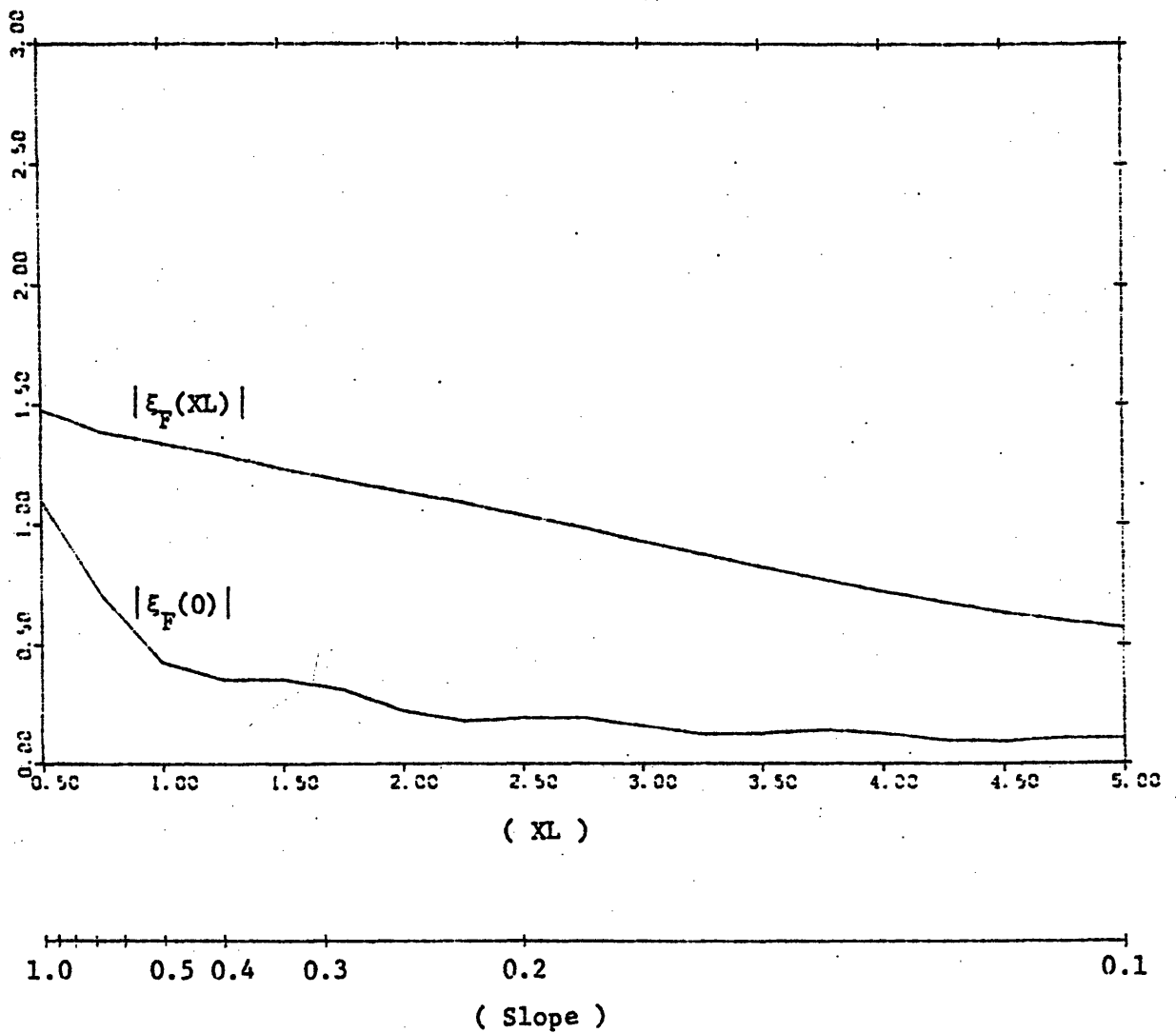


Figure 5.7 (Cont.)

(b) Oblique Incidence $\alpha_0 = \frac{\pi}{4}$

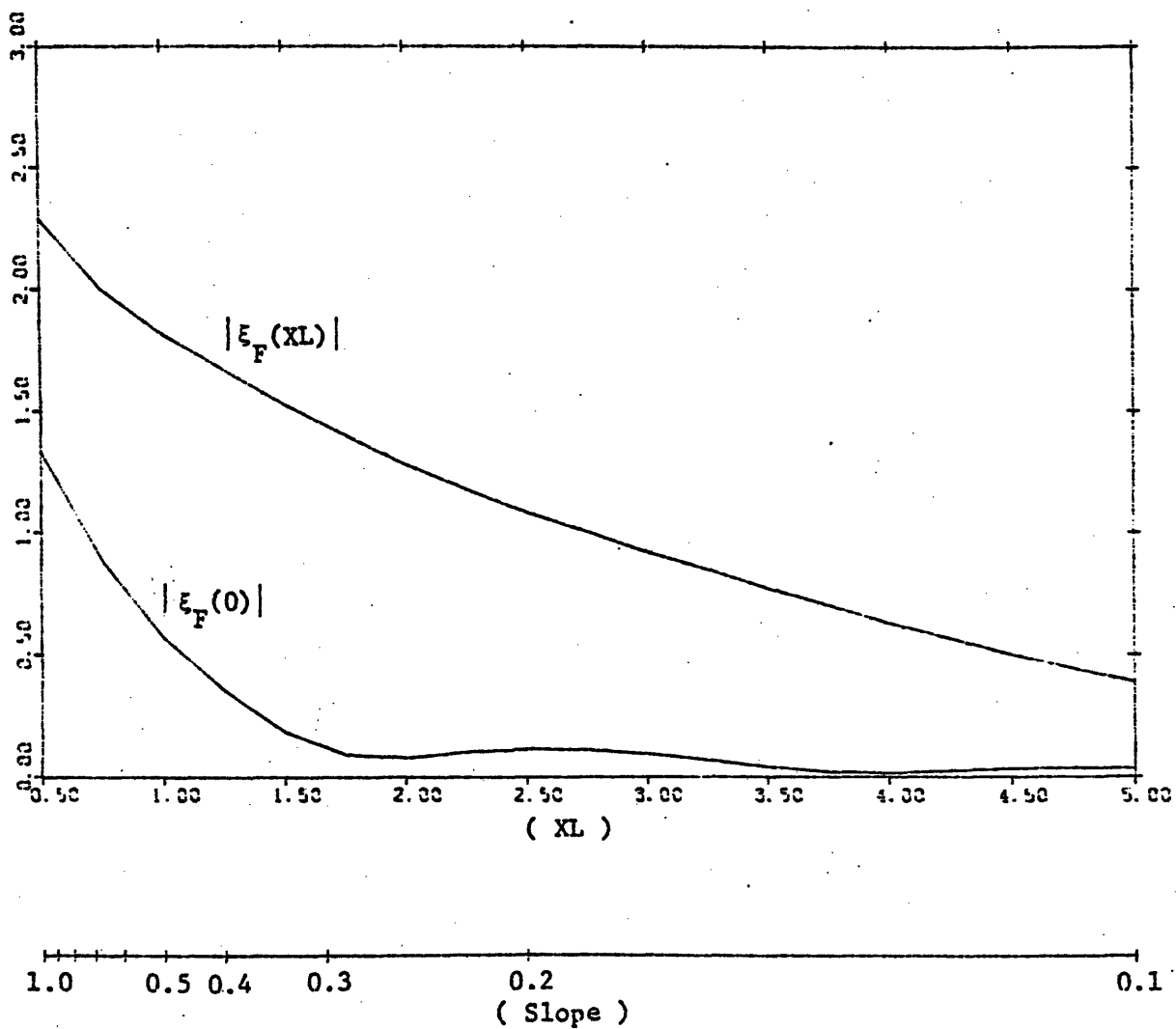


Figure 5.8 Forced Wave Amplitude on the Left and Right Hand Sides
of a Linearly Increasing Depth Region

$$h_0 = 0.5, dh = 0.5$$

(a) Normal Incidence $\alpha_0 = 0$

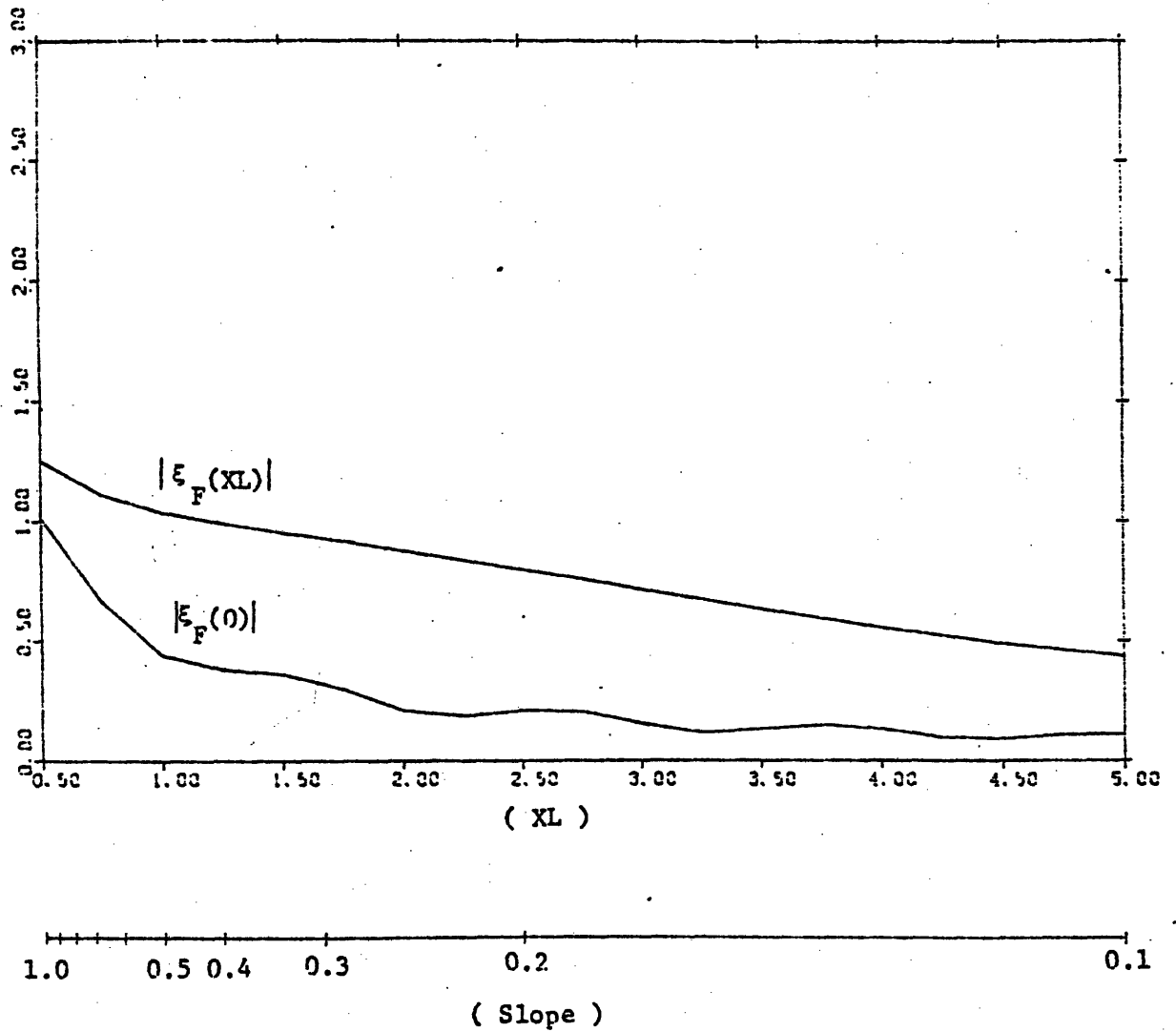
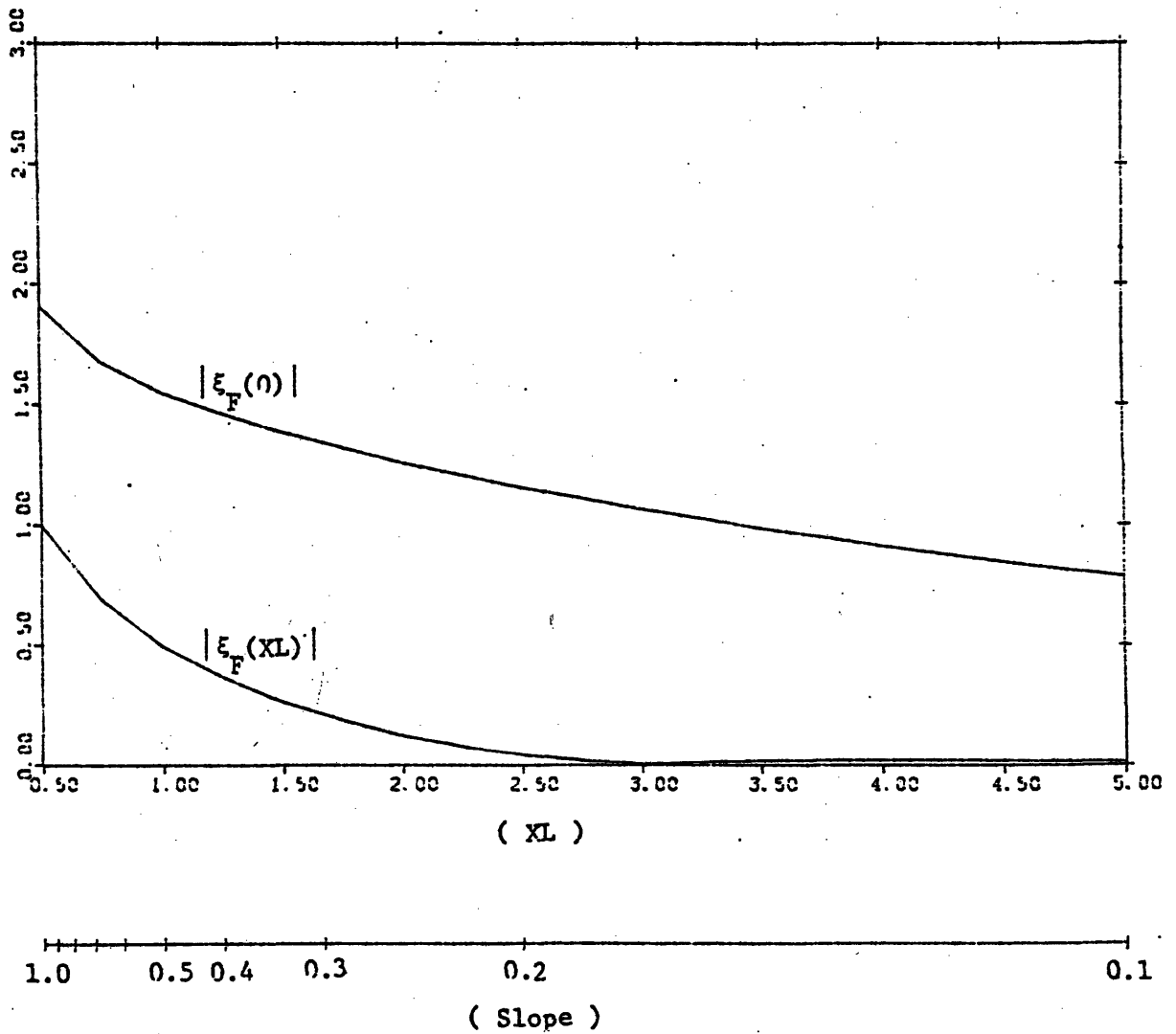


Figure 5.8 (Cont.)

(b) Oblique Incidence $\alpha_0 = \frac{\pi}{4}$



5.h. Canyons and Ridges

In this subsection we consider the depth variation to be a cosine profile:

$$h = h_0 + \frac{dh}{2} \left(1 - \cos \frac{2\pi x}{XL}\right)$$

The bottom profile corresponds to a canyon if $dh > 0$ and to a ridge if $dh < 0$. Figs. (5.9) and (5.10) show the forced wave amplitude and phase in the case of a canyon: $h_0 = 0.5$, $dh = 0.5$. The length of the transition zone is $XL = 2$ in Fig. (5.9) and $XL = 10$ in Fig. (5.10). For such depth variations progressive outgoing forced waves are present on both sides for normal incidence $\alpha_0 = 0$, and oblique incidence $\alpha_0 = \pi/6$ and $\pi/4$. However for $\alpha_0 = 0$ and $\pi/6$, λ^2 is positive everywhere. The wave amplitude is larger on the right hand side than on the left hand side. The phase distribution also shows that in the zone of varying depth the forced waves are propagating towards the right except in a small region in the neighborhood of $x = 0$. For $\alpha_0 = \pi/4$, λ^2 is negative for $h > 0.6$. The location of the turning points is marked on the plots by the dashed line. The right and left going waves have amplitudes of the same order of magnitude. In the case of normal incidence, the variations of the right going wave amplitude $|\xi_F|_R$ and left going wave amplitude $|\xi_F|_L$ with the length of the transition zone XL are displayed in Fig. (5.11). $|\xi_F|_L$ decreases rapidly towards zero with small oscillations while $|\xi_F|_R$ is much bigger and undergoes large oscillations. Depending on the length

Figure 5.9 Forced Waves over a Canyon, $h_0 = 0.5$, $dh = 0.5$, $XL = 2$

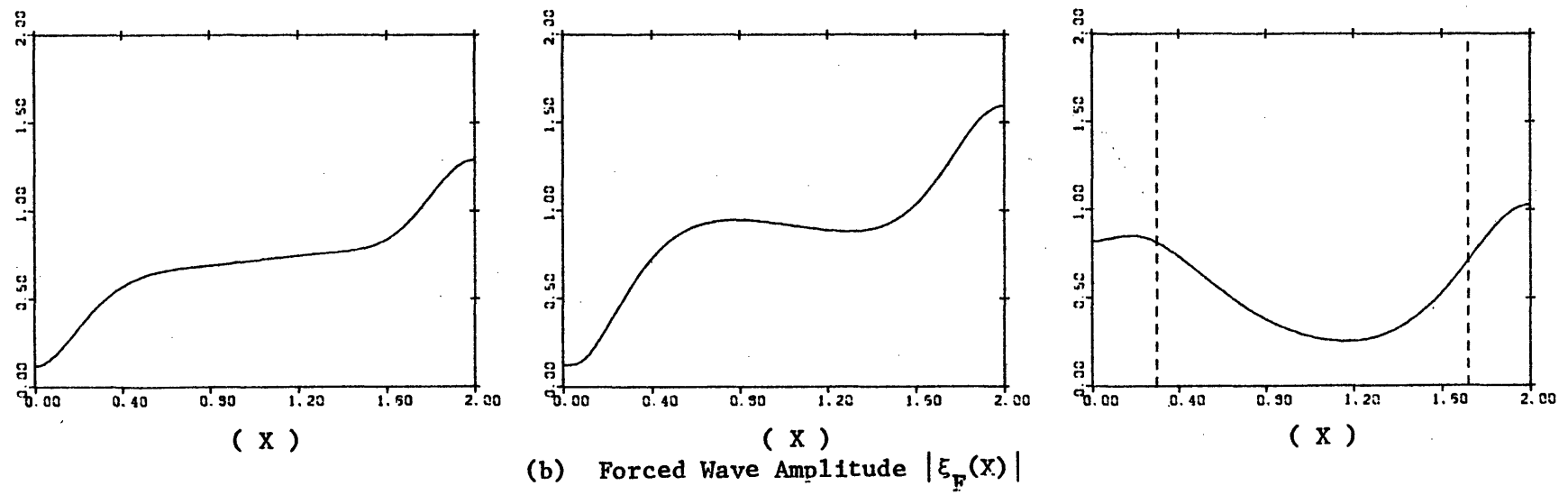
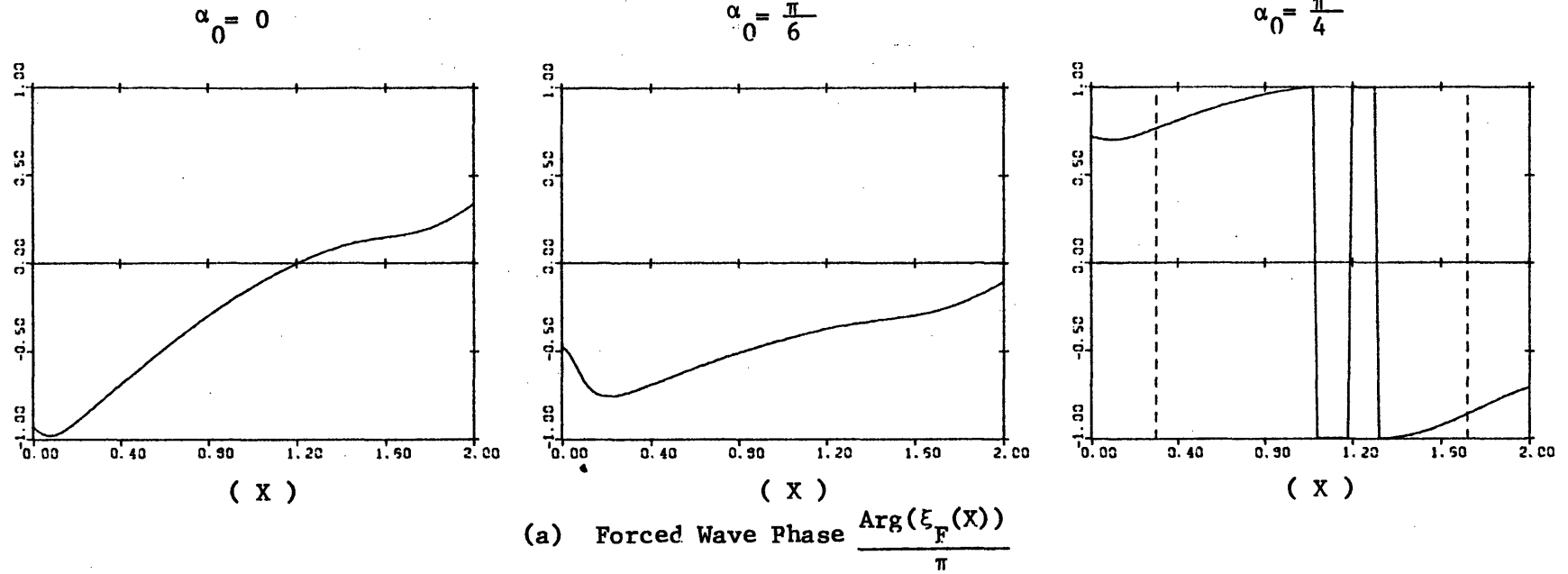
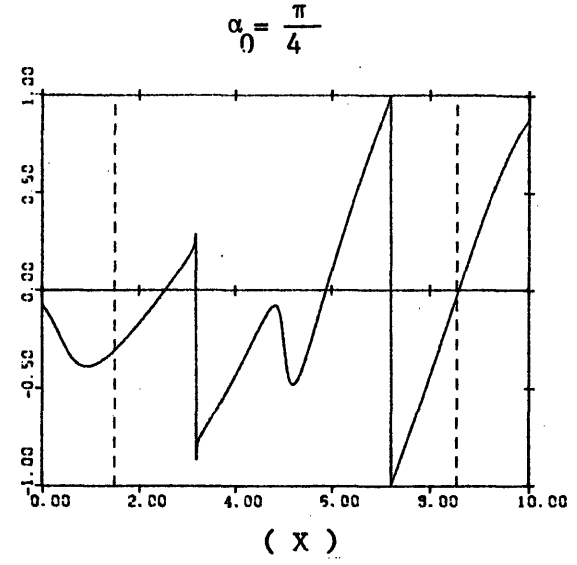
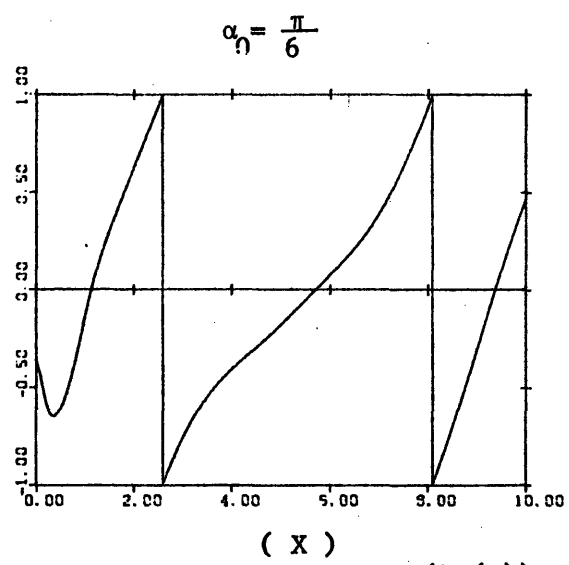
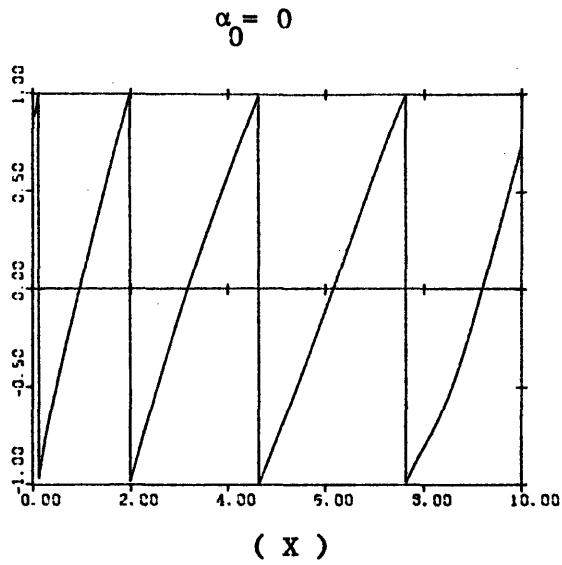
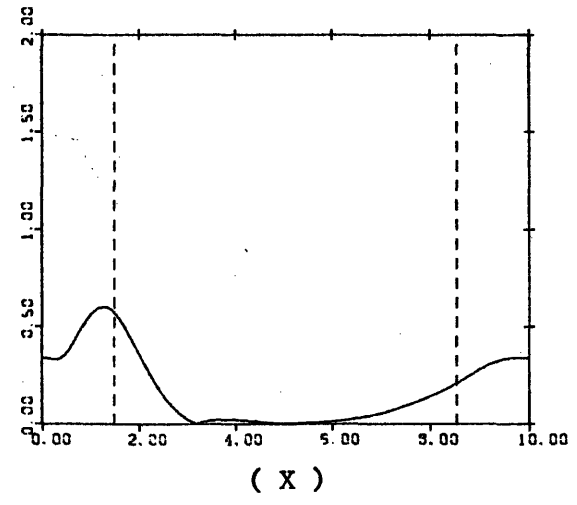
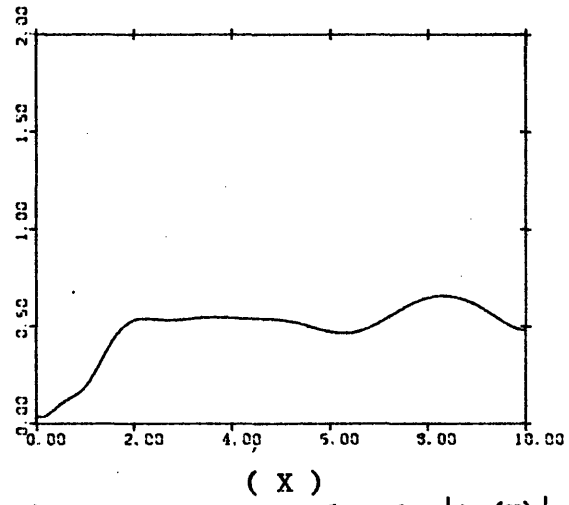
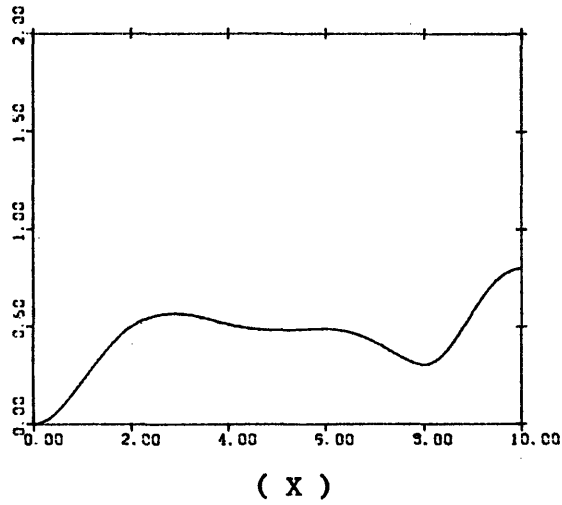


Figure 5.10 Forced Waves over a Canyon, $h_0 = 0.5$, $dh = 0.5$, $XL = 10$



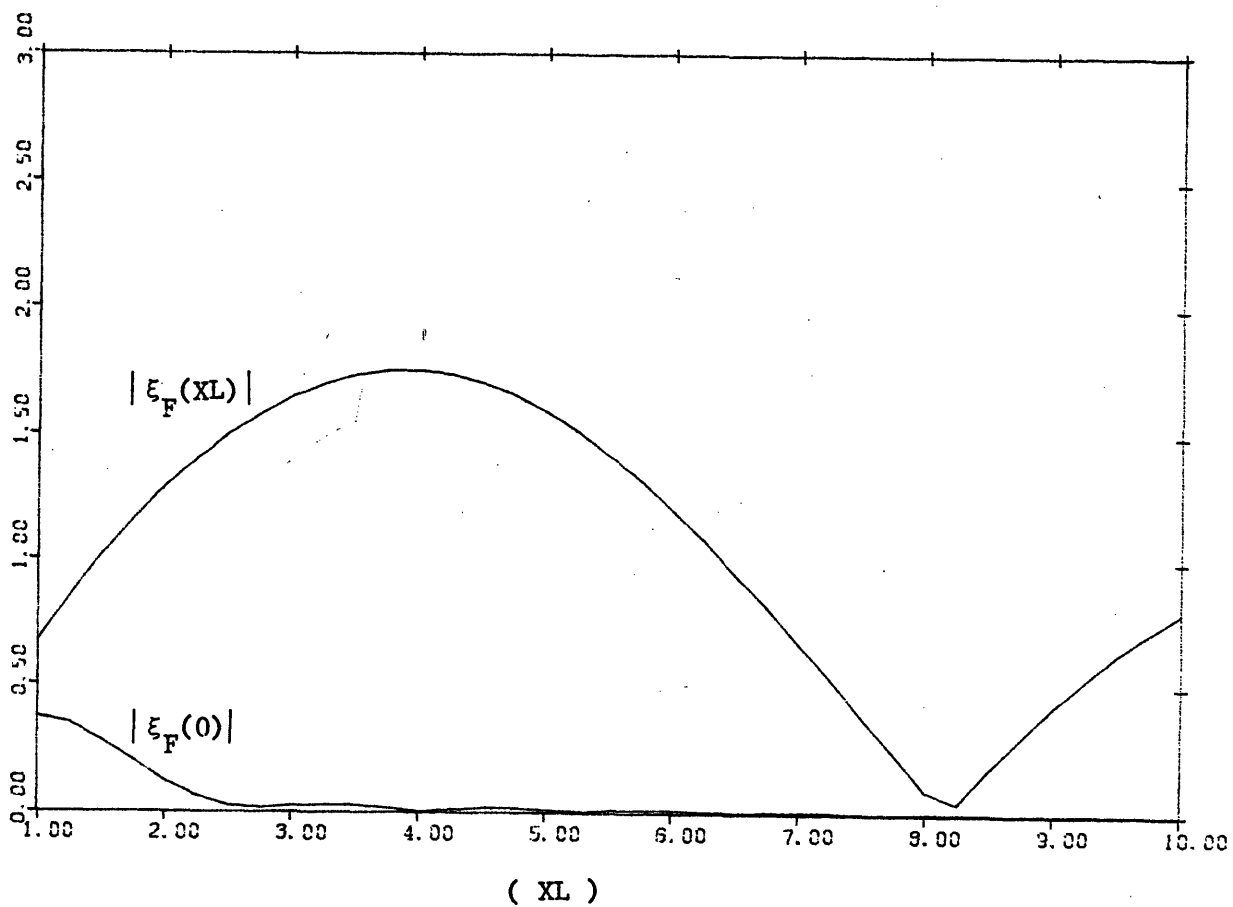
(a) Forced Wave Phase $\frac{\text{Arg}(\xi_F(X))}{\pi}$



(b) Forced Wave Amplitude $|\xi_F(X)|$

Figure 5.11 Forced Wave Amplitudes on the Left and Right Hand Sides

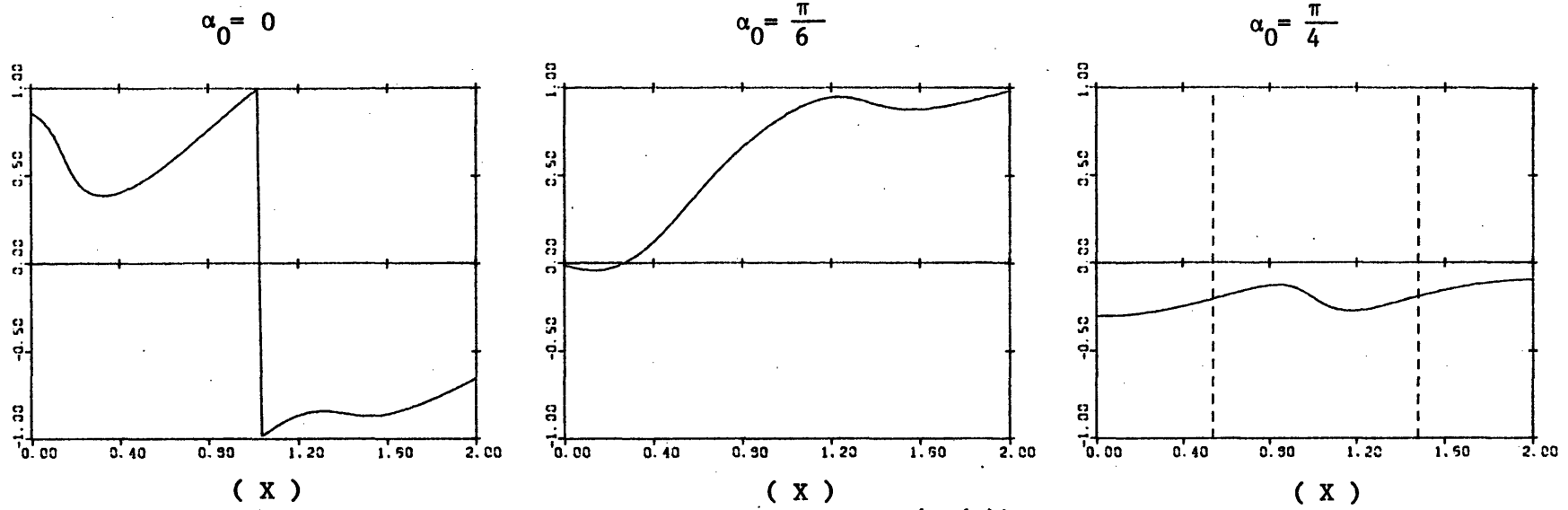
of a canyon, Normal Incidence, $h_0 = 0.5$, $dh = 0.5$



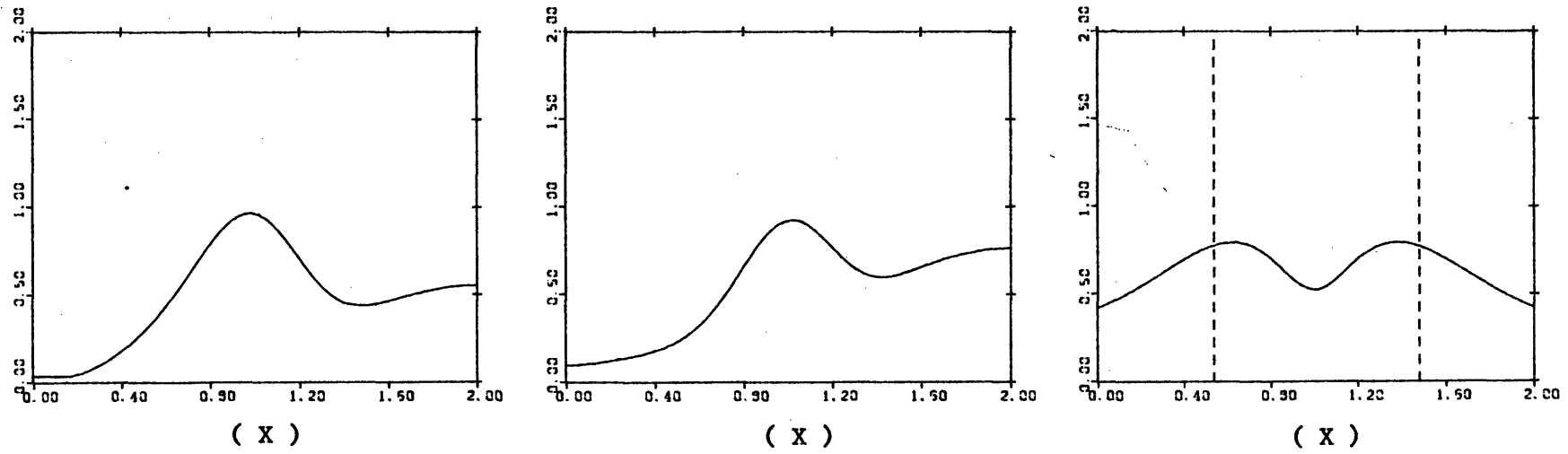
of the transition zone the right going wave can either have a very large amplitude or be absent. For $XL = 8$ there is hardly any ξ_F in both directions.

Fig. (5.12) and (5.13) correspond to the case of a ridge $h_0 = 1$, $dh = -0.5$, $\alpha_0 = 0, \pi/6, \pi/4$. The length of the transition zone is $XL = 2$ in Fig. (5.12) and $XL = 10$ in Fig. (5.13). For $\alpha_0 = 0$ and $\pi/6$ progressive outgoing waves are present in both sides of the region of variable depth. The left going wave amplitude is much smaller than the right going wave amplitude. For $\alpha_0 = \pi/4$ forced waves are trapped on both sides, their amplitudes at $X = 0$ and $X = XL$ are of the same order of magnitude. The ridge acts as a wave guide for the forced waves. In the case where progressive outgoing waves are present (i.e. $\alpha_0 = 0, \alpha_0 = \pi/6$), from the comparison of Fig. (5.12) and (5.13) we note that $|\xi_F|_R$ is larger for $XL = 10$ than for $XL = 2$. This seems to contradict our earlier experience that $|\xi_F|$ decreases with increasing XL . In Fig. (5.14) we have plotted the variations of $|\xi_F|_R$ and $|\xi_F|_L$ with XL for the case of normal incidence. It shows that $|\xi_F|_R$ is oscillating with a long period. The problem has now two different length scales: a length scale characterizing the oscillations and a much larger length scale over which the effect of the slope becomes important. On this long scale the maximum amplitude of the right going forced wave decreases.

Figure 5.12 Forced Waves over a Ridge, $h_0 = 1$, $dh = -0.5$, $XL = 2$



(a) Forced Wave Phase $\frac{\text{Arg}(\xi_F(X))}{\pi}$



(b) Forced Wave Amplitude $|\xi_F(X)|$

Figure 5.13 Forced Waves over a Ridge, $h_0 = 1$, $dh = -0.5$, $XL = 10$

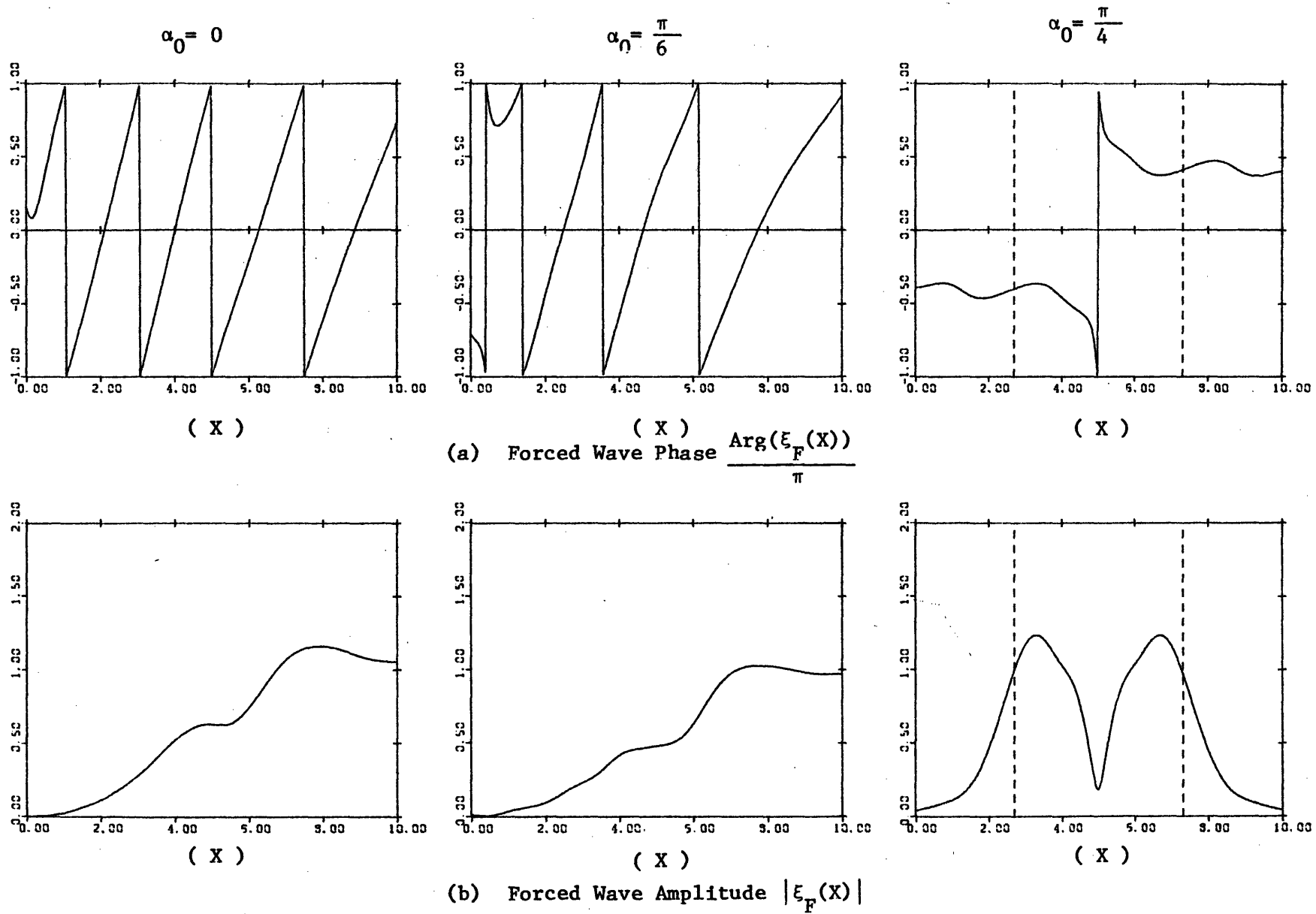
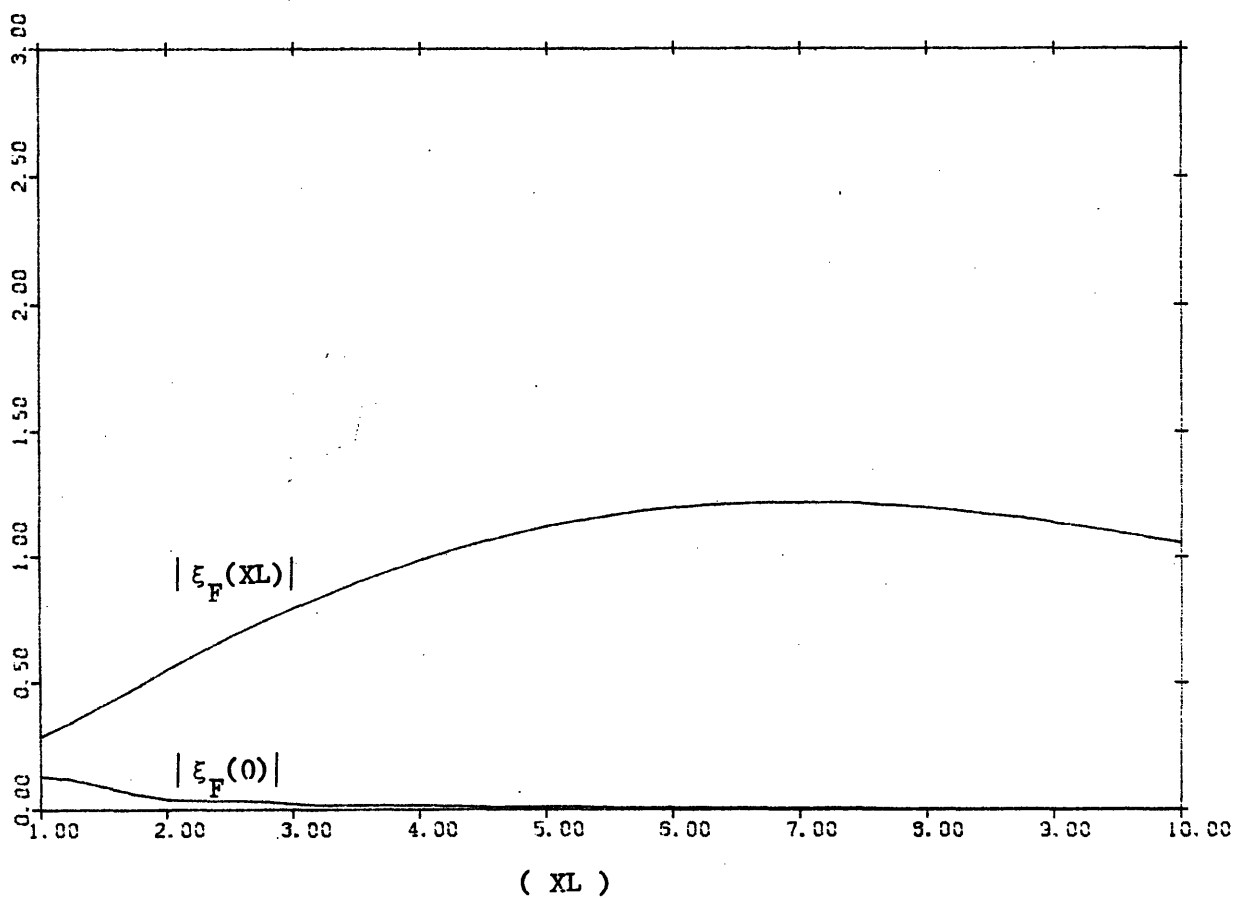


Figure 5.14 Forced Wave Amplitudes on the Left and Right Hand Sides

of a Ridge, Normal Incidence, $h_0 = 1$, $dh = -0.5$



6. Conclusion

A slowly modulated wave train propagating on varying depth generates second order long waves which can be decomposed into 'locked' and 'forced' waves. The locked waves propagate in the same direction and with the same velocity as the wave envelope. They are bound to it. The forced waves exist in the region of depth variation. In the case of normal incidence ($\lambda^2 > 0$ everywhere), they are radiated in the form of outgoing waves with constant amplitude. Their phase velocity and direction of propagation are different from those of the wave envelope. In the case of oblique incidence, the forced waves could be trapped along the zone of variable depth if the constant depth region is deep enough ($\lambda^2 < 0$). Their amplitude then decays exponentially as we move away from the transition zone.

In the case where λ^2 is everywhere positive, the forced waves are right going on most part of the region of depth variation. Their amplitude on the right hand side is in general larger than on the left hand side. In the case where λ^2 is somewhere negative, for linear depth variation the forced wave amplitude is smaller on the side where it is trapped, for a canyon or a ridge the forced wave amplitudes are of the same order on both sides whether they are trapped or not.

The effect of increasing depth is a rapid decrease of the forced wave amplitude. The effect of increasing the length of the transition

zone is a decrease of the right going and left going wave amplitude accompanied with some oscillations. These oscillations are small for a linear depth profile but have large amplitude and large period for a canyon or a ridge.

It should be noted that these results are valid everywhere but near a caustic. In the neighborhood of a caustic a more refined theory is needed to take into account the finiteness of the short wave amplitude. The numerical part of this study could also be extended by considering a two dimensional topography.

Figure Captions: Part II

Figure 3.1: Wavenumbers in the X-direction of the short waves (k_1) and their envelope (K) for different angles of incidence (a) $\alpha_0 = 0$, (b) $\alpha_0 = \pi/6$, (c) $\alpha_0 = \pi/4$, (d) $\alpha_0 = \pi/3$. The reference depth is $h_0 = 0.5$.

Figure 3.2: Wavenumbers in the X-direction of the short waves (k_1) and their envelope (K) for different angles of incidence (a) $\alpha_0 = 0$, (b) $\alpha_0 = \pi/6$, (c) $\alpha_0 = \pi/4$, (d) $\alpha_0 = \pi/3$. The reference depth is $h_0 = 1$.

Figure 3.3: Mean set-down for different angles of incidence $\alpha_0 = 0, \pi/6, \pi/4, \pi/3$ and reference depths (a) $h_0 = 0.5$, (b) $h_0 = 1$.

Figure 3.4: Set-down associated with the locked waves for different angles of incidence $\alpha_0 = 0, \pi/6, \pi/4, \pi/3$ and reference depths (a) $h_0 = 0.5$, (b) $h_0 = 1$.

Figure 5.1: Forced wave (a) amplitude $|\xi_F(X)|$, and (b) phase $\frac{\text{Arg}(\xi_F(X))}{\pi}$ over linearly increasing depth. $h_0 = 0.5, dh = 0.5, XL = 1$.

Figure 5.2: Forced wave (a) amplitude $|\xi_F(X)|$ and (b) phase $\frac{\text{Arg}(\xi_F(X))}{\pi}$ over linearly decreasing depth. $h_0 = 1, dh = -0.5, XL = 1$.

Figure 5.3: Forced wave (a) amplitude $|\xi_F(X)|$, and (b) phase $\frac{\text{Arg}(\xi_F(X))}{\pi}$ over linearly increasing depth. $h_0 = 1, dh = 0.5, XL = 1$.

Figure 5.4: Forced wave amplitudes on the left $|\xi_F(0)|$ and right $|\xi_F(XL)|$ hand sides of a linearly increasing depth region, for variable h_0 . Normal incidence, $dh = 0.5, XL = 1$.

- Figure 5.5: Forced wave (a) amplitude $|\xi_F(X)|$ and (b) phase $\frac{\text{Arg}(\xi_F(X))}{\pi}$ for linearly increasing depth. $h_0 = 0.5$, $dh = 0.5$, $XL = 5$.
- Figure 5.6: Forced wave (a) amplitude $|\xi_F(X)|$ and (b) phase $\frac{\text{Arg}(\xi_F(X))}{\pi}$ for linearly decreasing depth. $h_0 = 1$, $dh = -0.5$, $XL = 5$.
- Figure 5.7: Forced wave amplitudes on the left $|\xi_F(0)|$ and right $|\xi_F(XL)|$ hand sides of a linearly decreasing depth region, for variable XL . (a) Normal incidence, (b) oblique incidence $\alpha_0 = \pi/4$. $h_0 = 1$, $dh = -0.5$.
- Figure 5.8: Forced wave amplitudes on the left $|\xi_F(0)|$ and right $|\xi_F(XL)|$ hand sides of a linearly increasing depth region, for variable XL . (a) Normal incidence, (b) oblique incidence $\alpha_0 = \pi/4$. $h_0 = 0.5$, $dh = 0.5$.
- Figure 5.9: Forced wave (a) amplitude $|\xi_F(X)|$ and (b) phase $\frac{\text{Arg}(\xi_F(X))}{\pi}$ over a canyon. $h_0 = 0.5$, $dh = 0.5$, $XL = 2$.
- Figure 5.10: Forced wave (a) amplitude $|\xi_F(X)|$ and (b) phase $\frac{\text{Arg}(\xi_F(X))}{\pi}$ over a canyon. $h_0 = 0.5$, $dh = 0.5$, $XL = 10$.
- Figure 5.11: Forced wave amplitudes on the left $|\xi_F(0)|$ and right $|\xi_F(XL)|$ hand sides of a canyon, for variable XL . Normal incidence, $h_0 = 0.5$, $dh = 0.5$.
- Figure 5.12: Forced wave (a) amplitude $|\xi_F(X)|$ and (b) phase $\frac{\text{Arg}(\xi_F(X))}{\pi}$ over a ridge. $h_0 = 1$, $dh = -0.5$, $XL = 2$.
- Figure 5.13: Forced wave (a) amplitude $|\xi_F(X)|$ and (b) phase $\frac{\text{Arg}(\xi_F(X))}{\pi}$ over a ridge. $h_0 = 1$, $dh = -0.5$, $XL = 10$.
- Figure 5.14: Forced wave amplitudes on the left $|\xi_F(0)|$ and right $|\xi_F(XL)|$ hand sides of a ridge, for variable XL . Normal incidence, $h_0 = 1$, $dh = -0.5$.

*
*
*
*
*
*
*
*
*
*

ANNEXES

APPENDIX A1

The lower order terms which appear in Eqs. (3.10) are listed below:

$$I_{10} = I_{11} = 0$$

$$I_{20} = -2\rho(2k^2 u_{11} u_{1-1} - ik \frac{\partial u_{11}}{\partial z} W_{1-1} + ik \frac{\partial u_{1-1}}{\partial z} W_{11})$$

$$I_{21} = -\frac{2ik}{C_g} \frac{\partial p_{11}}{\partial \tau} - 2ik\rho \frac{\partial u_{10}}{\partial z} W_{11}$$

$$I_{22} = -2\rho(-k^2 u_{11} u_{11} + ik \frac{\partial u_{11}}{\partial z} W_{11})$$

$$I_{31} = -\frac{2ik}{C_g} \frac{\partial p_{21}}{\partial \tau} - 2ik \frac{\partial p_{11}}{\partial X} - \frac{i\partial k}{\partial X} p_{11} - \frac{1}{C_g^2} \frac{\partial^2 p_{11}}{\partial \tau^2} - 2\rho(2ik \frac{\partial u}{\partial X} u_{11} + \frac{2ik}{C_g} \frac{\partial u_{10}}{\partial \tau} u_{11} + 4k^2 u_{1-1} u_{22} + ik \frac{\partial u_{20}}{\partial z} W_{11} - ik \frac{\partial u_{22}}{\partial z} W_{1-1} + 2ik \frac{\partial u_{1-1}}{\partial z} W_{22})$$

$$J_{10} = J_{11} = J_{20} = J_{21} = J_{22} = 0$$

$$J_{31} = -ik \frac{\partial h}{\partial X} p_{11}$$

$$K_{10} = K_{11} = 0$$

$$K_{20} = -\frac{\partial u_{10}}{\partial \tau} - \frac{U}{C_g} \frac{\partial u_{10}}{\partial \tau} - W_{10} \frac{\partial u_{10}}{\partial z} - W_{11} \frac{\partial u_{1-1}}{\partial z} - W_{1-1} \frac{\partial u_{11}}{\partial z} - \frac{1}{\rho C_g} \frac{\partial p_{10}}{\partial \tau}$$

$$K_{21} = \frac{\partial u_{11}}{\partial \tau} - \frac{U}{C_g} \frac{\partial u_{11}}{\partial \tau} - ik u_{11} u_{10} - W_{10} \frac{\partial u_{11}}{\partial z} - W_{11} \frac{\partial u_{10}}{\partial z} - \frac{1}{\rho C_g} \frac{\partial p_{11}}{\partial \tau}$$

$$K_{22} = -ik u_{11} u_{1-1} - W_{11} \frac{\partial u_{11}}{\partial z}$$

$$\begin{aligned}
K_{30} &= \frac{\partial u_{20}}{\partial \tau} - \frac{\partial u_{10}}{\partial \tau} - \frac{\partial U}{\partial X} u_{10} - \frac{U}{C_g} \frac{\partial u_{20}}{\partial \tau} - U \frac{\partial u_{10}}{\partial X} + (z+h) \frac{\partial U}{\partial X} \frac{\partial u_{10}}{\partial z} \\
&+ \frac{\partial h}{\partial X} U \frac{\partial u_{10}}{\partial z} - \frac{1}{C_g} u_{10} \frac{\partial u_{10}}{\partial \tau} + ik u_{11} u_{2-1} - ik u_{1-1} u_{21} \\
&- \frac{1}{C_g} u_{11} \frac{\partial u_{1-1}}{\partial \tau} - \frac{1}{C_g} u_{1-1} \frac{\partial u_{11}}{\partial \tau} + ik u_{1-1} u_{21} - ik u_{11} u_{2-1} \\
&- W_{10} \frac{\partial u_{20}}{\partial z} - W_{1-1} \frac{\partial u_{21}}{\partial z} - W_{11} \frac{\partial u_{2-1}}{\partial z} - W_{2-1} \frac{\partial u_{11}}{\partial z} - \frac{1}{\rho C_g} \frac{\partial p_{20}}{\partial \tau} \\
&- \frac{1}{\rho} \frac{\partial p_{10}}{\partial X}
\end{aligned}$$

$$L_{10} = L_{11} = 0$$

$$L_{20} = -\frac{1}{C_g} \frac{\partial u_{10}}{\partial \tau}$$

$$L_{21} = -\frac{1}{C_g} \frac{\partial u_{11}}{\partial \tau}$$

$$L_{22} = 0$$

$$M_{10} = M_{20} = 0$$

$$\begin{aligned}
M_{20} &= \frac{\partial \eta_{10}}{\partial \tau} - \frac{U}{C_g} \frac{\partial \eta_{10}}{\partial \tau} + \eta_{10} \frac{\partial W_{10}}{\partial z} + ik u_{11} \eta_{1-1} - ik u_{1-1} \eta_{11} \\
&+ \eta_{1-1} \frac{\partial W_{11}}{\partial z} + \eta_{11} \frac{\partial W_{1-1}}{\partial z}
\end{aligned}$$

$$M_{21} = \frac{\partial \eta_{11}}{\partial \tau} - \frac{U}{C_g} \frac{\partial \eta_{11}}{\partial \tau} + \eta_{11} \frac{\partial W_{10}}{\partial z} + \eta_{10} \frac{\partial W_{11}}{\partial z} - ik u_{10} \eta_{11}$$

$$M_{22} = \eta_{11} \frac{\partial W_{11}}{\partial z} - ik u_{11} \eta_{11}$$

$$N_{10} = N_{11} = 0$$

$$N_{20} = \frac{\partial p_{10}}{\partial \tau} - \frac{U}{C_g} \frac{\partial p_{10}}{\partial \tau} - i\sigma\eta_{11} \frac{\partial p_{1-1}}{\partial z} + i\sigma\eta_{1-1} \frac{\partial p_{11}}{\partial z} + ik u_{11} p_{1-1}$$

$$-iku_{1-1} p_{11} - W_{10} \frac{\partial p_{10}}{\partial z} - W_{11} \frac{\partial p_{1-1}}{\partial z} - W_{1-1} \frac{\partial p_{11}}{\partial z} + \rho g \eta_{10} \frac{\partial w_{10}}{\partial z}$$

$$+ \rho g \eta_{11} \frac{\partial w_{1-1}}{\partial z} + \rho g \eta_{1-1} \frac{\partial w_{11}}{\partial z}$$

$$N_{21} = \frac{\partial p_{11}}{\partial \tau} - \frac{U}{C_g} \frac{\partial p_{11}}{\partial \tau} + i\sigma\eta_{10} \frac{\partial p_{11}}{\partial z} - ik u_{10} p_{11} - W_{10} \frac{\partial p_{11}}{\partial z} - W_{11} \frac{\partial p_{10}}{\partial z}$$

$$+ \rho g \eta_{10} \frac{\partial w_{11}}{\partial z} + \rho g \eta_{11} \frac{\partial w_{10}}{\partial z}$$

$$N_{22} = i\sigma\eta_{11} \frac{\partial p_{11}}{\partial z} - ik u_{11} p_{11} - W_{11} \frac{\partial p_{11}}{\partial z} + \rho g \eta_{11} \frac{\partial w_{11}}{\partial z}$$

To simplify the expressions for N_{30} and N_{31} we use the result

$$(3.24): \quad \eta_{10} = u_{10} = W_{10} = p_{10} = 0$$

$$N_{30} = \frac{\partial p_{20}}{\partial \tau} - \frac{U}{C_g} \frac{\partial p_{20}}{\partial \tau} - i\sigma\eta_{21} \frac{\partial p_{1-1}}{\partial z} + i\sigma\eta_{2-1} \frac{\partial p_{11}}{\partial z} - i\sigma\eta_{11} \frac{\partial p_{2-1}}{\partial z}$$

$$+ i\sigma\eta_{1-1} \frac{\partial p_{21}}{\partial z} + \eta_{11} \frac{\partial^2 p_{1-1}}{\partial \tau \partial z} - \frac{U}{C_g} \eta_{11} \frac{\partial^2 p_{1-1}}{\partial \tau \partial z} + \eta_{1-1} \frac{\partial^2 p_{11}}{\partial \tau \partial z}$$

$$- \frac{U}{C_g} \eta_{1-1} \frac{\partial^2 p_{11}}{\partial \tau \partial z} - ik u_{2-1} p_{11} + ik u_{21} p_{1-1} - ik u_{1-1} p_{21}$$

$$+ ik u_{11} p_{2-1} - \frac{1}{C_g} u_{11} \frac{\partial p_{1-1}}{\partial \tau} - \frac{1}{C_g} u_{1-1} \frac{\partial p_{11}}{\partial \tau} - W_{21} \frac{\partial p_{1-1}}{\partial z} - W_{2-1} \frac{\partial p_{11}}{\partial z}$$

$$- W_{11} \frac{\partial p_{2-1}}{\partial z} - W_{1-1} \frac{\partial p_{21}}{\partial z} + \rho g \eta_{11} \frac{\partial w_{2-1}}{\partial z} + \rho g \eta_{1-1} \frac{\partial w_{21}}{\partial z} + \rho g \eta_{21} \frac{\partial w_{1-1}}{\partial z}$$

$$+ \rho g \eta_{2-1} \frac{\partial w_{11}}{\partial z}$$

$$\begin{aligned}
N_{31} = & \frac{\partial p_{21}}{\partial \tau} - \frac{U}{C_g} \frac{\partial p_{21}}{\partial \tau} - \frac{\partial p_{11}}{\partial \tau} - \frac{U \partial p_{11}}{\partial X} + i \sigma \eta_{20} \frac{\partial p_{11}}{\partial z} - i \sigma \eta_{22} \frac{\partial p_{1-1}}{\partial z} \\
& - 2i \sigma \eta_{1-1} \frac{\partial p_{22}}{\partial z} + \frac{i \sigma}{2} (\eta_{11} \eta_{11} \frac{\partial^2 p_{1-1}}{\partial z^2} + 2 \eta_{11} \eta_{1-1} \frac{\partial^2 p_{11}}{\partial z^2}) - ik u_{20} p_{11} \\
& + ik u_{22} p_{1-1} - 2ik u_{1-1} p_{22} - ik (\eta_{11} p_{11} \frac{\partial u_{1-1}}{\partial z} - \eta_{11} p_{1-1} \\
& \frac{\partial u_{11}}{\partial z} + \eta_{1-1} p_{11} \frac{\partial u_{11}}{\partial z}) - ik (-\eta_{11} u_{11} \frac{\partial p_{1-1}}{\partial z} + u_{11} \eta_{1-1} \frac{\partial p_{11}}{\partial z} \\
& + u_{1-1} \eta_{11} \frac{\partial p_{11}}{\partial z}) - W_{22} \frac{\partial p_{1-1}}{\partial z} - W_{1-1} \frac{\partial p_{22}}{\partial z} - W_{11} \frac{\partial p_{20}}{\partial z} - (\eta_{11} \frac{\partial p_{11}}{\partial z} \\
& \frac{\partial W_{1-1}}{\partial z} + \eta_{11} \frac{\partial p_{1-1}}{\partial z} \frac{\partial W_{11}}{\partial z} + \eta_{1-1} \frac{\partial p_{11}}{\partial z} \frac{\partial W_{11}}{\partial z}) - (\eta_{11} W_{11} \frac{\partial^2 p_{1-1}}{\partial z^2} \\
& + \eta_{11} W_{1-1} \frac{\partial^2 p_{11}}{\partial z^2} + \eta_{1-1} W_{11} \frac{\partial^2 p_{11}}{\partial z^2}) - \rho g \frac{\partial \xi}{\partial X} u_{11} + (\xi+h) \frac{\partial U}{\partial X} \frac{\partial p_{11}}{\partial z} \\
& + U \frac{\partial h}{\partial X} \frac{\partial p_{11}}{\partial z} - \rho g \frac{\partial U}{\partial X} \eta_{11} + \rho g \eta_{1-1} \frac{\partial W_{22}}{\partial z} + \rho g \eta_{22} \frac{\partial W_{1-1}}{\partial z} + \rho g \eta_{20} \\
& \frac{\partial W_{11}}{\partial z} + \frac{\rho g}{2} (\eta_{11}^2 \frac{\partial^2 W_{1-1}}{\partial z^2} + 2 \eta_{11} \eta_{1-1} \frac{\partial^2 W_{11}}{\partial z^2}) \\
Q_{31} = & - \frac{\partial W_{11}}{\partial \tau} + (1 - \frac{U}{C_g}) \frac{\partial W_{21}}{\partial \tau} - \frac{U \partial W_{11}}{\partial X} + W_{11} \frac{\partial U}{\partial X} + (z+h) \frac{\partial U}{\partial X} \frac{\partial W_{11}}{\partial z} \\
& + \frac{\partial h}{\partial X} U \frac{\partial W_{11}}{\partial z} - 2iku_{1-1} W_{22} + ik W_{1-1} u_{22} - ik W_{11} u_{20} - W_{11} \frac{\partial W_{20}}{\partial z} \\
& - W_{1-1} \frac{\partial W_{22}}{\partial z} - W_{20} \frac{\partial W_{11}}{\partial z} - W_{22} \frac{\partial W_{1-1}}{\partial z}
\end{aligned}$$

The underlined terms are those which differ from the similar expression found by Turpin (1981)

Appendix A 2

FILE: WAVE FORTRAN A

```

*PROCESS SC(AXIS)
C *****
C *
C *   COMPUTE THE EVOLUTION OF A SECH PROFILE   *
C *
C *   OVER VARIABLE DEPTH AND CURRENT           *
C *
C *****
C A=AMPL.;H=DEPTH;XHI=TOTAL DEPTH(WITH CURRENT):
C T=ADIM.PERIOD;KA=WAVE NUMBER;Y1,Y2,Y3=COEF.OF EQUA.GOVER.A:
C CGG=GROUP VELOC.IN FIXED FRAME;UINF=CURRENT VEL. AT X=0
C ERR=CONSERVED QUANTITY( EVOLU.LAW)
C NA,2*JA1 ARE DIMEN. OF MATRIX A(AMPL.)
C NAV,DH,L=PARAM. OF DEPTH PROFILE
C DX,DTO=DISCR. LENGTH
C COMPLEX A(302,151)
C DIMENSION H(76),XHI(76),KA(76),Y1(76),Y2(76),Y3(76)
C S,CGG(76),ERR(500)
C REAL KA,CAA,L
C WRITE(10,100)
C READ(5,*)UINF,T,DH1,NAV,NA,JA1
100 FORMAT(5X,'UINF,T,DH1,NAV,NA,JA1')
C DTO=0.1
C JA=2*JA1
C L=1.
C DX=L/FLOAT(NAV-1)
C OME=2.*3.14159/T
C CALL DEPTH(NAV,DH1,H)
C GIVES THE DEPTH VARIATION
C DO 1 I=1,NAV
C HH=H(I)
C IF(ABS(UINF).LE.0.0001) GO TO 10
C CALL MEAFS(HH,UINF,XHII)
C GIVES THE SET UP DUE TO THE CURRENT
C GO TO 11
10 XHII=H(I)
11 XHI(I)=XHII
C CALL WAVENU(OME,UINF,XHII,CAA)
C GIVES THE WAVENUMBER
C IF WAVENUMBER NEGATIVE WAVES ARE STOPPED
C KA(I)=CAA
C IF(KA(I).GT.0.)GO TO 1
C WRITE(10,200)
C WRITE(10,300)UINF,T,H(I),XHII,KA(I)
200 FORMAT(5X,'WAVES CANNOT PROP. AGAINST THIS CURRENT')
300 FORMAT(5E12.4)
C GO TO 20
1 CONTINUE
C KA(NAV+1)=KA(NAV)
C XHI(NAV+1)=XHI(NAV)
C CALL COEFF(NAV,XHI,KA,H,UINF,OME,DX,Y1,Y2,Y3,CGG)
C GIVES THE COEFF. OF GOV. EQ.
C Y21=Y2(1)
C XX=ABS(Y3(1))
C CALL INIT(JA,DTO,Y21,XX,A,IS,ERR)
WAV00010
WAV00020
WAV00030
WAV00040
WAV00050
WAV00060
WAV00070
WAV00080
WAV00090
WAV00100
WAV00110
WAV00120
WAV00130
WAV00140
WAV00150
WAV00160
WAV00170
WAV00180
WAV00190
WAV00200
WAV00210
WAV00220
WAV00230
WAV00240
WAV00250
WAV00260
WAV00270
WAV00280
WAV00290
WAV00300
WAV00310
WAV00320
WAV00330
WAV00340
WAV00350
WAV00360
WAV00370
WAV00380
WAV00390
WAV00400
WAV00410
WAV00420
WAV00430
WAV00440
WAV00450
WAV00460
WAV00470
WAV00480
WAV00490
WAV00500
WAV00510
WAV00520
WAV00530
WAV00540
WAV00550

```

C	GIVES INITIAL PROFILE AT X2=0.	WAV00560
	CALL SOLUT(NA,NAV,JA,DX,DT0,Y1,Y2,Y3,IS,A,ERR,ADR,AN)	WAV00570
C	SOLVES THE LINEAR SYSTEM OF EQS.	WAV00580
	CALL IMPRES(NA,NAV,KA,XHI,Y2,Y3,ERR,ADR,AN)	WAV00590
	CALL WPLOT(NAV,NA,JA,DT0,DX,A)	WAV00600
20	CONTINUE	WAV00610
	STOP	WAV00620
	END	WAV00630
	SUBROUTINE DEPTH(NAV,DH1,H)	WAV00640
	DIMENSION H(1)	WAV00650
	DO 1 N=1,NAV	WAV00660
	R=FLOAT(N-1)*3.14159/FLOAT(NAV-1)	WAV00670
	H(N)=1.+DH1*(COS(R)-1.)/2.	WAV00680
1	CONTINUE	WAV00690
	H(NAV+1)=H(NAV)	WAV00700
	RETURN	WAV00710
	END	WAV00720
	SUBROUTINE MEAFS(HH,UINF,XHII)	WAV00730
	EPSI=0.001	WAV00740
	A2=(UINF**2)/2.	WAV00750
	X2=(A2**2)+4.*A2	WAV00760
	X1=(A2-SQRT(X2))/2.	WAV00770
	X2=(A2+SQRT(X2))/2.	WAV00780
	DELT=0.25*ABS(1.-X2)	WAV00790
	IF(DELT.LE.0.05) DELT=0.05	WAV00800
	XHII=1.	WAV00810
	N=0	WAV00820
	Z=HH-1.	WAV00830
	ER=ABS(Z)	WAV00840
	IF(ER.LE.EPSI) GO TO 20	WAV00850
	PTE=2.*(HH-1)-(1.-X1)*(1.-X2)	WAV00860
	IF(HH.LT.1.) GO TO 1	WAV00870
	IF(UINF.GT.1.) GO TO 10	WAV00880
	GO TO 11	WAV00890
12	IF(UINF.LT.1..AND.Z1.LE.O.) DELT=DELT/2.	WAV00900
	IF(UINF.GE.1..AND.Z1.GT.O.) DELT=DELT/2.	WAV00910
	N=N+1	WAV00920
	IF(N.GT.500) GO TO 20	WAV00930
11	XHII=XHII+DELT	WAV00940
	GO TO 14	WAV00950
13	IF(UINF.LT.1..AND.Z1.GT.O.) DELT=DELT/2.	WAV00960
	IF(UINF.GE.1..AND.Z1.LE.O.) DELT=DELT/2.	WAV00970
	N=N+1	WAV00980
	IF(N.GT.500) GO TO 20	WAV00990
10	XHII=XHII-DELT	WAV01000
14	Z1=Z	WAV01010
	Z=(XHII-1.)*(XHII-X1)+(XHII-X2)	WAV01020
	Z=(HH-1.)*(XHII**2)-Z	WAV01030
	ER=ABS(Z)	WAV01040
	IF(ER.LE.EPSI) GO TO 20	WAV01050
	IF(Z.GE.O..AND.UINF.LT.1.) GO TO 12	WAV01060
	IF(Z.LE.O..AND.UINF.LT.1.) GO TO 13	WAV01070
	IF(Z.LE.O..AND.UINF.GE.1.) GO TO 12	WAV01080
	IF(Z.GE.O..AND.UINF.GE.1.) GO TO 13	WAV01090
	GO TO 20	WAV01100
1	IF(UINF.GT.1.) GO TO 15	WAV01110
	GO TO 16	WAV01120
17	IF(UINF.GE.1.AND.(Z1.GT.O..OR.PT1.LE.O.)) DELT=DELT/2.	WAV01130
	IF(UINF.LT.1.AND.Z1.LE.O.AND.PT1.LE.O.) DELT=DELT/2.	WAV01140
	N=N+1	WAV01150
	IF(N.GT.500) GO TO 20	WAV01160
15	XHII=XHII+DELT	WAV01170
	GO TO 18	WAV01180
19	IF(UINF.GE.1.AND.Z1.LE.O.AND.PT1.GT.O.) DELT=DELT/2.	WAV01190
	IF(UINF.LT.1.AND.(Z1.GT.O..OR.PT1.GT.O.)) DELT=DELT/2.	WAV01200
	N=N+1	WAV01210
	IF(N.GT.500) GO TO 20	WAV01220

16	XHII=XHII-DELT	WAVO1230
18	Z1=Z	WAVO1240
	PT1=PTE	WAVO1250
	Z=(XHII-1.)*(XHII-X1)*(XHII-X2)	WAVO1260
	Z=(HH-1.)*(XHII**2)-Z	WAVO1270
	ER=ABS(Z)	WAVO1280
	IF(ER.LE.EPSI) GO TO 20	WAVO1290
	PTE=2.*(HH-1.)*XHII-(XHII-X1)*(XHII-X2)-(XHII-1.)*(2.*XHSI-X1-X2)	WAVO1300
	IF((Z.GT.O..OR.PTE.LE.O.).AND.UINF.GE.1.) GO TO 19	WAVO1310
	IF(Z.LE.O..AND.PTE.GT.O..AND.UINF.GE.1.) GO TO 17	WAVO1320
	IF(Z.LE.O..AND.PTE.LE.O..AND.UINF.LT.1.) GO TO 19	WAVO1330
	IF((Z.GT.O..OR.PTE.GT.O.).AND.UINF.LT.1.) GO TO 17	WAVO1340
20	RETURN	WAVO1350
	END	WAVO1360
	SUBROUTINE WAVENU(OME,UINF,XHII,CAA)	WAVO1370
	REAL K1,K2,CAA,K1INF,K2INF	WAVO1380
	EPSI=0.0001	WAVO1390
	X1=1.	WAVO1400
	X2=1.	WAVO1410
	X3=0.	WAVO1420
C	IF X1=1.(RES.-1.),X2=1.(RES.O.),X3=0.(RES.1.),WE STUD.THE	WAVO1430
C	SMALLEST(RES.LARGEST)ROOT	WAVO1440
	UN=UINF/XHII	WAVO1450
	N=0	WAVO1460
C	APPROXI.PLAC.OF ROOTS	WAVO1470
	K1=14.	WAVO1480
1	K1=K1/2.	WAVO1490
	FMG=(OME**2)/K1-2.*UN*OME+(UN**2)*K1-TANH(K1*XHII)	WAVO1500
	PTE=UN**2-(OME/K1)**2-XHII/((COSH(K1*XHII))**2)	WAVO1510
	IF(FMG.LE.O..OR.PTE.GT.O.) GO TO 1	WAVO1520
	DELT=K1	WAVO1530
	K2=K1	WAVO1540
2	FMG=(OME**2)/K2-2.*UN*OME+(UN**2)*K2-TANH(K2*XHII)	WAVO1550
	IF(FMG.LE.O.) GO TO 10	WAVO1560
	PTE=UN**2-(OME/K2)**2-XHII/((COSH(K2*XHII))**2)	WAVO1570
	IF(PTE.GT.O.) GO TO 11	WAVO1580
	K2=K2+DELT	WAVO1590
	GO TO 2	WAVO1600
11	DELT=DELT/2.	WAVO1610
	K2=K2-DELT	WAVO1620
	IF((DELT.LT.O.0005).AND.(UINF.LT.O.))GO TO 800	WAVO1630
C	K DOESNOT EXIST	WAVO1640
	GO TO 2	WAVO1650
10	K1INF=K2-DELT	WAVO1660
	FMG=1.	WAVO1670
	IF(X1.GE.O.) GO TO 131	WAVO1680
12	K2=K2+DELT	WAVO1690
	FMG=OME**2/K2-2.*UN*OME+(UN**2)*K2-TANH(K2*XHII)	WAVO1700
	IF(FMG.LE.O.) GO TO 12	WAVO1710
	K2INF=K2	WAVO1720
C	AT THIS PT.THE 2 ROOTS ARE K1(K2)BETW. K1INF AND K1INF+DE	WAVO1730
C	LT.(K2INF)	WAVO1740
131	K2=X2*K1INF+X3*K2INF	WAVO1750
	GO TO 130	WAVO1760
13	IF(FM1.LE.O.) DELT=DELT/2.	WAVO1770
130	K2=K2+X1*DELT	WAVO1780
	N=N+1	WAVO1790
	IF(N.GT.50) GO TO 1000	WAVO1800
	GO TO 15	WAVO1810
14	IF(FM1.GT.O.) DELT=DELT/2.	WAVO1820
	K2=K2-X1*DELT	WAVO1830
	N=N+1	WAVO1840
	IF(N.GT.50) GO TO 1000	WAVO1850
15	FM1=FMG	WAVO1860
	FMG=(OME**2)/K2-2.*UN*OME+(UN**2)*K2-TANH(K2*XHII)	WAVO1870
	ER=ABS(FMG)	WAVO1880
		WAVO1890

	IF(FMG.GE.O..AND.ER.GT.EPSI) GO TO 13	WAVO1900
	IF(FMG.LT.O..AND.ER.GT.EPSI) GO TO 14	WAVO1910
	KAA=K2	WAVO1920
	GO TO 1000	WAVO1930
900	KAA=-K2-DELT	WAVO1940
C	THE WAVE NUMBER IS SET TO BE NEGATIVE FOR STOPPED WAVES	WAVO1950
1000	RETURN	WAVO1960
	END	WAVO1970
	SUBROUTINE COEFF(NAV,XHI,KA,H,UINF,OME,DX,Y1,Y2,Y3,CGG)	WAVO1980
	DIMENSION XHI(1),KA(1),Y1(1),Y2(1),Y3(1),H(1),CGG(1)	WAVO1990
	REAL KA,KX1,KX,KH	WAVO2000
	DO 1 N=1,NAV	WAVO2010
	UN=UINF/XHI(N)	WAVO2020
	C=-UN+(OME/KA(N))	WAVO2030
	KX=KA(N)*XHI(N)	WAVO2040
	BET=TANH(KX)	WAVO2050
	CO=COSH(KX)	WAVO2060
	SI=SINH(KX)	WAVO2070
	CGM=C*0.5*(1.+KX/(SI*CO))	WAVO2080
	CG=CGM+UN	WAVO2090
	CGG(N)=CG	WAVO2100
	Y2(N)=1.-XHI(N)*(1.-BET*BET)*(1.-BET*KX)/(CGM**2)	WAVO2110
	Y2(N)=Y2(N)*(CGM**2)*KA(N)/(2.*C*(CG**3))	WAVO2120
	Y3(N)=4.*(C/CGM)**2)+4.*C/(CGM*CO*CO)+XHI(N)/((CGM*CO*CO)**2)	WAVO2130
	Y3(N)=-2.-Y3(N)-((BET*CGM)**2)/(XHI(N)-(CGM**2))+9.-10.*(WAVO2140
	SBET**2)+9.*(BET**4)	WAVO2150
	Y3(N)=KA(N)*Y3(N)/(4.*CG*C*((C*BET)**2))	WAVO2160
	KX1=KA(N+1)*XHI(N+1)	WAVO2170
	CG10S=0.5*(1.+KX1/(SINH(KX1)*COSH(KX1)))/KA(N+1)	WAVO2180
	CG10S=CG10S+UINF/(XHI(N+1)*(OME-UINF*KA(N+1)/XHI(N+1)))	WAVO2190
	Y1(N)=(CG10S-CG/(C*KA(N)))/DX	WAVO2200
	Y1(N)=Y1(N)/(CG10S+CG/C*KA(N))	WAVO2210
1	CONTINUE	WAVO2220
	RETURN	WAVO2230
	END	WAVO2240
	SUBROUTINE INIT(JA,DTO,Y21,XX,A,IS,ERR)	WAVO2250
	COMPLEX A(302,1)	WAVO2260
	DIMENSION ERR(1)	WAVO2270
	IS=1	WAVO2280
C	IF IS=1 INIT. PROF.SYM.IN TO	WAVO2290
C	IF IS=1 GIVE A AT X2=0 FOR TO=-DTO TO JA*DTO	WAVO2300
C	IF IS=0 INIT.PROF.NOT SYM.IN TO	WAVO2310
	QQ=1.	WAVO2320
	W=QQ*SQRT(ABS(XX/(2.*Y21)))/0.75	WAVO2330
	JA2=JA+1	WAVO2340
	E=0.	WAVO2350
	DO 1 I=1,JA2	WAVO2360
	R=FLOAT(I-2)	WAVO2370
	A(I,1)=CMPLX(QQ/COSH(W*R*DTO),0.)	WAVO2380
	IF(I.LE.2) GO TO 1	WAVO2390
	E=E+CABS(A(I,1))**2+CABS(A(I-1,1))**2	WAVO2400
1	CONTINUE	WAVO2410
	ERR(1)=E+DTO/2.	WAVO2420
	RETURN	WAVO2430
	END	WAVO2440
	SUBROUTINE SOLUT(NA,NAV,JA,DX,DTO,Y1,Y2,Y3,IS,A,ERR,ADR,AN)	WAVO2450
	COMPLEX AL(500),BE(500),GA(500),W(500),X(500),Y(500),	WAVO2460
	SA(302,1)	WAVO2470
	DIMENSION Y1(1),Y2(1),Y3(1),ERR(1)	WAVO2480
C	IF IS=0 A IS NOT SYMET.IN TO	WAVO2490
C	IF IS=1 A IS SYMET.IN TO	WAVO2500
	JA1=JA-1	WAVO2510
	YY=0.	WAVO2520
	KK=3-IS	WAVO2530
	DO 1 I=2,NA	WAVO2540
	E=0.	WAVO2550
	A(JA+1,I)=CMPLX(0.,0.)	WAVO2560

```

IF(IS.EQ.O) A(1,I)=CMLX(O.,O.)
IF(I.GT.NAV) GO TO 100
Y111=Y1(I-1)
Y222=Y2(I-1)
Y333=Y3(I-1)
Y11=(Y1(I-1)+Y1(I))/2.
Y22=(Y2(I-1)+Y2(I))/2.
Y33=(Y3(I-1)+Y3(I))/2.
GO TO 101
100 IF(I.GT.(NAV+1)) GO TO 101
Y111=O.
Y222=Y2(NAV)
Y333=Y3(NAV)
Y11=O.
Y22=Y222
Y33=Y333
101 DO 2 J=1,JA1
S=CABS(A(J+1,I-1))
AL(J)=CMLX(O.,Y22+DX/(2.*(DTO**2)))
GA(J)=AL(J)
W(J)=A(J+1,I-1)*CMLX(1.-DX*Y11/2.,DX*Y22/(DTO**2)-Y33*S+
SS+DX/2.)
W(J)=W(J)-(A(J+2,I-1)+A(J,I-1))*AL(J)
BE(J)=A(J+1,I-1)*CMLX(1.-DX*Y111,DX*2.*Y222/(DTO**2)-Y33
S3*S+S*DX)
BE(J)=BE(J)-(A(J+2,I-1)+A(J,I-1))*CMLX(O.,Y222+DX/(DTO**
S2))
S=CABS(BE(J))
BE(J)=CMLX(1.+DX*Y11/2.,-DX*Y22/(DTO**2)+DX*Y33*S+S/2.)
2 CONTINUE
X(JA-1)=-AL(JA-1)/BE(JA-1)
Y(JA-1)=W(JA-1)/BE(JA-1)
DO 3 J=3,JA
K=JA+1-J
X(K)=-AL(K)/(GA(K)*X(K+1)+BE(K))
Y(K)=(W(K)-GA(K)*Y(K+1))/(GA(K)*X(K+1)+BE(K))
3 CONTINUE
IF(IS.EQ.O) A(2,I)=(W(1)-GA(1)*Y(2))/(GA(1)*X(2)+BE(1))
IF(IS.EQ.1) A(1,I)=(X(2)*Y(1)+Y(2))/(1.-X(2)*X(1))
DO 4 J=KK,JA
A(J,I)=A(J-1,I)*X(J-1)+Y(J-1)
IF(J.LE.2) GO TO 4
E=E+CABS(A(J,I))**2+CABS(A(J-1,I))**2
4 CONTINUE
IF(I.GT.NAV) GO TO 103
YY=YY+Y1(I)+Y1(I-1)
103 ERR(I)=O.5*DTO*E*EXP(DX*YY)
1 CONTINUE
C AN,ADR ARE THE NUM. VALUE & THE D-R THEORY VALUE OF THE AREA
C UNDER THE WAVE PROFILE AT THE END OF THE DEPTH VARIATION
AN=O.
ADR=3.14159*SQRT(2.*Y2(1)/(ABS(Y3(1))*EXP(DX*YY)))
JA1=JA+1
DO5 J=3,JA1
SV=CABS(A(J,NAV))+CABS(A(J-1,NAV))
AN=AN+SV
5 CONTINUE
AN=AN*DTO
RETURN
END
SUBROUTINE IMPRES(NA,NAV,KA,XHI,Y2,Y3,ERR,ADR,AN)
DIMENSION Y2(1),Y3(1),ERR(1),XHI(1)
REAL KA(1),KH1,K1,KH2,K2
K1=Y3(1)/Y2(1)
KH1=XHI(1)*KA(1)
K2=Y3(NAV)/Y2(NAV)
K2=K2*((ADR/3.14159)**2)*ABS(K1)/2.
WAVO2570
WAVO2580
WAVO2590
WAVO2600
WAVO2610
WAVO2620
WAVO2630
WAVO2640
WAVO2650
WAVO2660
WAVO2670
WAVO2680
WAVO2690
WAVO2700
WAVO2710
WAVO2720
WAVO2730
WAVO2740
WAVO2750
WAVO2760
WAVO2770
WAVO2780
WAVO2790
WAVO2800
WAVO2810
WAVO2820
WAVO2830
WAVO2840
WAVO2850
WAVO2860
WAVO2870
WAVO2880
WAVO2890
WAVO2900
WAVO2910
WAVO2920
WAVO2930
WAVO2940
WAVO2950
WAVO2960
WAVO2970
WAVO2980
WAVO2990
WAVO3000
WAVO3010
WAVO3020
WAVO3030
WAVO3040
WAVO3050
WAVO3060
WAVO3070
WAVO3080
WAVO3090
WAVO3100
WAVO3110
WAVO3120
WAVO3130
WAVO3140
WAVO3150
WAVO3160
WAVO3170
WAVO3180
WAVO3190
WAVO3200
WAVO3210
WAVO3220
WAVO3230

```

C	PLOT THE WAVE AMPL.	WPLO0460
	DO1 I=2,JA1,IDELT	WPLO0470
	I1=I-2	WPLO0480
	XO=-FLOAT(I1)*SI*COS(AL)	WPLO0490
	YO=-FLOAT(I1)*SI*SIN(AL)+CABS(A(I,1))*1.4	WPLO0500
	CALL PLOT(XO,YO,3)	WPLO0510
	DO2 J=1,NA	WPLO0520
	J1=J-1	WPLO0530
	XP=XO+FLOAT(J1)*SJ*COS(AL)	WPLO0540
	YP=-FLOAT(I1)*SI*SIN(AL)-FLOAT(J1)*SJ*SIN(AL)	WPLO0550
	YP=YP+CABS(A(I,J))*1.4	WPLO0560
	CALL PLOT(XP,YP,2)	WPLO0570
2	CONTINUE	WPLO0580
1	CONTINUE	WPLO0590
	DO3 J=1,NA,JDELT	WPLO0600
	J1=J-1	WPLO0610
	XO=FLOAT(J1)*SJ*COS(AL)	WPLO0620
	YO=-FLOAT(J1)*SJ*SIN(AL)+CABS(A(2,J))*1.4	WPLO0630
	CALL PLOT(XO,YO,3)	WPLO0640
	DO4 I=2,JA1	WPLO0650
	I1=I-2	WPLO0660
	XP=XO-FLOAT(I1)*SI*COS(AL)	WPLO0670
	YP=-FLOAT(J1)*SJ*SIN(AL)-FLOAT(I1)*SI*SIN(AL)	WPLO0680
	YP=YP+CABS(A(I,J))*1.4	WPLO0690
	CALL PLOT(XP,YP,2)	WPLO0700
4	CONTINUE	WPLO0710
3	CONTINUE	WPLO0720
C	PLOT THE WAVE AMPL. AND ARG. AT XO=(IN(I)-1)*DX	WPLO0730
C	NU:NUMBER OF CURVES	WPLO0740
C	THE CURVES ARE PLOTTED FROM T=0 TO T=ISTOP	WPLO0750
C	D1:SUBDIVISION OF THE T AXIS	WPLO0760
C	WX:LENGTH OF THE T AXIS	WPLO0770
	NU=3	WPLO0780
	IN(1)=1	WPLO0790
	IN(2)=NAV	WPLO0800
	WRITE(10,300)	WPLO0810
300	FORMAT(5X,'ISTOP,IN(3),D1')	WPLO0820
	READ(5,*)ISTOP,IN(3),D1	WPLO0830
	WX=(ISTOP-2)*DT/D1	WPLO0840
	CALL PLOT(-9.5,-9.,-3)	WPLO0850
C	PLOT THE WAVE ARG. AT XO	WPLO0860
C	SUB. LIN PLOTS HOR. AND VERT. AXIS	WPLO0870
	XI=0.5+WX	WPLO0880
	CALL AXIS(0.5,1.5,'',2,4.,90.,-1.,0.5)	WPLO0890
	CALL AXIS(0.5,1.5,'',-2,WX,0.,0.,D1)	WPLO0900
	CALL LIN(0.5,5.5,WX,0.)	WPLO0910
	CALL LIN(0.5,3.5,WX,0.)	WPLO0920
	CALL LIN(XI,1.5,4.,90.)	WPLO0930
	DO5 J=1,NU	WPLO0940
	XP=0.5	WPLO0950
	W=AIMAG(A(2,IN(J)))	WPLO0960
	S=CABS(A(2,IN(J)))	WPLO0970
	YP=ARCOS(REAL(A(2,IN(J))/S))*SIGN(1.,W)	WPLO0980
	YP=(2*YP)/3.14159+3.5	WPLO0990
	CALL PLOT(XP,YP,3)	WPLO1000
	DO6 I=2,ISTOP	WPLO1010
	XP=0.5+(I-2)*WX/(ISTOP-2)	WPLO1020
	W=AIMAG(A(I,IN(J)))	WPLO1030
	S=CABS(A(I,IN(J)))	WPLO1040
	IF(S.LT.0.001)GO TO 5	WPLO1050
	YP=ARCOS(REAL(A(I,IN(J))/S))*SIGN(1.,W)	WPLO1060
	YP=(2*YP)/3.14159+3.5	WPLO1070
	CALL PLOT(XP,YP,2)	WPLO1080
6	CONTINUE	WPLO1090
5	CONTINUE	WPLO1100

	KH2=XHI(NAV)*KA(NAV)	
	WRITE(10,100)K1,KH1,K2,KH2	WAV03240
100	FORMAT(5X,'K1=',E12.4,2X,'KH1=',E12.4,/,5X,'K2=',	WAV03250
	&E12.4,2X,'KH2=',E12.4)	WAV03260
	WRITE(10,200)ADR,AN	WAV03270
	D03 J=1,NA,20	WAV03280
	WRITE(10,300)J,ERR(J)	WAV03290
3	CONTINUE	WAV03300
200	FORMAT(2X,'D-R=',E12.4,2X,'NUM=',E12.4)	WAV03310
300	FORMAT(5X,'QUANTITY CONSER.AT(',I3,')=',E12.4)	WAV03320
1000	RETURN	WAV03330
	END	WAV03340
		WAV03350

FILE: WPLOT FORTRAN A

@PROCESS SC(AXIS)		WPL00010
	SUBROUTINE WPLOT(NAV,NA,JA,DT,DX,A)	WPL00020
C	3-DIMENSIONAL PLOT OF AMPL. A(T,X)	WPL00030
	DIMENSION IN(4)	WPL00040
	COMPLEX A(302,1)	WPL00050
	WRITE(10,100)	WPL00060
100	FORMAT(5X,'DELX,DELT,JDELTA,IDELT')	WPL00070
	READ(5,*)DELX,DELT,JDELTA,IDELT	WPL00080
C	DELX,DELT:SUBDIVISION OF X AND T AXIS	WPL00090
C	JDELTA,IDELT:X AND T PLOTTING STEPS	WPL00100
C	WX,WY:LENGTH OF T AND X AXIS	WPL00110
C	AL:PROJECTION ANGLE	WPL00120
	JA1=JA+1	WPL00130
	WX=JA*DT/DELT	WPL00140
	WY=(NA-1)*DX/DELX	WPL00150
	JA2=JA-1	WPL00160
	NA2=NA-1	WPL00170
	SI=WX/FLOAT(JA2)	WPL00180
	SJ=WY/FLOAT(NA2)	WPL00190
	AL=35.*3.1416/180.	WPL00200
	X0=9.5	WPL00210
	Y0=9.	WPL00220
	CALL PLOTS(120,IDUM2,08)	WPL00230
	CALL FACTOR(0.6)	WPL00240
	CALL PLOT(X0,Y0,-3)	WPL00250
C	PLOT THE AXIS	WPL00260
	X0=-JA2*SI*COS(AL)	WPL00270
	Y0=-JA2*SI*SIN(AL)	WPL00280
	CALL PLOT(X0,Y0,2)	WPL00290
	CALL PLOT(0.,0.,3)	WPL00300
	XP=NA2*SJ*COS(AL)	WPL00310
	YP=-NA2*SJ*SIN(AL)	WPL00320
	CALL PLOT(XP,YP,2)	WPL00330
	XP=X0+WY*COS(AL)	WPL00340
	YP=Y0-WY*SIN(AL)	WPL00350
	CALL AXIS(X0,Y0,' ',-2,WY,-35.,0.,DELX)	WPL00360
	C=WX*DELT	WPL00370
	B=-DELT	WPL00380
	CALL AXIS(XP,YP,' ',-2,WX,35.,C,B)	WPL00390
	CALL PLOT(0.,0.,3)	WPL00400
	CALL PLOT(0.,2.8,2)	WPL00410
	CALL PLOT(0.,1.4,3)	WPL00420
	CALL PLOT(0.1,1.4,2)	WPL00430
	CALL PLOT(0.,2.8,3)	WPL00440
	CALL PLOT(0.1,2.8,2)	WPL00450

C	PLOT THE WAVE AMPL. AT XO	WPLO1110
	CALL AXIS(0.5,7.2,'',-2,WX,0.0.0.D1)	WPLO1120
	CALL AXIS(0.5,7.2,'',2.4.90.0.0.5)	WPLO1130
	CALL LIN(0.5,11.2,WX,0.)	WPLO1140
	CALL LIN(XI,7.2,4.90.)	WPLO1150
	DO7 J=1,NU	WPLO1160
	XP=0.5	WPLO1170
	YP=CABS(A(2,IN(J)))/0.5+7.2	WPLO1180
	CALL PLOT(XP,YP,3)	WPLO1190
	DO8 I=2,ISTOP	WPLO1200
	XP=0.5+(I-2)*WX/(ISTOP-2)	WPLO1210
	YP=CABS(A(I,IN(J)))/0.5+7.2	WPLO1220
	CALL PLOT(XP,YP,2)	WPLO1230
8	CONTINUE	WPLO1240
7	CONTINUE	WPLO1250
	CALL ENDPLT(15.0.,999)	WPLO1260
	STOP	WPLO1270
	END	WPLO1280

FILE: LIN FORTRAN A

	SUBROUTINE LIN(XO,YO,XL,XA)	LIN00010
C	PLOTS HOR. AND VERT. AXIS	LIN00020
C	XO,YO=COORD. OF AXIS	LIN00030
C	XL=LENGTH OF AXIS	LIN00040
C	XA=ANGLE OF AXIS (XA=0. OR 90.)	LIN00050
	CALL PLOT(XO,YO,3)	LIN00060
	N=INT(XL)+1	LIN00070
	IF(ABS(XA-90.).LT.0.1)GO TO 2	LIN00080
	X1=XO+XL	LIN00090
	CALL PLOT(X1,YO,2)	LIN00100
	Y2=YO-0.05	LIN00110
	Y1=YO+0.05	LIN00120
	X1=XO	LIN00130
	DO1 I=1,N	LIN00140
	CALL PLOT(X1,Y2,3)	LIN00150
	CALL PLOT(X1,Y1,2)	LIN00160
	X1=XO+I	LIN00170
1	CONTINUE	LIN00180
	GO TO 3	LIN00190
2	Y1=YO+XL	LIN00200
	CALL PLOT(XO,Y1,2)	LIN00210
	X2=XO-0.05	LIN00220
	X1=XO+0.05	LIN00230
	Y1=YO	LIN00240
	DO3 I=1,N	LIN00250
	CALL PLOT(X2,Y1,3)	LIN00260
	CALL PLOT(X1,Y1,2)	LIN00270
	Y1=YO+I	LIN00280
3	CONTINUE	LIN00290
	RETURN	LIN00300
	END	LIN00310

Appendix B1

The lower order terms appearing in eqs. (2.12) are listed below

$$R_{10} = F_{10} = G_{10} = H_{10} = 0$$

$$R_{20} = F_{20} = G_{20} = 0$$

$$H_{20} = \frac{\omega^2 a^2}{4 \sinh^2 kh} + \phi_{10T}$$

$$R_{21} = -2i \vec{k} \cdot \nabla \phi_{11} - i(\nabla \cdot \vec{k}) \phi_{11}$$

$$F_{21} = -\nabla h \cdot (i\vec{k} \phi_{11})|_{z=-h}$$

$$G_{21} = 2i\omega \phi_{11T}|_{z=0}$$

$$H_{21} = \phi_{11T}|_{z=0}$$

$$R_{30} = -\nabla^2 \phi_{10}$$

$$F_{30} = -\nabla h \cdot \nabla \phi_{10}|_{z=-h}$$

$$G_{30} = g \eta_{20T} - 2\nabla \cdot (\vec{k} \omega \phi_{11}^2)|_{z=0}$$

Appendix B2

FILE: FORCED FORTRAN A

```

#PROCESS SC(AXIS)
C *****
C * COMPUTE FORCED WAVES ON VARIABLE DEPTH *
C * USING *
C * HYBRID FINITE-ELEMENT METHOD *
C *****
C IP=1 THE PRG. COMPUTES & PLOTS THE FORCED WAVE AMPL.
C FOR N2(<4) DIFF. ANGLES OF INCIDENCE ALO;SAME LENGTH OF
C TRANSITION ZONE=XLO(DXL=0)
C IP=0 THE PRG. COMPUTES THE AMPL. OF THE WAVES AT THE ENDS OF
C THE REGION OF VAR. DEPTH;THE LENGTH OF THIS ZONE INCREASES
C FROM XLO WITH INCR. DXL;ANGLE OF INCID. CONST.=ALO(IAL)
C H=DEPTH,KA=WAVENUMBER,CG=GROUP VEL.,
C AL=DIR. OF PROP. OF SHORT WAVES
C ALO=DIR. OF PROP. AT REF. DEPTH
C KL=ENVELOPE WAVENUMBER IN X-DIR.
C A,ET= FORCED WAVE ,AML,AMR= AMPL. ON LEFT & RIGHT HAND SIDE
C OF VARYING DEPTH REGION
C Z=DIFF. MEAN SET-DOWN AND LOCKED WAVE AMPL.
C LA,LAM=COEF. OF GOV. EQ.
C ID=0 :LINEAR DEPTH VAR., ID=1 : COSINE DEPTH VAR.
C XL=LENGTH OF TRANSITION REGION
C XHO=REF. DEPTH, DH= AMPL. OF DEPTH VAR.
C DX=DISCR. LENGTH, NA=NUMB. OF INT.
C IMPLICIT REAL*8 (A-H,O-Z),INTEGER (I-N)
C REAL*8 H(1005),KA(1005),CG(1005),AL(1005),KL(1005)
C REAL*8 LA(1005),LAM(4,1005),AML(1005),AMR(1005),ALO(4),KAA
C COMPLEX*16 F(1005),A(1005),ET(4,1005)
C WRITE(10,200)
C READ(5,*)IP,ID,IAL,XLO,DXL,XHO,DH,N2
200 FORMAT(5X,'IP(0 NO PLOT,1 PLOT),ID(0 LIN.DEPTH,1 COS.)',/,
&5X,'IAL(ANGLE),XLO,DXL,XHO,DH,N2')
C DX=0.02
C ALO(1)=0.
C ALO(2)=3.1415900/6.
C ALO(3)=3.1415900/4.
C ALO(4)=3.1415900/3.
C H(1)=XHO
C K=1
C IF(IP.EQ.0)AL(1)=ALO(IAL)
C IF(IP.EQ.1)AL(1)=ALO(1)
7 CONTINUE
C XL=XLO+(K-1)*DXL
C NA=3+IDINT(XL/DX)
C CALL DEPTH(ID,H,NA,DH)
C GIVES THE DEPTH VAR.
C DO1 I=1,NA
C HH=H(I)
C CALL WAVENU(HH,KAA)
C GIVES THE WAVENUMBER
C KA(I)=KAA
C CG(I)=(1.+2.*KA(I)*HH/DSINH(2.*KA(I)*HH))/(2.*KA(I))
1 CONTINUE
C IF=0 NO CAUSTIC, IF>0 THERE IS A CAUSTIC
FOR00010
FOR00020
FOR00030
FOR00040
FOR00050
FOR00060
FOR00070
FOR00080
FOR00090
FOR00100
FOR00110
FOR00120
FOR00130
FOR00140
FOR00150
FOR00160
FOR00170
FOR00180
FOR00190
FOR00200
FOR00210
FOR00220
FOR00230
FOR00240
FOR00250
FOR00260
FOR00270
FOR00280
FOR00290
FOR00300
FOR00310
FOR00320
FOR00330
FOR00340
FOR00350
FOR00360
FOR00370
FOR00380
FOR00390
FOR00400
FOR00410
FOR00420
FOR00430
FOR00440
FOR00450
FOR00460
FOR00470
FOR00480
FOR00490
FOR00500
FOR00510
FOR00520
FOR00530
FOR00540
FOR00550

```

	IF=0	FOR00560
8	CONTINUE	FOR00570
	CALL FORC(IF,H,KA,AL,LA,DX,NA,F,CG)	FOR00580
C	COMPUTES THE FORCING FCT.	FOR00590
	IF(IF.GT.1)GO TO 10	FOR00600
	CALL SOLUT(H,LA,DX,NA,F,A)	FOR00610
C	SOLVES THE LINEAR SET OF EOS.	FOR00620
	IF(IP.EQ.0)GO TO 6	FOR00630
	DO3 I=1,NA	FOR00640
	ET(K,I)=A(I)	FOR00650
	LAM(K,I)=LA(I)	FOR00660
3	CONTINUE	FOR00670
	K=K+1	FOR00680
	IF(K.LE.N2)AL(1)=ALO(K)	FOR00690
	IF(K.LE.N2)GO TO 8	FOR00700
	CALL DRAW(XL,N2,NA,DX,ET,LAM)	FOR00710
C	PLOTS THE WAVE AMPL. AND PHASE	FOR00720
	GO TO 1000	FOR00730
6	AML(K)=CDABS(A(1))	FOR00740
	AMR(K)=CDABS(A(NA))	FOR00750
	K=K+1	FOR00760
	IF(K.LE.N2)GO TO 7	FOR00770
	WRITE(7,100)(AML(K),K=1,N2),(AMR(K),K=1,N2)	FOR00780
	GO TO 1000	FOR00790
10	WRITE(10,400)	FOR00800
	WRITE(10,401)IF,H(IF),AL(1)	FOR00810
400	FORMAT(6X,'CAUSTIC')	FOR00820
401	FORMAT(2X,'I=',I4,3X,'H(I)=',E10.4,3X,'AL(1)=',E10.4)	FOR00830
1000	CONTINUE	FOR00840
100	FORMAT(4(2X,E10.4))	FOR00850
	STOP	FOR00860
	END	FOR00870
	SUBROUTINE DEPTH(ID,H,NA,DH)	FOR00880
	IMPLICIT REAL*8 (A-H,O-Z),INTEGER (I-N)	FOR00890
	REAL*8 H(1005)	FOR00900
	N=NA-1	FOR00910
	IF(ID.EQ.0)GO TO 3	FOR00920
	DO1 I=2,N	FOR00930
	H(I)=H(1)+DH*(1.-DCOS(2.*3.14158DO*(I-2)/(N-2)))/2.	FOR00940
1	CONTINUE	FOR00950
	H(NA)=H(N)	FOR00960
	GO TO 1000	FOR00970
3	DO2 I=2,N	FOR00980
	H(I)=H(1)+DH*(I-2)/(N-2)	FOR00990
2	CONTINUE	FOR10000
	H(NA)=H(N)	FOR10100
1000	CONTINUE	FOR10200
	RETURN	FOR10300
	END	FOR10400
	SUBROUTINE WAVENU(HH,KA)	FOR10500
	IMPLICIT REAL*8 (A-H,O-Z),INTEGER (I-N)	FOR10600
	REAL*8 K1,K2,KA,K1INF,K2INF	FOR10700
	OME=1.	FOR10800
	EPSI=1.E-8	FOR10900
	X1=1.	FOR11000
	X2=1.	FOR11100
	X3=0.	FOR11200
C	IF X1=1.(RES.-1.),X2=1.(RES.0.),X3=0.(RES.1.),WE STUD.THE	FOR11300
C	SMALLEST(RES.LARGEST)ROOT	FOR11400
	N=0	FOR11500
C	APPROXI.PLAC.OF ROOTS	FOR11600
	K1=28.	FOR11700
1	K1=K1/2.	FOR11800
	FMG=(OME**2)/K1-DTANH(K1*HH)	FOR11900
	PTE=-((OME/K1)**2-HH/((DCOSH(K1*HH))**2)	FOR12000
	IF(FMG.LE.0..OR.PTE.GT.0.) GO TO 1	FOR12100
	DELT=K1	FOR12200

```

K2=K1
2 FMG=(OME**2)/K2-DTANH(K2*HH)
IF(FMG.LE.O.) GO TO 10
PTE=-(OME/K2)**2-HH/((DCOSH(K2*HH))**2)
IF(PTE.GT.O.) GO TO 11
K2=K2+DELT
GO TO 2
11 DELT=DELT/2.
K2=K2-DELT
GO TO 2
10 K1INF=K2-DELT
FMG=1.
IF(X1.GE.O.) GO TO 131
12 K2=K2+DELT
FMG=OME**2/K2-DTANH(K2*HH)
IF(FMG.LE.O.) GO TO 12
K2INF=K2
C AT THIS PT.THE 2 ROOTS ARE K1(K2)BETW. K1INF AND K1INF+DE
C LT.(K2INF)
131 K2=X2*K1INF+X3*K2INF
GO TO 130
13 IF(FM1.LE.O.) DELT=DELT/2.
130 K2=K2+X1*DELT
N=N+1
IF(N.GT.150) GO TO 1000
GO TO 15
14 IF(FM1.GT.O.) DELT=DELT/2.
K2=K2-X1*DELT
N=N+1
IF(N.GT.150) GO TO 1000
15 FM1=FMG
FMG=(OME**2)/K2-DTANH(K2*HH)
ER=DABS(FMG)
IF(FMG.GE.O..AND.ER.GT.EPSI) GO TO 13
IF(FMG.LT.O..AND.ER.GT.EPSI) GO TO 14
KAA=K2
1000 RETURN
END
SUBROUTINE FORC(IF,H,KA,AL,LA,DX,NA,F,CG)
C KY=WAVENUMBER IN Y-DIR.
C Z=DIFF. MEAN SET-DOWN AND LOCKED WAVE AMPL.
C XNU=DEF. RATIO OF FREQ. OF WAVE ENVEL. & SHORT WAVES
C F=FORCING FCT. TIMES DX
C THE MATCHING COND. ARE APPLIED AT X=DX & X=(NA-1)*DX
IMPLICIT REAL*8 (A-H,O-Z),INTEGER(I-N)
REAL*8 KA(1005),H(1005),CG(1005),Z(1005)
REAL*8 KL(1005),AL(1005),LA(1005)
REAL*8 KY
COMPLEX*16 F(1005)
DO1 I=1,NA
KY=KA(I)*DSIN(AL(I))
W=KY/KA(I)
IF(W.GE.1)GO TO 6
AL(I)=DARSIN(W)
KL(I)=CG(I)*KA(I)/(CG(I)*DCOS(AL(I)))
KL(I)=KL(I)-KY*DTAN(AL(I))
Z(I)=2.*KA(I)*H(I)*((KL(I)**2)+(KY**2))/DSINH(KA(I)*H(I)*2.)
Z(I)=Z(I)+2.*KA(I)*((CG(I)*KA(I)**2)/CG(I))
Z(I)=-Z(I)/(((CG(I)*KA(I)**2)-H(I)*((KL(I)**2)+(KY**2))))
Z(I)=Z(I)-1./((DSINH(KA(I)*H(I))**2)
Z(I)=Z(I)*CG(I)*DCOS(AL(I))/(8.*CG(I)*DCOS(AL(I)))
1 CONTINUE
XNU=1./((CG(I)*KA(I))
DO8 I=1,NA
LA(I)=(CG(I)**2-H(I)*((DSIN(AL(I))**2))*(KA(I)**2)
LA(I)=LA(I)*(XNU**2)
8 CONTINUE
FORO1230
FORO1240
FORO1250
FORO1260
FORO1270
FORO1280
FORO1290
FORO1300
FORO1310
FORO1320
FORO1330
FORO1340
FORO1350
FORO1360
FORO1370
FORO1380
FORO1390
FORO1400
FORO1410
FORO1420
FORO1430
FORO1440
FORO1450
FORO1460
FORO1470
FORO1480
FORO1490
FORO1500
FORO1510
FORO1520
FORO1530
FORO1540
FORO1550
FORO1560
FORO1570
FORO1580
FORO1590
FORO1600
FORO1610
FORO1620
FORO1630
FORO1640
FORO1650
FORO1660
FORO1670
FORO1680
FORO1690
FORO1700
FORO1710
FORO1720
FORO1730
FORO1740
FORO1750
FORO1760
FORO1770
FORO1780
FORO1790
FORO1800
FORO1810
FORO1820
FORO1830
FORO1840
FORO1850
FORO1860
FORO1870
FORO1880
FORO1890

```

TETA=0.	FORO1900
N=NA-1	FORO1910
DO2 I=2,N	FORO1920
IF(I.EQ.2)GO TO 3	FORO1930
IF(I.EQ.N)GO TO 4	FORO1940
DZ=(Z(I+1)-Z(I-1))/(2.*DX)	FORO1950
DDZ=(Z(I+1)-2.*Z(I)+Z(I-1))/((DX**2))	FORO1960
DH=(H(I+1)-H(I-1))/(2.*DX)	FORO1970
DA=KL(I)*DH+H(I)*(KL(I+1)-KL(I-1))/(2.*DX)	FORO1980
DB=(KA(I+1)-KA(I-1))-KA(I)*(CG(I+1)-CG(I-1))/CG(I)	FORO1990
DB=DB/(2.*DX*CG(I))	FORO2000
GO TO 5	FORO2010
3 DZ=(Z(I+1)-Z(I))/DX	FORO2020
DDZ=(Z(I+2)-2.*Z(I+1)+Z(I))/(DX**2)	FORO2030
DH=(H(I+1)-H(I))/DX	FORO2040
DA=DH*KL(I)+H(I)*(KL(I+1)-KL(I))/DX	FORO2050
DB=(KA(I+1)-KA(I))-KA(I)*(CG(I+1)-CG(I))/CG(I)	FORO2060
DB=DB/(DX*CG(I))	FORO2070
GO TO 5	FORO2080
4 DZ=(Z(I)-Z(I-1))/DX	FORO2090
DDZ=(Z(I)-2.*Z(I-1)+Z(I-2))/(DX**2)	FORO2100
DH=(H(I)-H(I-1))/DX	FORO2110
DA=DH*KL(I)+H(I)*(KL(I)-KL(I-1))/DX	FORO2120
DB=(KA(I)-KA(I-1))-KA(I)*(CG(I)-CG(I-1))/CG(I)	FORO2130
DB=DB/(DX*CG(I))	FORO2140
5 X1=DDZ*H(I)+DZ*DH	FORO2150
X2=DA*Z(I)+2.*H(I)*KL(I)*DZ-DB*(CG(I)**2)*KA(I)*DCOS(AL(I))/4.	FORO2160
X2=2.*XNU*X2	FORO2170
F(I)=DCMLPX(X1,X2)=DCMLPX(DCOS(TETA),DSIN(TETA))*DX	FORO2180
IF((I.EQ.2).OR.(I.EQ.N))F(I)=F(I)/2.	FORO2190
TETA=TETA+(KL(I)+KL(I+1))*XNU*DX	FORO2200
2 CONTINUE	FORO2210
F(I)=0.	FORO2220
F(NA)=0.	FORO2230
GO TO 1000	FORO2240
6 IF=I	FORO2250
1000 CONTINUE	FORO2260
RETURN	FORO2270
END	FORO2280
SUBROUTINE SOLUT(H,LA,DX,NA,F,A)	FORO2290
IMPLICIT REAL*8 (A-H,O-Z),INTEGER (I-N)	FORO2300
REAL*8 H(1005),LA(1005)	FORO2310
COMPLEX*16 F(1005),A(1005)	FORO2320
COMPLEX*16 W(1005),X(1005),Y(1005)	FORO2330
COMPLEX*16 GA(1005),BE(1005),AL(1005)	FORO2340
COMPLEX*16 S1,SN	FORO2350
N=NA-1	FORO2360
IF(LA(1).GE.O.)S1=DCMLPX(0.000,1.000)	FORO2370
IF(LA(1).LT.O.)S1=DCMLPX(-1.000,0.000)	FORO2380
IF(LA(NA).GE.O.)SN=DCMLPX(0.000,1.000)	FORO2390
IF(LA(NA).LT.O.)SN=DCMLPX(-1.000,0.000)	FORO2400
GA(1)=(2.*DX*LA(1)/3.+H(1)/DX)	FORO2410
BE(1)=(4.*DX*LA(1)/3.-H(1)/DX)	FORO2420
BE(1)=BE(1)+2.*S1*DSORT(H(1)*DABS(LA(1)))	FORO2430
BE(NA)=(4.*DX*LA(NA)/3.-H(NA)/DX)	FORO2440
BE(NA)=BE(NA)+2.*SN*DSORT(H(NA)*DABS(LA(NA)))	FORO2450
AL(NA)=(2.*DX*LA(NA)/3.+H(NA)/DX)	FORO2460
W(1)=0.	FORO2470
W(NA)=0.	FORO2480
DO1 I=2,N	FORO2490
GA(I)=(LA(I+1)+LA(I))*DX/3.+(H(I+1)+H(I))/(2.*DX)	FORO2500
BE(I)=2.*(LA(I+1)+2.*LA(I)+LA(I-1))*DX/3.	FORO2510
BE(I)=BE(I)-(H(I+1)+2.*H(I)+H(I-1))/(2.*DX)	FORO2520
AL(I)=(LA(I)+LA(I-1))*DX/3.+(H(I)+H(I-1))/(2.*DX)	FORO2530

	W(I)=F(I)	FOR02540
1	CONTINUE	FOR02550
	X(N)=-AL(NA)/BE(NA)	FOR02560
	Y(N)=W(NA)/BE(NA)	FOR02570
	NB=N-1	FOR02580
	DO2 I=1,NB	FOR02590
	I1=N-I	FOR02600
	I2=I1+1	FOR02610
	X(I1)=-AL(I2)/(GA(I2)*X(I2)+BE(I2))	FOR02620
	Y(I1)=(-GA(I2)+Y(I2)+W(I2))/(GA(I2)*X(I2)+BE(I2))	FOR02630
2	CONTINUE	FOR02640
	A(1)=(W(1)-GA(1)+Y(1))/(GA(1)*X(1)+BE(1))	FOR02650
	DO3 I=1,N	FOR02660
	A(I+1)=A(I)*X(I)+Y(I)	FOR02670
3	CONTINUE	FOR02680
	RETURN	FOR02690
	END	FOR02700
	@PROCESS SC(AXIS)	FOR02710
	SUBROUTINE DRAW(XL,N2,NA,DX,ET,LAM)	FOR02720
	IMPLICIT REAL*8 (A-H,O-Z),INTEGER(I-N)	FOR02730
	COMPLEX*16 ET(4,1005)	FOR02740
	REAL*8 LAM(4,1005)	FOR02750
	CALL PLOTS(120, IDUM2,08)	FOR02760
	CALL FACTOR(0.5)	FOR02770
	XO=1.	FOR02780
	YO=1.5	FOR02790
	N=NA-1	FOR02800
	DEL=N*DX/5.	FOR02810
	DEL=IDINT(10.*DEL)/10.	FOR02820
	DO6 K=1,N2	FOR02830
	X1=XO+5.	FOR02840
	Y1=YO+4.	FOR02850
	CALL AXIS(XO,YO,' ',-2.5,.0.,0.,DEL)	FOR02860
	CALL AXIS(XO,YO,' ',2.4..90..0..0.5)	FOR02870
	CALL LIN(XO,Y1,5..0.)	FOR02880
	CALL LIN(X1,YO,4..90.)	FOR02890
	DO2 I=2,N	FOR02900
	XP=XO+(I-2)*DX/DEL	FOR02910
	YP=YO+CDABS(ET(K,I))/0.5	FOR02920
	IF(I.EQ.2)CALL PLOT(XP,YP,3)	FOR02930
	CALL PLOT(XP,YP,2)	FOR02940
2	CONTINUE	FOR02950
	DO3 I=2,N	FOR02960
	S=LAM(K,I)*LAM(K,I-1)	FOR02970
	IF(S.GT.0.)GO TO 3	FOR02980
	XP=XO+(I-2)*DX/DEL	FOR02990
	YP=YO	FOR03000
	CALL PLOT(XP,YP,3)	FOR03010
5	YP=YP+0.1	FOR03020
	IF(YP.GT.Y1)GO TO 3	FOR03030
	CALL PLOT(XP,YP,2)	FOR03040
	YP=YP+0.1	FOR03050
	CALL PLOT(XP,YP,3)	FOR03060
	GO TO 5	FOR03070
3	CONTINUE	FOR03080
	YO=YO+6.	FOR03090
	Y1=YO+2.	FOR03100
	Y2=YO+4.	FOR03110
	CALL AXIS(XO,YO,' ',-2.5,.0.,0.,DEL)	FOR03120
	CALL AXIS(XO,YO,' ',2.4..90..-1..0.5)	FOR03130
	CALL LIN(XO,Y1,5..0.)	FOR03140
	CALL LIN(XO,Y2,5..0.)	FOR03150
	CALL LIN(X1,YO,4..90.)	FOR03160
	DO4 I=2,N	FOR03170
	ET(K,I)=ET(K,I)/CDABS(ET(K,I))	FOR03180
	WP=DARSIN(DIMAG(ET(K,I)))	FOR03190

	WS=SIGN(DARCOS(DREAL(ET(K,I))),WP)	FOR03200
	XP=XO+(I-2)*DX/DEL	FOR03210
	YP=Y1+WS/(0.5-3.14159)	FOR03220
	IF(I.EQ.2)CALL PLOT(XP,YP,3)	FOR03230
	CALL PLOT(XP,YP,2)	FOR03240
4	CONTINUE	FOR03250
	DO7 I=2,N	FOR03260
	S=LAM(K,I)=LAM(K,I-1)	FOR03270
	IF(S.GT.O.)GO TO 7	FOR03280
	XP=XO+(I-2)*DX/DEL	FOR03290
	YP=YO	FOR03300
	CALL PLOT(XP,YP,3)	FOR03310
8	YP=YP+0.1	FOR03320
	IF(YP.GT.Y2)GO TO 7	FOR03330
	CALL PLOT(XP,YP,2)	FOR03340
	YP=YP+0.1	FOR03350
	CALL PLOT(XP,YP,3)	FOR03360
	GO TO 8	FOR03370
7	CONTINUE	FOR03380
	XO=XO+S.	FOR03390
	YO=1.5	FOR03400
6	CONTINUE	FOR03410
	CALL ENOPLT(20.,O.,999)	FOR03420
	RETURN	FOR03430
	END	FOR03440

FILE: LIN FORTRAN A

	SUBROUTINE LIN(XO,YO,XL,XA)	LIN00010
C	PLOTS HOR. AND VERT. AXIS	LIN00020
C	XO,YO=COORD. OF AXIS	LIN00030
C	XL=LENGTH OF AXIS	LIN00040
C	XA=ANGLE OF AXIS (XA=0. OR 90.)	LIN00050
	CALL PLOT(XO,YO,3)	LIN00060
	N=INT(XL)+1	LIN00070
	IF(ABS(XA-90.).LT.O.1)GO TO 2	LIN00080
	X1=XO+XL	LIN00090
	CALL PLOT(X1,YO,2)	LIN00100
	Y2=YO-0.05	LIN00110
	Y1=YO+0.05	LIN00120
	X1=XO	LIN00130
	DO1 I=1,N	LIN00140
	CALL PLOT(X1,Y2,3)	LIN00150
	CALL PLOT(X1,Y1,2)	LIN00160
	X1=XO+I	LIN00170
1	CONTINUE	LIN00180
	GO TO 3	LIN00190
2	Y1=YO+XL	LIN00200
	CALL PLOT(XO,Y1,2)	LIN00210
	X2=XO-0.05	LIN00220
	X1=XO+0.05	LIN00230
	Y1=YO	LIN00240
	DO3 I=1,N	LIN00250
	CALL PLOT(X2,Y1,3)	LIN00260
	CALL PLOT(X1,Y1,2)	LIN00270
	Y1=YO+I	LIN00280
3	CONTINUE	LIN00290
	RETURN	LIN00300
	END	LIN00310

FILE: TEST2 FORTRAN A

```
C *****
C * FORCED WAVES ON VARIABLE DEPTH *
C * ANALYTICAL SOL. FOR LINEARLY INCREASING DEPTH *
C *****
C
C H:DEPTH ; AL:SLOPE ; XI,XF:END POINTS
C A:FORCED WAVES AMPLITUDE ; F:FORCING TERM
C Z:REL. DISPLACEMENT (ETO-ETL)
C KA:WAVELENGTH ; CG:GROUP VELOCITY
C DX:LENGTH INT. ;NA-1:NUM. OF INT
C IMPLICIT REAL*8 (A-H,O-Z),INTEGER (I-N)
REAL*8 KAA
REAL*8 H(1000),KA(1000),AM(1000)
COMPLEX*16 F(1000),A(1000)
WRITE(10,200)
READ(5,*)XI,XF,AL
200 FORMAT(5X,'XI,XF,AL')
DX=0.02
NA=1+IDINT((XF-XI)/DX)
DO2 I=1,NA
H(I)=AL*(XI+(XF-XI)*(I-1)/(NA-1))
2 CONTINUE
C FIND WAVELENGTH
DO1 I=1,NA
HH=H(I)
IF(DABS(HH).LT.0.01)GO TO 1000
CALL WAVENU(HH,KAA)
KA(I)=KAA
1 CONTINUE
C FINDS FORCING TERM
CALL FORC(H,KA,DX,NA,F)
C GIVES FORCED WAVE AMPLITUDE
CALL SOLUT(XI,XF,AL,DX,NA,F,A)
DO3 I=1,NA
AM(I)=CDABS(A(I))
3 CONTINUE
WRITE(7,100)(AM(I),I=1,NA)
100 FORMAT(2X,4(2X,E10.4))
1000 CONTINUE
STOP
END
SUBROUTINE WAVENU(HH,KAA)
IMPLICIT REAL*8 (A-H,O-Z),INTEGER (I-N)
REAL*8 K1,K2,KAA,K1INF,K2INF
OME=1.
EPSI=1.E-8
X1=1.
X2=1.
X3=0.
C IF X1=1.(RES.-1.),X2=1.(RES.0.),X3=0.(RES.1.),WE STUD.THE
C SMALLEST(RES.LARGEST)ROOT
N=0
C APPROXI.PLAC.OF ROOTS
K1=28.
1 K1=K1/2.
TES00010
TES00020
TES00030
TES00040
TES00050
TES00060
TES00070
TES00080
TES00090
TES00100
TES00110
TES00120
TES00130
TES00140
TES00150
TES00160
TES00170
TES00180
TES00190
TES00200
TES00210
TES00220
TES00230
TES00240
TES00250
TES00260
TES00270
TES00280
TES00290
TES00300
TES00310
TES00320
TES00330
TES00340
TES00350
TES00360
TES00370
TES00380
TES00390
TES00400
TES00410
TES00420
TES00430
TES00440
TES00450
TES00460
TES00470
TES00480
TES00490
TES00500
TES00510
TES00520
TES00530
TES00540
TES00550
```

	FMG=(OME**2)/K1-DTANH(K1*HH)	TESO0560
	PTE=-((OME/K1)**2-HH/((DCOSH(K1*HH))**2)	TESO0570
	IF(FMG.LE.O..OR.PTE.GT.O.) GO TO 1	TESO0580
	DELT=K1	TESO0590
	K2=K1	TESO0600
2	FMG=(OME**2)/K2-DTANH(K2*HH)	TESO0610
	IF(FMG.LE.O.) GO TO 10	TESO0620
	PTE=-((OME/K2)**2-HH/((DCOSH(K2*HH))**2)	TESO0630
	IF(PTE.GT.O.) GO TO 11	TESO0640
	K2=K2+DELT	TESO0650
	GO TO 2	TESO0660
11	DELT=DELT/2.	TESO0670
	K2=K2-DELT	TESO0680
	GO TO 2	TESO0690
10	K1INF=K2-DELT	TESO0700
	FMG=1.	TESO0710
	IF(X1.GE.O.) GO TO 131	TESO0720
12	K2=K2+DELT	TESO0730
	FMG=OME**2/K2-DTANH(K2*HH)	TESO0740
	IF(FMG.LE.O.) GO TO 12	TESO0750
	K2INF=K2	TESO0760
C	AT THIS PT.THE 2 ROOTS ARE K1(K2)BETW. K1INF AND K1INF+DE	TESO0770
C	LT.(K2INF)	TESO0780
131	K2=X2*K1INF+X3*K2INF	TESO0790
	GO TO 130	TESO0800
13	IF(FM1.LE.O.) DELT=DELT/2.	TESO0810
130	K2=K2+X1*DELT	TESO0820
	N=N+1	TESO0830
	IF(N.GT.150) GO TO 1000	TESO0840
	GO TO 15	TESO0850
14	IF(FM1.GT.O.) DELT=DELT/2.	TESO0860
	K2=K2-X1*DELT	TESO0870
	N=N+1	TESO0880
	IF(N.GT.50) GO TO 1000	TESO0890
15	FM1=FMG	TESO0900
	FMG=(OME**2)/K2-DTANH(K2*HH)	TESO0910
	ER=DABS(FMG)	TESO0920
	IF(FMG.GE.O..AND.ER.GT.EPSI) GO TO 13	TESO0930
	IF(FMG.LT.O..AND.ER.GT.EPSI) GO TO 14	TESO0940
	KAA=K2	TESO0950
1000	RETURN	TESO0960
	END	TESO0970
	SUBROUTINE FORC(H,KA,DX,NA,F)	TESO0980
	IMPLICIT REAL*8 (A-H,O-Z),INTEGER(I-N)	TESO0990
	REAL*8 KA(1000),H(1000),CG(1000),Z(1000)	TESO1000
	COMPLEX*16 F(1000)	TESO1010
	DO1 I=1,NA	TESO1020
	CG(I)=(1.+2.*KA(I)*H(I)/DSINH(2.*KA(I)*H(I)))/(2.*KA(I))	TESO1030
	Z(I)=(4.*CG(I)*KA(I)-1.)/((CG(I)**2)-H(I))	TESO1040
	Z(I)=Z(I)+1./((DSINH(KA(I)*H(I))**2)	TESO1050
	Z(I)=-Z(I)+CG(I)/(8.*CG(I))	TESO1060
1	CONTINUE	TESO1070
	TETA=0.	TESO1080
	DO2 I=1,NA	TESO1090
	IF(I.EQ.1)GO TO 3	TESO1100
	IF(I.EQ.NA)GO TO 4	TESO1110
	DZ=(Z(I+1)-Z(I-1))/(2.*DX)	TESO1120
	DOZ=(Z(I+1)-2.*Z(I)+Z(I-1))/(DX**2)	TESO1130
	DH=(H(I+1)-H(I-1))/(2.*DX)	TESO1140
	DA=DH/CG(I)-H(I)*(CG(I+1)-CG(I-1))/(2.*DX*(CG(I)**2))	TESO1150
	DB=(KA(I+1)-KA(I-1))-KA(I)*(CG(I+1)-CG(I-1))/CG(I)	TESO1160
	DB=DB/(2.*DX*CG(I))	TESO1170
	GO TO 5	TESO1180
3	DZ=(Z(I+1)-Z(I))/DX	TESO1190
	DH=(H(I+1)-H(I))/DX	TESO1200
	DOZ=(Z(I+2)-2.*Z(I+1)+Z(I))/(DX**2)	TESO1210
	DA=DH/CG(I)-H(I)*(CG(I+1)-CG(I))/(DX*(CG(I)**2))	TESO1220

	DB=(KA(I+1)-KA(I))-KA(I)*(CG(I+1)-CG(I))/CG(I)	TESO1230
	DB=DB/(DX-CG(I))	TESO1240
	GO TO 5	TESO1250
4	DZ=(Z(I)-Z(I-1))/DX	TESO1260
	DH=(H(I)-H(I-1))/DX	TESO1270
	DDZ=(Z(I)-2.*Z(I-1)+Z(I-2))/(DX**2)	TESO1280
	DA=DH/CG(I)-H(I)-(CG(I)-CG(I-1))/(DX*(CG(I)+2))	TESO1290
	DB=(KA(I)-KA(I-1))-KA(I)*(CG(I)-CG(I-1))/CG(I)	TESO1300
	DB=DB/(DX-CG(I))	TESO1310
5	X1=DDZ*H(I)+DH*DZ	TESO1320
	X2=(2.*DA+Z(I)+4.*H(I)*DZ/CG(I)-DB*CG(I))/2.)	TESO1330
	F(I)=DCMPLX(DCOS(TETA),DSIN(TETA))*X1	TESO1340
	F(I)=F(I)+DCMPLX(-DSIN(TETA),DCOS(TETA))*X2	TESO1350
	TETA=TETA+(1./CG(I)+1./CG(I+1))*DX	TESO1360
2	CONTINUE	TESO1370
	RETURN	TESO1380
	END	TESO1390
	SUBROUTINE SOLUT(XI,XF,AL,DX,NA,F,A)	TESO1400
	IMPLICIT REAL*8 (A-H,O-Z),INTEGER (I-N)	TESO1410
	COMPLEX*16 F(1000),A(1000)	TESO1420
	REAL*8 X(1000),Y(1000),ET(1000)	TESO1430
	COMPLEX*16 C1,C2,C3,C4,B1,B2	TESO1440
	COMPLEX*16 GA(1000),BE(1000)	TESO1450
	DO1 I=1,NA	TESO1460
	XX=XI+(XF-XI)*(I-1)/(NA-1)	TESO1470
	XX=DSORT(XX/AL)*4.	TESO1480
	CALL BESSEL(0,XX,XJ,XY)	TESO1490
	X(I)=XJ	TESO1500
	Y(I)=XY	TESO1510
1	CONTINUE	TESO1520
	GA(1)=0.	TESO1530
	BE(1)=0.	TESO1540
	DO2 I=2,NA	TESO1550
	GA(I)=GA(I-1)+(F(I)*Y(I)+F(I-1)*Y(I-1))*DX/2.	TESO1560
	BE(I)=BE(I-1)+(F(I)*X(I)+F(I-1)*X(I-1))*DX/2.	TESO1570
2	CONTINUE	TESO1580
	XX=4.*DSORT(XI/AL)	TESO1590
	CALL BESSEL(1,XX,XJ,XY)	TESO1600
	C1=DCMPLX(-XJ,X(1))	TESO1610
	C2=DCMPLX(-XY,Y(1))	TESO1620
	XX=4.*DSORT(XF/AL)	TESO1630
	CALL BESSEL(1,XX,XJ,XY)	TESO1640
	C3=DCMPLX(-XJ,-X(NA))	TESO1650
	C4=DCMPLX(-XY,-Y(NA))	TESO1660
	B1=C2*(C3+GA(NA)-C4+BE(NA))/(C2+C3-C1+C4)	TESO1670
	B2=-C1+B1/C2	TESO1680
	DO3 I=1,NA	TESO1690
	A(I)=(-GA(I)+B1)*X(I)+(BE(I)+B2)*Y(I)	TESO1700
	A(I)=A(I)*3.14159/AL	TESO1710
3	CONTINUE	TESO1720
	RETURN	TESO1730
	END	TESO1740
	SUBROUTINE BESSEL(ID,X,XJ,XY)	TESO1750
C	GIVES BESSEL FUNCTIONS J AND Y ACCORDING MATH. TABLE	TESO1760
C	ID:ORDER OF BESSEL FUNCTION ,ID=0 OR 1	TESO1770
	IMPLICIT REAL*8 (A-H,O-Z),INTEGER(I-N)	TESO1780
	IF(ID.EQ.1)GO TO 3	TESO1790
	IF(DABS(X).GT.3.)GO TO 2	TESO1800
	X1=(X/3.)**2	TESO1810
	XJ=1.+X1*(-2.2499997+X1*(1.2656208+X1*(-0.3163866+X1*(TESO1820
	&O.0444479+X1*(-0.0039444+X1*0.00021))))))	TESO1830
	XY=.36746691+X1*(.60559366+X1*(-.74350384+X1*(.25300117+	TESO1840
	&X1*(-0.04261214+X1*(0.00427916+X1*(-0.00024846))))))	TESO1850
	XY=XY+2.*DLOG(X/2.)*XJ/3.14159	TESO1860
	GO TO 11	TESO1870
2	X1=(3./X)	TESO1880
	XF=.79788456+X1*(-.00000077+X1*(-.0055274+X1*(-.00009512	TESO1890

	&+X1*(.00137237+X1*(-.00072805+X1*.00014476))))	TESO1900
	XT=X-.78539816+X1*(-.04166397+X1*(-.00003954+X1*(TESO1910
	&.00262573+X1*(-.00054125+X1*(-.00029333+X1*.00013558))))	TESO1920
	XJ=XF*DCOS(XT)/DSORT(X)	TESO1930
	XY=XF*DSIN(XT)/DSORT(X)	TESO1940
	GO TO 11	TESO1950
3	CONTINUE	TESO1960
	IF(DABS(X).GT.3.)GO TO 4	TESO1970
	X1=(X/3.)**2	TESO1980
	XJ=(.5+X1*(-.56249985+X1*(.21093573+X1*(-.03954289+X1*(TESO1990
	&.00443319+X1*(-.00031761+X1*.00001109)))))*X	TESO2000
	XY=-.6366198+X1*(.2212091+X1*(2.1682709+X1*(-1.3164827+X1*(TESO2010
	&.3123951+X1*(-.0400976+.0027873*X1))))	TESO2020
	XY=XY/X+2.*DLOG(X/2.)*XJ/3.14159	TESO2030
	GO TO 11	TESO2040
4	X1=3./X	TESO2050
	XF=.79788456+X1*(.00000156+X1*(-.01659667+X1*(.000017105+X1*(TESO2060
	&-.00249511+X1*(.00113653-X1*.00020033))))	TESO2070
	XT=X-2.35619449+X1*(.12499612+X1*(.0000565+X1*(-.00637879+	TESO2080
	&X1*(.00074348+X1*(.00079824-X1*.00029166))))	TESO2090
	XJ=XF*DCOS(XT)/DSORT(X)	TESO2100
	XY=XF*DSIN(XT)/DSORT(X)	TESO2110
11	CONTINUE	TESO2120
	RETURN	TESO2130
	END	TESO2140

Amplitude of Forced Waves over Linearly Increasing Depth,
 Normal Incidence, $XL= 1$, $h_0= 0.5$, $h_1= 1$

Numerical Results

0.4390D+00	0.4422D+00	0.4511D+00	0.4642D+00
0.4805D+00	0.4990D+00	0.5190D+00	0.5399D+00
0.5613D+00	0.5830D+00	0.6046D+00	0.6262D+00
0.6474D+00	0.6683D+00	0.6888D+00	0.7089D+00
0.7284D+00	0.7474D+00	0.7659D+00	0.7838D+00
0.8011D+00	0.8178D+00	0.8339D+00	0.8494D+00
0.8642D+00	0.8784D+00	0.8920D+00	0.9049D+00
0.9172D+00	0.9288D+00	0.9398D+00	0.9501D+00
0.9598D+00	0.9689D+00	0.9773D+00	0.9850D+00
0.9922D+00	0.9988D+00	0.1005D+01	0.1010D+01
0.1015D+01	0.1019D+01	0.1023D+01	0.1026D+01
0.1029D+01	0.1031D+01	0.1033D+01	0.1034D+01
0.1035D+01	0.1036D+01	0.1036D+01	

Analytical Results

0.4389D+00	0.4422D+00	0.4510D+00	0.4642D+00
0.4805D+00	0.4989D+00	0.5189D+00	0.5398D+00
0.5612D+00	0.5829D+00	0.6046D+00	0.6261D+00
0.6473D+00	0.6682D+00	0.6887D+00	0.7088D+00
0.7283D+00	0.7473D+00	0.7658D+00	0.7837D+00
0.8010D+00	0.8177D+00	0.8338D+00	0.8493D+00
0.8641D+00	0.8784D+00	0.8919D+00	0.9049D+00
0.9171D+00	0.9288D+00	0.9397D+00	0.9501D+00
0.9598D+00	0.9688D+00	0.9772D+00	0.9850D+00
0.9922D+00	0.9987D+00	0.1005D+01	0.1010D+01
0.1015D+01	0.1019D+01	0.1023D+01	0.1026D+01
0.1029D+01	0.1031D+01	0.1033D+01	0.1034D+01
0.1035D+01	0.1036D+01	0.1036D+01	

The relative difference is less than 0.1% .

REFERENCES

- Benjamin, T.B. and Feir, J.E. (1967) "The desintegration of Waves Trains on Deep Water," J. Fluid Mech., 27, 417.
- Bretherton, F.P. and Garret, C.J.R. (1968) "Wave Train in Inhomogeneous Moving Media," Proc. Roy. Soc., Series A, 302, 529.
- Chu, V.H. and Mei, C.C. (1970) "On Slowly Varying Stoke's Waves," J. Fluid Mech., 41, 873.
- Djordjevic, V.D. and Redekopp, L.G. (1978) "On the Development of Packet of Surface Gravity Waves Moving Over an Uneven Bottom," ZAMP, 29, 950.
- Longuet-Higgins, M.S. and Stewart, R.W. (1960) "Changes in the Form of Short Gravity Waves on Long Waves and Tidal Current," J. Fluid Mech., 10, 565.
- Longuet-Higgins, M.S. and Stewart, R.W. (1961) "The Change in Amplitude of Short Gravity Waves on Steady Non-uniform Currents," J. Fluid Mech., 12, 529.
- Longuet-Higgins, M.S. and Stewart, R.W. (1962) "Radiation Stress and Mass Transport in Gravity Waves, with Application to Surf Beats," J. Fluid Mech., 13, 481.
- Mei, C.C. (1978) "Numerical Methods in Water-Wave Diffraction and Radiation," Ann. Rev. Fluid Mech. 10, 393.
- Mei, C.C. (1982) "The Applied Dynamics of Ocean Surface Waves," Wiley Interscience, New-york.
- Molin, B. (1982) "On the Generation of Long-Period Second Order Free Waves Due to Changes in the Bottom Profile," Rapport IFP: 30167 Institut Fransais du Petrole.

- Ono, H. (1972) "Wave Propagation in an Inhomogeneous an. Harmonic Lattice," J. Phy. Society of Japan, 32, 332.
- Ono, H. (1974) "Nonlinear Wave Modulation in Inhomogeneous Media," J. Phy. Society of Japan, 37, 1668.
- Peregrine, D.H. (1976) "Interaction of Water Waves and Currents," Adv. Appl. Math. 16, 9.
- Phillips, O.M. (1966) "The Dynamic of the Upper Ocean," Cambridge University Press, London and New York.
- Potter, D. (1973) "Computational Physics," Wiley Interscience, New York.
- Satsuma, J. and N. Yajima, "Initial Value Problems of One Dimensional Self-Modulation of Nonlinear-Dispersive Waves," Suppl. of Prog. in Theor. Physics, 55, 284 (1975).
- Stiassnie, M. and Dagan, G. (1979) "Partial Reflexion of Water Waves by Non-uniform Adverse Currents," J. Fluid Mech., 92, 119.
- Stokes, G.G. (1847) "On the Theory of Oscillating Waves," Trans. Camb. Phil. Soc., 8, 441.
- Turpin, F.M. (1981) "Interaction Between Waves and Current Over a Variable Depth," Master Thesis, M.I.T.
- Whitham, G.B. (1962) "Mass Momentum and Energy Flux in Water Waves," J. Fluid Mech., 12, 135.
- Whitham, G.B. (1965) "A General Approach to Linear and Nonlinear Dispersive Waves Using a Lagrangian," J. Fluid Mech., 23, 273.
- Whitham, G.B. (1967) "Variational Methods and Application to Water Waves," Proc. Roy. Soc. Ser. A, 299, 6.
- Whitham, G.B. (1974) "Linear Nonlinear Waves," Wiley Interscience, New York.

Yue, D.K. (1980) "Numerical Study of Stoke's Waves Diffraction at Grazing Incidence," Ph.D. thesis, M.I.T.

Zakharov, V.E. and Shabat, A.B. (1972) "Exact Theory of two Dimensional Self-focusing and one Dimensional Self-modulation of Waves in Non Linear Media," Sov. Phys. JETP 34 , 62 .

Zakharov, V.E. and Shabat, A.B. (1973) "Interaction Between Solitons in a Stable medium," Sov. phys. JETP 37 , 823 .